

***Production and characterisation of analogues of the  
antimicrobial tyrocidine peptides with modified aromatic  
amino acid residues***

by

**Simon Nicholas Berge**

BSc Honours (Biochemistry)



UNIVERSITEIT  
UNIVERSITY  
STELLENBOSCH  
UNIVERSITY  
Dissertation approved for the degree  
***Magister Scientiae (Biochemistry)***



Faculty of Science

at the

University of Stellenbosch

Supervisor: Prof. Marina Rautenbach

Department of Biochemistry

University of Stellenbosch

## Declaration

By submitting this thesis electronically, I *Simon Nicholas Berge* declare that the entirety of the work contained therein is my own, original work, that I am the sole author thereof (save to the extent explicitly otherwise stated), that reproduction and publication thereof by Stellenbosch University will not infringe any third party rights and that I have not previously in its entirety or in part submitted it for obtaining any qualification.

*Simon Nicholas Berge*  
.....

**Name**

*March 2018*  
.....

**Date**

Copyright © 2018 Stellenbosch University

All rights reserved

## Summary

With the approach of a post-antibiotic era in which the current arsenal of antibiotic compounds can no longer combat common bacterial infections, the search for novel compounds to fight against antimicrobial resistance is more important than ever.

A group of forgotten antimicrobial peptides, termed the tyrocidines, have re-emerged as promising candidates for further development in clinical and industrial settings. These are basic, cyclic decapeptides, with the sequence cyclo(D-Phe<sup>1</sup>-L-Pro<sup>2</sup>-L-(Phe<sup>3</sup>/Trp<sup>3</sup>)-D-(Phe<sup>4</sup>/Trp<sup>4</sup>)-L-Asn<sup>5</sup>-L-Gln<sup>6</sup>-L-(Tyr<sup>7</sup>/Phe<sup>7</sup>/Trp<sup>7</sup>)-L-Val<sup>8</sup>-L-Orn<sup>9</sup>-L-Leu<sup>10</sup>), and are naturally synthesized, together with the neutral, linear pentadecapeptides, the gramicidins, by the soil bacterium *Brevibacillus parabrevis*. A multitude of structurally similar tyrocidines has been found in extracts of this organism. This arises due to the non-ribosomal, enzymatic, synthesis of these peptides in which certain domains within this multi-domain enzyme system have the ability to incorporate more than one kind of aromatic amino acid. The specific structural variations are at residue positions 3, 4 and 7 in the cyclic decapeptide. These structural variations produce tyrocidines with unique structure-activity relationships, imbuing them with activity against a wide variety of Gram-positive bacteria and fungi. Activity against the malarial parasite, *Plasmodium falciparum*, has also been observed.

This study aims to make use of the variability seen for incorporation of different aromatic amino acid residues, specifically of phenylalanine and tryptophan, to determine if non-natural derivatives of these amino acids can be incorporated, to biosynthesize novel tyrocidine, tryptocidine and phenycidine analogues (collectively termed the Trcs), with unique structure-activity relationships.

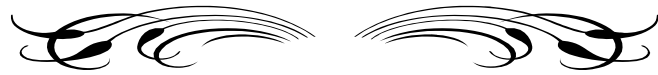
The initial objective of this study was to characterise different available strains of the producer organism, to determine if there was a difference in the production profiles of Trcs by the producer organism. A clear difference was found between the *Br. parabrevis* 5618, 362, 10068 and 8185 strains in terms of their production profiles, with the 5618 showing a marked improvement in Trc analogues rich in tryptophan. In addition to strain-determined differences in production profiles, differences in production as a result of altered nutrient conditions, in the form of nitrogen, sulphate and carbon sources, added on top of a base media, were also investigated. This was initially done by growth rate analysis of the producer organisms under different conditions, and then followed up by small scale culture to determine the effect on

production of Trcs. Altered productions in terms of biomass and extract mass were found, and to a lesser degree the Trc production profile. Urea appeared to have the most marked effect on Trc production, particularly for the 5618 strain.

The next objective was to determine if the selected phenylalanine analogues 4-methyl-phenylalanine (4-MeF), 2-flouro-phenylalanine (2-FF) and 4-trifluoro-phenylalanine (4-CF<sub>3</sub>F) and tryptophan analogues 5-methyl-tryptohan (5-MeW) and 1-methyl-trpyophan (1-MeW) could be incorporated into the Trcs. This investigation also used initial growth rate analysis of the strains 5618, 362 and 8185 under different supplementation concentrations of the non-natural and natural amino acids. With the exception of 1-MeW and CF<sub>3</sub>F, most amino acids appeared well tolerated by the strains tested, with a decrease in growth only being seen by most of the amino acids at concentrations of 22 mM. Following this, small scale cultures were done under selected conditions to test for their incorporation using the 5618 strain. Extensive incorporation was found for all the analogues, with the exception of 4-CF<sub>3</sub>F as determined by novel masses found using ESMS analysis.

Finally, medium-scale cultures were done using supplementation with 2-FF and 5-MeW to produce enough peptide for subsequent extraction, purification and analysis. Again, extensive incorporation of these analogues was found, with 5-MeW substituted Trc analogues having a large hydrophobic shift in retention time. A tyrocidine A analogue incorporating three 2-FF residues was found to be the predominate peptide in the 2-FF culture, while a tryptocidine B analogue incorporating either one or two 5-MeW was found on the 5-MeW culture. Subsequent semi-preparative reverse-phase HPLC was done in an attempt to purify individual non-natural analogues, however, difficulties in separation owing to the large variety of Trc analogues produced with overlapping retention times only allowed for enrichment of certain analogues. The enriched analogues were tested against *Micrococcus luteus*. The methylated tryptocidine B analogues appeared to have similar growth and metabolic inhibition activities to the natural analogues, while the fluorinated tyrocidine A analogues appeared to be more active compared to the natural analogue, being a more effective inhibitor of bacterial metabolism.

The production of novel tyrocidines with unique structure-activity relationships was shown to be possible by supplementation of the growth media of the producer organism with non-natural aromatic amino acids. This provides a rapid, affordable, and scalable method to produce novel antimicrobial peptides.



*Pain is nothing  
compared to  
the disgrace of  
giving up*

## Acknowledgements

I would like to express my thanks and gratitude to the following persons and institutions:

- Professor Marina Rautenbach for her unwavering supervision and support, and keeping the momentum of my research going when I needed it most;
- The BIOPEP group for their support and friendship, and making the lab environment feel like home;
- Dr Marietjie Stander and the other staff at the Central Analytical Facility (CAF) for their top-class expertise and assistance in Mass Spectrometry work;
- My Family for their unconditional love and support, without whom the opportunity to take part in post-graduate research would never have been possible;
- All the friends I have made both in the laboratory and out, who turned my journey through academia at Stellenbosch University into an adventure;
- The National Research Foundation and BIOPEP Peptide Fund for their financial support in achieving my MSc.

# Table of Contents

<b>CHAPTER 1: OVERVIEW OF ANTIMICROBIAL PEPTIDES FOCUSING ON THE TYROCIDINES AND ANALOGUES .....</b>	<b>1-1</b>
1.1 INTRODUCTION .....	1-1
1.2 DIVERSITY AND CATEGORISATION OF AMPS.....	1-1
1.3 MECHANISMS OF ACTION .....	1-2
1.3.1 Selectivity of AMPs for prokaryotic membranes.....	1-2
1.3.2 Membrane mediated mechanisms of action .....	1-2
1.3.3 Receptor or non-membrane mediated mechanisms.....	1-5
1.4 BIOSYNTHESIS OF AMPS.....	1-5
1.5 THE TYROCIDINES.....	1-5
1.5.1 Structure.....	1-6
1.5.2 Activity.....	1-9
1.5.3 Structure-activity.....	1-11
1.5.4 Mechanism of action .....	1-12
1.5.5 Tyrocidine biosynthesis .....	1-13
1.6 REFERENCES.....	1-16
<b>CHAPTER 2: TYROCIDINE PRODUCTION PROFILE CHARACTERISATION AND OPTIMISATION OF CARBON, NITROGEN AND SULPHATE SOURCES IN DIFFERENT USING STRAINS OF <i>BREVIBACILLUS PARABREVIS</i>.....</b>	<b>2-1</b>
2.1 INTRODUCTION .....	2-1
2.2 MATERIALS .....	2-2
2.3 METHODS.....	2-3
2.3.1 Medium-scale culturing of producer organisms .....	2-3
2.3.2 Production and extraction of tyrothricin .....	2-4
2.3.3 Bacterial growth using variable nutrient sources.....	2-6
2.3.4 Small scale cultures using optimised growth conditions .....	2-7
2.4 RESULTS.....	2-8
2.4.1 Extraction and UPLC-MS analysis of different producer strains.....	2-8
2.4.2 Growth rate analysis of selected strains under varying nutrient conditions .....	2-11
2.4.3 Small-scale culture extraction and ESMS analysis using selected nutrient conditions .....	2-18

2.5 DISCUSSION .....	2-21
2.6 REFERENCES .....	2-22
<b>CHAPTER 3: DETERMINATION OF THE INCORPORATION OF NON-NATURAL AMINO ACIDS INTO THE TYROCIDINES AND ANALOGUES .....</b>	<b>3-1</b>
3.1 INTRODUCTION .....	3-1
3.2 MATERIALS .....	3-4
3.3 METHODS.....	3-4
3.3.1 <i>Growth curve analysis of organisms using non-natural amino acids</i> .....	3-4
3.3.2 <i>Small scale cultures using selected, non-natural amino acids</i> .....	3-6
3.4 RESULTS.....	3-7
3.4.1 <i>Growth curve analysis of organisms using non-natural amino acids</i> .....	3-7
3.4.2 <i>ESMS analysis of small-scale cultures supplemented with non-natural amino acids ..</i>	3-15
3.5 DISCUSSION .....	3-33
3.6 REFERENCES .....	3-34
3.6 ADDENDUM.....	3-37
<b>CHAPTER 4: MEDIUM SCALE PRODUCTION AND CHARACTERISATION OF TYROCIDINE ANALOGUES CONTAINING NON-NATURAL AROMATIC AMINO ACIDS</b>	<b>4-1</b>
4.1 INTRODUCTION .....	4-1
4.2 MATERIALS .....	4-3
4.3 METHODS.....	4-4
4.3.1 <i>Medium-scale culturing and extraction using selected, non-natural amino acids</i> .....	4-4
4.3.2 <i>Purification of medium-scale extracts</i> .....	4-4
4.3.2 <i>ESMS Analysis of Trcs and analogues</i> .....	4-5
4.3.3 <i>Growth inhibition against M. luteus</i> .....	4-6
4.4 RESULTS.....	4-8
4.4.1 <i>Medium-scale culturing and extraction using selected, non-natural amino acids extracts</i> .....	4-8
4.4.2 <i>ESMS Analysis of crude extracts of Trcs and analogues</i> .....	4-9
4.4.3 <i>Reverse-phase semi-preparative HPLC purification and ESMS analysis of fractions.</i>	4-15
4.4.4 <i>Growth inhibition against M. luteus</i> .....	4-27
4.5 DISCUSSION .....	4-30



4.6 REFERENCES.....	4-32
<b>CHAPTER 5: SUMMARY, CONCLUSIONS AND FUTURE WORK.....</b>	<b>5-1</b>
5.1 INTRODUCTION.....	5-1
5.2 SUMMARY OF FINDINGS AND FUTURE WORK.....	5-2
5.2.1 <i>Strain production profile characterisation and optimisation of carbon, nitrogen and sulphate sources</i> .....	5-2
5.2.2 <i>Determination of the incorporation of non-natural amino acids into the tyrocidines and analogues</i> .....	5-4
5.2.3 <i>Medium scale production and characterisation of tyrocidine analogues containing non-natural aromatic amino acids</i> .....	5-5
5.3 LAST WORD.....	5-7
5.4 REFERENCES.....	5-8
 <b>THESIS ADDENDUM:</b>	
PEPTIDE REFERENCE TABLE.....	REFERENCE TABLE-1
REFERENCES.....	REFERENCE TABLE-5

## List of Abbreviations and Acronyms

2-FF	2-fluoro-phenylalanine
4-CF <sub>3</sub> F	4-CF <sub>3</sub> -phenylalanine
4-MeF	4-methyl-phenylalanine
1-MeW	1-methyl tryptophan
5-MeW	5-methyl tryptophan
[M]	molecular ion
ACN	Acetonitrile
AMP(s)	antimicrobial peptide(s)
ATCC	American type culture collection
<i>B. aneurinolyticus</i>	<i>Bacillus aneurinolyticus</i>
<i>B. subtilis</i>	<i>Bacillus subtilis</i>
<i>Br. parabrevis</i>	<i>Brevibacillus parabrevis</i>
<i>C. albicans</i>	<i>Candida albicans</i>
<i>C. glabrata</i>	<i>Candida glabrata</i>
<i>C. parapsilosis</i>	<i>Candida parapsilosis</i>
<i>C. tropicalis</i>	<i>Candida tropicalis</i>
CID	Collision Induced Dissociation
Da	Dalton
DSMZ	Deutsche Sammlung von Mikroorganismen und Zellkulturen
<i>E. coli</i>	<i>Escherichia coli</i>
ESI	Electrospray Ionisation
ESMS	electrospray mass spectrometry
EtOH	ethanol
Glc	glucose
Glr	glycerol
Grcs	linear gramicidins
GS	gramicidin S
HPLC	high performance liquid chromatography
HSV	herpes simplex virus

IC <sub>50</sub>	peptide concentration leading to 50 % microbial growth inhibition
IC <sub>max</sub>	peptide concentration leading to maximal microbial growth inhibition
<i>K. pneumoniae</i>	<i>Klebsiella pneumoniae</i>
Lys	Lysine
LB	Luria Bertani
LC	liquid chromatography
LC-MS	liquid chromatography linked mass spectrometry
<i>M. luteus</i>	<i>Micrococcus luteus</i>
m/v	mass per volume
m/z	mass over charge ratio
MBC	minimum bacteriocidal concentration
MIC	minimum inhibitory concentration
<i>Mr</i>	relative molar mass
MS	mass spectrometry
NCTC	national collection of type cultures
<i>N. gonorrhoea</i>	<i>Neisseria gonorrhoea</i>
NMR	nuclear magnetic resonance
NRPSs	non-ribosomal peptide synthetases
Orn/Ort/O	ornithine
OD	optical density
PBS	phosphate buffered saline
Phc(s)	phenycidine(s)
PhcA	phenycidine A
Phe	Phenylalanine
<i>P. falciparum</i>	<i>Plasmodium falciparum</i>
RP-HPLC	reverse phase high performance liquid chromatography
Rt	retention time of analyte in column chromatography
SAR	structure-activity relationship
SD	standard deviation
SEM	standard error of the mean
sp.	specie
spp.	species (plural)
ssp	sub-specie

<i>S. aureus</i>	<i>Staphylococcus aureus</i>
<i>S. pneumoniae</i>	<i>Streptococcus pneumoniae</i>
Tcn	tyrothricin
TE	thioesterase
TFA	trifluoroacetic acid
TGS	tryptone glucose and salts culture medium
TOF	time of flight
Tpc(s)	tryptocidines(s)
TpcA	tryptocidine A
TpcA <sub>1</sub>	tryptocidine A <sub>1</sub>
TpcB	tryptocidine B
TpcB <sub>1</sub>	tryptocidine B <sub>1</sub>
TpcC	tryptocidine C
TpcC <sub>1</sub>	tryptocidine C <sub>1</sub>
Trc C	tyrocidine C
Trc C <sub>1</sub>	tyrocidine C <sub>1</sub>
Trc(s)	tyrocidine(s)
TrcA	tyrocidine A
TrcA <sub>1</sub>	tyrocidine A <sub>1</sub>
TrcB	tyrocidine B
TrcB <sub>1</sub>	tyrocidine B <sub>1</sub>
Trp	tryptophan
TS	tryptone and salts culture medium
TSA	tryptone soy agar
TSB	tryptone soy broth
UPLC	ultra performance liquid chromatography
UPLC-MS	ultra performance liquid chromatography linked mass spectrometry
UV	ultraviolet
VGA	linear gramicidin A
VGB	linear gramicidin B
v/v	volume per volume

Standard 3-letter and 1 letter abbreviations were used for the natural amino acids, with uppercase 1-letter abbreviations for L-amino acid residues and lower case 1-letter abbreviations for D-amino acid residues in peptide sequences. For the abbreviations used for the modified peptides refer to the monomer reference tables in thesis addendum.

## Preface

The increase in antimicrobial resistance has sparked a revival in the search for new antimicrobial agents. The tyrocidines, originally discovered by Rene Dubos in 1939, are a group of non-ribosomally synthesized anti-microbial peptides showing activity against a wide variety of Gram-positive bacteria, as well as activity against a broad range of fungal species. The tyrocidines are basic, cyclic, decapeptides with a strong amphipathic structure which are synthesized by the soil bacteria *Brevibacillus parabrevis*, together with the neutral, linear gramicidins (Grcs). Collectively, Trcs and Grcs extracted from cultures of *Br. parabrevis* are known as tyrothricin (Tcn). The Trcs are receiving renewed interest to help combat antimicrobial resistance due to their rapid, membranolytic activity. Their ability to target and disrupt bacterial membranes is important due to the fact that these membranes contain highly conserved structures, which makes the development of antimicrobial resistance unlikely. The Trcs are non-ribosomally synthesized in an enzymatic process using a thiotemplate mechanism. Certain domains within the non-ribosomal synthetase enzymes that incorporate amino acids into the growing Trc chain lack specificity for a single amino acid, and as a result domains responsible for incorporations of amino acids at positions 3,4 and show affinity for both phenylalanine and tryptophan, while position 7 also shows affinity for tyrosine. This leads to the production of a wide variety of Trcs with unique structure activity relationships with the sequence cyclo(Phe<sup>1</sup>-Pro<sup>2</sup>-X<sup>3</sup>-x<sup>4</sup>-Asn<sup>5</sup>-Gln<sup>6</sup>-X<sup>7</sup>-Val<sup>8</sup>-Orn<sup>9</sup>-Leu<sup>10</sup>), where upper-case X represents variable L amino acids and the lower-case x represents a variable D amino acid. The lack of specificity of the variable domains, as well as the non-ribosomal mechanism of synthesis, provide a basis for testing for the incorporation of non-natural aromatic amino acid derivatives into the Trcs, on which minimal work has been done. In addition, different strains of the producer organism as well as nutrient conditions have also been shown to play a role on the levels of Trc production.

This study's major goal was to determine the possibility of creating novel Trcs with unique structure-activity relationships by supplementing the growth media of the producer organisms with selected aromatic amino acid derivatives. In order to reach this goal a number of aims were set in this study as detailed below.

## **Research Aims**

### **Aim 1. Cultivation of *Brevibacillus parabrevis* strains and comparison of the production of tyrocidine and analogues by the producer organism**

- 1.1. Selection and base-line peptide production of tyrocidine producing strains from four available strains.
- 1.2. Assessment of growth rates of three of the strains under altering nutrient conditions relating to urea, sodium sulphate, ammonium sulphate, glucose and glycerol content.
- 1.3. Small-scale deep-well cultures using one of the strains to assess the effect of selected nutrient conditions determined to have largest positive effect on growth rate.
- 1.4. Assessment of the effect of selected natural and non-natural amino acids on growth rate on three strains of the producer organism.
- 1.5. Small-scale deep-well cultures using one of the strains to assess the effect of selected nutrient amino acids, as well as selected nutrient conditions, on the production profile of the Trecs.

The results of these objectives are reported in Chapter 2 (1.1, 1.2, 1.3) and Chapter 3 (1.4, 1.5).

### **Aim 2: Characterisation of peptide production profile**

- 2.1 High throughput organic extraction and isolation of the tyrocidines and their analogues from the small and medium scale cultures produced under Aim 1.
- 2.2 Characterisation of the crude extract peptide production profiles via electrospray mass spectrometry (ESMS) and ultraperformance liquid chromatography linked to mass spectrometry (UPLC-MS).

The results of these studies are reported in Chapters 2 and Chapter 3.

### **Aim 3. Medium scale production using selected natural and non-natural amino acids**

- 3.1 Medium scale production (200 mL) and extraction of cultures supplemented with selected natural and non-natural amino acids.
- 3.2 Purification of novel peptides using semi-preparative reverse phase high performance liquid chromatography (RP-HPLC) using established protocols.
- 3.3 Characterisation of the purified/enriched cyclic decapeptide preparations extracts via ESMS and UPLC-MS.

3.4 Assessment of the antibacterial activity of the novel cyclic decapeptides and their natural analogues against *Micrococcus luteus* in liquid culture and in agar-based antimicrobial assays.

The results of these studies are reported in the final experimental chapter, Chapter 4.

## **Thesis Content**

The thesis comprises of literature background in Chapter 1 on antimicrobial peptides and the experimental results and discussion is given in Chapters 2-4. Chapter 5 comprises of the conclusion and future studies. As this study refers to many different peptide structures peptide reference table were added to the end of the thesis for quick referencing. Independent chapter units were used in this thesis to ease future publication of result and some repetition was unavoidable, however I attempted to minimise repetitions as far as possible.



## Outputs of MSc study

- Berge S.N.\* (March 2017) The production and characterisation of analogues of the antimicrobial tyrocidine peptides with modified aromatic amino acid residues, Biochemistry Forum, University of Stellenbosch, Oral presentation
- Berge S.N.\* (February 2018) Production and characterisation of analogues of the antimicrobial tyrocidine peptides with modified aromatic amino acid residues, Biochemistry Forum, University of Stellenbosch, Oral defence of the MSc thesis
- Berge S.N.\*, Rautenbach M. (July 2016) The in-culture production of antimicrobial tyrocidine analogues with modified aromatic amino acid residues, SASBMB 2016 Conference, East London, South Africa, Poster was voted runner-up in the Biotechnology Section.
- Berge S.N., Laubscher W.E, Vosloo J. A. and Rautenbach M.\* Production and characterisation of tyrocidine analogues containing 5-methyl tryptophan residues, IMAP 2016, 6<sup>th</sup> International Meeting on Antimicrobial Peptides, Leipzig, Germany
- Berge S.N., Rautenbach M. Comparison of tyrocidine production profiles of different *Brevibacillus parabrevis* strains in a variety of supplemented culture media. Article in preparation from Chapter 2 to be submitted to *AMB Express* in March 2018
- Berge S.N., Rautenbach M. Mass spectrometric characterisation of fluorinated tyrocidines produced by *Brevibacillus parabrevis*. Article planned from Chapters 3 and 4 to be submitted to *Rapid Communications in Mass Spectrometry* in May 2018

\*Presenter

# Chapter 1

## Overview of antimicrobial peptides focusing on the tyrocidines and analogues

### 1.1 Introduction

Antimicrobial resistance (AMR) is fast becoming a major burden on human health due primarily to their misuse within both the healthcare and agricultural sectors. A report published by the World Health Organisation in 2014 states that the economic burden in the US alone, as a result of increasing levels of AMR, amounts to between \$21 and \$31 billion dollars per year (1). Five or more of the six regions monitored by the WHO have reported over 50% resistance to commonly used anti-microbials by *Escherichia coli*, *Klebsiella pneumoniae*, *Staphylococcus aureus*. Resistance levels above 25 % have also been reported in some regions for *Streptococcus pneumoniae*, non-typhoidal *Salmonella* species, certain *Shigella* species and *Neisseria gonorrhoea* (1). As of 2014 the pipeline for the implementation of new antimicrobials is virtually empty, highlighting the need for further research and development within this field (1).

All kingdoms of life produce compounds which provide the host with protection against invading microbes, of these compounds, a large group, known as antimicrobial peptides (AMPs), serve as a rapid-responding, non-specific defence system to the host organism, which is furthermore complemented by a slower acting, more specific cell-mediated response in higher eukaryotic organisms (2). The rapid increase in levels of AMR have sparked renewed interest in AMPs, with hundreds being discovered and thousands more being synthesized and designed *de novo* (3). AMPs are a promising avenue for solving the problem of AMR as they tend to target the highly conserved structures of microbial cell membranes, making the development of resistance unlikely (4–10). In addition, the large variety of AMPs makes it unlikely for target organisms to develop proteases able to recognize the unique epitopes of different AMPs (11).

### 1.2 Diversity and categorisation of AMPs

The diversity of AMPs can make them difficult to categorise, however there are a few characteristics that are shared by the majority of AMPs, namely, they mostly fall within a size of between 9 and 100 amino acids, have mostly L-amino acids, are amphipathic, generally have a net positive (cationic) charge and act on the membranes of their target organisms (3, 11). Despite their wide range of structures and activities against various organisms (including fungi, bacteria and

viruses (12)), AMPs can be grouped based on the organisms against which they have activity. The first major group being peptides that are non-toxic to normal mammalian cells but are toxic to selective microorganisms, the second group being non-toxic to mammalian cells but toxic to a broad range of both Gram-positive and Gram-negative bacteria, the third being non-toxic towards mammalian cells while being toxic towards bacteria and fungi or fungi only, and lastly peptides with a broad toxicity that are only slightly selective toward microbial targets (13–17).

Epanand and Vogel (18) grouped peptides by structural motifs which were common to certain groups of AMPs, into six categories. These groups are: peptides that form hydrophobic and amphipathic  $\alpha$ -helices, cyclic peptides and small proteins which form  $\beta$ -sheet structures, peptides possessing unique amino acid compositions, cyclic peptides with thio-ester groups present in the ring structure, and lipopeptides terminating in an amino-alcohol and macro-cyclic knotted peptides.

## **1.3 Mechanisms of action**

### **1.3.1 Selectivity of AMPs for prokaryotic membranes**

A commonality to many AMPs is a mechanism of action which primarily involves interaction with the lipid bilayer of a target membrane, which is largely due to their cationic nature and subsequent interaction with anionic phospholipids present on the target membrane (18). This is also the main factor behind the preferential interaction of AMPs with bacterial membranes over the zwitterionic phospholipids such as phosphatidylcholine and sphingomyelin present in mammalian cell membranes (18, 19).

Unlike bacterial membranes, plants and animals have their anionic components segregated into inner leaflet of their cell membranes (11). In addition, the presence of cholesterol in the membrane of multicellular animals is believed to reduce the activity of the AMPs on these membranes, either due to the stabilizing effect of cholesterol on the membrane or due to interaction of the AMP with cholesterol (20).

### **1.3.2 Membrane mediated mechanisms of action**

In the context of bacteria, some AMPs may act on intracellular targets, while many act via disruption of cell membranes, particularly at higher concentrations. Either way, the AMPs must initially interact with and traverse the cell wall (consisting primarily of a peptidoglycan polymer) in Gram-positive bacteria and the outer membrane (and cell wall) in the case of Gram-negative bacteria.

Many AMPs appear to readily cross the porous, 40 to 80 nm thick, cell wall of Gram-positive bacteria (21). In the case of Gram-negative bacteria, AMPs can rapidly traverse the outer membrane via a charge-exchange mechanism whereby the cationic AMPs compete with  $\text{Ca}^{2+}$  and  $\text{Mg}^{2+}$  bound to lipopolysaccharides. Interactions with these ions may enhance the binding of the peptides to outer membrane proteins, a process called the self-promoted uptake hypothesis (22). Once these peptides have crossed the outer membrane of Gram-negative bacteria they are free to interact with the cell wall and cell membrane. Studies on the interactions of AMPs with bacterial cell-walls (outer-most thick peptidoglycan layer on Gram-positive bacteria, and thin peptidoglycan layer between outer membrane and cell membrane of Gram-negative bacteria) show that there is not an equal distribution of bound peptides on the cell wall. Recent single-cell experiments using fluorescent probes have shown that AMPs are restricted to cell-wall foci associated with cell division, cell wall remodelling, and secretion (23, 24), with interference of these processes leading to cell lysis. Initial interaction of AMPs with cell walls is dependent primarily on negatively charged components, including lipoteichoic acids and teichoic acids.

Once the AMPs have crossed the bacterial outer-membrane and/or cell wall, they interact with bacterial cell membranes (the last external barrier before the cytosol). This is likely to occur in the same manner as for outer-membranes and cell walls (21, 25). The amphipathic conformation of AMPs (resulting from their distribution of charged and hydrophobic amino acid residues) leads to interactions with negatively charged cell membrane components and/or insertion into the lipid-bilayer of these membranes. There are four models typically associated with this amphipathic interaction of linear  $\alpha$ -helical cationic AMPs with bacterial membranes. These are the aggregate (26), toroidal-pore, barrel-stave and carpet models (27, 28). The conformation of an interacting AMP can also be altered by the specific membrane environment (29).

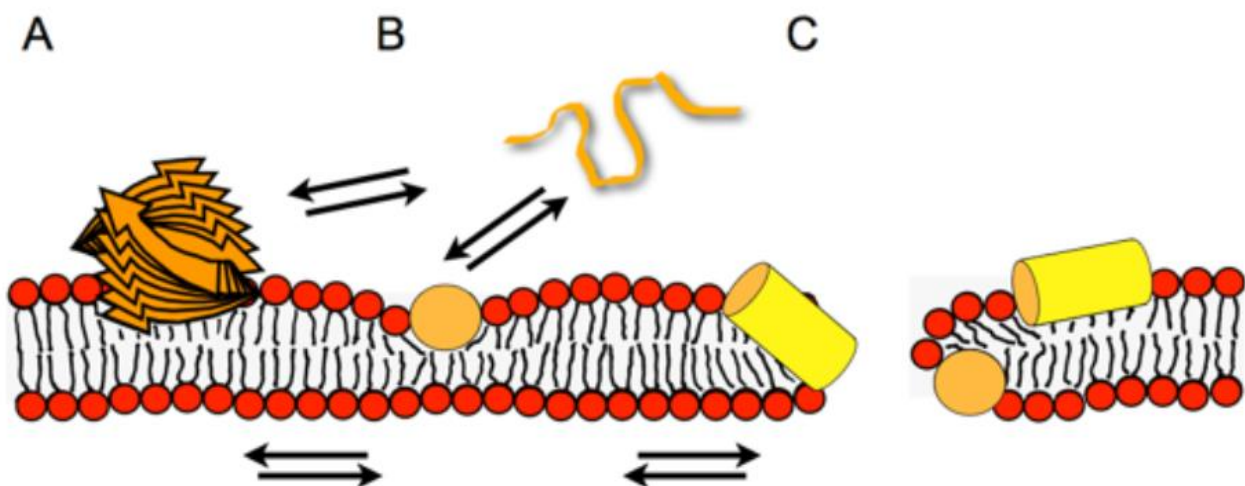


*Figure 1.1* SMART model depicting interaction of AMPs (yellow and orange) with bacterial membranes. **A**, a  $\beta$ -sheet peptide aggregate interacting with the lipid-monolayer at its interface, **B**, random coil-string peptide forming a helical structure upon membrane interaction, **C**, helical structure peptides interacting with cell membrane. At low densities of peptide on the membrane surface the membrane can adapt to maintain membrane integrity (**B**), while at higher local peptide concentrations peptide-induced strain curvature on the lipid bilayer starts to cause transient openings (**C**). The equilibrium between the different states (shown by reversible arrows) is dependent on a wide variety of AMP and membrane-related factors (figure adapted from 30).

A single type of AMP is likely to act through a combination of aspects of the toroidal-, barrel-stave, carpet-models. This is primarily due to differences in membrane structure, membrane topology, AMP aggregation levels, AMP-lipid interactions, AMP structure, AMP:lipid ratio and properties of the lipid membrane (30). This led to the proposal of a more generalised model by Bechinger (31), termed the SMART model (Soft Membranes Adapt and Respond, also Transiently, in the presence of AMPs). Bechinger (31) also proposed an additional aspect to this model due to the effect of AMP-induced curvature strain of bacterial membranes. Curvature strain starts at relatively low peptide concentrations, where AMPs lie at the interface of the cell membrane (with more hydrophobic peptide residues associating with hydrophobic membrane lipids, and more hydrophilic residues associating with the outer cell membrane surface). Curvature strain occurs as a result of the AMPs having an asymmetric distribution, as they do not completely fill the top lipid monolayer of the lipid bilayer (Figure 1.1, B). The curvature strain is initially high, but is relieved as peptides distribute evenly between the outer and inner surface of the membrane thanks to membrane transport and membrane openings (30). The ‘soft’ membranes can adjust at lower peptide concentrations, but as more peptide associates with the cell membrane, transient opening and membrane deformation begins to occur (Figure 1.1, C) (31). At even higher peptide concentrations, both local and global disruptions of the cell membrane begin to occur.

### 1.3.3 Receptor or non-membrane mediated mechanisms

While interaction with target membranes is a prerequisite for all antimicrobial activity, some peptides, either as a function of their structure and/or concentration, translocate across target membranes without causing permeabilisation and act on intracellular targets (12). Cytosolic mechanisms of action include inhibition of nucleic acid synthesis, protein synthesis, enzyme activity and cell wall synthesis (32). Examples of this include the frog peptide buforin II which has the ability to translocate the bacterial membrane without the bacterial membrane becoming leaky or lysing. Once in the cytoplasm this AMP inhibits both DNA and RNA synthesis in *E. coli* (33). The proline-rich insect AMP pyrrohocidin binds to the heat shock protein DnaL, inhibiting its ATPase activity which ultimately leads to the accumulation of misfolded proteins and cell death (34, 35). A peptide which inhibits cell wall synthesis is the lantibiotic mersacidin, which interrupts the process of transglycosylation of lipid II, a step essential in the formation of peptidoglycan (36).

### 1.4 Biosynthesis of AMPs

The majority of AMPs synthesized by multicellular organisms are produced by traditional gene transcription preceded by translation via ribosomes, and will often undergo post-translational modification (18). An example of post-translational proteolysis is the formation of individual magainin peptides from a preprotein made of six copies of the peptide (37). Other peptides which undergo proteolytic cleavage include lactoferricin B produced in milk proteins, peptides resulting from denatured lysozyme, the cecropin like AMPs produced by *Helicobacter pylori*, bifuron I and parasin I (38–41). Other post-translational modification include glycosylation (42–45) and bromination (46).

When it comes to microorganisms, many of the AMPs synthesized contain non-natural or uncommon amino acids. This is most often due to the fact that these AMPs are synthesized non-ribosomally in an enzymatic process, or through proteolytic cleavage following ribosomal synthesis (18). Non-ribosomally produced AMPs are synthesized by large, multifunctional peptide synthetases using a thiotemplate mechanism with multiple carrier domains, examples of peptides produced in this way include polymyxin B, colistin (polymyxin E or colimycin) and the tyrocidines, all of which have been used clinically (47–49).

### 1.5 The tyrocidines

The tyrocidines and their analogues are basic, cyclic decapeptides which form part of a group of antimicrobial AMPs extracted, together with neutral gramicidins, from a soil bacterium known as

*Brevibacillus parabrevis* (*Br. Parabrevis*), and are produced in the late logarithmic phase of growth (50–53). The collective term for this antimicrobial extract is tyrothricin (Tcn), and was first isolated by René Dubos in 1939 who found an extract of a cultured soil bacillus to be active against Gram-positive cocci (54). It was the first antibiotic to be used in a clinical setting but had limited use due to its haemolytic effect on red blood cells (55), and as such its main use was as a topical agent for treatment for surface wounds (56–59), as an active ingredient in throat lozenges (60) and for the treatment of eye ulcers (61).

### 1.5.1 Structure

The Trcs are cationic, consisting of a balance of hydrophobic and hydrophilic amino acid residues. There are many structural Trc analogues synthesized together by the producer organism which differ by one-another at specific amino acid positions within the peptide, with the sequence *cyclo*[f<sup>1</sup>P<sup>2</sup>X<sup>3</sup>x<sup>4</sup>N<sup>5</sup>Q<sup>6</sup>Y<sup>7</sup>V<sup>8</sup>X<sup>9</sup>L<sup>10</sup>] (residues depicted with a lower-case x represent variable D-amino while an upper-case X represents an L-amino acid). These variable amino acid residues include those found at positions three and four (Phe and/or Trp), seven (Tyr, Trp or Phe) and nine (ornithine (Orn or O) or Lys). (50, 62, 63). Figure 1.2 depicts a tyrocidine A with the relatively hydrophobic amino acid Phe at positions three and four. Bearing this variability mind, a study by Tang *et al* (1992) identified the primary structures of 28 natural tyrocidine analogues, shown in Table 1.1 (62). While up to 72 different analogues are possible in theory, practically, only a smaller subset are produced, or at least at a high enough concentration to be detected (64). Tyrocidine A, A<sub>1</sub>, B, B<sub>1</sub>, C and C<sub>1</sub> are produced in the highest abundance by the producer organism and can be thought of as the major tyrocidines, while those present in smaller amounts are considered as analogues of these major Trcs (62, 65).

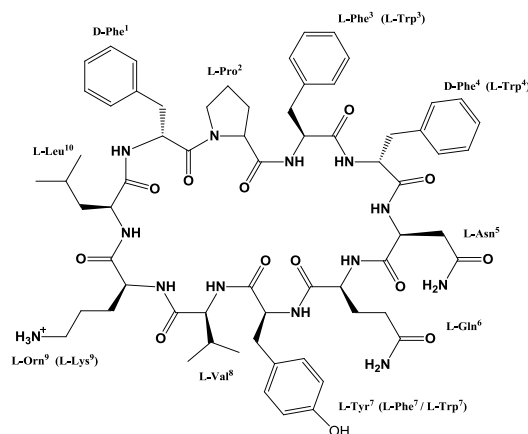


*Figure 1.2* Tyrocidine A peptide as defined by having two Phe residues at positions 3 and 4 (making it an A analogue) and a Tyr residue at position 7 (making it a Tyrocidine). Numbers indicate order of incorporation of amino acids during biosynthesis. Residues in brackets are other possible amino acids which can be incorporated at these variable positions to produce the various tyrocidines and analogues as observed by Tang *et al* (62) and listed in Table 1.1.



*Table 1.1* Tyrocidines and analogues identified and characterised from tyrothricin by Tang *et al.* (62). Standard one letter abbreviations for the L-amino acid residues are used, except O for ornithine. The lower-case letters depict D-amino acid residues in the sequence.

Number	Identity	Abbreviation	Sequence	Monoisotopic $M_r$	Abundance
1	Tyrocidine D *	TrcD	VOLfPYwNQY	1324.7	2.1
2	Tyrocidine D <sub>1</sub> *	TrcD <sub>1</sub>	VKLfPYwNQY	1338.7	1.7
3	-	-	VOLyPWwNQY	1363.7	< 1
4	Tyrocidine E' *	TrcE'	VOLfPFyNQY	1285.7	< 1
5	Tyrocidine E <sub>1</sub> ' *	TrcE <sub>1</sub> '	VKLfPFyNQY	1299.7	< 1
6	Tyrocidine C	TrcC	VOLfPWwNQY	1347.7	100
7	Tyrocidine C <sub>1</sub>	TrcC <sub>1</sub>	VKLfPWwNQY	1361.7	30
8	Tryptocidine C	TpcC	VOLfPWwNQW	1370.7	23
9	Tryptocidine C <sub>1</sub> *	TpcC <sub>1</sub>	VKLfPWwNQW	1384.7	2.3
10	Tyrocidine B' *	TrcB'	VOLfPFwNQY	1308.7	14
11	Tyrocidine B <sub>1</sub> ' *	TrcB <sub>1</sub> '	VKLfPFwNQY	1322.7	5.8
12	Tyrocidine B	TrcB	VOLfPWfNQY	1308.7	109
13	Tyrocidine B <sub>1</sub>	TrcB <sub>1</sub>	VKLfPWfNQY	1322.7	44
14	Tryptocidine B	TpcB	VOLfPWfNQW	1331.7	26
15	Tryptocidine B <sub>1</sub>	TpcB <sub>1</sub>	VKLfPWfNQW	1345.7	13
16	Tyrocidine A	TrcA	VOLfPFfNQY	1269.7	88
17	Tyrocidine A <sub>1</sub>	TrcA <sub>1</sub>	VKLfPFfNQY	1283.7	39
18	Tryptocidine A	TpcA	VOLfPFfNQW	1292.7	15
19	Phencyidine A **	PhcA	VOLfPFfNQF	1253.7	3.1
20	Tyrocidine E *	TrcE	VOLfPYfNQY	1285.7	2.2
21	Tyrocidine E <sub>1</sub> *	TrcE <sub>1</sub>	VKLfPYfNQY	1299.7	1.1
22	-	-	VOLfPF(?)NQY	1336.7	4.5
23	-	-	VKLfPF(?)NQY	1350.7	9.4
24	Phencyidine B *	PhcB	VOLfPWfNQF	1292.7	3.7
25	-	-	(L/I)OLfPWfNQY	1322.7	1.9
26	-	-	(L/I)KLfPWfNQY	1336.7	2.6
27	-	-	VOLfP(L/I)fNQY	1325.7	1.2
28	-	-	VKLfP(L/I)fNQY	1249.7	< 1

\* Peptides renamed in this study

\*\* Peptides renamed by our group



The secondary structure of TrcA (Figure 1.3) has been found to be composed of a two-stranded antiparallel  $\beta$ -sheet structure which is connected by a type II  $\beta$ -turn on the one end and a type I  $\beta$ -turn on the other end of the molecule (66–71). The residues Leu<sup>10</sup>, D-Phe<sup>1</sup>, Pro<sup>2</sup> and Phe<sup>3</sup> form a type II  $\beta$ -turn, and the residues Asn<sup>5</sup>, Gln<sup>6</sup>, Tyr<sup>7</sup> and Val<sup>8</sup> at the other end form a slightly distorted type I  $\beta$ -turn.

The two strands are connected via three hydrogen bonds which lie between the backbone amide and carbonyl groups, with a fourth hydrogen bond between the backbone amide of Val<sup>8</sup> and the side chain of Asn<sup>5</sup>. The association of the strands in TrcA are stabilised by hydrophobic interactions between the side chains of D-Phe<sup>4</sup>, Val<sup>8</sup> and Leu<sup>10</sup> (70). While these structural characteristics were determined for TrcA, differences in amino acid composition, particularly for the aromatic residues, are still believed to result in the same backbone structure among different tyrocidine analogues (72)

From the studies of Loll *et al.* (70) and Munyuki *et al.* (71) it was observed that the homodimer form TrcA is formed by a strong association between the two monomers. The  $\beta$ -sheets of each monomer align edge-on, leading to the formation of continuous four-stranded antiparallel sheet, which possess four hydrogen bonds between the backbones of each monomer. The dimer is also stabilised by hydrophobic interactions between the side chains of Val<sup>8</sup> of one monomer with the Leu<sup>10</sup> of another monomer. There is also a stabilising effect between the aromatic rings of D-Phe<sup>1</sup> and Tyr<sup>7</sup> on the opposing monomers (70). The dimer form of the tyrocidine has been proposed to be the active conformation of these cyclic decapeptides (70).

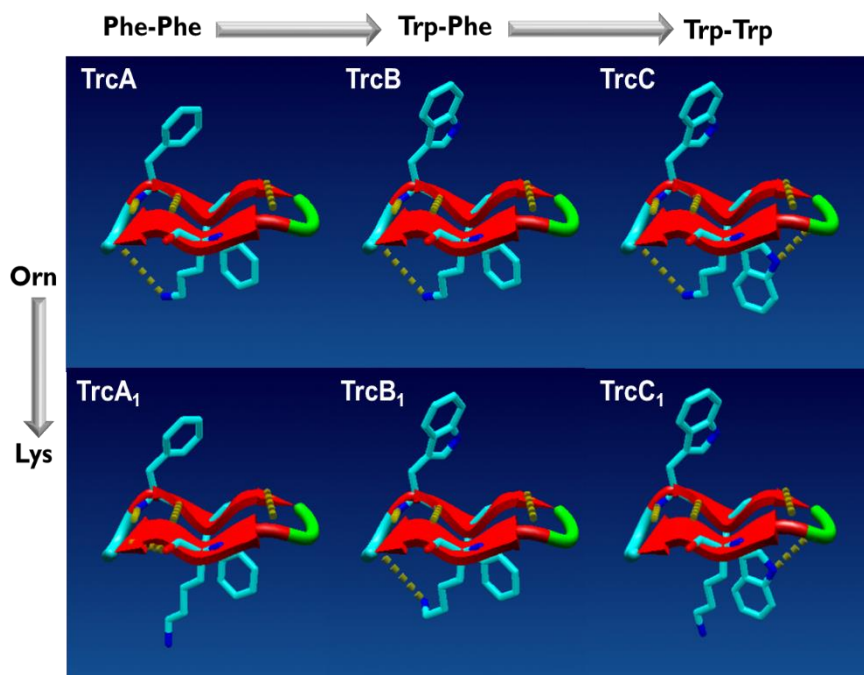


Figure 1.3 Secondary structure of the six major tyrocidines showing the side chains of the variable aromatic dipeptide moiety, two turns (type II and I  $\beta$  turns) leading to the formation of an anti-parallel  $\beta$ -sheet structure. The differences in sequence of major peptides are shown above and on the left side of the figure. Also refer to Table 1.1 above. Figure courtesy of M. Rautenbach, structures created from the TrcC and TrcA models of Munyuki *et al.* (71)

### 1.5.2 Activity

The Tcn extract from *Br. parabrevis* was first tested against a variety of Gram-positive and Gram-negative bacteria by its discoverer, Dubos, who demonstrated its bactericidal effect on various strains of *Diplococcus pneumoniae*, *Streptococcus hemolyticus*, *Streptococcus viridans* and *Streptococcus viridans* but found no bactericidal effect on the Gram-negative bacteria tested (73). In the years since this initial research, research has shown this same extract to have a wide variety of activity, including, but not limited to fungi, viruses and malarial parasites.

*Antibacterial:* Kretschmar *et al.* (75) tested several reference strains, and clinical isolates, of streptococci, staphylococci and enterococci against tyrothricin and found their minimum inhibitory concentration ranges (MICs) to be between 0.048-1.526  $\mu\text{g/mL}$ , 1.562-3.125  $\mu\text{g/mL}$  and 0.195-1.562  $\mu\text{g/mL}$  respectively. A study by Spathelf and Rautenbach (76) found the Tcn extract to be active against the Gram-positive bacteria *Micrococcus luteus*, as well as two different strains of *Listeria monocytogenes*, with  $\text{IC}_{50}$  concentration (concentration of peptide that leads to 50%

inhibition of maximum growth of the target organism) of 3.5 µg/mL, 12.0 µg/mL and 9.7 µg/mL respectively.

*Antifungal:* Tcn was found to be active against a variety of *Candida* species (with both reference strains and clinical isolates), being *C. albicans*, *C. tropicalis* and *C. glabrata*, with MICs of between 4 µg/ml and 16 µg/ml for the different strains and isolates of *C. albicans* tested, between 5.3 µg/ml and 7.8 µg/ml for the strains isolates of *C. tropicalis* tested and between 6.4 and 8.6 µg/ml for the different strains and isolates of *C. glabrata* tested (77, 78). Several clinical isolates of *C. parapsilosis* were also found to have their growth inhibited by tyrothricin (78). A study by Troskie *et al.* (79) showed the activity of Tcn extract (which had been treated to remove gramicidins) against a wide array of phytopathogenic fungi, with IC<sub>50</sub> values ranging from 2.0 µg/mL for a strain of *Cylindrocarpon liriodendra*, to 8.9 µg/mL for a strain of *Penicillium glabrum*.

*Antiviral:* An *in vitro* experiment against the parainfluenza virus (type Sendai) showed that tyrothricin had anti-infectious activity, with a similar anti-infective activity being shown for mumps, herpes and influenza viruses (80). Similar experiments using the herpes-simplex-virus (HSV) type 1 showed that incubating the virus with tyrothricin in suspension significantly decreased the lethality of the virus in a mouse model, but this effect was dependent on initial, direct contact with the virus and the peptide before contact with the mice (81).

*Antiplasmodial:* A study by Taliaferro *et al.* (1944) found daily tyrothricin dosages of 0.2 mg to effectively rid chickens of *Plasmodium gallinaceum* when administered intravenously in a 9.5% ethanol solution. Tyrothricin acted in a parasitocidal manner, killing extracellular merozoites produced at the segmentation phase of growth most effectively, and to a lesser extent acting via inhibition of growth and reproduction of the parasite (82). A study by Rautenbach *et al.* (2007) assessed the *in vitro* activity of six purified Trc analogues on the malaria causing parasite *Plasmodium falciparum* (strain 3D7) and found that all the analogues tested had antiplasmodial activity in the nanomolar range, with the Trc analogue TrcA having the best relative activity with an IC<sub>50</sub> value of 580 picomolar (83). A study by Leussa (84) also assessed the effects of isolated Trcs on the growth of several strains of *P. falciparum*, showing a wide range of IC<sub>50</sub> depending on both Trc structure and strain of target organism. These values ranged from 15 nM for PhcA against the 3D7 strain of *P. falciparum*, to 1920 nM for TrcA against the Dd2 strain.

*Activity in mammalian cell infections:* The Tcn complex, and both the Trcs and Grcs individually, have haemolytic activity (85–89), however, the haemolytic activity of the Trcs is less, particularly over longer periods of time (55, 87). The tyrothricin peptides have been shown to be safe when applied topically to skin ulcers and cutaneous infections (61, 90–93), but will lyse blood cells if

exposure to the blood stream occurs via deeper, sub-cutaneous wounds (88, 94). Oral administration of tyrothricin has been reported by some to treat microbial infections in mice (52, 95) but other studies showed tyrothricin to only slow infections of pathogens which typically invade the upper gastro intestinal tract (95). It appears that the tyrothricin peptides may be inactivated within the mammalian gastrointestinal tract as oral treatment of mice with these peptides showed no change in their intestinal microbiota (94, 96).

### 1.5.3 Structure-activity

Significant research has been done the importance of the residues D-Phe<sup>4</sup> and Gln<sup>6</sup>, highlighting their role on the therapeutic ratio (the ratio between minimum haemolytic concentration and minimum concentration required to inhibit bacterial growth) (97–99).

The hydrophobic amino acid D-Phe<sup>4</sup> is important due to its role in inserting into hydrophobic core of lipid bi-layers, and substitution of this amino acid with other hydrophobic residues does not have a significant effect on Trc activity (97, 98), but substitution with basic D-amino acids leads to a reduction in activity (63, 97, 100), believed to be primarily due to a loss in amphipathicity. Replacing D-Phe<sup>4</sup> with basic L-amino acids does not lead to a loss in activity, unlike the basic D-amino acid, this residue has a reversed orientation of its side chain, allowing it to orientate with the basic face of the Trc dimer, potentially reinforcing the amphipathicity of the molecule (97).

A wide variety of amino acid substitutions in place of Gln<sup>6</sup>, ranging in size and hydrophobicity, are well tolerated, with 13 out of 14 substitutions tested leading to improved antibacterial activity (98). It appears that irrespective of the amino acid substituted at this position, the residue will still lie at the interface between the hydrophobic interior of the lipid bilayer and the lipid head group following interaction with a bacterial membrane, allowing for more hydrophobic residues to associate with the nearby hydrophobic face of the molecule, and the phospholipid head groups for more hydrophilic residues (70).

A study by Rautenbach *et al.* (2007) found that the six major tyrocidine analogues (A, A<sub>1</sub>, B, B<sub>1</sub>, C and C<sub>1</sub>) all showed activity in the nanomolar range against *P. falciparum*. An increase in the apparent hydrophobicity and a decrease in the side chain surface area of these analogues correlated well with an increase in their selective activity against this malaria parasite. In terms of amino acid composition, the tyrocidines with phenylalanine residues at positions 3 and 4 and ornithine at position 9 (TrcA) was therefore the most active against the parasite while TrcC<sub>1</sub> was the least active, with tryptophan residues at positions 3 and 4 and lysine at position 9.

A study by Spathelf and Rautenbach (2009) looked at the same six major analogues on the Gram-positive bacterium *L. monocytogenes*, a potentially deadly food-borne pathogen. Unlike malaria however, the more polar tyrocidines showed improved activity. TrcC showed better activity than TrcB while both were superior to TrcA. The presence of the more hydrophilic residues at positions 3 and 4 in the form of tryptophan therefore appear to improve the activity of these peptides against this organism (76).

A study by Leussa and Rautenbach (101) found that activity against selected strains of *L. monocytogenes* was dependant on Tyr or Phe in position 7 of the sequence, ornithine (Orn, O) as cationic residue at position 9, and Trp in position 3 or 4. The roles of Trp and Orn in the tyrocidines were confirmed with most active peptide being a TrcB containing Orn and a Trp-D-Phe in the aromatic dipeptide moiety. However, a modified TrcA, which typically had reduced activity against this target organism, was found to have an  $IC_{max}$  (concentration causing 100% growth inhibition) of 18  $\mu$ M, rivalling that of TrcB (16  $\mu$ M) which was the most active peptide. The increased activity of this TrcA analogue resulted from the insertion of a trimethylated Orn residue at position 9 in place of the natural Orn residue. This lead to a relatively more hydrophobic peptide, which had reduced hydrogen bonding with the aromatic amino acids at position 3 and 4, and was likely more active due to deeper insertion into the target membrane. This result supports the importance and the nature of the interactions between aromatic amino acids present at positions 3 and 4, and interaction with the cationic ornithine residue at position 9. Any residue change resulting in tighter membrane interaction is likely to trap TrcA in the membrane and impede its mechanism of action.

#### **1.5.4 Mechanism of action**

Like many AMPs, the activity of the Trcs is believed primarily be mediated by their interaction with a target membrane largely though hydrophobic interaction (102), leading to membrane permeabilisation (103) and ultimately cell lysis (73). Trc dimers are likely the most active membrane configuration, due to their increased amphipathicity relative to monomers (70, 71). A study by Loll *et al.* (70) used X-ray crystallography to determine the crystal structure of TrcA. It was found that TrcA forms strongly associated, highly amphipathic homodimers consisting of four  $\beta$ -strands that associate into a single, highly curved, anti-parallel  $\beta$ -sheet. The dimerisation of TrcA enhances the amphipathic nature of the TrcA peptides by partitioning hydrophobic and hydrophilic residues. In the dimer structure all of the amino acid side chains on the convex face of the dimer are hydrophobic, with the exception of the neutral, polar Asn<sup>5</sup> residue, which takes part in the backbone hydrogen bonding of the dimer. Only a relatively hydrophilic, charged, Orn<sup>9</sup> residue is found protruding off the convex face of the dimer. The backbone carbonyl oxygens of D-Phe<sup>1</sup>, Asn<sup>5</sup> and

Gln<sup>6</sup> all point outward on the convex face of the dimer. The Gln<sup>6</sup> residue lies in an equatorial region between the concave and convex faces, but is also well positioned to turn towards the concave face. This configuration of amino acids ultimately produces a highly polar concave face, and a strongly non-polar convex face (Figure 1.4, A). The hydrophobic face of this amphipathic dimer is hypothesised to insert deeply into the lipid bilayer in target membranes, with the hydrophilic residues protruding outwards (Figure 1.4, B).

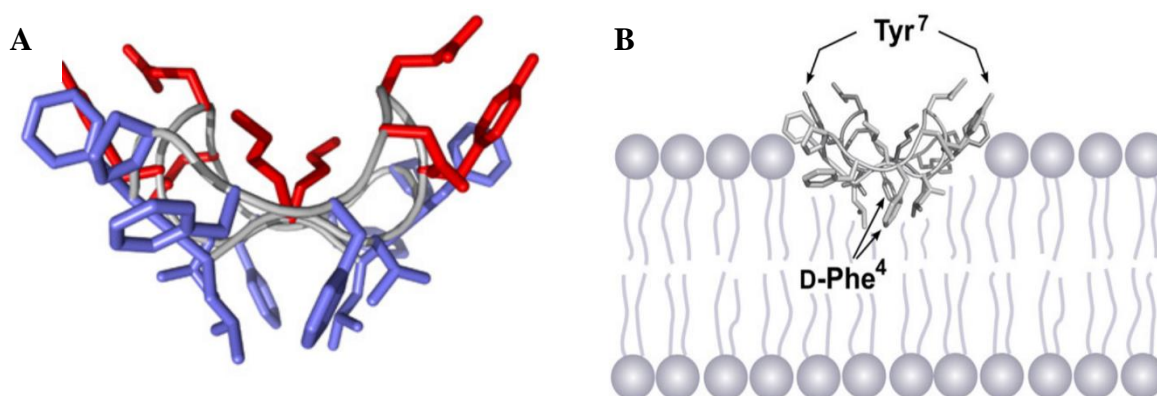


*Figure 1.4* The dimer structure of TrcA with **A** the highly amphipathic structure (hydrophilic side chains shown in red, hydrophobic side chains shown in blue) showing the polar concave face and the non-polar convex face of the dimer and **B** showing the proposed mechanism of interaction of this dimer with a model bacterial membrane, with the hydrophobic, convex face inserting into the lipid-bilayer (with Phe<sup>4</sup> at its center and Gln<sup>6</sup> lying at the interface of the lipid layer), and the polar face lying at the level of the lipid head groups, extending outward (images from Loll *et al.* (70)).

Membrane-bound tyrocidines, especially at higher concentrations, appear to oligomerise to form pore-like structures in a manner similar to gramicidin S (50, 104–107). While hydrophobic interaction is essential for association with membrane lipids, hydrogen bonding and ionic interactions also play a role (101). In addition to membrane-mediated mechanisms of action, other non-lytic mechanisms have been proposed (76, 79, 83, 84). In the case of the Trcs antiplasmodial activity, it is suggested that there are other intracellular targets, such as the food vacuole (84) or regulators of the cell cycle (83). In Gram-positive bacteria the Trcs have been shown to disrupt glucose metabolism (85, 108). The Trcs may also inhibit replication and/or transcription (102) which is hypothesized partly due to the observation that it binds to DNA in the producer organism (109–111) where it inhibits transcription *in vitro* (112).

### 1.5.5 Tyrocidine biosynthesis

Unlike traditional protein and peptide synthesis, the tyrocidines produced by *Br. Parabrevis* are created without the use of ribosomes but rather enzymatically in a process known as non-ribosomal



peptide synthesis. These large modular enzymes have multiple domains and are known as non-ribosomal peptide synthetases, which incorporate amino acids directly into a growing peptide (113). In the case of tyrocidines, there are three major NRPS involved, TycA, TycB and TycC, which activate and incorporate one, three and six amino acids respectively into the final decapeptide product (114). Experiments involving the purification of TycA, TycB and TycC found them to consist of 100, 230 and 440 kDa proteins respectively, and as a result the purified enzymes were commonly referred to as the light (TycA), intermediate (TycB) and heavy fractions (TycC) respectively (114).

Following the incorporation of ten amino acids into a linear tyrocidine, the synthesis process is completed by ring closure between the Leu<sup>10</sup> and Phe<sup>1</sup> (114). Within each of the three tyrocidine synthetases there exists a number of modules, which in turn contain all the necessary domains for the incorporation of a single amino acid (although not always a specific amino acid), into a given Trc (115). The process of Trc synthesis begins with the activation of an amino acid substrate in the adenylation domain (A) of the enzyme module consuming ATP with dependence on Mg<sup>2+</sup> as a cofactor in the process (116). The A-domain of modules three, four, seven and nine have affinity for more than one amino acid, allowing activation and subsequent incorporation of different amino acids at these positions in the peptide (117). This forms an activated aminoacyl-*O*-AMP.

The Ppan-arm assists in the delivery of the aminoacyl- and peptidyl-S-PCP intermediates to the condensation domain (C), which catalyses the nucleophilic attack of the activated amino acid's  $\alpha$ -carbon group on the thio-esterified carboxy group of an adjacent amino-acyl-S-Ppan moiety (another single activated amino acid) or a peptidyl-S-Ppan moiety (elongating peptide) on the preceding module to form a peptide bond (126). During this condensation process, all intermediates are covalently attached to the multienzyme complex. In summary, the biosynthesis of tyrocidine is mediated by the 4'PP cofactors, which assist in the ordered shuttling of carboxy activated substrates between the active units that constitute the peptide synthetases (115). At modules one and four there exists an additional epimerase (E) domain which catalyses the epimerisation of the activated amino acid bound there before its incorporation into the peptide (127, 128). These E-domains are found at the C-terminal ends of the TycA and TycB domains. A thioesterase (TE) domain catalyses the release of the peptide from the enzyme template and is therefore found at the C-terminal module of the NRPS (129). This process involves the formation of an acyl-*O*-TE intermediate which is cleaved by a regio- or stereoselective macrocyclization process, which uses an internal nucleophile to generate a cyclic product in the case of the tyrocidines (130, 131). The number of separate modules, with all the necessary enzyme domains needed for incorporation of an activated amino acid, as well as their order, determine the size and sequence of the produced peptide (115). We will

report in this research study on the elasticity of the tyrocidine synthesis machinery in terms of the incorporation of natural aromatic amino acids and non-natural amino acids in the four aromatic positions of the cyclodecapeptide structure.

The Ppan-arm assists in the delivery of the aminoacyl- and peptidyl-S-PCP intermediates to the condensation domain (C), which catalyses the nucleophilic attack of the activated amino acid's  $\alpha$ -carbon group on the thio-esterified carboxy group of an adjacent amino-acyl-S-Ppan moiety (another single activated amino acid) or a peptidyl-S-Ppan moiety (elongating peptide) on the preceding module to form a peptide bond (126). During this condensation process, all intermediates are covalently attached to the multienzyme complex. In summary, the biosynthesis of tyrocidine is mediated by the 4'PP cofactors, which assist in the ordered shuttling of carboxy activated substrates between the active units that constitute the peptide synthetases (115). At modules one and four there exists an additional epimerase (E) domain which catalyses the epimerisation of the activated amino acid bound there before its incorporation into the peptide (127, 128). These E-domains are found at the C-terminal ends of the TycA and TycB domains. A thioesterase (TE) domain catalyses the release of the peptide from the enzyme template and is therefore found at the C-terminal module of the NRPS (129). This process involves the formation of an acyl-O-TE intermediate which is cleaved by a regio- or stereoselective macrocyclization process, which uses an internal nucleophile to generate a cyclic product in the case of the tyrocidines (130, 131). The number of separate modules, with all the necessary enzyme domains needed for incorporation of an activated amino acid, as well as their order, determine the size and sequence of the produced peptide (115). We will report in this research study on the elasticity of the tyrocidine synthesis machinery in terms of the incorporation of natural aromatic amino acids and non-natural amino acids in the four aromatic positions of the cyclodecapeptide structure.



## 1.6 References

1. World Health Organisation Antimicrobial Resistance Global Report on Surveillance, [online] [http://apps.who.int/iris/bitstream/10665/112642/1/9789241564748\\_eng.pdf](http://apps.who.int/iris/bitstream/10665/112642/1/9789241564748_eng.pdf) (Accessed November 22, 2017)
2. Andreu, D., and Rivas, L. (1998) Animal antimicrobial peptides: An overview. *Biopolym. - Pept. Sci. Sect.* **47**, 415–433
3. Shai, Y. (2002) Mode of action of membrane active antimicrobial peptides. *Biopolym. - Pept. Sci. Sect.* **66**, 236–248
4. Boman, H. G. (1991) Antibacterial peptides: Key components needed in immunity. *Cell.* **65**, 205–207
5. Lehrer, R. I., and Ganz, T. (1999) Antimicrobial peptides in mammalian and insect host defence. *Curr. Opin. Immunol.* **11**, 23–27
6. Hoffmann, J. A., Kafatos, F. C., Janeway, C. A., and Ezekowitz, R. A. (1999) Phylogenetic perspectives in innate immunity. *Science.* **284**, 1313–1318
7. Zasloff, M. (1992) Antibiotic peptides as mediators of innate immunity. *Curr. Opin. Immunol.* **4**, 3–7
8. Nicolas, P., and Mor, A. (1995) Peptides as weapons against microorganisms in the chemical defense system of vertebrates. *Annu. Rev. Microbiol.* **49**, 277–304
9. R, H., and G, D. (2000) The role of cationic antimicrobial peptides in innate host defences. *Trends Microbiol.* **8**, 402–410
10. Guder, A., Wiedemann, I., and Sahl, H.G. (2000) Posttranslationally modified bacteriocins—the lantibiotics. *Biopolymers.* **55**, 62–73
11. Zasloff, M. (2002) Antimicrobial peptides of multicellular organisms. *Nature.* **415**, 389–395
12. Jenssen, H., Hamill, P., and Hancock, R. E. W. (2006) Peptide antimicrobial agents. *Clin. Microbiol. Rev.* **19**, 491–511
13. Steiner, H., Hultmark, D., Engström, A., Bennich, H., and Boman, H. G. (1981) Sequence and specificity of two antibacterial proteins involved in insect immunity. *Nature.* **292**, 246–248
14. Zasloff, M. (1987) Magainins, a class of antimicrobial peptides from *Xenopus* skin: isolation, characterization of two active forms, and partial cDNA sequence of a precursor. *Proc. Natl. Acad. Sci. U. S. A.* **84**, 5449–5453
15. Mor, A., Nguyen, V. H., Delfour, A., Migliore-Samour, D., and Nicolas, P. (1991) Isolation, Amino Acid Sequence, and Synthesis of Dermaseptin, a Novel Antimicrobial Peptide of Amphibian Skin1. *Biochemistry.* **30**, 8824–8830
16. Landon, C., Sodano, P., Hetru, C., Hoffmann, J., and Ptak, M. (1997) Solution structure of drosomycin, the first inducible antifungal protein from insects. *Protein Sci.* **6**, 1878–1884

17. Johansson, J., Gudmundsson, G. H., Rottenberg, M. E., Berndt, K. D., and Agerberth, B. (1998) Conformation-dependent antibacterial activity of the naturally occurring human peptide LL-37. *J. Biol. Chem.* **273**, 3718–3724
18. Epand, R. M., and Vogel, H. J. (1999) Diversity of antimicrobial peptides and their mechanisms of action. *Biochim. Biophys. Acta - Biomembr.* **1462**, 11–28
19. Verkleij, A. J., Zwaal, R. F. A., Roelofsen, B., Comfurius, P., Kastelijn, D., and van Deenen, L. L. M. (1973) The asymmetric distribution of phospholipids in the human red cell membrane. A combined study using phospholipases and freeze-etch electron microscopy. *Biochim. Biophys. Acta - Biomembr.* **323**, 178–193
20. Matsuzaki, K. (1999) Why and how are peptide-lipid interactions utilized for self-defense? Magainins and tachyplesins as archetypes. *Biochim. Biophys. Acta.* **1462**, 1–10
21. Malanovic, N., and Lohner, K. (2016) Gram-positive bacterial cell envelopes: The impact on the activity of antimicrobial peptides. *Biochim. Biophys. Acta - Biomembr.* **1858**, 936–946
22. Anunthawan, T., de la Fuente-Núñez, C., Hancock, R. E. W., and Klaynongsruang, S. (2015) Cationic amphipathic peptides KT2 and RT2 are taken up into bacterial cells and kill planktonic and biofilm bacteria. *Biochim. Biophys. Acta - Biomembr.* **1848**, 1352–1358
23. Choi, H., Rangarajan, N., and Weisshaar, J. C. (2016) Lights, camera, action! Antimicrobial peptide mechanisms imaged in space and time. *Trends Microbiol.* **24**, 111–122
24. Rashid, R., Veleba, M., and Kline, K. A. (2016) Focal targeting of the bacterial envelope by antimicrobial peptides. *Front. Cell. Dev. Biol.* **4**, 1-13
25. Koprivnjak, T., and Peschel, A. (2011) Bacterial resistance mechanisms against host defense peptides. *Cell. Mol. Life Sci.* **68**, 2243–2254
26. Wu, M., Maier, E., Benz, R., and Hancock, R. E. W. (1999) Mechanism of interaction of different classes of cationic antimicrobial peptides with planar bilayers and with the cytoplasmic membrane of *Escherichia coli* †. *Biochemistry.* **38**, 7235–7242
27. Guilhelmelli, F., Vilela, N., Albuquerque, P., Derengowski, L. da S., Silva-Pereira, I., and Kyaw, C. M. (2013) Antibiotic development challenges: The various mechanisms of action of antimicrobial peptides and of bacterial resistance. *Front. Microbiol.* **4**, 1–12
28. Jenssen, H., Hamill, P., and Hancock, R. E. W. (2006) Peptide antimicrobial agents. *Clin. Microbiol. Rev.* **19**, 491–511
29. Balhara, V., Schmidt, R., Gorr, S-U., and DeWolf, C. (2013) Membrane selectivity and biophysical studies of the antimicrobial peptide GL13K. *Biochim. Biophys. Acta - Biomembr.* **1828**, 2193–2203
30. Bechinger, B., and Gorr, S-U. (2017) Antimicrobial Peptides: Mechanisms of Action and Resistance. *J. Dent. Res.* **96**, 254–260
31. Bechinger, B. (2015) The SMART model: Soft Membranes Adapt and Respond, also Transiently, in the presence of antimicrobial peptides. *J. Pept. Sci.* **21**, 346–355
32. Brogden, K. A. (2005) Antimicrobial peptides: Pore formers or metabolic inhibitors in bacteria? *Nat. Rev. Microbiol.* **3**, 238–250

33. Park, C. B., Kim, H. S., and Kim, S. C. (1998) Mechanism of action of the antimicrobial peptide buforin ii: buforin ii kills microorganisms by penetrating the cell membrane and inhibiting cellular functions. *Biochem. Biophys. Res. Commun.* **244**, 253–257
34. Kragol, G., Lovas, S., Varadi, G., Condie, B. A., Hoffmann, R., and Otvos, L. (2001) The antibacterial peptide pyrrocoricin inhibits the ATPase actions of DnaK and prevents chaperone-assisted protein folding. *Biochemistry.* **40**, 3016–3026
35. Lehrer, R. I., Szklarek, D., Ganz, T., and Selsted, M. E. (1985) Correlation of binding of rabbit granulocyte peptides to *Candida albicans* with candidacidal activity. *Infect. Immun.* **49**, 207–211
36. Brötz, H., Bierbaum, G., Reynolds, P. E., and Sahl, H. G. (1997) The lantibiotic mersacidin inhibits peptidoglycan biosynthesis at the level of transglycosylation. *Eur. J. Biochem.* **246**, 193–199
37. Terry, A. S., Poulter, L., Williams, D. H., Nutkins, J. C., Giovannini, M. G., Moore, C. H., and Gibson, B. W. (1988) The cDNA sequence coding for prepro-PGS (prepro-magainins) and aspects of the processing of this prepro-polypeptide. *J. Biol. Chem.* **263**, 5745–5751
38. Bellamy, W., Takase, M., Yamauchi, K., Wakabayashi, H., Kawase, K., and Tomita, M. (1992) Identification of the bactericidal domain of lactoferrin. *Biochim. Biophys. Acta (BBA)/Protein Struct. Mol.* **1121**, 130–136
39. Ibrahim, H. R., Higashiguchi, S., Koketsu, M., Juneja, L. R., Kim, M., Yamamoto, T., Sugimoto, Y., and Aoki, T. (1996) partially unfolded lysozyme at neutral pH agglutinates and kills Gram-negative and Gram-positive bacteria through membrane damage mechanism. *J. Agric. Food Chem.* **44**, 3799–3806
40. Kim, H. S., Park, C. B., Kim, M. S., and Kim, S. C. (1996) cDNA Cloning and characterization of buforin I, an antimicrobial peptide: A cleavage product of histone h2a. *Biochem. Biophys. Res. Commun.* **229**, 381–387
41. Park, I. Y., Park, C. B., Kim, M. S., and Kim, S. C. (1998) Parasin I, an antimicrobial peptide derived from histone H2A in the catfish, *Parasilurus asotus*. *FEBS Lett.* **437**, 258–262
42. Bulet, P., Hegy, G., Lambert, J., Van Dorsselaer, A., Hoffmann, J. A., and Hetru, C. (1995) Insect immunity. The inducible antibacterial peptide diptericin carries two O-glycans necessary for biological activity. *Biochemistry.* **34**, 7394–7400
43. Mackintosh, J. A., Veal, D. A., Beattie, A. J., and Gooley, A. A. (1998) Isolation from an ant *Myrmecia gulosa* of two inducible O-glycosylated proline-rich antibacterial peptides. *J. Biol. Chem.* **273**, 6139–6143
44. Hara, S., and Yamakawa, M. (1995) A novel antibacterial peptide family isolated from the silkworm, *Bombyx mori*. *Biochem. J.* **310 (Pt 2)**, 651–656
45. Cociancich, S., Dupont, A., Hegy, G., Lanot, R., Holder, F., Hetru, C., Hoffmann, J. A., and Bulet, P. (1994) Novel inducible antibacterial peptides from a hemipteran insect, the sap-sucking bug *Pyrrhocoris apterus*. *Biochem. J.* **300 (Pt 2)**, 567–575

46. Craig, A. G., Jimenez, E. C., Dykert, J., Nielsen, D. B., Gulyas, J., Abogadie, F. C., Porter, J., Rivier, J. E., Cruz, L. J., Olivera, B. M., and McIntosh, J. M. (1997) A novel post-translational modification involving bromination of tryptophan. Identification of the residue, L-6-bromotryptophan, in peptides from *Conus imperialis* and *Conus radiatus* venom. *J. Biol. Chem.* **272**, 4689–4698
47. Koczulla, A. R., and Bals, R. (2003) Antimicrobial Peptides. *Drugs.* **63**, 389–406
48. Beringer, P. (2001) The clinical use of colistin in patients with cystic fibrosis. *Curr. Opin. Pulm. Med.* **7**, 434–440
49. Evans, M. E., Feola, D. J., and Rapp, R. P. (1999) Polymyxin b sulfate and colistin: Old antibiotics for emerging multiresistant gram-negative bacteria. *Ann. Pharmacother.* **33**, 960–967
50. Spathelf, B. (2010) Qualitative structure-activity relationships of the major tyrocidines, cyclic decapeptides from *Bacillus aneurinolyticus*. **Ph.D. thesis**, Stellenbosch University, <http://hdl.handle.net/10019.1/4001>
51. Fujikawa, K., Suzuki, T., and Kurahashi, K. (1968) Biosynthesis of tyrocidine by a cell-free enzyme system of *Bacillus brevis* ATCC 8185. I. Preparation of partially purified enzyme system and its properties. *Biochim. Biophys. Acta.* **161**, 232–246
52. Dubos, R. J., and Cattaneo, C. (1939) Studies on a bactericidal agent extracted from a soil bacillus: III. preparation and activity of a protein-free fraction. *J. Exp. Med.* **70**, 249–56
53. Hotchkiss, R. D., and Dubos, R. J. (1941) the Isolation of Bactericidal Substances From Cultures of *Bacillus Brevis*. *J. Biol. Chemistry.* **141**, 155–162
54. Dubos, R. J. (1939) Bactericidal effect of an extract of a soil bacillus on Gram-positive cocci. *J. Exp. Med.* **70**, 3–4
55. Dimick, K. P. (1951) The hemolytic action of gramicidin and tyrocidin. *Exp. Biol. Med.* **78**, 782–784
56. Henderson, J. (1946) The status of tyrothricin as an antibiotic agent for topical application\*†. *J. Am. Pharm. Assoc. (Scientific ed.).* **35**, 141–147
57. Goldman, L., Feldman, M. D., and Altemeier, W. A. (1948) Contact dermatitis from topical tyrothricin and associated with polyvalent hypersensitivity to various antibiotics. *J. Invest. Dermatol.* **11**, 243–244
58. Wigger-Alberti, W., Stauss-Grabo, M., Grigo, K., Atiye, S., Williams, R., and Korting, H. C. (2012) Efficacy of a tyrothricin-containing wound gel in an abrasive wound model for superficial wounds. *Skin Pharmacol. Physiol.* **26**, 52–56
59. Rankin, L. M. (1944) The use of tyrothricin in the treatment of ulcers of the skin. *Amer. J. Surg.* **65**, 391–392
60. Kagan, G., Huddleston, L., and Wolstencroft, P. (1982) Two lozenges containing benzocaine assessed in the relief of sore throat. *J. Int. Med. Res.* **10**, 443–446
61. Bloomfield, S. (1944) The use of tyrothricin, a bacterial extract, in the treatment of marginal ulcers of the cornea\*. *Am. J. Ophthalmol.* **27**, 500–504

62. Tang, X-J., Thibault, P., and Boyd, R. K. (1992) Characterisation of the tyrocidine and gramicidin fractions of the tyrothricin complex from *Bacillus brevis* using liquid chromatography and mass spectrometry. *Int. J. Mass Spectrom. Ion Process.* **122**, 153–179
63. Marques, M. A., Citron, D. M., and Wang, C. C. (2007) Development of tyrocidine analogues with improved antibacterial activity. *Bioorg. Med. Chem.* **15**, 6667–6677
64. Vosloo, J. A. (2016) Optimised bacterial production and characterisation of natural antimicrobial peptides with potential application in agriculture. **Ph.D. thesis**, University of Stellenbosch, <http://scholar.sun.ac.za/handle/10019.1/98411>
65. Troskie, A. M. (2013) Tyrocidines, cyclic decapeptides produced by soil bacilli, as potent inhibitors of fungal pathogens. **Ph.D. thesis**, University of Stellenbosch, <http://hdl.handle.net/10019.1/86162>
66. Gibbons, W. A., Beyer, C. F., Dadok, J., Sprecher, R. F., and Wyssbrod, H. R. (1975) Studies of individual amino acid residues of the decapeptide tyrocidine A by proton double-resonance difference spectroscopy in the correlation mode. *Biochemistry.* **14**, 420–9
67. Kuo, M. C., and Gibbons, W. A. (1979) Total assignments, including four aromatic residues, and sequence confirmation of the decapeptide tyrocidine A using difference double resonance. Qualitative nuclear overhauser effect criteria for beta turn and antiparallel beta-pleated sheet conformations. *J. Biol. Chem.* **254**, 6278–6287
68. Kuo, M. C., and Gibbons, W. A. (1979) Determination of individual side-chain conformations, tertiary conformations, and molecular topography of tyrocidine A from scalar coupling constants and chemical shifts. *Biochemistry.* **18**, 5855–5867
69. Kuo, M. C., and Gibbons, W. A. (1980) Nuclear overhauser effect and cross-relaxation rate determinations of dihedral and transannular interproton distances in the decapeptide tyrocidine A. *Biophys. J.* **32**, 807–836
70. Loll, P. J., Upton, E. C., Nahoum, V., Economou, N. J., and Cocklin, S. (2014) The high resolution structure of tyrocidine A reveals an amphipathic dimer. *Biochim. Biophys. Acta.* **1838**, 1199–1207
71. Munyuki, G., Jackson, G. E., Venter, G. A., Kövér, K. E., Szilágyi, L., Rautenbach, M., Spathelf, B. M., Bhattacharya, B., and Van Der Spoel, D. (2013)  $\beta$ -sheet structures and dimer models of the two major tyrocidines, antimicrobial peptides from *Bacillus aneurinolyticus*. *Biochemistry.* **52**, 7798–7806
72. Laiken, S., Printz, M., and Craig, L. C. (1969) Circular dichroism of the tyrocidines and gramicidin S-A. *J. Biol. Chem.* **244**, 4454–4457
73. Dubos, R. J. (1939) Studies on a bactericidal agent extracted from a soil bacillus I. Preparation of the agent. Its activity in vitro. *J. Exp. Med.* **70**, 1–10
74. Ruckdeschel, G., Beaufort, F., Nahler, G., and Belzer, O. (1983) In vitro antibacterial activity of gramicidin and tyrothricin. *Arzneimittelforschung.* **33**, 1620–1622
75. Kretschmar, M., Nichterlein, T., Hof, H., and Burger, K. (1995) Tyrothricin: Bactericidal effect on facultative pathogenic Gram positive aerobic bacteria of the oral flora and MRSA. *Chemother. J.* **4**, 156–159

76. Spathelf, B. M., and Rautenbach, M. (2009) Anti-listerial activity and structure-activity relationships of the six major tyrocidines, cyclic decapeptides from *Bacillus aneurinolyticus*. *Bioorganic Med. Chem.* **17**, 5541–5548
77. Kretschmar, M., Nichterlein, T., Nebe, C. T., Hof, H., and Burger, K. J. (1996) Fungicidal effect of tyrothricin on *Candida albicans*. *Mycoses.* **39**, 45–50
78. Stauss-Grabo, M., Atiye, S., Le, T., and Kretschmar, M. (2014) Decade-long use of the antimicrobial peptide combination tyrothricin does not pose a major risk of acquired resistance with gram-positive bacteria and *Candida* spp. *Pharmazie.* **69**, 838–841
79. Troskie, A. M., de Beer, A., Vosloo, J. A., Jacobs, K., and Rautenbach, M. (2014) Inhibition of agronomically relevant fungal phytopathogens by tyrocidines, cyclic antimicrobial peptides isolated from *Bacillus aneurinolyticus*. *Microbiology.* **160**, 2089–2101
80. Grossgebauer, K., and Hartmann, D. (1978) Antiviral activity of tyrothricin against Sendai virus in suspension tests. *Zentralbl. Bakteriolog. Orig. B.* **166**, 434–442
81. Hartmann, D., and Grossgebauer, K. (1979) Experimental protection with tyrothricin against herpes simplex virus infections in mice. *Arzneimittelforschung.* **29**, 50–54
82. Taliaferro, L. G., Coulston, F., and Silverman, M. (1944) The antimalarial activity of tyrothricin against *Plasmodium gallinaceum*. *J. Infect. Dis.* **75**, 179–211
83. Rautenbach, M., Vlok, N. M., Stander, M., and Hoppe, H. C. (2007) Inhibition of malaria parasite blood stages by tyrocidines, membrane-active cyclic peptide antibiotics from *Bacillus brevis*. *Biochim. Biophys. Acta - Biomembr.* **1768**, 1488–1497
84. Leussa, N.-N. A. (2014) Characterisation of small cyclic peptides with antilisterial and antimalarial activity. **Ph.D. thesis**, Stellenbosch University, <http://hdl.handle.net/10019.1/86161>
85. Dubos, R. J., and Hotchkiss, R. D. (1941) The production of bactericidal substances by aerobic sporulating bacilli. *J. Exp. Med.* **73**, 629–640
86. Herrell, W. E., and Heilman, D. (1943) Tissue culture studies on cytotoxicity of bactericidal agents. I. Effects of gramicidin, tyrocidine and penicillin on cultures of mammalian lymph node. *Am. J. Med. Sci.* **205**, 157–162
87. Mann, F. C., Heilman, D., and Herrell, W. E. (1943) Effect of serum on hemolysis by gramicidin and tyrocidine. *Exp. Biol. Med.* **52**, 31–33
88. Rammelkamp, C. H., and Weinstein, L. (1941) Hemolytic effect of tyrothricin. *Exp. Biol. Med.* **48**, 211–214
89. Herrell, W. E., and Heilman, D. (1941) Experimental and clinical studies on gramicidin. *J. Clin. Invest.* **20**, 583–591
90. Tulloch, L. G. (1954) Nasal carriage in staphylococcal skin infections. *Br. Med. J.* **2**, 912–913
91. Anderson, H. E. (1946) Tyrothricin in cutaneous infections. *Arch. Derm. Syphilol.* **53**, 20–25
92. Bayerl, C., and Völp, A. (2004) Tyrothricin powder in the treatment of cutaneous lesions. *Pharmazie.* **59**, 864–868



93. Franks, A. G., Dobes, W. L., and Jones, J. (1946) Tyrothricin in the treatment of diseases of the skin. *Arch. Derm. Syphilol.* **53**, 498–502
94. Rammelkamp, C. H., and Weinstein, L. (1942) Toxic effects of tyrothricin, gramicidin and tyrocidine. *J. Infect. Dis.* **71**, 166–173
95. Kolmer, J. A., and Rule, A. M. (1946) Toxicity and therapeutic activity of tyrothricin by oral administration. *Exp. Biol. Med.* **63**, 315–317
96. Weinstein, L., and Rammelkamp, C. H. (1941) A study of the effect of gramicidin administered by the oral route. *Exp. Biol. Med.* **48**, 147–149
97. Kohli, R. M., Walsh, C. T., and Burkart, M. D. (2002) Biomimetic synthesis and optimization of cyclic peptide antibiotics. *Nature.* **418**, 658–661
98. Qin, C., Zhong, X., Bu, X., Ng, N. L. J., and Guo, Z. (2003) Dissociation of antibacterial and hemolytic activities of an amphipathic peptide antibiotic. *J. Med. Chem.* **46**, 4830–4833
99. Qin, C., Bu, X., Zhong, X., Ng, N. L. J., and Guo, Z. (2004) Optimization of antibacterial cyclic decapeptides. *J. Comb. Chem.* **6**, 398–406
100. Xiao, Q., Xiao, Q., Pei, D., and Pei, D. (2007) High-throughput synthesis and screening of cyclic peptide antibiotics. *J. Med. Chem.* **4**, 3132–3137
101. Leussa, A. N. Yango N., and Rautenbach, M. (2014) Detailed SAR and PCA of the tyrocidines and analogues towards leucocin A-sensitive and leucocin A-resistant *Listeria monocytogenes*. *Chem. Biol. Drug Des.* **84**, 543–557
102. Aranda, F. J., and de Kruijff, B. (1988) Interrelationships between tyrocidine and gramicidin A' in their interaction with phospholipids in model membranes. *Biochim. Biophys. Acta.* **937**, 195–203
103. Goodall, M. C. (1970) Structural effects in the action of antibiotics on the ion permeability of lipid bilayers. I. Tyrocidine B. *Biochim. Biophys. Acta.* **203**, 28–33
104. Eyeghe-Bickong, H. (2011) Role of surfactin from *Bacillus subtilis* in protection against antimicrobial peptides produced by *Bacillus* species. **Ph.D. thesis**, Stellenbosch University, <http://hdl.handle.net/10019.1/6773>
105. Breshow, R., and Chipman, D. (1965) The use of the tyrocidines for the study of conformation and aggregation behaviour. *J. Am. Chem. Soc.* **87**, 4196–4198
106. Ruttenberg, M. A., King, T. P., and Craig, L. C. (1966) The chemistry of tyrocidine. VII. Studies on association behavior and implications regarding conformation \*. *Biochemistry.* **5**, 2857–2864
107. Williams, R. C., Yphantis, D. A., and Craig, L. C. (1972) Noncovalent association of tyrocidine B. *Biochemistry.* **11**, 70–77
108. Dubos, R. J., Hotchkiss, R. D., and Coburn, A. F. (1942) The effect of gramicidin and tyrocidine on bacterial metabolism. *J. Biol. Chem.* **146**, 421–426
109. Schazschneider, B., Ristow, H., and Kleinkauf, H. (1974) Interaction between the antibiotic tyrocidine and DNA in vitro. *Nature.* **249**, 757–759

110. Bohg, A., and Ristow, H. (1987) Tyrocidine-induced modulation of the DNA conformation in *Bacillus brevis*. *Eur. J. Biochem.* **170**, 253–258
111. Bohg, A., and Ristow, H. (1986) DNA-supercoiling is affected in vitro by the peptide antibiotics tyrocidine and gramicidin. *Eur. J. Biochem.* **160**, 587–591
112. Danders, W., Marahiel, M. A., Krause, M., Kosui, N., Kato, T., Izumiya, N., and Kleinkauf, H. (1982) Antibacterial action of gramicidin S and tyrocidines in relation to active transport, in vitro transcription, and spore outgrowth. *Antimicrob. Agents Chemother.* **22**, 785–790
113. Mootz, H. D., and Marahiel, M. A. (1997) The tyrocidine biosynthesis operon of *Bacillus brevis*: complete nucleotide sequence and biochemical characterization of functional internal adenylation domains. *J. Bacteriol.* **179**, 6843–6850
114. Lee, S. G., and Lipmann, F. (1975) [45] Tyrocidine synthetase system. *Methods Enzymol.* **43**, 585–602
115. Marahiel, M. A., Stachelhaus, T., and Mootz, H. D. (1997) Modular Peptide Synthetases Involved in Nonribosomal Peptide Synthesis. *Chem. Rev.* **97**, 2651–2674
116. Conti, E., Stachelhaus, T., Marahiel, M. A., and Brick, P. (1997) Structural basis for the activation of phenylalanine in the non-ribosomal biosynthesis of gramicidin S. *EMBO J.* **16**, 4174–4183
117. Marahiel, M. A., and Essen, L. O. (2009) *Nonribosomal Peptide Synthetases: Mechanistic and Structural Aspects of Essential Domains*, 1st Ed., Elsevier Inc.
118. Stein, T., Vater, J., Kruft, V., Wittmann-Liebold, B., Franke, P., Panico, M., McDowell, R., and Morris, H. R. (1994) Detection of 4'-phosphopantetheine at the thioester binding site for L-valine of gramicidinS synthetase 2. *FEBS Lett.* **340**, 39–44
119. Stein, T., Vater, J., Kruft, V., Otto, A., Wittmann-Liebold, B., Franke, P., Panico, M., McDowell, R., and Morris, H. R. (1996) The multiple carrier model of nonribosomal peptide biosynthesis at modular multienzymatic templates. *J. Biol. Chem.* **271**, 15428–15435
120. Stachelhaus, T., Schneider, A., and Marahiel, M. A. (1996) Engineered biosynthesis of peptide antibiotics. *Biochem. Pharmacol.* **52**, 177–186
121. Stachelhaus, T., Hüser, A., and Marahiel, M. A. (1996) Biochemical characterization of peptidyl carrier protein (PCP), the thiolation domain of multifunctional peptide synthetases. *Chem. Biol.* **3**, 913–921
122. Lambalot, R. H., Gehring, A. M., Flugel, R. S., Zuber, P., LaCelle, M., Marahiel, M. A., Reid, R., Khosla, C., and Walsh, C. T. (1996) A new enzyme superfamily - the phosphopantetheinyl transferases. *Chem. Biol.* **3**, 923–936
123. Reuter, K., Mofid, M. R., Marahiel, M. A., and Ficner, R. (1999) Crystal structure of the surfactin synthetase-activating enzyme sfp: a prototype of the 4'-phosphopantetheinyl transferase superfamily. *EMBO J.* **18**, 6823–6831
124. Finking, R., Solsbacher, J., Konz, D., Schobert, M., Schäfer, A., Jahn, D., and Marahiel, M. A. (2002) Characterization of a new type of phosphopantetheinyl transferase for fatty acid and siderophore synthesis in *Pseudomonas aeruginosa*. *J. Biol. Chem.* **277**, 50293–50302



125. Mootz, H. D., Finking, R., and Marahiel, M. A. (2001) 4'-Phosphopantetheine transfer in primary and secondary metabolism of *Bacillus subtilis*. *J. Biol. Chem.* **276**, 37289–37298
126. Stachelhaus, T., Mootz, H. D., Bergendahl, V., and Marahiel, M. A. (1998) Peptide bond formation in nonribosomal peptide biosynthesis. Catalytic role of the condensation domain. *J. Biol. Chem.* **273**, 22773–22781
127. Stein, T., Kluge, B., Vater, J., Franke, P., Otto, A., and Wittmann-Liebold, B. (1995) Gramicidin S synthetase 1 (phenylalanine racemase), a prototype of amino acid racemases containing the cofactor 4'-phosphopantetheine. *Biochemistry.* **34**, 4633–4642
128. Linne, U., Doekel, S., and Marahiel, M. A. (2001) Portability of epimerization domain and role of peptidyl carrier protein on epimerization activity in nonribosomal peptide synthetases. *Biochemistry.* **40**, 15824–15834
129. Bruner, S. D., Weber, T., Kohli, R. M., Schwarzer, D., Marahiel, M. A., Walsh, C. T., and Stubbs, M. T. (2002) Structural basis for the cyclization of the lipopeptide antibiotic surfactin by the thioesterase domain SrfTE. *Structure.* **10**, 301–310
130. Kopp, F., and Marahiel, M. A. (2007) Macrocyclization strategies in polyketide and nonribosomal peptide biosynthesis. *Nat. Prod. Rep.* **24**, 735-749
131. Trauger, J. W., Kohli, R. M., Mootz, H. D., Marahiel, M. A., and Walsh, C. T. (2000) Peptide cyclization catalysed by the thioesterase domain of tyrocidine synthetase. *Nature.* **407**, 215–218
132. Powers, J-P. S., Tan, A., Ramamoorthy, A., and Hancock, R. E. W. (2005) Solution structure and interaction of the antimicrobial polyphemusins with lipid membranes. *Biochemistry.* **44**, 15504–15513
133. Ehrenstein, G., and Lecar, H. (1977) Electrically gated ionic channels in lipid bilayers. *Q. Rev. Biophys.* **10**, 1-34
134. Breukink, E., and de Kruijff, B. (1999) The lantibiotic nisin, a special case or not? *Biochim. Biophys. Acta.* **1462**, 223–234
135. Rotem, S., and Mor, A. (2009) Antimicrobial peptide mimics for improved therapeutic properties. *Biochim. Biophys. Acta - Biomembr.* **1788**, 1582–1592
136. Oren, Z., and Shai, Y. (1998) Mode of action of linear amphipathic  $\alpha$ -helical antimicrobial peptides. *Biopolymers.* **47**, 451–463
137. Pouny, Y., Rapaport, D., Mor, A., Nicolas, P., and Shai, Y. (1992) Interaction of antimicrobial dermaseptin and its fluorescently labeled analogues with phospholipid membranes. *Biochemistry.* **31**, 12416–12423

## Chapter 2

### Tyrocidine production profile characterisation and optimisation of carbon, nitrogen and sulphate sources in different strains of *Brevibacillus parabrevis*

#### 2.1 Introduction

Tyrothricin (Tcn) is an antimicrobial peptide complex produced by the gram-positive soil bacteria *Brevibacillus parabrevis* (previously known as *Bacillus brevis* and *Bacillus aneurinolyticus*) consists of two major peptide groups, namely the tyrocidines (Trc) and gramicidines (Grcs) (1, 2). The Trcs are basic, cyclic decapeptides and the Grcs are neutral, linear pentadecapeptides (2, 3). The tyrocidines are synthesised by multienzyme complex (Trc synthetase complex) which sequentially incorporates the constituent amino acids into the growing peptide, with three major enzyme complexes (Trc synthetases I, II and III) consisting of enzyme subunits which in turn have domains specific for the activation and incorporation of an amino acids into the growing peptide (4). The sequence variability seen between Trc analogues is largely due to the ability of the Trc synthetase sub-units to incorporate different amino acids at positions 3,4 and 7 within the Trc cyclic decapeptide (3–5).

Trc inhibits the growth of a wide variety of Gram-positive microorganisms (6, 7), as well as the blood-borne malaria parasite *Plasmodium falciparum*, and are toxic in the blood stream due to their haemolytic activity (2, 8). They, however, show little toxicity when applied topically or locally, for example, via the subcutaneous, intramuscular or intrapleural routes (2). The Trcs have shown their ability to induce cell death of target organisms via lysis of the cell membrane but other mechanisms of action may cause or contribute to cell death, including a secondary effect of autolytic enzymes, inactivation of the target cell enzymes (resulting in disruption of metabolic activity) and DNA binding leading to non-specific repression of transcription (1, 9–13).

The yield of Tcn was found to vary greatly depending on the composition of the growth media used in the initial work done on Tcn production by Dubos *et al.* (1). Complex nitrogen sources such as acid hydrolysed casein, tryptic digest of soybean meal, corn-steep liquor, tryptone and press juice concentrates have been found most effective in Tcn production. Using 0.2% tryptone in conjunction with glutamic acid, asparagine or ammonium sulphate plus citric acid or malic acid was shown to be moderately effective for Tcn production (14). Fermentable carbon compounds, such as glucose, mannitol or glycerol, were also required at levels ranging between 3% to 5% for optimal yields (14). A study by Okuda *et al.* (15) supported this, finding that a combination of tryptone, yeast extract,

mineral salts and glucose gave the best yield. The need for calcium and either magnesium or manganese was also found, particularly since the latter two compounds act as co-factors for the production of tyrocidine by the tyrocidine producing peptide synthetases (1, 16).

In addition to media composition, significant variability has been found for Grc production between different strains of the producer organism (1). Within the total amount of Tcn produced, the ratio of Grcs and Trcs may also be altered (15). Okuda *et al.* (15) produced between 0.38 mg Grc and 1.37 mg Trc, and 3.28 mg Grc and 9.65 mg Trc per 100 ml culture media depending on the composition of the media.

Tcn production is slow during the initial phase of bacterial growth but tends to accelerate during the log phase where observed yields of 103 mg/100 mL Trc and 95 mg/100 mL Grc after 108 hours of growth in a simple Tryptone-NaCl growth media (15). Mach *et al.* (17) found that tyrocidine production occurred 26 hours after inoculation, correlating with the completion of the exponential growth, or log phase, in a media composition used previously by Stokes and Woodward (18), which contained a mixture of mineral salts, L-asparagine and glycerol.

Little work has been done to assess and compare the variability of the growth of different strains of Tcn-producing *Br. parabrevis*. In this study, we first assessed the Trc production of four different strains in TGS media using medium-scale cultures then proceeded to investigate the effect of various nitrogen, sulphate and carbon sources, both in varying combinations and concentrations, on the growth of three selected strains of the producer organism. Following this, small-scale, medium throughput culturing was done to assess any correlation between growth rate and peptide production.

## 2.2 Materials

The producer organisms *Brevibacillus parabrevis* (*Br. parabrevis*) 362 and 5618 originate from the Deutsche Sammlung von Mikroorganismen und Zellkulturen (DSMZ) in Braunschweig, Germany. The *Br. parabrevis* 8185 and 10068 strains originate from the American Type Culture Collection (ATCC) based in Manassas (Virginia, USA). *Micrococcus luteus* (*M. luteus*) was sourced from the National Collection of Type Cultures (NCTC) in Porton Down (Salisbury, England).

Tryptic soy broth (TSB), yeast extract, tryptone, agar, glucose (Glc), glycerol (Glr), ethanol (EtOH), hydrochloric acid (HCl), sodium chloride (NaCl) and ammonium sulphate ((NH<sub>4</sub>)<sub>2</sub>SO<sub>4</sub>) were from Merck (Darmstadt, Germany). Trifluoroacetic acid (TFA, > 98% purity) was from Sigma-Aldrich (St. Louis, USA). Acetonitrile (ACN, far UV cut-off, > 98% purity) was obtained from Romil Ltd (Cambridge, UK). Analytical grade, deionised water was obtained by filtering reverse osmosis water through a Millipore<sup>®</sup> water purification system. Urea was obtained from ICN Biomedicals Inc (Aurora, USA). Sodium sulphate (Na<sub>2</sub>SO<sub>4</sub>) was from Univar (Illinois, US).

Falcon<sup>®</sup> tubes were from SPL Life Sciences Co (Gyeonggi-do, South Korea). 0.22 µm syringe filters were from GVS Filter Technology (Morecambe, UK). The Acquity UPLC<sup>®</sup> BEH Phenyl column (2.1 mm × 100 mm, 1.7 µm particle size) was from Waters (Milford, MA, USA). Ninety-six well deep-well plates were from Thermo Fisher Scientific (Waltham, MA, USA).

## 2.3 Methods

### 2.3.1 Medium-scale culturing of producer organisms

*Pre-culturing of producer organisms:* The four available strains, *Br. parabrevis* ATCC 8185, *Br. parabrevis* ATCC 10068, *Br. parabrevis* DSMZ 362 and *Br. parabrevis* DSMZ 5618 (Note: strains will be referred to only by strain number throughout rest of chapter) were grown from glycerol freezer stocks stored at -80 °C. A wire loop was used to scoop a dollop of the partially defrosted glycerol stocks onto tryptone soy agar (TSA) (3% (*m/v*) TSB, 1.5% (*m/v*) agar) petri dishes and subsequently streaked out and incubated at 37 °C for 48 hours to allow for the growth of individual colonies.

*Selection of producer colonies:* To ensure that Tcn producing colonies were selected and used in subsequent experiments, a spot-on-lawn assay was done. Individual colonies were chosen and spotted onto a TSA agar petri dish in a grid like fashion so that the placement of each colony could be recorded. This plate is referred to as the seed plate. These colonies were chosen from the previously streaked out glycerol stocks, and were selected primarily based on size, with larger, darker coloured colonies being preferred. In order to determine if the selected colonies were producing tyrothricin, activity against *M. luteus* was tested for in the form of growth inhibition zones. *M. luteus* was grown

from freezer stocks on LB agar plates (1% (*m/v*) tryptone, 0.5 % (*m/v*) yeast extract, 1% (*m/v*) NaCl, 1.5 % *m/v* agar), and a colony was used to inoculate 20 mL of Luria Bertani broth (LB) (1% (*m/v*) tryptone, 0.5 % (*m/v*) yeast extract, 1% (*m/v*) NaCl). This was then incubated at 37 °C, together with an LB blank, while being mixed at 150 rpm for 16 hours to allow for an OD at 595 nm of 0.6 (representing the exponential phase of the organism's growth) to develop relative to the LB blank. This was then sub-cultured by adding 200 uL of the 0.6 culture to 20 mL of fresh LB media. This was then incubated in the same manner but only for 5-6 hrs, to again reach an OD at 595 nm of 0.6. Following incubation, the sub-cultured *M. luteus* was mixed with warm LB agar (1% (*m/v*) tryptone, 0.5 % (*m/v*) yeast extract, 1% (*m/v*) NaCl), which was allowed to cool sufficiently following autoclaving so as not to kill organism, at a ratio of 1:9 culture to LB agar. After this, 5 mL of the mixture of *M. luteus* and agar was added on top of a previously made LB agar petri dish and allowed to cool and solidify. Once cooled, colonies of the producer organism were spotted on top of the *M. luteus* using sterile pipette tips and were spotted from the same grid configuration of colonies on the original seed plate. These petri dishes were then incubated for 48 hours to allow for the growth of the colonies and the possible formation of zones of inhibition, where tyrothricin production halts the growth of *M. luteus*. The colonies with the largest inhibition zones were then used as a reference to find the original colony on the TSB plate, which was then used to create new glycerol freezer stocks.

### ***2.3.2 Production and extraction of tyrothricin***

*Production of media:* The previously optimised TGS (tryptone, glucose and inorganic salts) media was used based on a media composition developed by Lewis *et al.* (14). Due to an existing non-disclosure agreement regarding a patent surrounding the production and extraction of tyrothricin, the details of this process will be omitted. TGS media (200 mL) was added into a 2-liter Erlenmeyer flask and autoclaved at 121 °C for 25 minutes at a pressure of 100 kPa. Twelve large scale cultures were prepared to allow for triplicate productions ( $n = 3$ ) for each of the four strains used.

*Culturing and production of tyrothricin:* In order to inoculate the 200 mL, medium-scale cultures, starter cultures were made. Glycerol stocks were streaked out onto tryptone soy agar (TSA) ( plates in the same manner as previously described and grown for 48 hours to allow for colony growth. Single colonies were then used to inoculate the starter culture, which was made using 20 mL of autoclaved TSB (3% (*m/v*)) in a 50 mL Falcon<sup>®</sup> tube. Following inoculation, the starter cultures were incubated (together with a blank) at 37°C for 16 hours while shaking at 150 rpm, allowing the cultures to reach an OD at 595 nm of between 0.6 and 0.9 relative to the TSB blank. Following incubation, 2 mL of the starter culture was added to the 200 mL culture (1% *v/v*) in a sterile manner. These medium-scale

cultures were then incubated, while stationary, for a period of 10 days. On the tenth day, the cultures were stopped by acidification.

*Extraction of tyrothricin:* The initial acidification step is the first stage in tyrothricin extraction, and serves to both terminate bacterial growth and assist in cell lysis and precipitation of organic material. The details of extraction fall under the protection of a non-disclosure agreement with BIOPEP® and Stellenbosch University, and as such only the general principles will be briefly described. Following acidification, the biomass went through several extraction steps including organic solvent extraction, precipitation steps, and treatment with activated carbon. The aim is to maximise the concentration of the Trcs relative to co-extracted compounds at the end of the extraction steps. Crude extract masses were recorded.

*Analysis of extracts via UPLC-ESMS:* Aliquots obtained from the first round of extraction with organic solvent were used for ultraperformance liquid chromatography (UPLC) linked to electrospray mass spectrometry (UPLC-MS). Freeze dried samples were made up to 50 mg/mL in 50% (v/v) acetonitrile diluted with deionised analytical grade water. The samples were then centrifuged at  $8600 \times g$  for 10 minutes to remove any particulate or insoluble material from the sample. Following centrifugation, a 10 fold dilution was made using the supernatant and deionised water in a 200  $\mu$ L vial insert. An injection of 3  $\mu$ L was done using a Waters Acquity UPLC™ system and separation of Trcs and Grcs was done on an Acquity UPLC® BEH Phenyl column. The conditions for UPLC separation were as follows: a column temperature of 60 °C, a flow rate of 300  $\mu$ L/min and a linear buffer gradient using two eluents, eluent A (1% (v/v) formic acid in analytical grade deionised water) and eluent B (ACN). Table 2.1 shows the UPLC method gradient that was used.

*Table 2.1* UPLC linear gradient program used for separation of peptides during the UPLC-MS analysis of medium and small scale culture extracts

Step	% eluent B Start	% eluent B End	Time interval (min)
1	0	0	0 - 0.5
2	0	30	0.5 - 1
3	30	60	1 - 10
4	60	80	10 - 15
5	80	100	15 - 15.1
6	100	100	15.1-18

The visualization of the chromatography was done via mass spectrometry utilizing a Waters Synapt G2 mass spectrometer. Two microliters of analyte was injected and ionised via electrospray in positive mode, using a Z-spray configuration. A capillary voltage of 2.5 kV was used together with a cone voltage of 15 V at a temperature of 120 °C at the source. Desolvation gas (N<sub>2</sub>) was applied at a

rate of 650 L/hour and a desolvation temperature 275 °C. The data were acquired by scans covering a mass-to-charge ( $m/z$ ) range of 300 to 2000 in continuum mode with a rate of 0.2 scans per second.

### 2.3.3 Bacterial growth using variable nutrient sources

*Growth curves for nitrogen and sulphate sources:* Using TGS as a base media, different nitrogen or sulphate sources were added over a range of concentrations and the effect on the growth rate of producer organism was recorded. A four times concentrated solution of TGS media was made to allow for dilution with analytical grade water and the variable nitrogen and/or sulphate source. For the nitrogen sources, stocks of 100 g/L urea ( $\text{CO}(\text{NH}_2)_2$ ) and ammonium sulphate ( $(\text{NH}_4)_2\text{SO}_4$ ) were used. The ammonium sulphate served both as a nitrogen and sulphate sources, while sodium sulphate ( $\text{Na}_2\text{SO}_4$ ) was used as a sulphate source only. All stocks were sterilised by autoclaving in Falcon<sup>®</sup> tubes. In a 96-well microtiter plate, 50  $\mu\text{L}$  of concentrated TGS was added to all wells after which the stock solutions of urea, ammonium sulphate or sodium sulphate were added. In addition, a combination of both urea and sodium sulphate was used. A range of concentrations was used starting at 0.4 g/L going up to 8.0 g/L. In the case of the urea and sodium sulphate combination, one concentration range used a fixed urea concentration of 5 g/L urea together with variable sodium sulphate, while another used a fixed sodium sulphate concentration of 2.5 g/L combined with a variable urea concentration. TGS on its own was used as both a standard to measure growth under unmodified conditions and as a blank to check for contamination of the base media. To get TGS and the added nitrogen or sulphate sources to the correct concentration sterilised analytical grade water was added to the wells for a final volume of 200  $\mu\text{L}$  per well. Overnight starter cultures of the 5618, 362 and 8185 strains were made by inoculating TSB (3% ( $m/v$ ) dissolved in analytical grade water) media with a colony of the producer organism and incubating at 37 °C for 16 hours. After reaching an OD at 595 nm of between 0.6 and 0.9 the starter culture was diluted with TSB to an OD of 0.2. Ten microliters of the diluted starter culture was added to each well with the exception of the blank, where 10  $\mu\text{L}$  of the sterile blank was added. Three replicates were done for ammonium sulphate ( $n = 3$ ), four for sodium sulphate ( $n = 4$ ), four for urea ( $n = 4$ ), 6 for variable sodium sulphate and fixed urea ( $n = 6$ ) and 5 for variable urea and fixed sodium sulphate ( $n = 5$ ). Plates were incubated at 37 °C and their OD at 595 nm was read every hour for the first 8 hours and then at 10 and 12 hours using a BioRad<sup>™</sup> Model 680 microplate reader.

*Growth curves for carbon sources:* Here the tryptone and salts from TGS were used but glucose was removed to allow for the addition of variable glucose (Glc) or glycerol (Glr) concentrations (or a combination of the two). Stock solutions of 50% ( $m/v$ ) Glc and Glr were sterilised via autoclaving. A four times concentrated solution of tryptone and salts (TS) was made to allow for dilution with Glc



and/or Glr and analytical-grade water. A concentration range for Glc was used ranging from 10 g/L to 45 g/L while a Glr concentration range of 12.6 g/L to 94.5 g/L was used. A fixed Glc concentration of 30 g/L together with a variable Glr concentration range was also used as well as a fixed Glr concentration of 63 g/L together with a variable Glc concentration. Concentrated Glc or Glr was added to the appropriate wells followed by the addition of 50  $\mu$ L of four times concentrated TS and finally analytical grade water. A final volume of 200  $\mu$ L was used in each well. The growth control and the blank used TS together with a Glc concentration of 30 g/L. Overnight night cultures of the three strains were made and added to the wells in the same manner as for the nitrogen and sulphate sources. OD readings were taken at 595 nm for the first 8 hours then at 10 and 12 hours using a BioRad<sup>TM</sup> microtiter plate reader. Six replicates ( $n = 6$ ) were done for Glc and five for Glr ( $n = 5$ ). Five repeats were done for the variable Glr and fixed Glc ( $n = 5$ ) and six for variable Glc and fixed Glr ( $n = 6$ ).

*Generating growth rates from growth curves:* Using the growth curves generated from change in optical density over time, growth rates could be calculated. The steepest, linear section of this growth curve, which lies between the lag phase and the stationary phase, represents the exponential growth rate where maximal bacterial growth occurs. For each nitrogen, sulphate or carbon source a maximum number of data points were chosen within the linear section of the exponential phase. After this a linear regression was used to generate a first-order polynomial equation (i.e. straight line) using the data points. The gradient of this line represents the growth rate and is expressed in change in OD at 595 nm per hour. A growth rate was generated for each analytical repeat and the mean of the repeats was calculated.

### ***2.3.4 Small scale cultures using optimised growth conditions***

*Deep well assay:* To assess the correlation between growth rate and tyrothricin production, small scale medium-throughput stationary cultures were done in 96-well deep well plates using urea as an additional nitrogen source. This was chosen after determining that urea produced, overall, the most significant effect on growth rate for both the nitrogen and sulphate sources. Concentrations of 1 g/L, 4 g/L and 8 g/L were chosen to represent below optimal growth rate, optimal growth rate, and above the concentration that produced optimal growth rate respectively. No additional sulphate source was used and a glucose concentration of 35 g/L was used for the 5618 strain while 30 g/L was used for the 8185 and 362 strains. These glucose concentrations were selected based on growth rate. Again, a four-fold concentrated solution of TGS was made up (with 3.5 % ( $m/v$ ) Glc concentration being chosen for the 5618 strain). Two-hundred and fifty microliters of TGS was added to each well, together with glucose. Five microliters, 20  $\mu$ L or 40  $\mu$ L of concentrated urea stock solution (50%



(*m/v*) was then added and finally analytical grade, deionised water was added to a final volume of 500  $\mu\text{L}$ . TGS on its own was used as a growth and peptide production control. Starter cultures were made as previously described and 10  $\mu\text{L}$  were used to inoculate each well. The deep-well plates were incubated for 10 days at 37 °C while remaining stationary. On the tenth day, the cultures were acidified and extracted.

*Extraction and ESMS analysis of deep well extracts:* Following the 10 days of incubation the cultures were acidified using HCl to a pH of 4. After 3 hours, the cultures were spun down for 20 minutes at  $3000 \times g$ . The supernatant was removed, and the pellet was freeze-dried to get the cell mass. The cell mass was then extracted using 50% ACN for 30 minutes while sonicating. The extracts were then spun down again for 30 minutes at  $3000 \times g$  after which the supernatant was collected and freeze dried. After freeze drying the mass was recorded. The samples were then made up to 1 mg/mL using 50% ACN and analytical grade water and spun down to remove insoluble material and particulate. The supernatant was removed and placed into a glass insert for ESMS analysis on a Waters Synapt G2 mass spectrometer.

## 2.4 Results

### 2.4.1 Extraction and UPLC-MS analysis of different producer strains

The two tyrocidine producer strains of *Br. parabrevis* used for Tcn production in our lab are *Br. parabrevis* ATCC 10068 and *Br. parabrevis* ATCC 8185. Two more strains, *Br. parabrevis* DSMZ 362 and *Br. parabrevis* DSMZ 5618, became available for use in tyrocidine production. Variability in strain production profiles has been observed in addition to growth media composition (22). UPLC-MS analysis was done on medium-scale culture extracts using the different strains to determine if there were strain-dependant differences in their production profiles.

TGS (tryptone, glucose, inorganic salts) media was used in these experiments and has been shown to give tyrothricin yields in the order of 2-3 g/L for stationary, 200 mL cultures grown in 2 litre Erlenmeyer flasks (22). Table 2.2 shows the yields of extracts of the medium-scale cultures for the four strains used. The 8185 strain gave the highest yield 770.6 mg, followed by the 5618 and 362 strains, which gave similar yields of around 650 mg, and lastly the 10068 strain, which produced under half the yield of the 5618 and 362 strains and just over a quarter of the 8185 strain yield.

*Table 2.2* Three rounds of extraction using organic solvent were done for each biological repeat giving the mean freeze-dried extract mass and the SEM

Strain	10068	5618	362	8185
Extract	Extract Mass (mg)/200 mL culture ( $n=3$ ; $\pm$ SEM)			
1	166.1 $\pm$ 14.9	505.7 $\pm$ 20.4	436.7 $\pm$ 96.1	557 $\pm$ 98
2	35.6 $\pm$ 5.7	97 $\pm$ 6.6	140.4 $\pm$ 66.4	156.6 $\pm$ 15.1
3	13.9 $\pm$ 2.8	62 $\pm$ 32.7	56.8 $\pm$ 27.4	57 $\pm$ 9
Total	215.6	664.7	633.9	770.6

The percentage contribution of each analogue to the total area-under-curve can be seen in Table 2.3. This gives a clearer indication of the relative production of each tyrocidine analogue for each strain. Here the superior production of C-analogues by 5618 can clearly be seen, with TpcC and TrcC<sub>1</sub> showing the largest increase in production relative to the other tryptophan containing analogues. For the B-analogues there was no strain that had a clearly superior production profile.

The 362 strain showed the best TpcB<sub>1</sub> and TrcB<sub>1</sub> production, perhaps indicating a preference for incorporation of a lysine residue over an ornithine residue. For TpcB, the 8185-strain showed a marginally better production over 10068 while 10068 produced the highest relative amount of TrcB. The 362 strain showed the best overall production of the A analogues with the exception of TrcA, where the 10068-strain showed the best production.

Figure 2.1 shows the UPLC-MS chromatograms of the extracts, with ESMS and area-under-curve (AUC) being used to determine the relative contributions of each Trc analogue to the entire production profile.

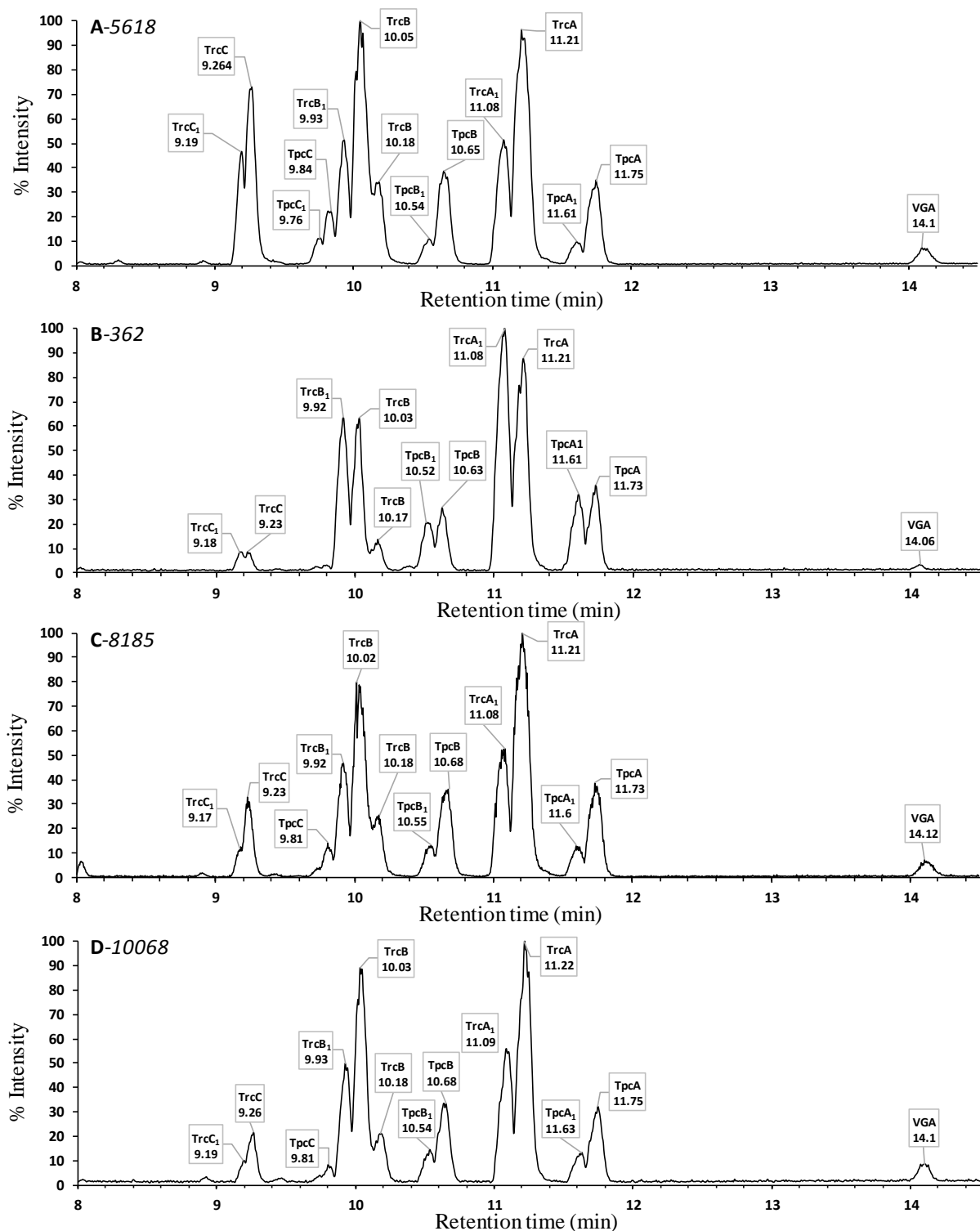


**Figure 2.1** UPLC-MS analysis of the first round of culture extraction using organic solvent. The first repeat was used from of the four strains as a representative base-peak intensity (BPI) UPLC chromatogram. Freeze-dried extracts were dissolved in 2.5% ACN and separated on a reverse phase BEH Phenyl column linked to ESMS to determine the  $m/z$  and subsequent peptide identity for each peak, which is shown above the retention time for each peak. The height of each peak is given as percentage signal intensity relative to the highest peak signal intensity in the chromatogram. Letters correspond with, **A**, *Br. parabrevis* 5618, **B**, *Br. parabrevis* 362, **C** *Br. parabrevis* 8185 and **D** *Br. parabrevis* 10068

**Table 2.3** The first round of extractions was analysed via UPLC-ESMS to give the mean area-under-curve and SEM for each of the major tyrocidine analogues detected. The detected  $m/z$  ratio represent ionization of the analyte by two protons. One injection was done for each extract. The expected theoretical mass is shown in the last column (See thesis addendum for complete list of theoretical Trc masses)

Strain	10068		5618		362		8185		Theoretical $m/z$ (Doubly charged)
	Average AUC $\pm$ SEM ( $n=3$ )	Detected $m/z$ (Doubly charged)	Average AUC $\pm$ SEM ( $n=3$ )	Detected $m/z$ (Doubly charged)	Average AUC $\pm$ SEM ( $n=3$ )	Detected $m/z$ (Doubly charged)	Average AUC $\pm$ SEM ( $n=3$ )	Detected $m/z$ (Doubly charged)	
TpcC <sub>1</sub>	1.1 $\pm$ 0.24	693.3624	2.5 $\pm$ 0.4	693.3624	1 $\pm$ 0.03	693.3624	1.4 $\pm$ 0.06	693.3624	693.3618
TpcC	1.7 $\pm$ 0.09	686.3550	3.7 $\pm$ 0.52	686.3550	0.8 $\pm$ 0.02	686.3549	2.6 $\pm$ 0.1	686.3550	686.3540
TrcC <sub>1</sub>	3.7 $\pm$ 0.17	681.8551	6.4 $\pm$ 0.58	681.8551	2.8 $\pm$ 0.16	681.8550	3.2 $\pm$ 0.06	681.8551	681.8539
TrcC	6.2 $\pm$ 0.21	674.8494	10.9 $\pm$ 0.91	674.8494	Trace	674.8494	6.8 $\pm$ 0.05	674.8494	674.8460
TpcB <sub>1</sub>	2.6 $\pm$ 0.18	673.8541	1.9 $\pm$ 0.08	673.8628	6.8 $\pm$ 0.28	673.8628	2.8 $\pm$ 0.07	673.8628	673.8564
TpcB	8 $\pm$ 0.71	666.8533	7.3 $\pm$ 0.07	666.8533	5.5 $\pm$ 0.01	666.8533	8.2 $\pm$ 0.18	666.8533	666.8486
TrcB <sub>1</sub>	11.1 $\pm$ 0.86	662.3500	8.8 $\pm$ 0.23	662.3505	14.5 $\pm$ 0.48	662.3505	10.8 $\pm$ 0.17	662.3505	662.3484
TrcB	22.4 $\pm$ 0.73	655.3342	21.5 $\pm$ 0.58	655.3453	14.8 $\pm$ 0.18	655.3453	20.6 $\pm$ 0.48	655.3453	655.3406
TpcA <sub>1</sub>	2.6 $\pm$ 0.24	654.3508	1.8 $\pm$ 0.11	654.3508	6.17 $\pm$ 0.21	654.3508	2.8 $\pm$ 0.15	654.3508	654.3509
TpcA	7.9 $\pm$ 0.77	647.3439	6.9 $\pm$ 0.31	647.3439	8.49 $\pm$ 0.38	647.3439	8.3 $\pm$ 0.28	647.3493	647.3431
TrcA <sub>1</sub>	9.4 $\pm$ 1.22	642.8411	8 $\pm$ 0.25	642.8411	18.05 $\pm$ 0.5	642.8411	10.6 $\pm$ 0.46	642.8411	642.8430
TrcA	21.9 $\pm$ 0.87	635.8411	19.1 $\pm$ 1.24	635.8411	18.96 $\pm$ 1.45	635.8411	20.4 $\pm$ 0.28	635.8411	635.8351
PhcA	1.3 $\pm$ 0.07	627.8395	1.1 $\pm$ 0.09	627.8395	1.59 $\pm$ 0.1	627.8395	1.4 $\pm$ 0.03	627.8395	627.8377

#### 2.4.2 Growth rate analysis of selected strains under varying nutrient conditions

The variable nitrogen or carbon sources used were all added on top of the TGS media, which was used as a base media for media modification as well as a control on its own to look at the relative effect of the additional nitrogen source. In the case of the carbon source, the 3% glucose used in TGS was replaced with the variable carbon source, being glucose or glycerol.

In terms of nitrogen and sulphate sources, three sources were tested: ammonium sulphate ((NH<sub>4</sub>)<sub>2</sub>SO<sub>4</sub>) as a nitrogen source and sulphate source, sodium sulphate (Na<sub>2</sub>SO<sub>4</sub>) as a sulphate source,

and urea ( $\text{CO}(\text{NH}_2)_2$ ) as a nitrogen source. These three compounds were tested on their own at different concentrations on top of the base media. In addition, varying concentrations of  $\text{Na}_2\text{SO}_4$  were tested in conjunction with a fixed concentration of urea (5 g/L). Inversely, variable concentrations of urea were tested together with a fixed concentration of  $\text{Na}_2\text{SO}_4$  (2.5 g/L). Glucose and glycerol were used at varying concentrations and their effect on growth rate recorded. In addition, a variable concentration of glucose was used with a fixed glycerol concentration of 63.5 g/L while a fixed concentration of glucose (30 g/L) was used together with a variable glycerol concentration.

To assess the effects of altering nitrogen, sulphate and carbon sources on the available producer strains, growth curves were done to determine exponential-phase growth rates under a range of concentrations for a given nitrogen, sulphate or carbon source, represented as the natural logarithmic change in optical density per hour at 595 nm wavelength, or  $\Delta \ln \text{OD}_{595}/\text{hour}$ . Only three concentrations were chosen over the range of concentrations used (8 in total). These concentrations represent the low, middle and high end of the concentrations range used.

While four strains were available for use it was decided that the 10068-strain would be omitted as its growth and production profile has already been extensively characterised by Vosloo *et al* (22). The results of these growth curves for the 5618, 362 and 8185 strains are given below in Figure 2.2 and Figure 2.4. While one cannot assume that a relatively high growth rate will result in high levels of peptide production, it does provide a more rapid method of testing which nitrogen, sulphate or carbon sources and concentrations will sustain bacterial growth. It is in fact hypothesized that the highest yields of peptide occur when the producer organism is put under nutrient limiting conditions to mimic a stressful or competitive environment (24, 25).

A large variation in concentrations of nitrogen sources appeared to be well tolerated across the concentration range for all three strains (Figure 2.2) with the 5618 strain showing the smallest deviation in growth rates (Figure 2.2, A). Overall,  $\text{CO}(\text{NH}_2)_2$  produced the highest growth rates with the exception of the 8185-strain, where it was difficult to elucidate a clearly superior nitrogen and/or sulphate source. The 5618-strain responded most positively to an increase in concentration of  $\text{CO}(\text{NH}_2)_2$  together with a fixed concentration of 2.5 g/L  $\text{Na}_2\text{SO}_4$ .  $\text{Na}_2\text{SO}_4$  and  $(\text{NH}_4)_2\text{SO}_4$  alone gave the lowest relative growth rates, however, the 8185 strain again seemed to not show a preference for these compounds in terms of its growth rate. In terms of the positive control (representing the unmodified TGS base-media) the 8185-strain showed the clearest preference for TGS alone as a growth medium. This is expected as this strain was used for media optimisation (for Trc production) that resulted in the TGS media composition.

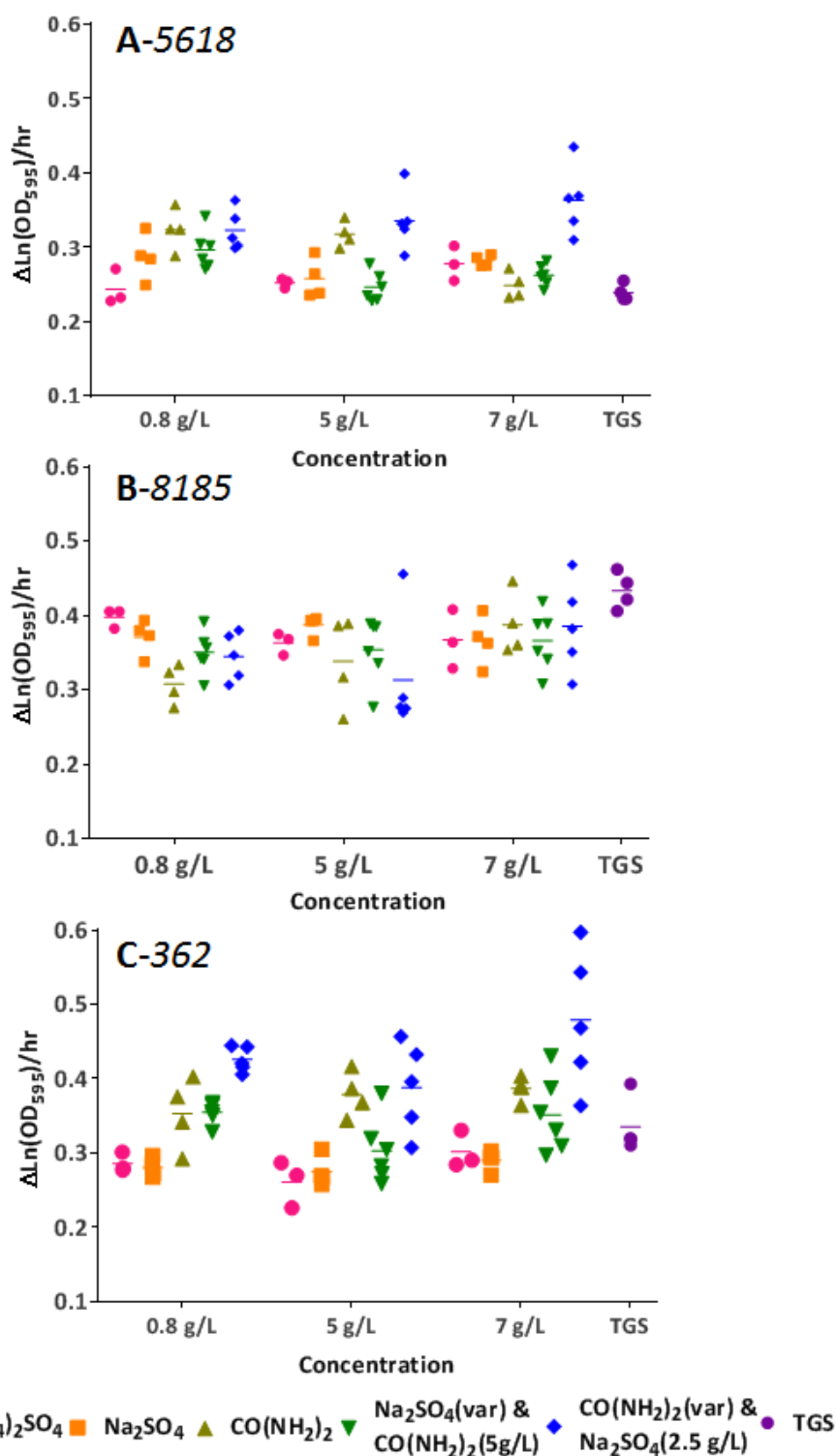
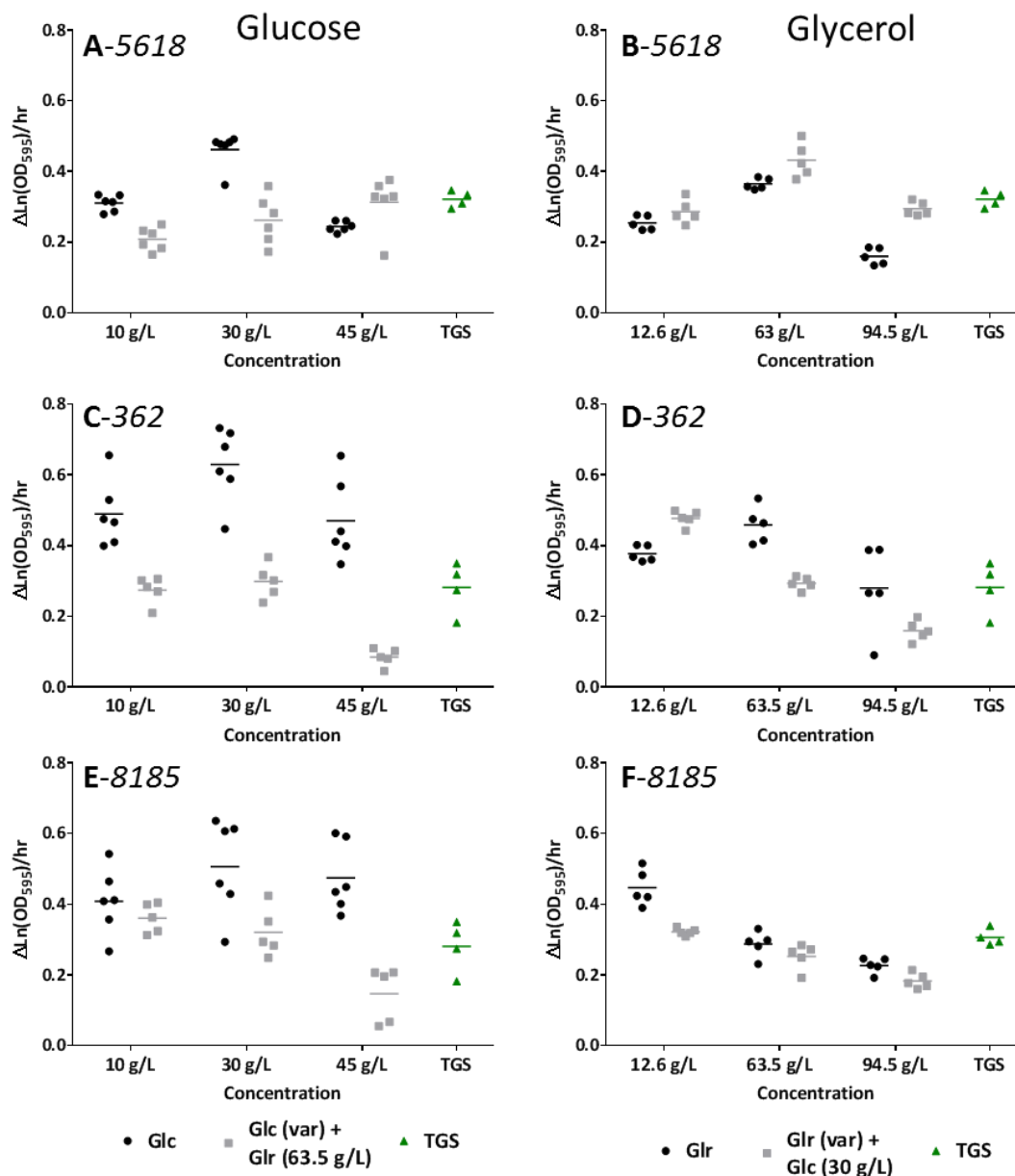


Figure 2.2 Selected growth rates calculated from exponential growth rates for each growth curve. Scattered points represent repeats for each concentration while the line of the same colour represents the mean of the repeats. Three concentrations were chosen to represent the low, middle and high end of the concentration range used. TGS media was used as a control for growth under unmodified conditions. Letters represent growth rates for strains, **A** 5618, **B**, 8185 and **C**, 362 under the same set of nutrient conditions

For the 5618 and 362 strains, urea ( $\text{CO}(\text{NH}_2)_2$ ) alone, and variable urea concentration together with 2.5 g/L sodium sulphate ( $\text{Na}_2\text{SO}_4$ ) led to the increase in growth rate relative to TGS alone. Genetic variation in the 5618 and 362 strains may lead to an altered metabolism and a unique ability to utilise these tested nitrogen and sulphate sources in a preferential manner. In most cases, the spread of growth rate data was clustered, indicating similar responses in the cultures (Figure 2.2). However, some growth rates, such as those determined with mixtures of urea and sodium sulphate, gave a large spread in growth rate values which made it difficult to elucidate the difference in growth rates between nitrogen/sulphate sources used for a given strain.

For the 5618 strain Glc appeared to be a preferable carbons source, exemplified by the fact that the addition of Glr to a variable Glc concentration led to a reduced growth rate (Figure 2.3, A) (with the exception of the 45 g/L Glc, where the addition of Glr led to an increased growth rate), while the addition of Glc to a variable Glr concentration led to an increase in growth rate relative to glycerol alone (Figure 2.3, B). For the 362 and 8185 strains Glr again led to a reduction in growth when added to a variable Glc concentration, however, unlike 5618, both 362 and 8185 preferred Gly alone compared to the addition of a 30 g/L Glc (with the exception of the 12.6 g/L Glr for the 362-strain, (Figure 2.3, D)). Looking at growth rates using Glc between strains we can see that the 362-strain appears to produce the highest growth rates, albeit with a large relatively larger spread of data points. The 362 strain also has the largest difference between variable Glc concentrations and variable Glc concentrations with the addition of Glr. The addition of Glr to Glc reduced growth rate at all Glc concentrations for all three strains used (Except for 45 g/L Glc mixed with Glr). In addition, a Glc concentration of 30 g/L (representing the middle of the concentration range used) lead to the best growth rates overall.

Looking at Glr alone, a concentration of 63.5 g/L appeared to produce the best growth rate, with the exception of the 8185-strain where a concentration of 12.6 g/L was superior. The 8185-strain appeared to be the least tolerant to Glr with a steady decline in growth rate as Glr concentration increased.



*Figure 2.3* Selected growth rates calculated from exponential growth rates for each growth curve. Scattered points represent repeats for each concentration while the line of the same colour represents the mean of the repeats. Three concentrations were chosen to represent the low, middle and high end of the concentration range used. The left column represents variable Glc concentrations while the right represents variable glycerol concentrations. TGS media was used as a control for growth under unmodified conditions

Besides the quantitative assessment of growth rate, the shape of the growth curves under varying conditions could also be inspected. The large difference between some of the growth rates is due to the fact that some of the technical repeats entered a clear logarithmic growth phase after a short lag phase while others showed a markedly slower growth rate over the same time period. Some repeats showed a growth curve more characteristic of diauxic growth. Diauxic growth can be attributed to a



metabolic change in nutrient preference of the growing bacteria. Eventually, the bacteria adapt to the media and surrounding environment after a period of slow growth, as observed by Vosloo (23). In these cases, bacteria will generally reach a similar OD in the stationary phase as the bacterial populations which showed a more typical exponential growth curve. The growth rates however represent the average change in optical density over a time period at which most repeats showed clear exponential growth. Figure 2.4, A, gives some examples of growth curves considered as having only one exponential phase, versus examples of growth curves showing at least two exponential phases (Figure 2.4, B). Table 2.4 shows the lag time and number of diauxy (as well as the number of repeats) following visual inspection of the growth curves under varying growth conditions.

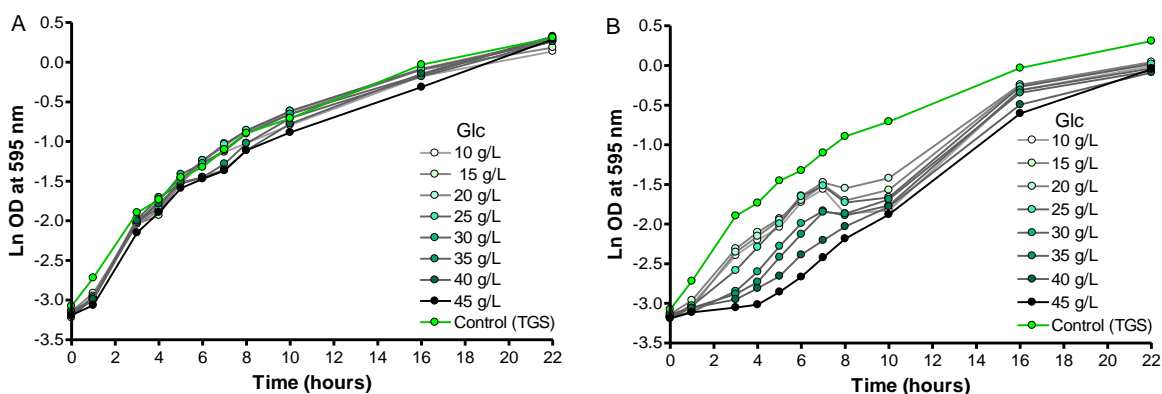


*Figure 2.4* Selected growth curves from *Br. parabrevis* 362. **A**, an example of a normal growth curves with varying glucose concentration and **B** growth curves with more than one apparent exponential growth phase showing a diauxy-type metabolic response. The growth curves in B was generated under varying glucose concentrations together with a fixed glycerol concentration of 63.5 g/L

**Table 2.4** Summary of the conditions, number of repeats, lag times and number of exponential growth phases observed (represented in the Diauxy column) for selected growth curves. The growth rates were determined using the first apparent exponential growth phase following the lag phase

5618					362				
Compound added	Concentration (g/L)	<i>n</i>	Lag Time (hrs)	Diauxy	Compound added	Concentration (g/L)	<i>n</i>	Lag Time (hrs)	Diauxy
(NH <sub>4</sub> ) <sub>2</sub> SO <sub>4</sub>	0.8	3	2	2-3	(NH <sub>4</sub> ) <sub>2</sub> SO <sub>4</sub>	0.8	3	1-2	(NH <sub>4</sub> ) <sub>2</sub> SO <sub>4</sub>
	5	3	2	2		5	3	1-2	
	7	3	2	2		7	3	2-3	
Na <sub>2</sub> SO <sub>4</sub>	0.8	4	2	2-3	Na <sub>2</sub> SO <sub>4</sub>	0.8	4	1-2	Na <sub>2</sub> SO <sub>4</sub>
	5	4	2	2-3		5	4	2-3	
	7	4	2-3	2-3		7	4	2-3	
CO(NH <sub>2</sub> ) <sub>2</sub>	0.8	4	2-3	1-2	CO(NH <sub>2</sub> ) <sub>2</sub>	0.8	4	2-3	CO(NH <sub>2</sub> ) <sub>2</sub>
	5	4	2-3	1-2		5	4	2	
	7	4	3-4	1		7	4	2-3	
Na <sub>2</sub> SO <sub>4</sub> (var) + CO(NH <sub>2</sub> ) <sub>2</sub> (5 g/L)	0.8	6	2	1-2	Na <sub>2</sub> SO <sub>4</sub> (var) + CO(NH <sub>2</sub> ) <sub>2</sub> (5 g/L)	0.8	6	1-2	Na <sub>2</sub> SO <sub>4</sub> (var) + CO(NH <sub>2</sub> ) <sub>2</sub> (5 g/L)
	5	6	2	1		5	6	1-2	
	7	6	2	1-2		7	6	2-3	
CO(NH <sub>2</sub> ) <sub>2</sub> (5 g/L) + Na <sub>2</sub> SO <sub>4</sub> (var)	0.8	5	2-3	1-2	CO(NH <sub>2</sub> ) <sub>2</sub> (5 g/L) + Na <sub>2</sub> SO <sub>4</sub> (var)	0.8	5	1-2	CO(NH <sub>2</sub> ) <sub>2</sub> (5 g/L) + Na <sub>2</sub> SO <sub>4</sub> (var)
	5	5	2-3	2		5	5	2-3	
	7	5	2-3	1-2		7	5	2-3	
Glc	10	6	3-4	1	Glc	10	6	0-1	Glc
	30	6	5	1-2		30	6	1-2	
	45	6	7	1		45	6	2	
Glr	12.6	5	3	1	Glr	12.6	5	0-1	Glr
	63	5	4-5	1-2		63	5	2	
	94.5	5	4-5	1		94.5	5	1-2	
Glr (var) + Glc (30 g/L)	12.6	5	4	1	Glr (var) + Glc (30 g/L)	12.6	5	0-1	Glr (var) + Glc (30 g/L)
	63	5	6-7	1		63	5	1-2	
	94.5	5	7-9	1		94.5	5	5-6	
Glc (var) + Glr (63 g/L)	10	6	5-6	1	Glc (var) + Glr (63 g/L)	10	6	0-1	Glc (var) + Glr (63 g/L)
	30	6	6-7	1		30	6	1-2	
	45	6	7-8	1		45	6	2-3	
<b>8185</b>									
(NH <sub>4</sub> ) <sub>2</sub> SO <sub>4</sub>	0.8	3	0-1	2	Glc	10	5	1	Glc
	5	3	0-1	2		30	5	1-2	
	7	3	0-1	2		45	5	1-2	
Na <sub>2</sub> SO <sub>4</sub>	0.8	4	0-1	2	Glr	12.6	5	1	Glr
	5	4	0-1	1		63	5	1	
	7	4	0-1	2		94.5	5	1	
CO(NH <sub>2</sub> ) <sub>2</sub>	0.8	4	1-2	1	Glr (var) + Glc (30 g/L)	12.6	5	0-1	Glr (var) + Glc (30 g/L)
	5	4	1-2	1-2		63	5	0-1	
	7	4	0-1	1		94.5	5	1	
Na <sub>2</sub> SO <sub>4</sub> (var) + CO(NH <sub>2</sub> ) <sub>2</sub> (5 g/L)	0.8	6	1-2	2	Glc (var) + Glr (63 g/L)	10	6	0-1	Glc (var) + Glr (63 g/L)
	5	6	0-1	1-2		30	6	0-1	
	7	6	1-2	2-3		45	6	0-1	
CO(NH <sub>2</sub> ) <sub>2</sub> (5 g/L) + Na <sub>2</sub> SO <sub>4</sub> (var)	0.8	5	2-3	1-2	CO(NH <sub>2</sub> ) <sub>2</sub> (5 g/L) + Na <sub>2</sub> SO <sub>4</sub> (var)	0.8	5	2-3	CO(NH <sub>2</sub> ) <sub>2</sub> (5 g/L) + Na <sub>2</sub> SO <sub>4</sub> (var)
	5	5	1-2	1		5	5	1-2	
	7	5	1-2	1		7	5	1-2	

### ***2.4.3 Small-scale culture extraction and ESMS analysis using selected nutrient conditions***

As mentioned earlier, one cannot necessarily presume that an optimised growth rate in a microtiter equates to increased yields of peptides under larger scale culture conditions. A medium-throughput assay done in deep well 96-well plates (in which peptides are eventually extracted and analysed) provides a better approximation of peptide production and can also be used to test different media compositions. Using growth rates as a preliminary indication of media composition on bacterial growth, one can pick a set of conditions to be used in the deep well assay. In this case both carbon and nitrogen concentrations were chosen at points which produce below optimal growth, optimal growth, and above optimal growth.

The 5618-strain was more sensitive to an increase in urea concentration, with a decline in detected signal intensities as the urea concentration increased. The opposite was true for the 8185 and 362 strains, which showed increasing peptide intensities as urea concentration increased. In terms of the TGS control, the 8185-strain showed a clear preference, with moderate levels of production in the 362 and 8185-strain.

Figure 2.5 represents the peptide production profiles of the major tyrocidines and analogues under growth conditions selected from the growth curve data, while Table 2.5 shows the cell and extract mass of the deep-well cultures. The 362-strain showed poor production under the selected conditions when compared to the 5618 and 8185 strains. The 5618-strain produced a more diverse production profile and produced and was only able to produce detectable amounts of TrcA<sub>1</sub> at lower urea concentrations of 1 g/L. The 8185-strain also produced TrcA<sub>1</sub> at 1g/L urea but preferred an increasing amount of urea, producing higher ESMS signal intensities.

In terms of extract masses (Table 2.5), the 5618-strain had the best response to urea in terms of cell mass and extract mass, specifically with an addition of 8 g/L urea. Relative to the TGS control, the 5618-strain produced, 34% more cell mass and 44% more extract mass at 8g/L urea. The 362-strain responded poorly to increasing urea concentration, with both a decrease in cell mass and extract mass. Only a urea concentration of 1 g/L led to an increase in extract yield over that of TGS for the 362-strain. The 8185-strain also responded well to an increase in urea concentration, but the difference between TGS yields and urea at 8 g/L were not as pronounced as the 5618-strain, with the large standard deviation making differences insignificant.

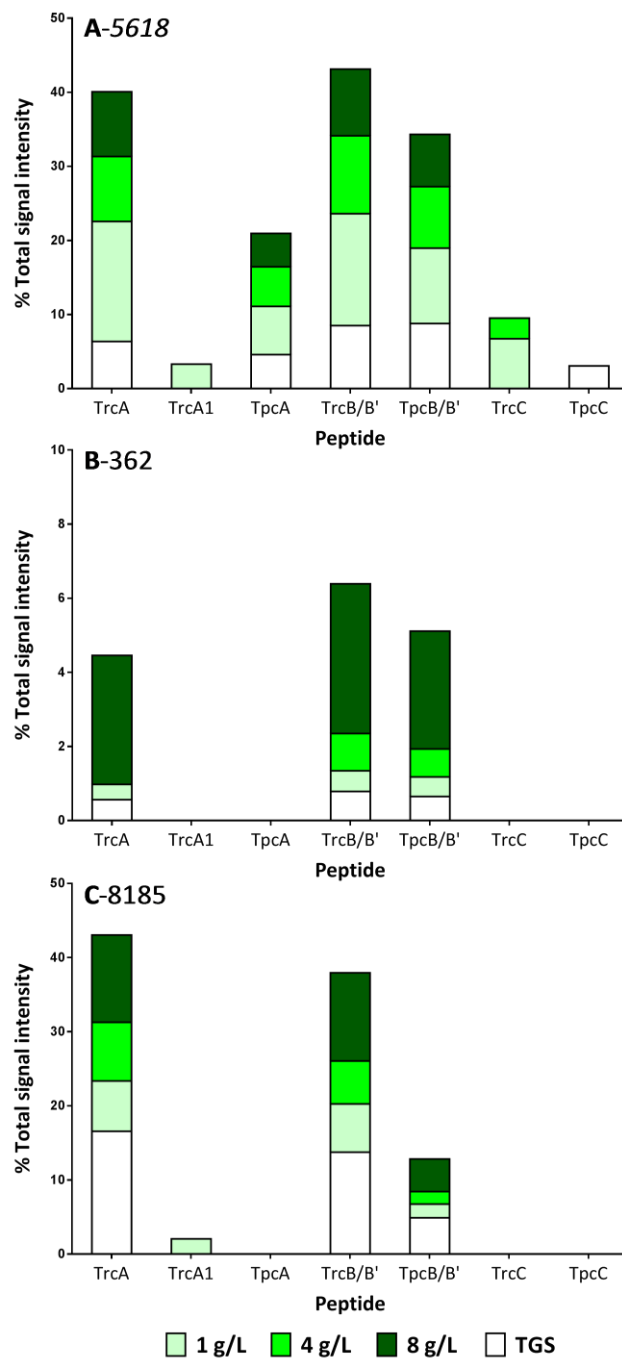


*Figure 2.5* Direct injection ESMS analysis of the tyrocidine analogue production profile of deep-well extracts. Media contained TGS together with 1 g/L, 4g/L and 8 g/L respectively of urea. Analysis was done in duplicate with 6 wells being combined and extracted together for each replicate under each growth condition. The y-axis represents the signal intensity produced by the tyrocidine analogue compared to the total signal of all compounds detected via ESMS in the sample. Letters in bold represent the strains used (**A**: 5618, **B**: 362, **C**: 8185) under the same nutrient conditions

*Table 2.5* Deep-well extraction masses for the 5618, 326 and 8185 strains under varying urea concentrations on top of TGS together with TGS alone as a control. Six deep-well wells were combined per replicate for a total of two replicates per condition. Cell mass of culture after acidification, centrifugation and lyophilization of pellet is shown together with the standard deviation (SD). Extract mass represents lyophilized mass of the supernatant following extraction of cell mass, also shown with SD. Colour codes correspond with those in Figure 2.5

Strain	5618			326			8185		
Urea (g/L)	Cell Mass (mg) (n=2; ± SD)*	Extract mass (mg)*	Ratio - Extract Mass: Cell mass	Cell Mass (mg)*	Extract mass (mg)*	Ratio - Extract Mass: Cell mass	Cell Mass (mg)*	Extract mass (mg)*	Ratio - Extract Mass: Cell mass
1	9.4 ± 1.9	7.4 ± 2.5	0.79	9.4 ± 1.1	7.5 ± 1.2	0.8	9.8 ± 0.3	8.3 ± 0.2	0.84
4	8.5 ± 2.2	6.6 ± 0.2	0.77	6.7 ± 0.4	5.4 ± 0.2	0.8	10.1 ± 1.7	8.6 ± 1.8	0.85
8	11.5 ± 1.8	10.3 ± 1.1	0.89	5.6 ± 0.3	4.5 ± 0.2	0.8	11 ± 3.3	8.8 ± 3.5	0.8
TGS	7.5 ± 2.1	5.8 ± 2	0.78	6.9 ± 0.4	5.6 ± 0.8	0.81	11.4 ± 1.3	8.2 ± 2.5	0.72

## 2.5 Discussion

There is a clear difference in the Trc production profiles of different strains of the producer organism, using TGS media, as exemplified by the UPLC chromatograms and AUC (Figure 2.1 & Table 2.2). Since strain differences in GS production have been observed (26, 27), it is likely that variability in Trc production by different strains would occur, especially due to the similar synthesis mechanisms and overlapping use of common amino acids.

In addition to production profiles using the same media between strains, the same argument for variable production of Trcs analogues under altered nutritional requirements can be made. This is clearly observed by both the growth rates of the different organisms (Figure 2.2 and Figure 2.3) and the production profiles determined by ESMS-analysis of deep-well extracts (Figure 2.5). Of particular interest is the 5618-strain, which possessed what could be described as a good nutritional and peptide production flexibility. This strain utilised varying nitrogen, sulphate and carbon source compositions well in relation to the 8185 and 362-strains, and produced the major tyrocidines in easily detectable amounts for almost all growth conditions selected (Figure 2.5).

The 5618-strain showed an increase in growth rate from the highest urea concentration to the lowest urea concentration, with the lowest concentration's growth rate being higher than the TGS control, indicating that this strain may benefit from exploration of additional nitrogen sources to improve yields. The 8185-strain showed an increase in growth rate from low to high urea concentrations, with the growth rate moving towards that of TGS. TGS produced the both the best growth rate and best Trc production profile in terms of signal intensities for the 8185-strain. This, together with no clear trend for the other nitrogen and/or sulphate sources on growth rate, indicates that there may not be much room for optimisation of the TGS media for peptide production in the 8185-strain. This is to be expected as most of the work done on optimisation of production in previous literature was done with this strain, with the creation of the TGS being based on such research (23). While it was difficult to observe a clear growth rate trend for either urea or the nitrogen and sulphate sources used for the 362-strain, the increase in urea concentration showed a marked effect on the Trc production profile, producing increased signal intensities as urea concentration increased.

The extract yields for 5618, for both cell mass and following extraction with 50% ACN, were improved at the highest urea concentration of 8 g/L. This and the TGS yields for the 8185 strain, were the top producing strains and conditions.

The importance of a complex nitrogen source described by previous investigators is supported (14, 28). In this case tryptone served this role, and provided an adequate base on which to test various other nitrogen sources, sulphate sources and carbon sources. Glycerol served as a rather poor carbon source compared to glucose, which was effective in the concentration similar to that reported by Lewis *et al* (14), particularly when combined with tryptone. The concentration of 3% Glc used in the TGS base media is adequate and any deviation from this is unlikely to produce any significant change in Trc production.

After exploring the difference occurring in both growth rate and peptide production under different nutrient conditions, the 5618-strain was chosen going forwards for both its good response to urea in terms of growth rate and peptide production, and its relatively high production of Trp containing Trc analogues. This was of particular interest as the first non-natural amino acid tested in the next chapter was the Trp derivative 5-methyl-tryptophan.

## 2.6 References

1. Dubos, R. J., and Hotchkiss, R. D. (1941) The production of bactericidal substances by aerobic sporulating bacilli. *J. Exp. Med.* **73**, 629–640
2. Hotchkiss, R. D., and Dubos, R. J. (1941) The isolation of bactericidal substances from cultures of *Bacillus Brevis*. *J. Biol. Chemistry.* **141**, 155–162
3. Tang, X-J., Thibault, P., and Boyd, R. K. (1992) Characterisation of the tyrocidine and gramicidin fractions of the tyrothricin complex from *Bacillus brevis* using liquid chromatography and mass spectrometry. *Int. J. Mass Spectrom. Ion Process.* **122**, 153–179
4. Kambe, M., Sakamoto, Y., and Kurahashi, K. (1971) Biosynthesis of tyrocidine by a cell-free enzyme system of *Bacillus brevis* ATCC 8185 IV. Further separation of component II into two fractions. *J. Biochem.* **69**, 1131–1133
5. Lee, S. G., Roskoski, R., Bauer, K., and Lipmann, F. (1973) Purification of the polyenzymes responsible for tyrocidine synthesis and their dissociation into subunits. *Biochemistry.* **12**, 398–405
6. Spathelf, B. M., and Rautenbach, M. (2009) Anti-listerial activity and structure-activity relationships of the six major tyrocidines, cyclic decapeptides from *Bacillus aneurinolyticus*. *Bioorganic Med. Chem.* **17**, 5541–5548

7. Leussa, A. N. Yango N., and Rautenbach, M. (2014) Detailed SAR and PCA of the tyrocidines and analogues towards leucocin A-sensitive and leucocin A-resistant *Listeria monocytogenes*. *Chem. Biol. Drug Des.* **84**, 543–557
8. Rautenbach, M., Vlok, N. M., Stander, M., and Hoppe, H. C. (2007) Inhibition of malaria parasite blood stages by tyrocidines, membrane-active cyclic peptide antibiotics from *Bacillus brevis*. *Biochim. Biophys. Acta - Biomembr.* **1768**, 1488–1497
9. Dubos, R. J. (1939) Studies on a bactericidal agent extracted from a soil bacillus I. Preparation of the agent. its activity in vitro. *J. Exp. Med.* **70**, 1–10
10. Bohg, A., and Ristow, H. (1986) DNA-supercoiling is affected in vitro by the peptide antibiotics tyrocidine and gramicidin. *Eur. J. Biochem.* **160**, 587–591
11. Bohg, A., and Ristow, H. (1987) Tyrocidine-induced modulation of the DNA conformation in *Bacillus brevis*. *Eur. J. Biochem.* **170**, 253–258
12. Chakraborty, T., Hansen, J., Schazschneider, B., and Ristow, H. (1978) The DNA-tyrocidine complex and its dissociation in the presence of dramycin D. *Eur. J. Biochem.* **90**, 261–270
13. Changeux, J. P., Ryter, A., Leuzinger, W., Barrand, P., and Podleski, T. (1969) On the association of tyrocidine with acetylcholinesterase. *Proc. Natl. Acad. Sci. U. S. A.* **62**, 986–993
14. Lewis, J. C., Dimick, K. P., and Feustel, I. C. (1945) Production of tyrothricin in cultures of *Bacillus brevis*. *Ind. Eng. Chem.* **37**, 996–1004
15. Okuda, K., Edwards, G. C., and Winnick, T. (1963) Biosynthesis of gramicidin and tyrocidine in the Dubos strain of *Bacillus brevis*. I. Experiments with growing cultures. *J. Bacteriol.* **85**, 329–338
16. Fujikawa, K., Suzuki, T., and Kurahashi, K. (1968) Biosynthesis of tyrocidine by a cell-free enzyme system of *Bacillus brevis* ATCC 8185. I. Preparation of partially purified enzyme system and its properties. *Biochim. Biophys. Acta.* **161**, 232–246
17. Mach, B., Reich, E., and Tatum, E. L. (1963) Separation of the biosynthesis of the antibiotic polypeptide tyrocidine from protein biosynthesis\*. *Proc. Natl. Acad. Sci. U. S. A.* **50**, 175–181
18. Stokes, J. L., and Woodward Jr., C. R. (1943) Formation of tyrothricin in submerged cultures of *Bacillus brevis*. *J. Bacteriol.* **46**, 83–88



19. Kurahashi, K. (1974) Biosynthesis of small peptides. *Annu. Rev. Biochem.* **43**, 445–459
20. Laland, S. G., and Zimmer, T. L. (1973) The protein thiotemplate mechanism of synthesis for the peptide antibiotics produced by *Bacillus brevis*. *Essays Biochem.* **9**, 31–57
21. Lipmann, F. (1972) Nonribosomal polypeptide synthesis on polyanzyme templates. *Acc. Chem. Res.* **6**, 161–168
22. Vosloo, J. A., Stander, M. A., Leussa, A. N. N., Spathelf, B. M., and Rautenbach, M. (2013) Manipulation of the tyrothricin production profile of *Bacillus aneurinolyticus*. *Microbiol. (United Kingdom)*. **159**, 2200–2211
23. Vosloo, J. A. (2016) Optimised bacterial production and characterisation of natural antimicrobial peptides with potential application in agriculture, **Ph.D. thesis**, University of Stellenbosch, <http://scholar.sun.ac.za/handle/10019.1/98411>
24. Seddon, B., and Fynn, G. (1973) Energetics of growth in a tyrothricin-producing strain of *Bacillus brevis*. *J. Gen. Microbiol.* **74**, 305–314
25. Trach, K., Burbulys, D., Strauch, M., Wu, J. J., Dhillon, N., Jonas, R., Hanstein, C., Kallio, P., Perego, M., Bird, T., Spiegelman, G., Fogher, C., and Hoch, J. A. (1991) Control of the initiation of sporulation in *Bacillus subtilis* by a phosphorelay. *Res. Microbiol.* **142**, 815–823
26. Lykov, V. P., Bodnar, I. V., Khovrychev, M. P., and Polin, A. N. (1986) [Biosynthesis of the antibiotic gramicidin S by a *Bacillus brevis* culture associated with a change in growth kinetics]. *Mikrobiologiya.* **55**, 792–795
27. Winnick, R. E., and Winnick, T. (1961) Biosynthesis of gramicidin S II. Incorporation experiments with labelled amino acids analogs, and the amino acid activation process. *Biochem. Biophys Acta.* **53**, 461–468
28. Okuda, K., Edwards, G. C., and Winnick, T. (1962) Biosynthesis of gramicidin and tyrocidine in the dubos strain of *Bacillus brevis* I. Experiments with growing cultures. *J. Bacteriol.* **85**, 329–338

## Chapter 3

### Determination of the incorporation of non-natural amino acids into the tyrocidines and analogues

#### 3.1 Introduction

The tyrocidines are secondary metabolites synthesised by multi-domain enzyme complex known as non-ribosomal peptide synthetases. These multi-domain enzyme complex are most broadly grouped into three synthetases, namely TycA, TycB and TycC (1). These synthetases consist of several modules responsible for the activation and incorporation of an amino acid into the growing peptide chain (2–4). The process terminates with the cyclisation of the linear peptide to form a cyclic decapeptide (1, 5, 6) (refer to Figure 1.8 in Chapter 1).

Tang *et al.* (7) has identified 28 tyrocidine (Trc) analogues based on the variability observed at residue positions 3, 4, 7, 8 and 9 (refer to Table 1.1 in Chapter 1). The enzyme domains responsible for incorporation of amino-acids into positions 3, 4 and 7 of the peptide show a partial lack of specificity, allowing for incorporation of more than one possible aromatic amino acid. It has been shown that the residues 3 and 4 can be Trp and/or Phe while residue 7 can be occupied by Tyr, Phe or Trp. Residue 9 can be either Ort or Lys (7–9). Residue 8 has a lower overall variability showing a preference for Val, but minor analogues containing Leu and Ile in this position was also identified by Tang *et al.* (7).

The amino acid composition of any given Trc analogue has an effect on its hydrophobicity, mass-to-charge ratio, as well as its side chain surface area (10). In addition, amino acid composition may have an effect on the tertiary structure of the peptide, altering how the hydrophobic, charged and polar residues interact within peptide oligomers, as well as with possible target cells, and ultimately effecting its antimicrobial activity (11).

The aromatic amino acids (Phe, Trp and Tyr) content were found to play a role in the ability of the Trc analogue to cause inhibition of Gram-positive organisms. A study by Spathelf and Rautenbach (10) looked at the structure-activity relationships of six major tyrocidine analogues against three Gram-positive target organisms. Against *Micrococcus luteus*, four analogues (TrcB<sub>1</sub>, TrcC<sub>1</sub>, TrcB and TrcB) had similar IC<sub>50</sub> values which were much lower than the more hydrophobic TrcA and TrcA<sub>1</sub> analogues. A similar trend was observed against *L. monocytogenes*, but with a less pronounced difference, the order of IC<sub>50</sub> values from lowest to highest here was TrcB<sub>1</sub>, TrcC, TrcC<sub>1</sub>, TrcB, TrcA and TrcA<sub>1</sub> (10). For *L. monocytogenes*, the ascending order of the cyclic-

decapeptides in terms of their  $IC_{50}$  values was  $TrcB_1 > TrcC$ , and as the most active  $TrcB$ , with  $TrcC_1 > TrcA$  and  $TrcA_1$  together having the highest relative  $IC_{50}$  values (most active). Overall, the more hydrophobic tyrocidine analogues had better activity, which appeared to correspond well with analytical HPLC retention times, with the order of elution from first to last being  $TrcC_1$ ,  $TrcC$ ,  $TrcB_1$ ,  $TrcB$ ,  $TrcA_1$  and  $TrcA$  (10). Amino acid composition is hypothesized to alter the  $Trc$  antimicrobial activity via its effect on dimerization of the peptide (12, 13).

The importance of the amino acid composition on activity has also been highlighted by several experiments aimed at increasing antimicrobial activity while decreasing haemolytic activity via synthetic insertion of selected amino acids into the  $Trcs$  and analogues (9, 14). Increasing the positive charge of  $TrcA$  by the replacement of  $Gln^6$  by an  $Orn$  led to enhanced activity against *Bacillus subtilis* while simultaneously decreasing its toxic haemolytic affect (14). Insertion of a  $Lys$  in position 6 of  $TrcA$  led to an increase in activity against a variety of selected Gram-positive bacteria, also due to an increase in the positive charge relative to the unmodified  $TrcA$  (9). The replacement of  $Phe^4$  by a  $Lys^4$  formed a  $TrcA$  analogue with three positively charged residues that possessed activity against Gram-negative bacteria (9). The importance of the distribution of hydrophilic and hydrophobic amino acids within the  $Trcs$ , and the resultant amphipathic nature of the tyrocidines also plays a key role in activity. The insertion of a hydrophobic penta-fluoro-phenylalanine residue in positions 3 and 7 (position 7 generally contain a more polar  $Tyr$  residue) potentially disrupts the amphipathic nature of  $TrcA$ , leading to a decrease in antibacterial activity (9). Enhancing the amphipathic nature of  $TrcA$  by insertions of  $Lys$  residues at position 4 and/or 6, together with the insertion of a penta-flouro-phenylalanine residue at position 3, led to enhanced activity against selected Gram-positive and Gram-negative bacteria (9).

Due to the expensive and time-consuming nature of chemical synthesis and modification of the  $Trcs$ , it is of interest to investigate if the producer organisms can incorporate non-natural amino acids supplemented into the growth media into the  $Trcs$ , and the effect of these amino-acid analogues on growth and overall peptide production of the producer organism. The ability of the  $Trc$  producer organisms to incorporate amino acids supplemented into the growth media into the  $Trcs$  as well as their effect on growth and peptide production was investigated in several studies (15–17). Okuda *et al.* (15) found that  $\beta$ -hydroxyglutamic acid, pipercolic acid,  $\beta$ -2-thienylalanine, *p*-flourophenylalanine and phenylglycine all selectively reduced  $Trc$  synthesis relative to non-supplemented nutrient media while simultaneously enhancing gramicidin production. Isotopically labelled non-natural  $\beta$ -2-thienylalanine, as well as isotopically labelled isoleucine, valine, proline and ornithine were found to give rise to isotopically labelled  $Trcs$  (15). The supplementation of the nutrient media with non-natural amino acid analogues 5-methyl-tryptophan (5-MeW) and

thioproline exerted a generalised inhibitory effect on both growth and peptide production (15). A study by Mach *et al.* (16) found that the Phe analogues *m*-, *o*-, and *p*-fluorophenylalanine were found to inhibit Trc synthesis without a marked effect on protein synthesis. This study also found that  $\beta$ -methyltryptophan did not inhibit Trc synthesis while  $\alpha$ -methyltryptophan did. Ruttenberg *et al.* (17) found that allo-Ile was preferentially incorporated into the Trcs over Ile.

Given the flexibility of the tyrocidine synthetase system to incorporate different amino acids, both natural and non-natural, one can potentially produce a large library of Trc analogues with novel structures and activities. Of course, this is also dependent on the amino acid being non-toxic to the host organism, as an amino acid (specifically a non-natural derivative) may act as an antagonist to protein synthesis, or as an antagonist in peptide production. Modern experimental techniques allow us to easily assess both the ability of the producer organism to grow in the presence of a given amino acid (using growth curve analysis) and to determine the identity of the produced tyrocidines (using direct-injection ESMS or UPLC-ESMS). Observed experimental masses can be compared to expected theoretical masses to assess if non-natural amino acids were incorporated into the Trc analogue.

In this chapter, we aim to determine the effect of the selected non-natural aromatic amino acids (Figure 3.1) and their naturally occurring analogues on the growth of three selected strains of the Trc producer organisms. One of these strains was then selected for medium-throughput deep-well cultures using the selected aromatic amino acids to allow for determination of the identity of the Trc analogues detected in the extract.

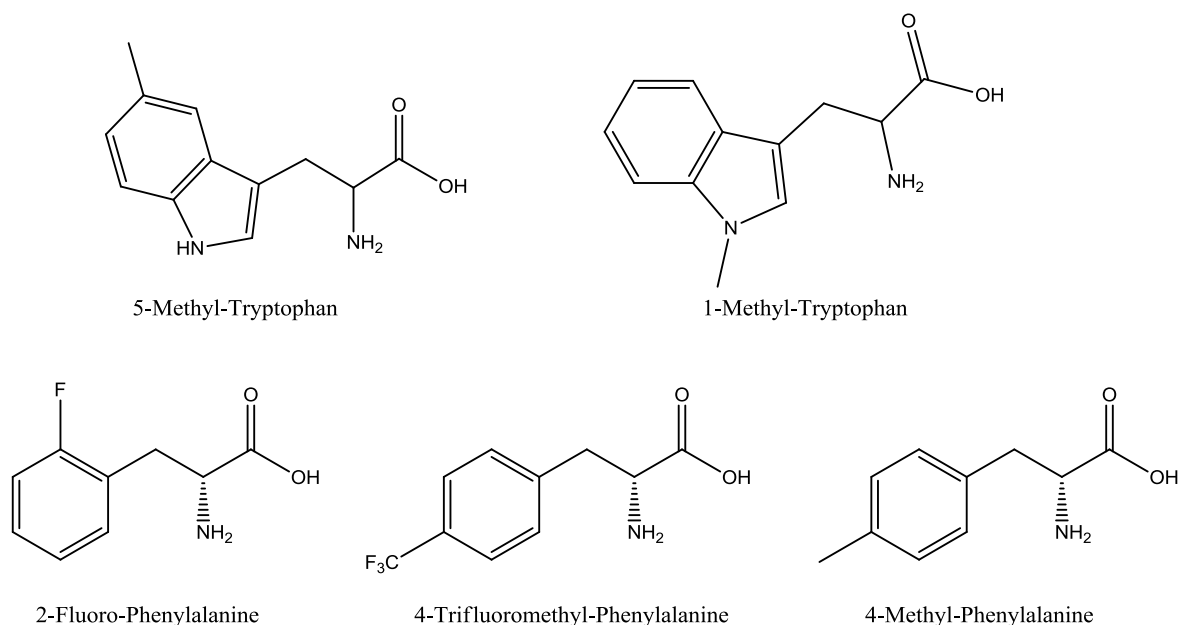


*Figure 3.1* The selected non-natural Trp and Phe analogues supplemented into cultures of the producer organism to determine their effect on growth and peptide production.

## 3.2 Materials

The producer organisms *Brevibacillus parabrevis* 362 and 5618 originate from the Deutsche Sammlung von Mikroorganismen und Zellkulturen (DSMZ) in Braunschweig, Germany. The *Brevibacillus parabrevis* 8185 and 10068 strains originate from the American Type Culture Collection (ATCC) based in Manassas (Virginia, USA). *Micrococcus luteus* NCTC 8340 was sourced from the National Collection of Type Cultures (NCTC) in Porton Down (Salisbury, England).

Tryptic soy broth (TSB), tryptone, agar, glucose (Glc), ethanol (EtOH), hydrochloric acid (HCl) and sodium chloride (NaCl) were from Merck (Darmstadt, Germany). Trifluoroacetic acid (TFA, > 98% purity) was from Sigma-Aldrich (St. Louis, USA). Acetonitrile (ACN, far UV cut-off, > 98% purity) was obtained from Romil Ltd. (Cambridge, UK). Analytical grade, deionised water was obtained by filtering reverse osmosis water through a Milli-Q<sup>®</sup> water purification system (Merck Millipore, Ma, USA). The modified amino acids, 2-fluorophenylalanine (2-FF), 4-trifluoro-methyl-phenylalanine (4-CF<sub>3</sub>F) and 4-methyl-phenylalanine (4-MeF) were from GL Biochem Ltd. (Shanghai, China). L-Tryptophan (Trp), 1-methyl-L-tryptophan (1-MeW), 5-methyl-DL-tryptophan (5-MeW) and L-phenylalanine (Phe) were from Sigma-Aldrich (Steinheim, Germany). Glycerol (Glr, > 99.5% purity) is from Merck (Kenilworth, USA).

Falcon<sup>®</sup> tubes were from Corning (Corning, NY, USA). The 96-well deep-well plates were sourced from Nunc (Roskilde, Denmark) and 96-well microtiter plates were from Corning Incorporated (NY, USA). Petri dishes were from Lasec (Cape Town, South Africa). The 96-well flat bottom microtiter plates were from Corning (NY, USA). Round bottom 96-well plates were from Greiner Bio-One (Kremsmünster, Austria).

## 3.3 Methods

### 3.3.1 Growth curve analysis of organisms using non-natural amino acids

*Growth curves using 5-methyl tryptophan and tryptophan supplementation:* Here the selected amino acids were incubated and their effect on the growth rate of the selected producer organisms (5618, 362 and 8185 strains) was recorded. A five times concentrated solution of TGS was made up to allow for dilution with 5-MeW and Trp stocks and 1.25 concentrated (relative to final assay concentration) dilutions of 5-MeW were made in a 300 µL round-bottom microtiter plate. NaOH addition was used to improve amino acids solubility and pH was adjusted with HCl to neutrality. Controls with similar amounts of NaOH and HCl were used as pH growth controls to rule out the influence of these components on growth. The concentration ranges of the supplemented amino

acids were started from a 34.375 mM analytically prepared stock solution. A series of dilutions were made with analytical grade to a final concentration of 0.859 mM. A Trp dilution series was made in a similar manner with a 5-fold dilution range from 137.5 mM to 3.438 mM. Both the 34.375 mM and 137.5 mM 5-MeW and Trp TGS stocks were sterilised by filtration through a 0.22  $\mu\text{m}$  filter. Growth curves were done in standard 96-well microtiter plates by transferring the concentrated amino acid solution to the final assay plate from the round bottom plate. The concentrated amino acid solutions were then diluted with concentrated TGS and/or analytical grade water to get all components to the correct concentration and a final volume of 200  $\mu\text{L}$ . TGS on its own was used as normal culture growth control and sterility blank. Overnight cultures of the producer organisms were made as previously described for the growth curves in Chapter 2, and 10  $\mu\text{L}$  culture was used to inoculate the wells. Cultures were incubated at 37°C. Bacterial growth was monitored by recording the OD at 595 every two hours for the first eight hours then at 16 hrs, 24 hrs and 36 hrs on BioRad™ microtiter plate reader.

*Growth curve using 1-methyl tryptophan supplementation:* Growth curves were done for 1-MeW in a similar manner to Trp and 5-MeW. A 27.5 mM stock of 1-MeW was dissolved in TGS and dilutions were made in a 300  $\mu\text{L}$  round-bottom 96-well plate using TGS down to 0.69 mM. A volume of 200  $\mu\text{L}$  was then pipetted into each well of a standard 96-well microtiter plate. TGS on its own was used as a control. Overnight cultures of the 5618, 362 and 8185 strains were grown up as previously described and 10  $\mu\text{L}$  was used to inoculate each well. Growth was monitored by recording the change in OD at 595 nm every hour for 12 hours.

*Growth curves using phenylalanine and non-natural phenylalanine derivatives in supplementation:* Three non-natural phenylalanine derivatives 2-FF, 4-CF<sub>3</sub>F and 4-MeF, as well as Phe as control were chosen to for growth curve analysis. Here, a stock solution of TGS was made containing 27.5 mM of the selected amino acid for each amino acid. Amino acid solubility was improved by using NaOH and HCl as described above. Stocks were sterilised by filtration through a 0.22  $\mu\text{m}$  filter. Normal TGS was also made up for use in growth controls and for diluting the TGS-amino acid stock. A range of dilutions was made in round-bottom 300  $\mu\text{L}$  microtiter plates starting with the undiluted 27.5 mM stock going down to 0.7 mM. Dilutions of the TGS-amino acid stock were done with normal TGS. A volume of 200  $\mu\text{L}$  of each dilution was added to a standard 96-well microtiter plate. Unmodified TGS was used as a sterility blank and normal culture growth control. Overnight starter cultures were made as previously described and 10  $\mu\text{L}$  was added to the wells. Cultures were incubated at 37°C. Growth was measured by recording the change in OD at 595 nm every hour for the first eight hours then every two hours up to 14 hours using a BioRad™ microtiter plate reader.

Four repeats were done for phenylalanine ( $n=4$ ), five were done for 2-FF ( $n=5$ ), four for 4-CF<sub>3</sub>F ( $n=4$ ) and five repeats were done for 4-MeF ( $n=5$ ).

### ***3.3.2 Small scale cultures using selected, non-natural amino acids***

*Deep well assay for tryptophan, 1-methyl tryptophan and 5-methyl tryptophan supplemented cultures:* In order to determine the incorporation of the selected non-natural amino acids, small scale, medium-throughput cultures were done. The concentrations of amino acid were chosen based on the results from the growth curves, with a lower and a higher concentration chosen to see if incorporation of the amino acid increased in a dose dependant manner. Concentrations of 5 mM and 10 mM were chosen for Trp, 5-MeW and 1-MeW in the deep well assay. Stocks of 20 mM for Trp and 5-MeW, and 40 mM for 1-MeW were made in analytical grade water and sterilised via filtration through a 0.22 µm filter. Two four times concentrated TGS stocks were made, one with a glucose concentration of 3% ( $m/v$ ) and one with a glucose concentration of 3.5% ( $m/v$ ). In addition, urea and Na<sub>2</sub>SO<sub>4</sub> stocks of 100 g/L were made and sterilised by autoclaving. For urea and Na<sub>2</sub>SO<sub>4</sub>, concentration of 1 g/L and 4 g/L were chosen for use in the deep well assay. Each well consisted of a combination of one of the selected amino acids and either urea or Na<sub>2</sub>SO<sub>4</sub> (with both components at one of two varying concentrations) together with TGS and made up to the final concentration and volume (500 µL) with analytical grade water. The TGS with 3% ( $m/v$ ) glucose was used for controls with no added amino acid or urea/ Na<sub>2</sub>SO<sub>4</sub> while the 3.5% ( $m/v$ ) was used for the rest (based on the growth curve for variable glucose concentrations). Overnight starter cultures of 5618 were made as previously described and 10 µL was used to inoculate each well. Cultures were then incubated at 37°C for 10 days after which they were extracted as previously described.

*Deep well assay for Phe, 2-FF, 4-CF<sub>3</sub>F and 4-MeF:* The incorporation of Phe and the selected non-natural Phe analogues were tested for using small scale, medium throughput cultures. Urea and Na<sub>2</sub>SO<sub>4</sub> were also used to determine their effect on peptide production using stocks of 50.00 g/L. For the amino acids, stocks of 40.00 mM were made in analytical grade water and sterilised by filtration through a 0.22 µm filter. Four times concentrated TGS stocks were made, one with a Glc concentration of 3.5% ( $m/v$ ) and another with 3% ( $m/v$ ). In the deep well plate each well consisted of either 10 or 20 mM amino acid, 1 g/L or 4 g/L urea or Na<sub>2</sub>SO<sub>4</sub> and finally TGS with 3.5% ( $m/v$ ) glucose (control wells only contained 3% ( $m/v$ ) glucose in TGS). All wells were made up to the correct volume (500 µL) and concentration using analytical grade water. Overnight cultures of the 5618-strain were made as previously described and 10 µL were used to inoculate each well. Cultures were incubated for 10 days and extracted as previously described.



*Deep well culture extraction and ESMS analysis of extracts:* Following the 10 days of incubation the cultures were acidified using HCl to a pH of 4. After 3 hours the cultures were spun down for 20 minutes at  $3000 \times g$ . Extraction was then done on the pellet by resuspending it in 75% ACN for 30 minutes while sonicating. The extracts were then spun down again for 30 minutes at  $3000 \times g$  after which the supernatant for each duplicate repeat (combining supernatant of six wells per repeat) was collected and freeze dried. After freeze drying the mass was recorded. The samples were then made up to 1.00 mg/mL using 50% ACN and analytical grade water and spun down to remove insoluble material and particulate. The supernatant was removed and placed into a glass insert for ESMS analysis as described in Chapter 2.

*Analysis of ESMS data:* For determining the % signal contribution of the Trcs and analogues in the deep-well extracts, an  $m/z$  spectrum was generated from ESMS analysis of the Trc extracts. This spectrum was then deconvoluted using the MaxEnt 3 function in MassLynx<sup>®</sup> 4.1. A mass range of 600-2000 Da and two charges was used for the MaxEnt 3 conditions to generate a mass-spectrum covering the expected monomer range. The mass-spectra generated were then exported to Excel where the Trcs and non-natural analogues were identified using their theoretical masses. The % signal contribution of the identified Trcs was then calculated by dividing their signals by the sum of all the signals for the ionised species detected. This was done for all the deep-well extracts to determine the effect of the different media compositions and amino-acid supplementations on the relative amount of Trcs produced. A breakdown of the process of deconvolution of the  $m/z$  spectrum is given in the results section. In addition to this, selected deep-well extract from each of the amino acid supplementations used was selected to give an idea of the levels of oligomerisation of the Trcs in the extract as well as displaying more detailed mass-spectra for the monomers by these extracts. Here the MaxEnt 3 conditions covers a mass range of 600-10000 Da and six charges to display the expected mass range for monomers up to tetramers. Monomers were then identified based on theoretical masses to assess the difference between theoretical and observed masses as well as the putative identifications of novel Trcs.

## **3.4 Results**

### ***3.4.1 Growth curve analysis of organisms using non-natural amino acids***

For the 5618-strain, both Trp and its analogue 5-MeW appeared to be well tolerated when compared to TGS (Figure 3.2, A). The 1-MeW analogue was well tolerated, particularly at a lower concentration of 2.75 mM, however, growth was markedly inhibited at higher concentrations, with no growth occurring at 22 mM. Similar trends were observed for both the 362 and 8185-strains (Figure 3.2, B & C) with the 8185-strain appearing to be the least tolerant to both the Trp analogues



used at concentrations of 11 mM and 22 mM. The 362-strain appeared to grow the best in the presence of 1-MeW, having the highest growth rate at a concentration of 11 mM, while the 5618-strain appeared to be the most amenable to increasing 5-MeW concentrations.

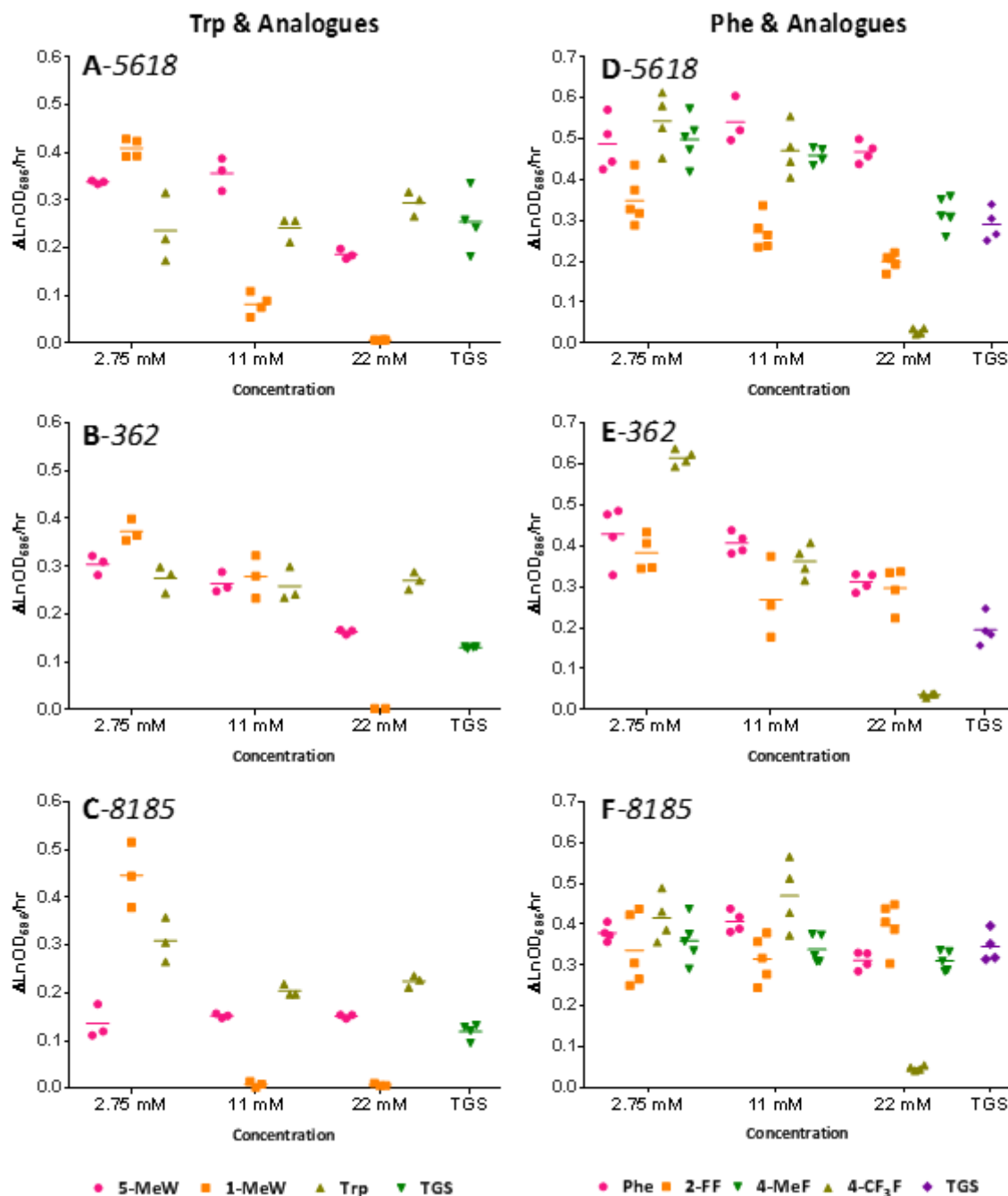


**Figure 3.2** Growth rates for producer strains using Trp and Phe and analogues at concentrations of 2.75, 11.0 and 22.0 mM respectively, together with a TGS control. Concentrations were chosen to represent low, medium and high concentrations respectively of those used in the growth curves. All repeats are shown under each growth condition together with the mean represented by the horizontal line of the same colour. Bold letters **A-C** represent growth rates for selected strains (A: 5618, B: 362, C: 8185) under varying Trp and Trp derivative concentrations with TGS as a control while bold letters **D-F** represent growth rates under varying concentrations of Phe and Phe derivative for selected strains (D: 5618, E: 362, F: 8185).

In terms of Phe and its analogues, the 5618-strain has markedly elevated growth rates for Phe, 4-CF<sub>3</sub>F and 4-MeF relative to TGS (Figure 3.2, D). Only the 2-FF analogue appeared to induce equal or slightly reduced growth rates relative to TGS for this strain (Figure 3.2, D). For all strains, the 4-CF<sub>3</sub>F analogue appeared to drastically inhibit growth at higher concentrations of 22 mM (Figure 3.2, D – F). Relative to TGS, all strains had more-a-less equal or elevated growth rates for all amino acids and concentrations used, again with the exception of 4-CF<sub>3</sub>F at 22 mM and 2-FF at a concentration of 22 mM for the 5618-strain only.

### 3.4.2 Analysis of direct-injection ESMS data processing

For the discussion of the results generated from direct-injection ESMS analysis for the deep-well extracts, it is important to explain which assumptions were made and how results were analysed and interpreted using the raw output, depicted as the mass-to-charge ratio. Figure 3.3 depicts the output of a direct-injection ESMS analysis of a deep-well extract supplemented with Phe (expected to produce a higher proportion Phe containing Trc analogues (18)). The *x*-axis depicts the centroid (average mass for molecular ions detected in peak) mass-to-charge ratios of the analytes as detected in the Synapt G2 mass spectrometer, which was set to only detect analytes in the *m/z* range of 300 to 2000. In Figure 3.3, A, four large clusters of molecular ions can be observed. The molecular ions detected in the highest relative % signal intensities (*y*-axis) in these peaks are 426.1260, 635.8792, 922.6049 and 1270.7557 respectively. The peak cluster around *m/z* 426.1260 most likely represents contaminants extracted in the sample such as plasticisers resulting from exposure to plastics during the culturing, extraction and analysis process, as well as triply charged peptides. The peaks surrounding the *m/z* 635.8792 cluster represent Trcs monomers which are doubly charged with two protons [Trc + 2H]<sup>2+</sup>. This molecular ion represents a doubly charged TrcA monomer, which has a theoretical mass of 635.8351 Da. The detected molecular ion at *m/z* = 635.8792 has a 70 ppm error, which is somewhat higher than expected, possibly because of the low concentration of analytes and a minor problem with the calibrant Leu-enkephalin.

The cluster of peaks around the *m/z* = 922.6049 molecular ion was hypothesised to represent the linear gramicidins. The doubly charged linear gramicidin B analogue, VGB, is the most likely candidate for this molecular ion, with a theoretical *m/z* of 922.0415. However, when the -611 ppm error is considered, together with previous results (19) that indicated that gramicidins are not produced in Phe supplemented cultures, the presence of VGB and analogues would be unlikely. Alternatively, this *m/z* cluster can be attributed to either contamination, partially synthesised Trcs or quadruply charged trimers.

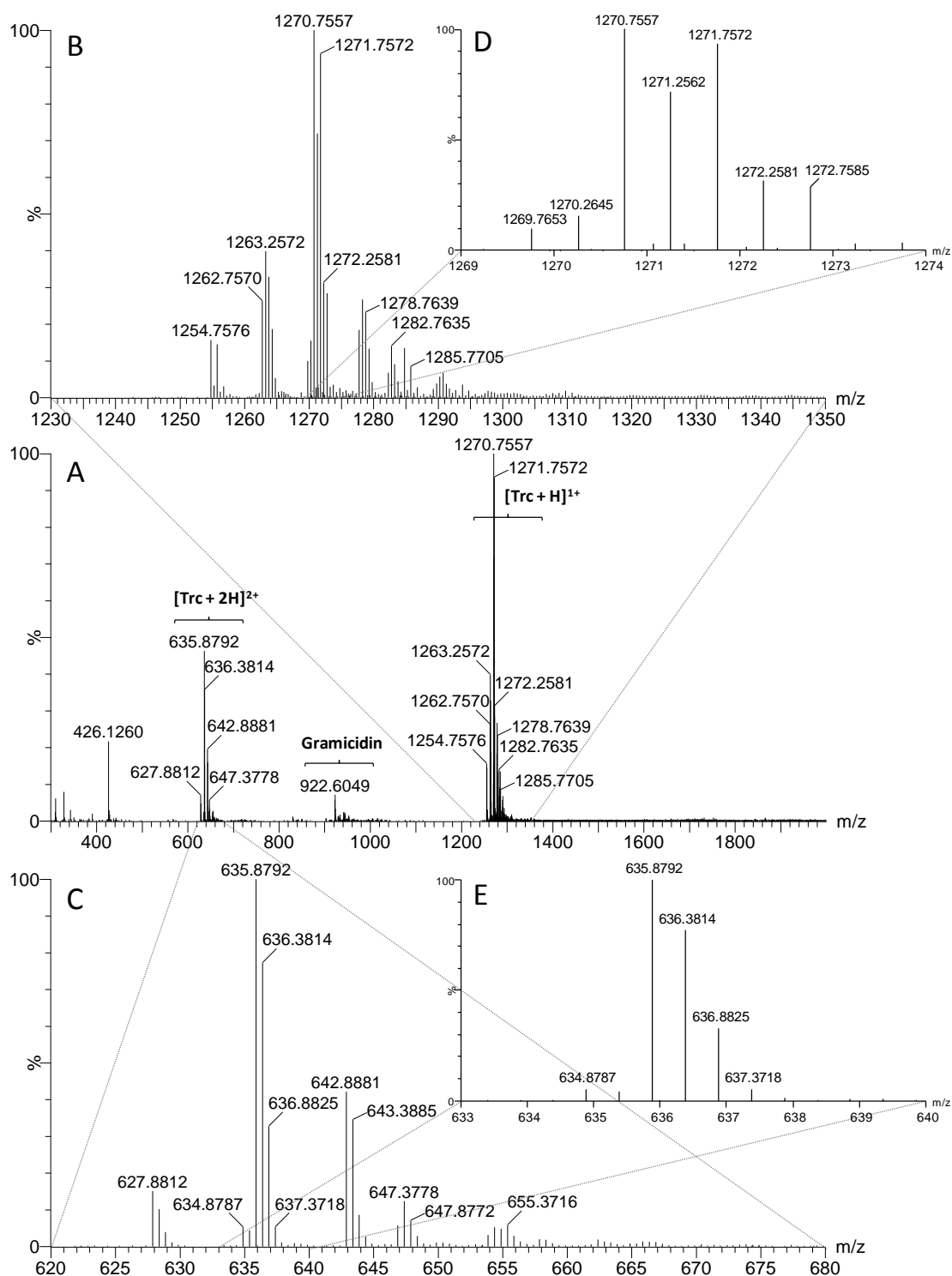


**Figure 3.3** Direct-injection ESMS analysis results of deep-well extract supplemented with 20 mM Phe together with TGS base-media. Centroid mass-spectra depict  $m/z$  of detected analytes. **A** Averaged spectrum over  $m/z$  range of 350 to 2000 Da. **B** Zoomed-in spectrum of  $m/z$  range depicting singly charged monomers and doubly charged dimers. **C** Zoomed-in spectrum of  $m/z$  range typically associated with doubly charged monomers. **D** Zoomed-in spectrum of singly charged TrcA peak (Expected  $m/z = 1270.6624$ ). **E** Zoomed-in spectrum of doubly charged TrcA peak (Expected  $m/z = 635.8351$ ).

The next large cluster of molecular ions can be seen to be present in the highest relative signal intensities, and these represent both singly protonated monomers and doubly charged dimers, which have overlapping  $m/z$  values. In this cluster, the  $m/z = 1270.7295$  represents a singly protonated TrcA ( $[\text{TrcA}+\text{H}]^+$ ) (52.8 ppm error). From previous studies (19) it is expected that the Trc analogue with the highest % signal intensity in the monomer range will also have the highest % signal intensity in the dimer range.

Zooming in on the monomer  $m/z$  range (Figure 3.3, B insert), we can observe in more detail several more clusters of molecular ions. There are six clusters of peptides which stand out following visual inspection. From left to right the first cluster of molecular ions has a major monoisotopic  $m/z$  of 1254.7567, which represents a PhcA with a theoretical mass of 1254.6675 (71 ppm error). Following this  $m/z$ , we come across an  $m/z$  of 1262.7570, which cannot be readily identified from the list of most commonly observed ionised Trc species. However, from the isotopic pattern it was deduced to be a doubly charge ion identified as a TrcA-PhcA heterodimer.

If we extract the  $m/z$  range from 1269 to 1274 (Figure 3.3, D insert) it reveals the atypical isotope pattern of the major peptide, TrcA, in this cluster of ions. Here, the peak at  $m/z$  1270.7557 represents the monoisotopic mass of protonated TrcA. In general, the largest peak in such a cluster with the lowest  $m/z$  represents the monoisotopic mass of the singly charged monomer ( $[\text{TrcA}+\text{H}]^+$ ) or doubly charged dimer ( $[\text{2TrcA}+2\text{H}]^{2+}$ ). Trcs, particularly those with a higher Phe content, readily aggregate to form dimers, trimers and tetramers (19). Due to the high resolution of the Synapt G2 mass spectrometer, one can observe isotopes pattern of TrcA. In this case the peaks at 1271.7557 and 1272.7585 are most likely representative of a TrcA monomer and dimer with one or two heavier isotopes of primarily carbon-13 ( $\text{C}^{13}$ ) respectively, as these masses differ by a mass of 1.0028  $mu$  (mass units), which equates, to the mass of a neutron (1.008664  $mu$ ). The isotope  $m/z$  values of the monomeric TrcA would overlap with those of a doubly charged homodimer of TrcA, in which both monomers making up the dimer possess a heavier isotope of carbon. If, however, only one of the monomers making up the dimer has a  $\text{C}^{13}$  while the other does not, we observe a  $m/z$  ratio in-line with those observed at 1271.2562 and 1272.2581, where the mass difference from the preceding peak is  $m/z = 0.5005$  (1271.2562 - 1270.7557) and  $m/z = 0.5009$  (1272.2581 - 1271.7572  $m/z$ ) respectively. This mass difference corresponds, with half the mass of a neutron (0.504332  $mu$ ). The reason that there is only half an  $m/z$  difference results from fact that the dimer is doubly charged. If only one of the monomers in the dimer has an extra neutron (from  $\text{C}^{13}$ ), and the dimer is doubly charged, then the  $m/z$  ratio difference from a dimer with two heavier TrcA isotopes that is doubly charged, will be half that. A similar isotope distribution pattern is observed for the doubly-charged monomers (Figure 3.3, E insert). Here, however, the isotope pattern is a more classical

representation of an isotope distribution pattern for peptides, as there is little or no overlap with multiply charged oligomers. Here the peaks represent doubly charged isotopes of a TrcA monomer. The largest peak at an  $m/z$  of 635.8792 represents the doubly charged TrcA monomer. Each subsequent peak represents an  $m/z$  resulting from a TrcA heavier by a single neutron mass.

Next, a cluster with major molecular ion at  $m/z$  1278.7639 is observed. From the isotopic pattern it is likely a doubly charged dimer, namely TrcA-TrcA<sub>1</sub> heterodimer. The molecular ion peak cluster with major monomeric  $m/z$  of 1282.7635, could be correlated with a sodium adduct of a TrcA dimer. TrcA<sub>1</sub> is likely the molecular ion with  $m/z$  of 1284.7689 (not labelled) present in the same peak cluster, which corresponds closely with the theoretical  $m/z$  for this peptide of 1284.6781 (71 ppm error). The next cluster has a major  $m/z$  of 1290.7627 Da, which is also not identified from the list of most likely ionised Trc monomers. The isotope pattern is a classical one produced by doubly charged ions and the monoisomeric  $m/z$  value correlating to a TrcA-TrcB heterodimer.

As can be seen, if large-scale analysis of such spectra for many different extracts is done, it would be beneficial to simplify, or deconvolute the  $m/z$  spectra to ease the identification because of the propensity of the peptides to form dimers, as well as higher order oligomers. The deconvolution would also simplify the calculation of the relative contribution of Trc analogues to the tyrothricin (Tcn) extract within sample and within multiple samples grown, extracted and analysed under the same conditions. While using UPLC-MS is the standard for both accurate identification and quantification of Trc analogues, to analyse all the extracts from the deep-well cultures in such a manner would be too time consuming (due to the duration of a UPLC-MS run) and the high cost (time on instrument, column and solvents). As such direct-injection ESMS analysis provides a faster, cheaper alternative, by making use of a maximum entropy algorithm to deconvolute the  $m/z$  spectra to produce an accurate mass spectrum. In this case the MaxEnt 3 (built into the Waters<sup>®</sup> MassLynx 4.1 software suite) function designed specifically for the deconvolution of  $m/z$  spectra with multiply charged ions, such as peptides, was used. This algorithm produces the most likely distribution of masses based on a complex algorithm which makes use of the isotope pattern of detected peptides. As such we can determine the original mass of the uncharged oligomers from their charged counterparts (i.e. generate a mass using the  $m/z$  equation:  $m/z = (MW + (n \times H))/n$ , where MW = molecular weight,  $n$  = number of charges and H = mass of a proton), as well as the mass of the monomers. The details of the algorithm are proprietary information in the MassLynx software, therefore only the MaxEnt 3 output of the sample is detailed in Figure 3.4.

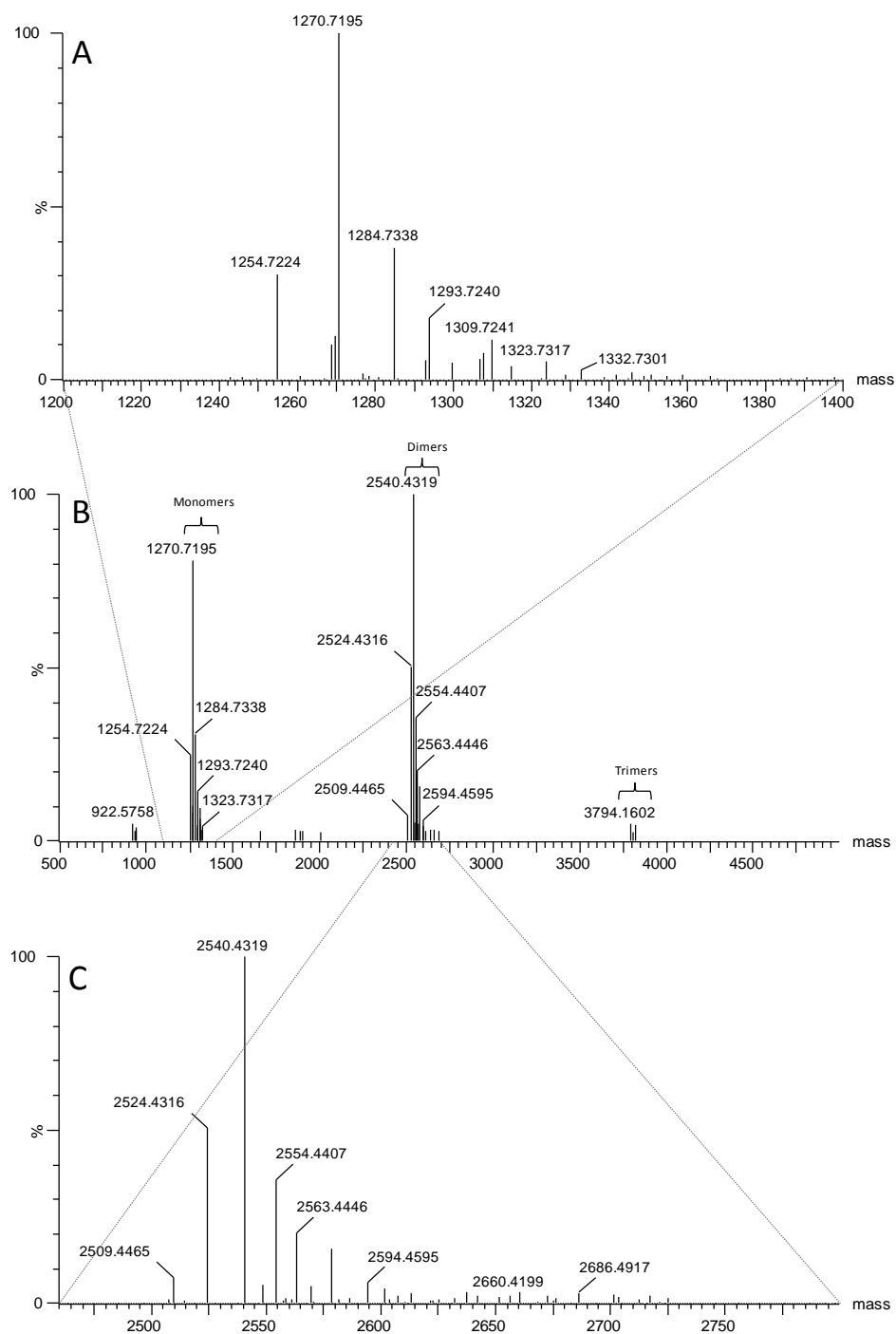


**Figure 3.4** Mass-spectra generated with MaxEnt 3 algorithm using the  $m/z$  spectrum of the 20 mM Phe supplemented deep-well sample. **A** Extracted mass spectrum of monomers in the sample. **B** Full mass spectrum (500 – 6000 Da) depicting Trc monomers, dimers and trimers. **C** Extracted mass spectrum of the peptide dimers.

Figure 3.4 represents the MaxEnt 3 output of the  $m/z$  spectra in Figure 3.3. Figure 3.4 shows the deconvoluted mass spectra for the 20 mM Phe supplemented sample. The masses here predominantly depict the experimentally detected masses of the monomer or oligomer with the addition of a single hydrogen (and to a lesser degree adducts of Na and K). The masses given are

centroid values representing the centroid monoisotopic mass ( $m/z$  with  $z = 1$ ) for a given peak. In Figure 3.4, A, can be seen the monomeric monoisotopic mass peaks produced following the deconvolution by the MaxEnt 3 algorithm. All labelled mass peaks can be identified as protonated Trc analogues (identities not shown). In Figure 3.4, C, the accurate masses of the dimers can also be derived from the deconvoluted mass spectrum. Looking only at the theoretical values of the homodimers we can only identify the mass at 2540.4319 Da as a dimer of TrcA. The rest are heterodimers consisting of various combinations of monomers present in the highest % signal intensities in spectrum A of Figure 3.4. (Refer to addendum at end of chapter for theoretical dimer masses (for Phe supplemented extract) and addendum of chapter 4 for theoretical monomer masses).

Figure 3.5 shows the MaxEnt output (Figure 3.5, A) and the original  $m/z$  spectrum (Figure 3.5, B). Here it can be seen how the algorithm gave the most likely monomer masses using the original isotopic-distribution patterns of the detected peptides in this range.

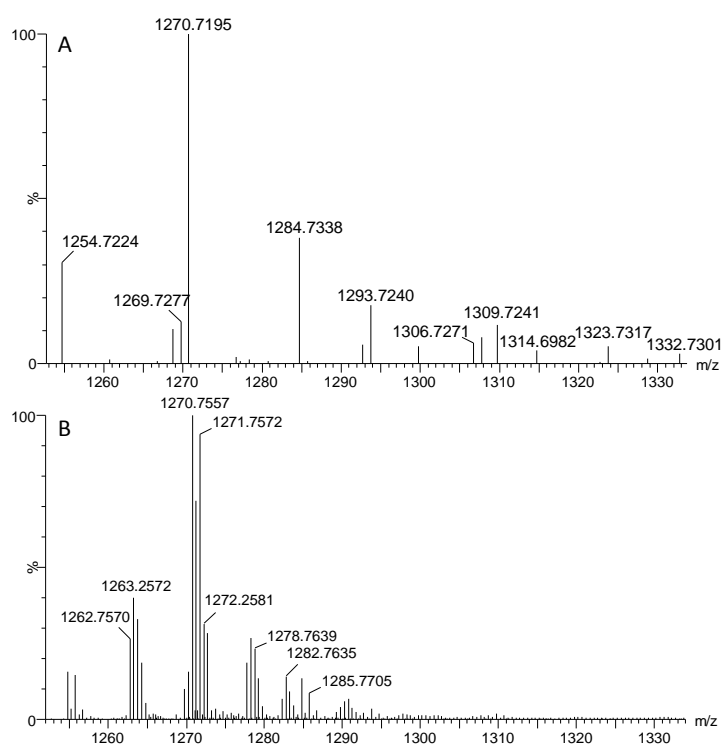


*Figure 3.5* Comparison of 20 mM Phe supplemented deep-well extract showing, **A** the output of MaxEnt 3 algorithm over monomer-mass range versus **B**  $m/z$  values for molecular ions detected in singly charged monomer  $m/z$  range and doubly charged dimer  $m/z$  range.

From the deconvoluted mass spectra we identified the most likely peptides candidates and extracted the signal intensities of the monomeric species to compare the contribution of each peptide in a specific extract. In these calculations a general assumption was made that the monomeric peptide

signal reflected the peptide contribution in the extract and that the peptides have similar signal response in the mass spectrometer.

The 5618-strain was used for all deep-well cultures as it had been first used in deep-well cultures with 5-MeW (due to its good production of Trp containing Trcs) and was therefore used for other amino acid analogues.

### **3.4.2 ESMS analysis of small-scale cultures supplemented with non-natural amino acids**

For a list of theoretical monomer masses of both natural and non-natural Trc analogues identified in this chapter see the thesis addendum.

A detailed ESMS analysis of deep-well cultures that were supplemented with different Phe and Trp analogues revealed that strain 5618 were able to incorporate different Phe and Trp derivatives into the Trc and Tpc peptides. Figure 3.6 to Figure 3.12 show the mass-spectra of selected samples, while summaries of the possible Trc analogues which could theoretically produce the detected mass are given in Table 3.1 to Table 3.7. The masses shown were generated using the in-built MassLynx<sup>®</sup> MaxEnt 3 function to identify the most probable masses of the peptides using the detected mass-to-charge ( $m/z$ ) ratios generated by direct-injection ESMS analyses. For the mass spectra, only masses (or  $m/z$  values) with % signal intensity higher than 5 % above the background are shown and only masses with a % signal intensity higher than 10 % were labelled if a corresponding theoretical mass could be identified. Mass intensities (% signal intensity) are given as a percentage of the maximum detected intensity for a particular spectrum. In the tables presenting the possible identities of the theoretical Trc analogues, the most probable peptide identity (as protonated peptide (mass + 1.007825 *mu*) and/or a sodium adduct (mass + 22.989769 *mu*)) is given above the corresponding mass.

Figure 3.6 and Table 3.1 depict the mass spectra and possible peptide identities for a 20 mM Phe supplemented deep-well extract. Seven monomeric peptides were identified that met the criteria for identification. The majority of the identified peptides were A analogues corresponding with the incorporation of phenylalanine residues at positions 3 and 4. As previously found by Vosloo *et al.* (18) it was also observed that with Phe supplementation TrcA gave the highest signal intensity, followed by PhcA and TrcA<sub>1</sub> in the second tier of highest signals, and finally TpcA, PhcA<sub>1</sub>, TpcA<sub>1</sub> and TrcB/B' producing in the lowest, but still readily detectable amounts. Any masses not labelled most likely represent peptides with adducts that were not identified (i.e. an adduct other than sodium), partially formed or degraded peptides, or contaminants. Due to problems with the in-analysis calibrant used in the mass-spectrometer, some samples were calibrated using the theoretical mass of the Trc analogue present in the highest relative amount within the sample. In these cases,



the difference between the detected mass and theoretical mass for this analogue was subtracted from all the other detected monomer masses. The Trc analogue used as the internal calibrant will therefore have the same detected mass as the theoretical mass, and a ppm mass error of zero. In addition, some of the observed masses can be produced by Trc analogues which possess the same molecular formula but have a different structure. For instance, in Table 3.1, any TrcB and TrcB' analogue have the same molecular formula, but differ structurally in that the amino acids in positions 3 and 4 (Phe and Trp) are swapped around. As a result, any peptide which matches the mass of a TrcB analogue is given the identity Trc B/B' as one cannot predict exactly which amino acids occupies which position (without the use of MS/MS fragmentation). However, from previous studies by Spathelf (8) and Tang *et al.* (7) it is known that TrcB' is a minor peptide in the tyrocidine complex.

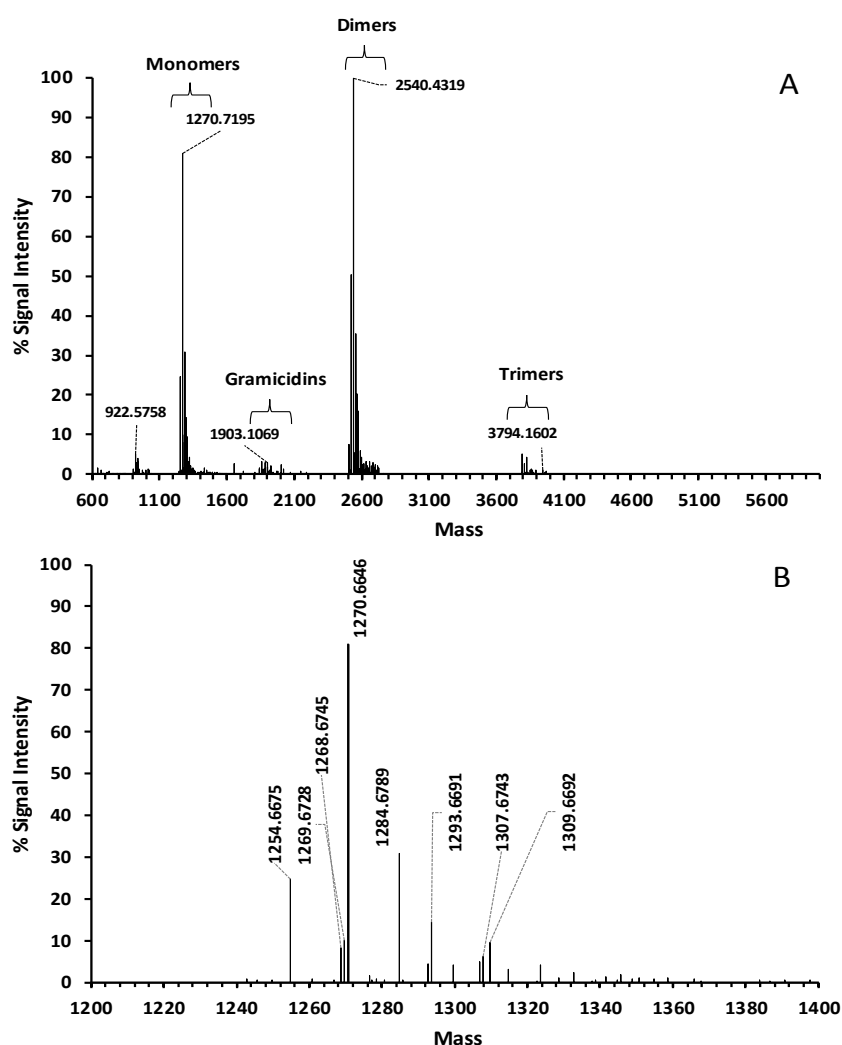


**Figure 3.6** ESMS mass-spectra generated using the MaxEnt 3 algorithm for 20 mM Phe supplemented deep-well culture extract of strain 5618. **A** Full spectrum over the mass range from 600-6000 Da, **B** Extracted spectrum showing mass range (1200-1400 Da) in which the monomeric peptides would be detected. Refer to Table 3.1 for the list possible peptide identities from detected masses above.

**Table 3.1** List of detected masses for 20 mM supplemented Phe deep-well extracts which could be putatively identified based on theoretical masses. Labels correspond to mass-spectra in Figure 3.6, B.

Detected Mass	Possible Identities	Theoretical $M_r$ of protonated peptide	ppm error
1254.6653	PhcA	1254.6675	-2
1268.6723	PhcA <sub>1</sub>	1268.6832	-9
1270.6624 <sup>#</sup>	TrcA	1270.6624	0
1284.6767	TrcA <sub>1</sub>	1284.6781	-1
1293.6669	TpcA	1293.6784	-9
1307.6721	TpcA <sub>1</sub>	1307.6941	-17
1309.6670	TrcB/B'	1309.6733	-5

<sup>#</sup> Detected mass of TrcA adjusted to theoretical mass. Mass difference used to adjust TrcA detected mass to theoretical mass used to calibrate all other masses

Figure 3.7 depicts the mass-spectra for a deep-well culture extract supplemented with 20 mM 2-FF on top of TGS base media. Fourteen possible peptide masses were detected. A TrcA with three 2-FF residues gave the highest signal. For the gramicidins, which lie in the mass range of 1882.0862 to 1873.0858 Da, only a trace amount of protonated VGA (gramicidin A) and its sodium adduct were detected. Table 3.2 lists the possible peptides with theoretical masses that correspond with the detected masses. For the peptides identified, all have a potential incorporation of the Phe analogue containing a fluorine group (Table 3.2). Fluorinated analogues of PhcA, PhcA<sub>1</sub>, TrcA, TrcA<sub>1</sub>, TpcA, TpcA<sub>1</sub> and TrcB/B' are likely to be identified correctly as their natural counterparts in the 20 mM Phe supplemented extract were observed. The mass of 1346.6374 Da corresponds closely with that of a TpcB<sub>1</sub>/B<sub>1</sub>', but given the fact that this is not observed in the Phe supplemented culture extract it is more likely a TrcA (3\*2-FF) with a sodium adduct, as TrcA gave the largest relative signal in the Phe extract. The same principle can be used to eliminate the TrcC (mass at 1348.6450 Da), TrcC<sub>1</sub> (1362.6329 Da), TpcB/B' (2\*2-FF) (1368.6329 Da), TpcB<sub>1</sub>/B<sub>1</sub>' (1368.6329 Da) as possible Trc analogues. There also appears to be less dimerization by the 2-FF extract (Figure 3.7, A), but far higher levels of trimers and tetramers detected (possibly explaining the loss of dimer signal).

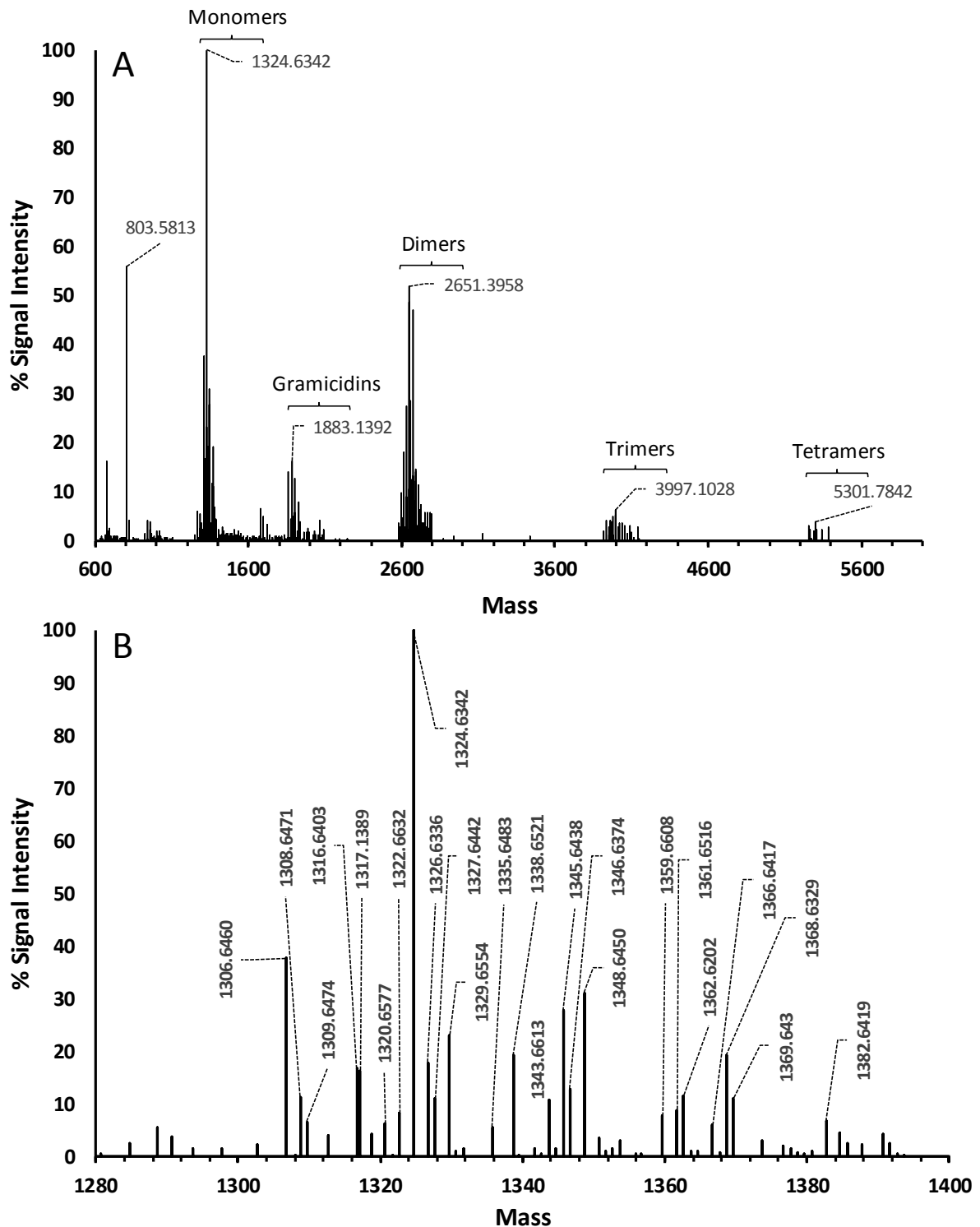


*Figure 3.7* ESMS mass-spectra generated using the MaxEnt 3 algorithm for 20 mM 2-FF supplemented deep-well culture extract of strain 5618. **A** Full spectrum over the mass range 600-6000 Da, **B** Extracted spectrum showing the mass range (1280-1400 Da) in which monomeric peptides would be detected. Refer to Table 3.2 for the list possible peptide identities from detected masses above.

**Table 3.2** List of detected masses for 20 mM 2-FF supplemented deep-well extracts which could be putatively identified based on theoretical masses. Labels correspond to mass-spectra in Figure 3.7, B.

Detected Mass	Possible Identities*	Theoretical masses	ppm error
1306.6460	TrcA (2*2-FF)	1306.6436	2
	TrcA <sub>1</sub> + Na	1306.6600	-11
1308.6471	PhcA (3*2-FF)	1308.6393	6
	PhcA <sub>1</sub> (1*2-FF) + Na	1308.6557	-7
1324.6342 <sup>#</sup>	TrcA (3*2-FF)	1324.6342	0
	TrcA <sub>1</sub> (1*2-FF) + Na	1324.6506	-12
1326.6336	PhcA (4*2-FF)	1326.6298	3
	PhcA <sub>1</sub> (2*2-FF) + Na	1326.6463	-10
1327.6442	TrcB (1*2-FF)	1327.6639	-15
1329.6554	TpcA (2*2-FF)	1329.6596	-3
	TpcA <sub>1</sub> + Na	1329.6760	-15
1338.6521	TrcA <sub>1</sub> (3*2-FF)	1338.6498	2
1343.6613	TpcA <sub>1</sub> (2*2-FF)	1343.6752	-10
1345.6438	TrcB/B' (2*2-FF)	1345.6545	-8
	Trc B <sub>1</sub> /B <sub>1</sub> ' + Na	1345.6709	-20
1346.6374	TrcA (3*2-FF) + Na	1346.6161	16
	TpcB <sub>1</sub> /B <sub>1</sub> '	1346.7050	-50
1348.6450	TrcC	1348.6842	-29
	PhcA (4*2-FF) + Na	1348.6118	25
1362.6329	PhcA <sub>1</sub> (4*2-FF) + Na	1362.6274	4
	TrcC <sub>1</sub>	1362.6999	-49
1368.6329	TpcB/B' (2*2-FF)	1368.6705	-27
	TpcB <sub>1</sub> /B <sub>1</sub> ' + Na	1368.6869	-39
1369.6430	TpcA (3*2-FF) + Na	1369.6321	8

<sup>#</sup> Detected mass of TrcA (3\*2-FF) adjusted to theoretical mass. Mass difference used to adjust TrcA (3\*2-FF) detected mass to theoretical mass used to calibrate all other masses

Figure 3.8 represents the mass-spectra of a 20 mM 4-MeF supplemented deep-well culture, using TGS as a base media. Methylated analogues of PhcA, PhcA<sub>1</sub>, TrcA, TrcA<sub>1</sub>, TpcA, TpcA<sub>1</sub> and TrcB/B' (Table 3.3) are also likely to be identified correctly as their natural counterparts in the 20 mM Phe supplemented extract were also observed. This lack of detection of TrcB<sub>1</sub>/B<sub>1</sub>' in the Phe supplemented culture extract, makes TrcB<sub>1</sub>/B<sub>1</sub>' with one 4-MeF residue (TrcB<sub>1</sub>/B<sub>1</sub>'(1\*4MeF), mass 1337.7656 Da) a less likely peptide in the 4-MeF supplemented extract. The peptides in this extract appeared to dimerise less (Figure 3.8, A) than those found in the Phe supplemented extract, but produced higher levels of trimers and tetramers.

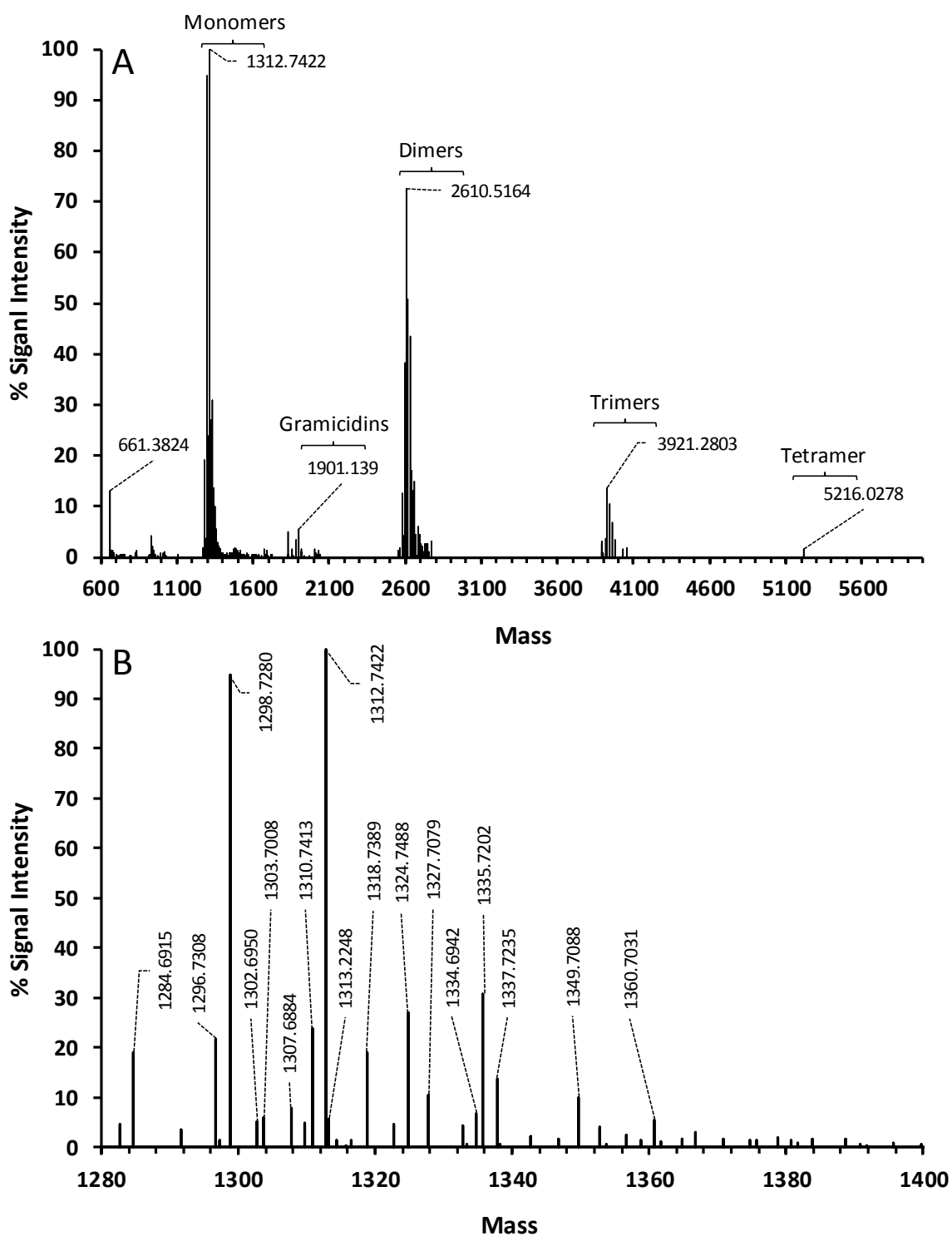


*Figure 3.8* ESMS mass-spectra generated using the MaxEnt 3 algorithm for 20 mM 4-MeF supplemented deep-well culture extract of strain 5618. **A** Full spectrum over the mass range from 600-6000 Da, **B** Extracted spectrum showing mass range (1280-1400 Da) in which the monomeric peptides would be detected. Refer to Table 3.3 for the list possible peptide identities from detected masses above.

**Table 3.3** List of detected masses for 20 mM 4-MeF supplemented deep-well culture extracts which could be putatively identified based on theoretical masses. Labels correspond to mass-spectra in Figure 3.8, B.

Detected Mass	Possible Identities*	Theoretical masses	ppm error
1284.6915	TrcA (1*MeF)	1284.6890	2
	TrcA <sub>1</sub>	1284.6781	10
1296.7308	PhcA (3*MeF)	1296.7470	-12
	PhcA <sub>1</sub> (2*MeF)	1296.7363	-4
1298.7280	TrcA (2*MeF)	1298.7156	10
	TrcA <sub>1</sub> (1*MeF)	1298.7047	18
1310.7413	PhcA (4*MeF)	1310.7738	-25
	PhcA <sub>1</sub> (3*MeF)	1310.7629	-16
1312.7422 <sup>#</sup>	TrcA (3*MeF)	1312.7422	0
	TrcA <sub>1</sub> (2*MeF)	1312.7312	8
1318.7389	PhcA (3*MeF) + Na	1318.7292	7
	PhcA <sub>1</sub> (2*MeF) + Na	1318.7183	16
1324.7448	PhcA <sub>1</sub> (4*MeF)	1324.7895	-34
1335.7202	TpcA (3*MeF)	1335.7582	-28
	TpcA <sub>1</sub> (2*MeF)	1335.7472	-20
1337.7235	TrcB/B' (2*MeF)	1337.7265	-2
	TrcB <sub>1</sub> /B <sub>1</sub> ' (1*MeF)	1337.7156	6

<sup>#</sup> Detected mass of TrcA (3\*2-MeF) adjusted to theoretical mass. Mass difference used to adjust TrcA (3\*2-MeF) detected mass to theoretical mass used to calibrate all other masses

Figure 3.9 and Table 3.4 represent the mass-spectra and possible peptides containing a 4-CF<sub>3</sub>F residue. Fifteen possible peptides were found, with only the mass 1332.6678 Da having more than one possible identity. Of the nine monomers identified, the masses 1338.6361 Da, 1360.6684 Da, 1361.6549 Da, 1377.6450 Da, 1392.6464 Da and 1400.6491 Da had masses which indicated the possible incorporation of a single 4-CF<sub>3</sub>F residue. This signal produced by the peptides in this extract were relatively low compared to the background, with the highest signals being produced by TrcB and TrcC analogues (masses at 1309.6733, 1323.6590, 1348.6753). This indicated that the 4-CF<sub>3</sub>F analogue of Phe might not be readily incorporated into the peptide structure. None the less there were possible novel TrcA and TpcA analogues detected, which would be the most likely candidates for incorporation when considering the high signal intensities of their natural counterparts in the Phe supplemented extract. There appeared to be relatively low levels of dimerization of these peptides compared to the Phe extract, with similar trimer levels but more tetramer formation (Figure 3.9, A).

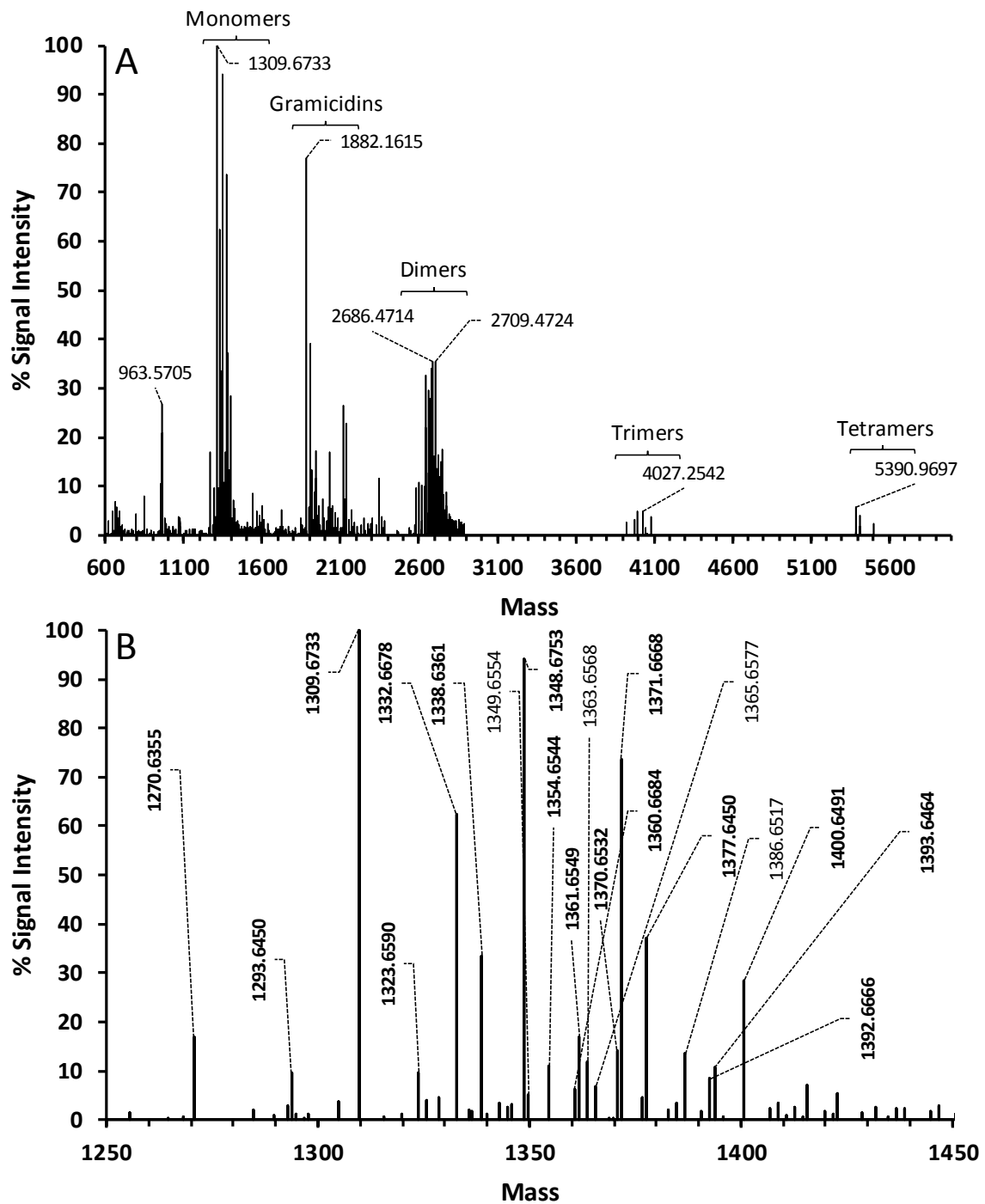


*Figure 3.9* ESMS mass-spectra generated using the MaxEnt 3 algorithm for 20 mM 4-CF<sub>3</sub>F supplemented deep-well culture extract of strain 5618. **A** Full spectrum over the mass range from 600-6000 Da, **B** Extracted spectrum showing mass range (1250-1400 Da) in which the monomeric peptides would be detected. Refer to Table 3.4 for the list possible peptide identities from detected masses above.

**Table 3.4** List of detected masses for 20 mM supplemented 4-CF<sub>3</sub>F deep-well culture extracts which could be putatively identified based on theoretical masses. Labels correspond to mass-spectra in Figure 3.9, B.

Detected Mass	Possible Identities*	Theoretical masses	ppm error
1270.6355	TrcA	1270.6624	-21
1293.6450	TrcA + Na	1293.6522	-6
1309.6733 <sup>#</sup>	TrcB/B'	1309.6733	0
1323.6590	TrcB <sub>1</sub> /B <sub>1</sub> '	1323.689	-23
1332.6678	TpcB/B'	1332.6893	-16
	TrcB/B' + Na	1332.6631	4
1338.6361	TrcA (1*4-CF <sub>3</sub> F)	1338.6605	-18
1348.6753	TrcC	1348.6842	-7
1354.6544	TpcB/B' + Na	1354.6713	-12
1360.6684	TrcA (1*4-CF <sub>3</sub> F) + Na	1360.6425	19
1361.6549	TpcA (1*4-CF <sub>3</sub> F)	1361.6765	-16
1370.6532	TrcC + Na	1370.6662	-9
1377.6450	Trc B/B' (1*4-CF <sub>3</sub> F)	1377.6714	-19
1392.6666	TrcAv (1*CF <sub>3</sub> F)	1392.643	17
1393.6464	TpcC + Na	1393.6822	-26
1400.6491	TpcB/B' (1*CF <sub>3</sub> F)	1400.6874	-27

<sup>#</sup> Detected mass of TrcB/B' adjusted to theoretical mass. Mass difference used to adjust TrcB/B' detected mass to theoretical mass used to calibrate all other masses

Figure 3.10 and Table 3.5 depict the results for 10 mM supplementation with the natural amino acid tryptophan (W). There were higher levels of gramicidin production relative to the Phe extract, possibly due to Trp-rich structure of the gramicidins. There were also lower levels of dimerization, but more tetramer formation observed for the cyclic decapeptides in the extract. As previously found by Vosloo *et al.* (19), we also observed only four major peptides with a clear shift towards the production of Trp containing analogues relative to the Phe extract. As expected from previous studies (19, 20), TpcC was the major peptide observed, and generated a significantly higher signal compared to the other peptides in this extract.



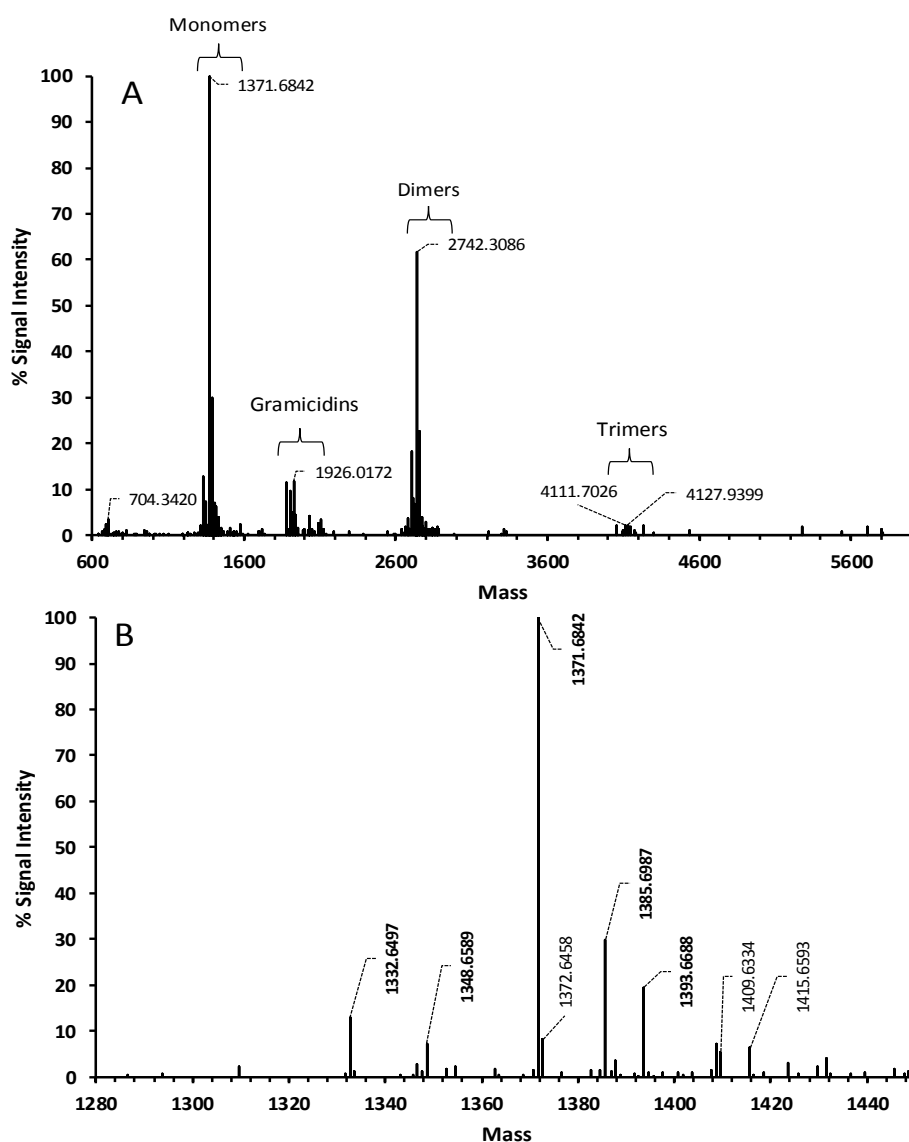
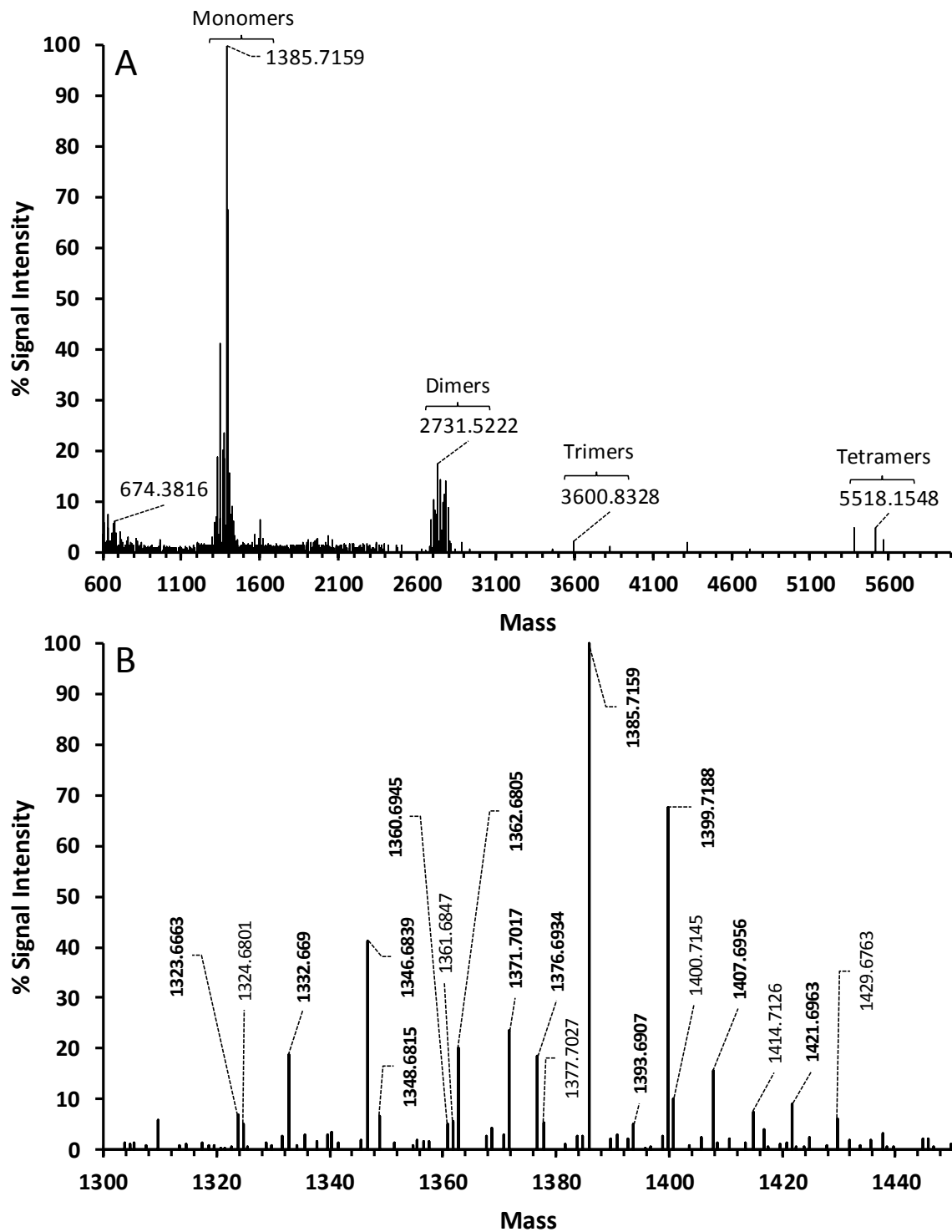


Figure 3.10 ESMS mass-spectra generated using the MaxEnt 3 algorithm for 10 mM Trp supplemented deep-well culture extract of strain 5618. **A** Full spectrum over the mass range from 600-6000 Da, **B** Extracted spectrum showing mass range (1280-1450 Da) in which the monomeric peptides would be detected. Refer to Table 3.5 for the list possible peptide identities from detected masses above.

*Table 3.5* List of detected masses for 10 mM supplemented Trp deep-well extracts which could be putatively identified based on theoretical masses. Labels correspond to mass-spectra in Figure 3.10.

<b>Detected Mass</b>	<b>Possible Identities*</b>	<b>Theoretical masses</b>	<b>ppm error</b>
1332.6497	TpcB/B'	1332.6893	-30
1348.6589	TrcC	1348.6842	-19
1371.6842	TpcC	1371.7002	-12
1385.6987	TpcC <sub>1</sub>	1385.7159	-12
1393.6688	TpcC + Na	1393.6822	-10

Figure 3.11 and Table 3.6 represent the mass spectra and possible peptide identities found in cultures supplemented with the methylated tryptophan analogue 1-MeW. Eight possible peptides were identified. Given the production profile of the Trp supplemented extract, the mass at 1362.6805 Da is more likely a Trc with a single 1-MeW residue incorporated than a TrcC<sub>1</sub>, which was not observed in the Trp extract. Similarly, the mass at 1376.6934 Da is likely a TrcC with two 1-MeW residues or TrcC (2\*1MeW). There appeared to be much lower levels of dimerization of in this extract, as well as virtually no readily observable gramicidin production, which is in stark contrast to the Trp extract.



*Figure 3.11* ESMS mass-spectra generated using the MaxEnt 3 algorithm for 10 mM 1-MeWsupplemented deep-well culture extract of strain 5618. **A** Full spectrum over the mass range from 600-6000 Da, **B** Extracted spectrum showing mass range (1300-1450 Da) in which the monomeric peptides would be detected. Refer to Table 3.6 for the list possible peptide identities from detected masses above.

**Table 3.6** List of detected masses for 10 mM supplemented 1-MeW deep-well extracts which could be putatively identified based on theoretical masses. Labels correspond to mass-spectra in *Figure 3.11*, B.

Detected Mass	Possible Identities*	Theoretical masses	ppm error
1332.6690	TpcB/B'	1332.6893	-15
1346.6839	TpcB/B' (1*1MeW)	1346.7050	-16
	TpcB <sub>1</sub> /B <sub>1</sub> '	1346.7050	-16
1362.6805	TrcC (1*1MeW)	1362.6999	-14
	TrcC <sub>1</sub>	1362.6999	-14
1371.7017	TpcC	1371.7002	1
1376.6934	TrcC (2*1MeW)	1376.7158	-16
	TrcC <sub>1</sub> (1*1MeW)	1376.7157	-16
1385.7159 <sup>#</sup>	TpcC (1*1MeW)	1385.7159	0
	TpcC <sub>1</sub>	1385.7159	0
1399.7188	TpcC (2*1MeW)	1399.7315	-9
	TpcC <sub>1</sub> (1*1MeW)	1399.7315	-9
1407.6956	TpcC (1*1MeW) + Na	1407.6978	-2
	TpcC <sub>1</sub> + Na	1407.6978	-2

Figure 3.12 and Table 3.7 represent the ESMS analysis of the 5-MeW supplemented deep-well culture extract. Six possible peptide masses were identified. The mass of 1323.6554 Da gives two possible theoretical identities, either a TrcB<sub>1</sub>/B<sub>1</sub>' or a TrcB/B' (1\*5MeW), which are unique in the sense that neither TrcB<sub>1</sub>/B<sub>1</sub>' or TrcB/B' were readily produced in the Trp supplemented culture. The peptide with  $m/z$  at 1346.6774 is likely a TpcB/B' (1\*5MeW) given that this was readily produced in the Trp supplemented culture. The peptide correlating to  $m/z$  of 1360.6869 Da could be a TpcB<sub>1</sub>/B<sub>1</sub>' (1\*5MeW), as its sodium adduct at  $m/z$  1382.6908 was also detected. However, very little TpcB<sub>1</sub>/B<sub>1</sub>' is produced in Trp supplemented culture, which could indicate that 5-MeW incorporation leads to selective synthesis of the B and B<sub>1</sub> type tryptocidine analogues. This extract appeared to form fewer dimers than the Trp supplemented culture extract, but more tetramers. Its gramicidin content appeared to be similar to that of the Trp supplemented culture extract.

Due to the complicated nature of dimerization and oligomerisation in the cyclic decapeptide mixtures this was not discussed in detail in this chapter. However, a preliminary analysis of the possible dimers in the different supplemented extracts is given in the addendum.

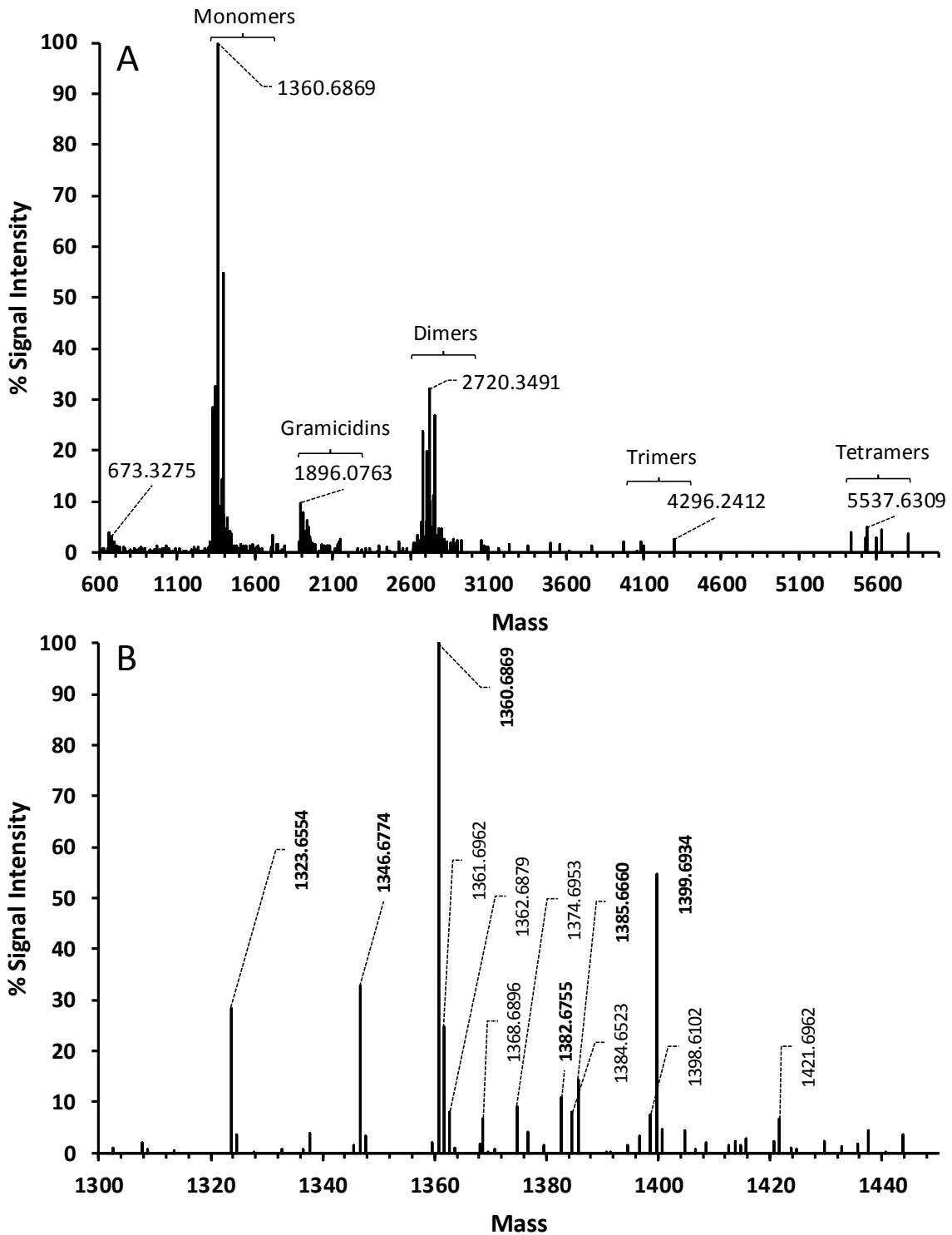
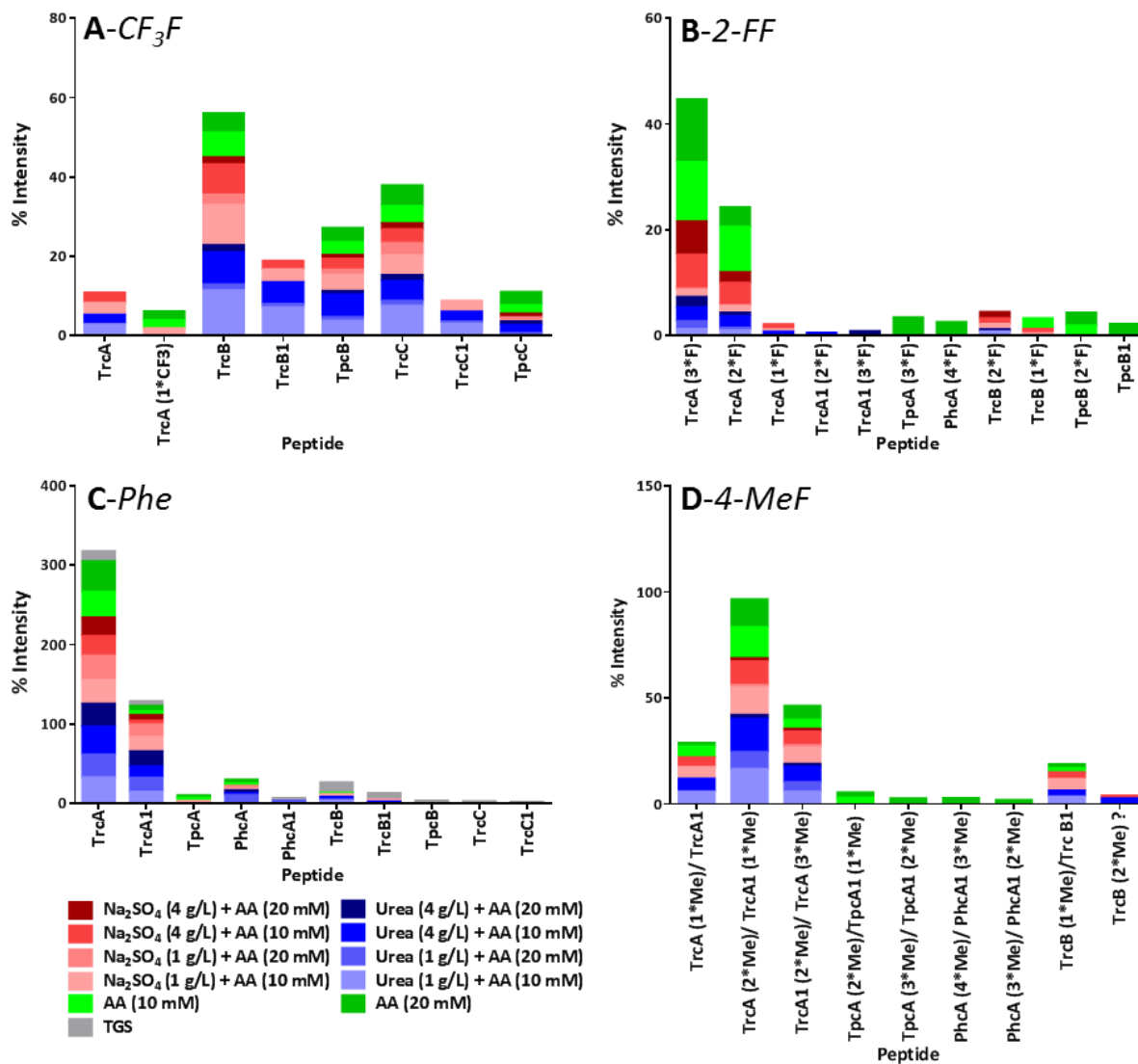


Figure 3.12 ESMS mass-spectra generated using the MaxEnt 3 algorithm for 10 mM 5-MeW supplemented deep-well culture extract of strain 5618. **A** Full spectrum over the mass range from 600-6000 Da, **B** Extracted spectrum showing mass range (1300-1450 Da) in which the monomeric peptides would be detected. Refer to Table 3.7 for the list possible peptide identities from detected masses above.

*Table 3.7* List of detected masses for 10 mM supplemented 5-MeW deep-well extracts which could be putatively identified based on theoretical masses. Possible identities correspond to mass-spectra in Figure 3.12, B.

Detected Mass	Possible Identities*	Theoretical masses	ppm error
1323.6554	TrcB/B' (1*5MeW)	1323.6890	-25
	TrcB <sub>1</sub> /B <sub>1</sub> '	1323.6890	-25
1346.6774	TpcB/B' (1*5MeW)	1346.7050	-20
	TpcB <sub>1</sub> /B <sub>1</sub> '	1346.7050	-20
1360.6869	TpcB/B' (2*5MeW)	1360.7206	-25
	TpcB <sub>1</sub> /B <sub>1</sub> ' (1*5MeW)	1360.7206	-25
1382.6908	TpcB/B' (2*5MeW) + Na	1382.7026	-9
	TpcB <sub>1</sub> /B <sub>1</sub> ' (1*5MeW) + Na	1382.7026	-9
1385.6660	TpcC (1*5MeW)	1385.7159	-36
	TpcC <sub>1</sub>	1385.7159	-36
1399.9634	TpcC (2*5MeW)	1399.7315	-27
	TpcC <sub>1</sub> (1*5MeW)	1399.7315	-27

*Comparison of Trc production under varying growth conditions using ESMS analysis of extracts:* Figure 3.13 represents the results of combined analysis of all the Phe and Phe derivative supplemented cultures. These deep-well cultures were extracted and analysed by ESMS to determine if the growth rate under certain conditions had an effect on both natural and novel Trc productions. The % intensity on the in this figure gives an idea of how the signal of Trcs identified in the monomer mass range (after MaxEnt 3 processing), using ESMS analysis, changes relative to the background of detected compounds, which gives a good estimation of peptide production. Concentrations of amino acids were chosen from the middle and high end the concentration range used for growth-rate analysis. In addition, urea and sodium sulphate were used at two different concentration to determine if their apparent positive effect on growth rate observed in Chapter 2 has an effect peptide production.



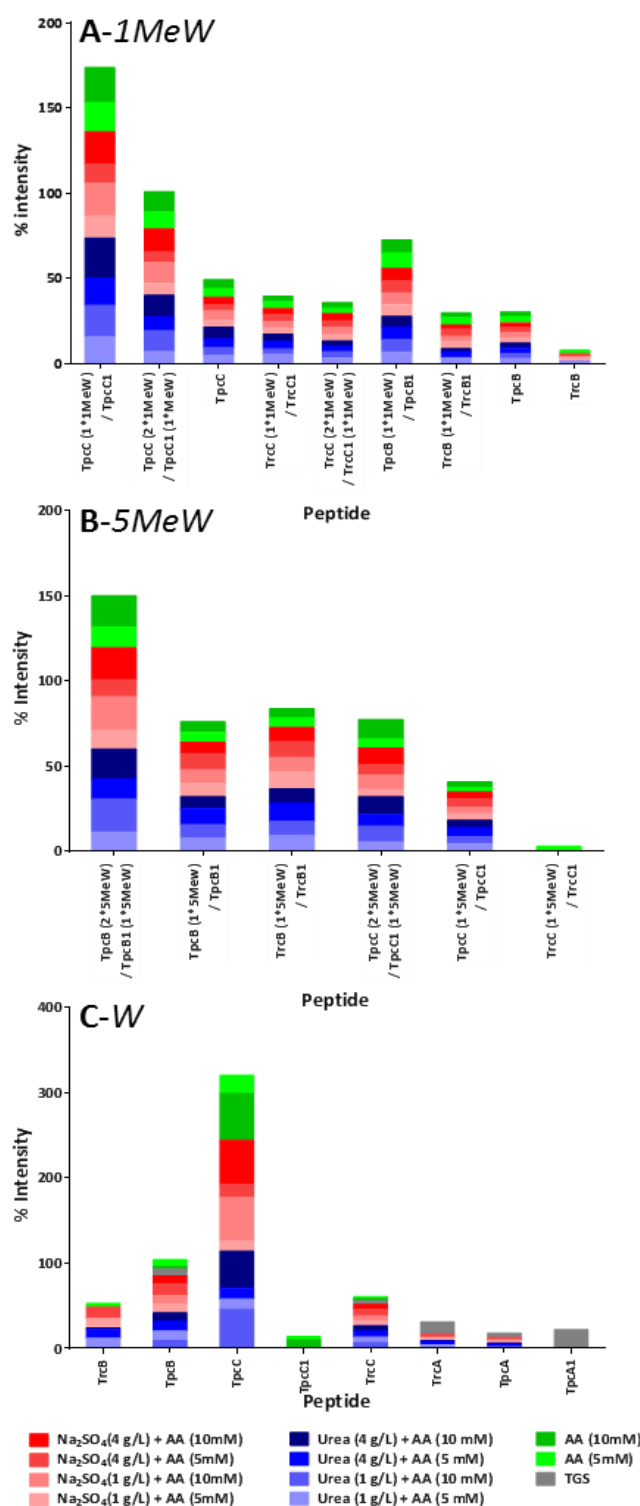
**Figure 3.13** Comparison of the medium-throughput deep-well culture extracts for phenylalanine and its derivatives supplemented into the growth media of the 5618 strain. The % intensity represents the percentage contribution that was observed for each Trc analogue under that specific growth condition. The AA in the figure legend is a placeholder for the particular amino acid used in that assay, together with the urea or Na<sub>2</sub>SO<sub>4</sub> concentration. The F-analogue used is shown at the top-left of each graph. The % intensity shown is the mean of two analytical repeats obtained by combining six deep-well cultures for each extraction and subsequent analysis.

Figure 3.13, C, compares the Trc production in the Phe supplemented growth media of strain 5618. As expected relatively high signal intensities were found for TrcA and PhcA relative to the TGS. All Phe supplemented extracts, irrespective of Phe, urea or Na<sub>2</sub>SO<sub>4</sub> concentration produced similar signal intensities relative to TGS. Looking at the growth rates for the 5618 strain at 11 mM and 22 mM (Figure 3.2, D), there was an improvement in growth rate over TGS, but the improvement seen in peptide production may not correlate with this. For the Phe derivative 2-FF (Figure 3.13, B), TrcA analogues with three and two 2-FF residues were found in the highest % signal intensities

respectively. For these two Trc analogues, TGS together with 10 mM or 20 mM of 2-FF produced the highest total signal intensity. Eight other potential Trc analogues containing 2-FF were found but at a considerably lower contribution. The addition of either urea or Na<sub>2</sub>SO<sub>4</sub> (irrespective of concentration) did appear to improve the production of a TrcB analogue with two 2-FF residues. In Figure 3.2, B, supplementation of TGS with 2-FF led to a dampening of growth rate relative to the other amino acids tested, but one that was closer to that of TGS. The Phe derivative 4-MeF (Figure 3.13, D) appeared to be incorporated into the Trcs well under all conditions tested, with the exception of a Na<sub>2</sub>SO<sub>4</sub> concentration of 4 g/L together with 20 mM 4-MeF. The 4-CF<sub>3</sub>F analogue only showed one potential novel Trc analogue producing a significant signal, with a mass found corresponding to the incorporation of a single 4-CF<sub>3</sub>F incorporated into a TrcA (Figure 3.13, A)).

Figure 3.14 shows the Trp and Trp derivative supplemented deep-well extracts, using different concentrations of these amino acids together with urea and Na<sub>2</sub>SO<sub>4</sub>. For the samples supplemented with Trp (Figure 3.14, C) TpcC (as expected from previous studies (18)) was produced in the highest amount, followed by TpcB and TrcC. Looking at the TpcC analogue there is an increase in TpcC signal contribution from a 5 mM supplementation to a 10 mM supplementation. There does not appear to be any major influence of Na<sub>2</sub>SO<sub>4</sub> or urea on production. Comparing the signal contributions to that of the TGS control, it is observed that the TGS produced more appreciable amounts of the TrcA, TpcA and TpcA<sub>1</sub> analogues, together with some TpcB. The supplementation of the growth media with Trp leads to a higher relative production of analogues containing tryptophan, particularly TpcC and TrcC. For the direct-injection ESMS results obtained from the Trp derivative supplemented extracts (Figure 3.14, A & B) there appears to be incorporation of both the 1-MeW and 5-MeW analogues for all growth conditions. For the two highest contributions of analogues produced, there appeared to be a marginal preference for urea and Na<sub>2</sub>SO<sub>4</sub> at 4 g/L and 10 mM 1-MeW, Na<sub>2</sub>SO<sub>4</sub> at 1 g/L together with 10 mM 1-MeW, and for TGS alone together with 5 mM or 10 mM 1-MeW, although observed differences are minimal.





**Figure 3.14** Comparison of the medium-throughput deep-well culture extracts for tryptophan and its analogues supplementation of strain 5618. The % intensity represents the percentage contribution that was observed for each Trc analogue under that specific growth condition. The AA in the figure legend is a placeholder for the particular amino acid used in that assay, together with the urea or  $\text{Na}_2\text{SO}_4$  concentration. The Trp-analogue used is shown at the top-left of each graph. The % intensity shown is the mean of two analytical repeats obtained by combining six deep-well cultures for each extraction and subsequent analysis. Letters in bold show represent amino acids used with **A**: 1-methyl-tryptophan (1-MeW), **B**: 5-methyl-tryptophan (4-MeW) and **C**: tryptophan (W).

### 3.5 Discussion

Using growth rate analysis under different supplementation conditions has been shown to be a good starting point to assess the effect of these altered conditions on the growth of the producer organism. It is particularly useful to determine if an amino acid derivative is toxic to the organism. This then provides a relatively quick and easy basis by which to select growth conditions for analysis of peptide production using a medium-throughput deep-well assay, which in turn provides a basis for eventual large-scale production of peptides for detailed analysis and purification of individual Trc analogues.

The relative sensitivity of the producer organisms to certain amino acids has been observed, most noticeable is the effect of 1-MeW versus that of 5-MeW on growth rate for all the strains, while fluorinated phenylalanine also inhibited growth rate for both the 362 and 5618-strains. Even though there are differences in growth rate between both amino acid type and concentration, almost all the conditions tested led to growth rate comparable to the supplemented TGS media, with the only exception being the 11 mM and 22 mM 1-MeW supplemented cultures.

Looking at selected deep-well extracts (Figure 3.6 – Figure 3.12, Table 3.1 – Table 3.7), it is clear that the 5618 strain of *Brevibacillus parabrevis*, and possibly the other strains used in growth rate analysis, readily incorporate all the amino acids supplemented into TGS, while only the 4-CF<sub>3</sub>F derivative did not appear to produce the expected production profile of Phe and its other two derivatives tested. All the Phe derivatives used appeared to lead to increased levels of oligomerisation, particularly the formation of trimers and tetramers. Both the 1-MeW and 5-MeW extracts appeared to produce lower oligomers compared to the natural analogue (with the exception of an increase in tetramer formation for the 5-MeW extract). Interesting to note is that there is often an increase in gramicidin production following supplementation with tryptophan, which was also observed for its derivative 5-MeW. Supplementation with 1-MeW, however, appeared to suppress gramicidin production, but still allow for the formation of Trcs.

The direct-injection ESMS analysis of the deep well extracts showed that while both the 2-FF and 1-MeW amino acid analogues led to inhibited growth in the 5618-strain, they still produced detectable Trc analogues. This may indicate that the some analogues may act as antagonists in protein synthesis, while still being able to bind to tyrocidine synthetase domains, a result supported by Okuda *et al.* (15).

Even though an amino acid analogue may inhibit the growth of the producer organism it is still possible for the producer organism to synthesise detectable amounts of the cyclic decapeptides over

an incubation period of 10 days. This is exemplified by the fact that even though 1-MeW appeared to suppress growth at a concentration of 11 mM, using a concentration of 10 mM in the deep-well cultures still produced detectable amounts of peptide which were likely incorporated into tryptophan analogue.

The ability of the 5618-strain of *Br. parabrevis* (and possibly other strains) to incorporate non-natural amino acids provides even more structural and potential functional diversity to the already extensive library of identified Trc analogues. This opens the door for the creation of Trc analogues with a higher therapeutic index either on their own or acting synergistically in a formulated combination of peptides, as the ability of the monomers to dimerize has been extensively shown. Novel Trc analogues retained the ability to form homo- and heterodimers, which could be essential for activity. In Chapter 4 the ability of the 5618-strain to produce novel modified cyclodecapeptides in the Trc family will be further explored using larger scale production and HPLC purification protocols to isolate these novel peptides and assess their antibacterial activity..

### 3.6 References

1. Mootz, H. D., and Marahiel, M. A. (1997) The tyrocidine biosynthesis operon of *Bacillus brevis*: complete nucleotide sequence and biochemical characterization of functional internal adenylation domains. *J. Bacteriol.* **179**, 6843–6850
2. Linne, U., Stein, D. B., Mootz, H. D., and Marahiel, M. A. (2003) Systematic and quantitative analysis of protein-protein recognition between nonribosomal peptide synthetases investigated in the tyrocidine biosynthetic template. *Biochemistry.* **42**, 5114–5124
3. Kopp, F., and Marahiel, M. A. (2007) Macrocyclization strategies in polyketide and nonribosomal peptide biosynthesis. *Nat. Prod. Rep.* **24**, 735-749
4. Marahiel, M. A. (2009) Working outside the protein-synthesis rules: insights into non-ribosomal peptide synthesis. *J. Pept. Sci.* **15**, 799–807
5. Trauger, J. W., Kohli, R. M., Mootz, H. D., Marahiel, M. A., and Walsh, C. T. (2000) Peptide cyclization catalysed by the thioesterase domain of tyrocidine synthetase. *Nature.* **407**, 215–218
6. Kohli, R. M., Walsh, C. T., and Burkart, M. D. (2002) Biomimetic synthesis and optimization of cyclic peptide antibiotics. *Nature.* **418**, 658–661

7. Tang, X-J., Thibault, P., and Boyd, R. K. (1992) Characterisation of the tyrocidine and gramicidin fractions of the tyrothricin complex from *Bacillus brevis* using liquid chromatography and mass spectrometry. *Int. J. Mass Spectrom. Ion Process.* **122**, 153–179
8. Spathelf, B. (2010) Qualitative structure-activity relationships of the major tyrocidines , cyclic decapeptides from *Bacillus aneurinolyticus*. **Ph.D. thesis**, Stellenbosch University, <http://hdl.handle.net/10019.1/4001>
9. Marques, M. A., Citron, D. M., and Wang, C. C. (2007) Development of tyrocidine A analogues with improved antibacterial activity. *Bioorg. Med. Chem.* **15**, 6667–6677
10. Spathelf, B. M., and Rautenbach, M. (2009) Anti-listerial activity and structure-activity relationships of the six major tyrocidines, cyclic decapeptides from *Bacillus aneurinolyticus*. *Bioorganic Med. Chem.* **17**, 5541–5548
11. Leussa, A. N. yango N., and Rautenbach, M. (2014) Detailed SAR and PCA of the tyrocidines and analogues towards leucocin A-sensitive and leucocin A-resistant *Listeria monocytogenes*. *Chem. Biol. Drug Des.* **84**, 543–557
12. Loll, P. J., Upton, E. C., Nahoum, V., Economou, N. J., and Cocklin, S. (2014) The high resolution structure of tyrocidine A reveals an amphipathic dimer. *Biochim. Biophys. Acta.* **1838**, 1199–1207
13. Munyuki, G., Jackson, G. E., Venter, G. a., Kövér, K. E., Szilágyi, L., Rautenbach, M., Spathelf, B. M., Bhattacharya, B., and Van Der Spoel, D. (2013)  $\beta$ -sheet structures and dimer models of the two major tyrocidines, antimicrobial peptides from *Bacillus aneurinolyticus*. *Biochemistry.* **52**, 7798–7806
14. Qin, C., Zhong, X., Bu, X., Ng, N. L. J., and Guo, Z. (2003) Dissociation of antibacterial and hemolytic activities of an amphipathic peptide antibiotic. *J. Med. Chem.* **46**, 4830–4833
15. Okuda, K., Edwards, G. C., and Winnick, T. (1962) Biosynthesis of gramicidin and tyrocidine in the Dubos strain of *Bacillus brevis* I. Experiments with growing cultures. *J. Bacteriol.* **85**, 329–338
16. Mach, B., Reich, E., and Tatum, E. L. (1963) Separation of the biosynthesis of the antibiotic polypeptide tyrocidine from protein biosynthesis\*. *Proc. Natl. Acad. Sci. U. S. A.* **50**, 175–181

17. Ruttenberg, M. A, and Mach, B. (1966) Studies on amino acid substitution in the biosynthesis of the antibiotic polypeptide tyrocidine. *Biochemistry*. **5**, 2864–2869
18. Vosloo, J. A., Stander, M. A., Leussa, A. N. N., Spathelf, B. M., and Rautenbach, M. (2013) Manipulation of the tyrothricin production profile of *Bacillus aneurinolyticus*. *Microbiol. (United Kingdom)*. **159**, 2200–2211
19. Vosloo, J. A. (2016) Optimised bacterial production and characterisation of natural antimicrobial peptides with potential application in agriculture. **Ph.D. thesis**, University of Stellenbosch, [scholar.sun.ac.za/handle/10019.1/98411](https://scholar.sun.ac.za/handle/10019.1/98411), pp 3.7 -3.13
20. Mach, B., and Tatum, E. L. (1964) Environmental control of amino acid substitutions in the biosynthesis of the antibiotic polypeptide tyrocidine. *Proc. Natl. Acad. Sci. U. S. A.* **52**, 876–884

### 3.6 Addendum

The incorporation of the non-natural amino acids used in the deep-well extracts leads to a wide array of novel tyrocidine, tryptocidine and some phenycidine analogues. The increase in the diversity of monomers incorporating non-natural amino acid derivatives leads to an even more diverse array of dimers, which the Trcs have been shown to readily form. In this addendum a breakdown of the dimers observed for both Trp and Phe supplemented cultures, as well as their non-natural derivatives, is given. The extracted spectrums are shown covering the expected dimer ranges from the mass-spectra in Figures 3.6 to 3.12.

Figures 3.16 to 3.21 depict the extracted mass-ranges for the expected dimers, generated using the MaxEnt 3 function. Figures 3.8 to 3.21 show the detected masses in this range as well as their possible identities (i.e. their monomer constituents). The dimers are putatively identified by the monomers positively identified for the extracts, whose theoretical masses were combined and compared against the detected masses. The theoretical dimer masses and detected dimer masses are protonated masses (no adducts were tested for). The theoretical dimer identity can be determined by looking at the masses highlighted in yellow in the theoretical dimer mass tables. The corresponding monomer identities in the first column and top row represent the constituent monomers.

For a full list of theoretical monomer masses for observed Trcs, see addendum of chapter 4.

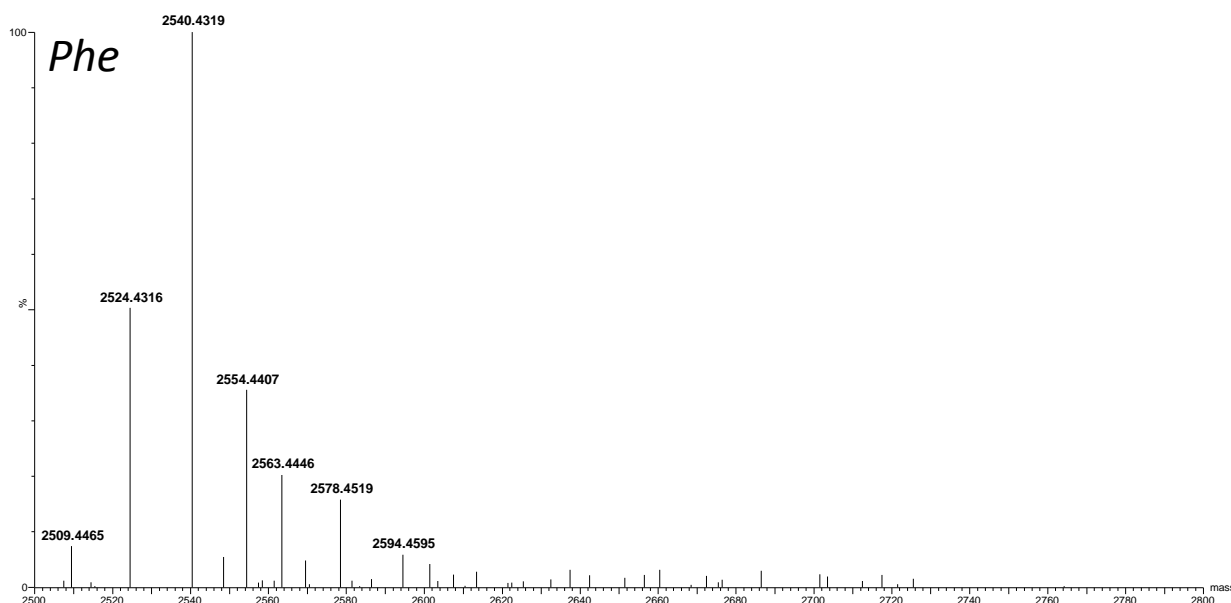


*Figure 3.15* ESMS mass-spectra generated using the MaxEnt 3 algorithm for 20 mM Phe supplemented deep-well culture extract of strain 5618 depicting mass-range for dimers and detected masses. Refer to Table 3.9 for % signal contribution of detected masses to this spectrum and Table 3.8 for possible dimer identities.

*Table 3.9* Detected MaxEnt 3 masses in dimer range for Phe supplemented culture contributing over 2% to total signal in this range.

Detected Mass (Da)	% Total Signal
2540.4319	33.55
2524.4316	16.87
2554.4407	11.92
2563.4446	6.78
2578.4519	5.29
2509.4465	2.47

*Table 3.8* Theoretical dimer masses and constituent monomers determined from combinations of detected monomers in Phe extract. Highlighted masses are theoretical dimer masses which correspond with detected masses in Table 3.9.

TrcB/B'	TpcA <sub>1</sub>	TpcA	TrcA <sub>1</sub>	TrcA	PhcA <sub>1</sub>	PhcA	Monomer Abbreviation
2563.3330	2561.3538	2547.3381	2538.3378	2524.3221	2522.3429	2508.3272	PhcA
2577.3487	2575.3694	2561.3538	2552.3534	2538.3378	2536.3585		PhcA <sub>1</sub>
2579.3280	2577.3487	2563.3330	2554.3327	2540.3171			TrcA
2593.3436	2591.3643	2577.3487	2568.3483				TrcA <sub>1</sub>
2602.3439	2600.3647	2586.3490					TpcA
2616.3596	2614.3803						TpcA <sub>1</sub>
2618.3389							TrcB'

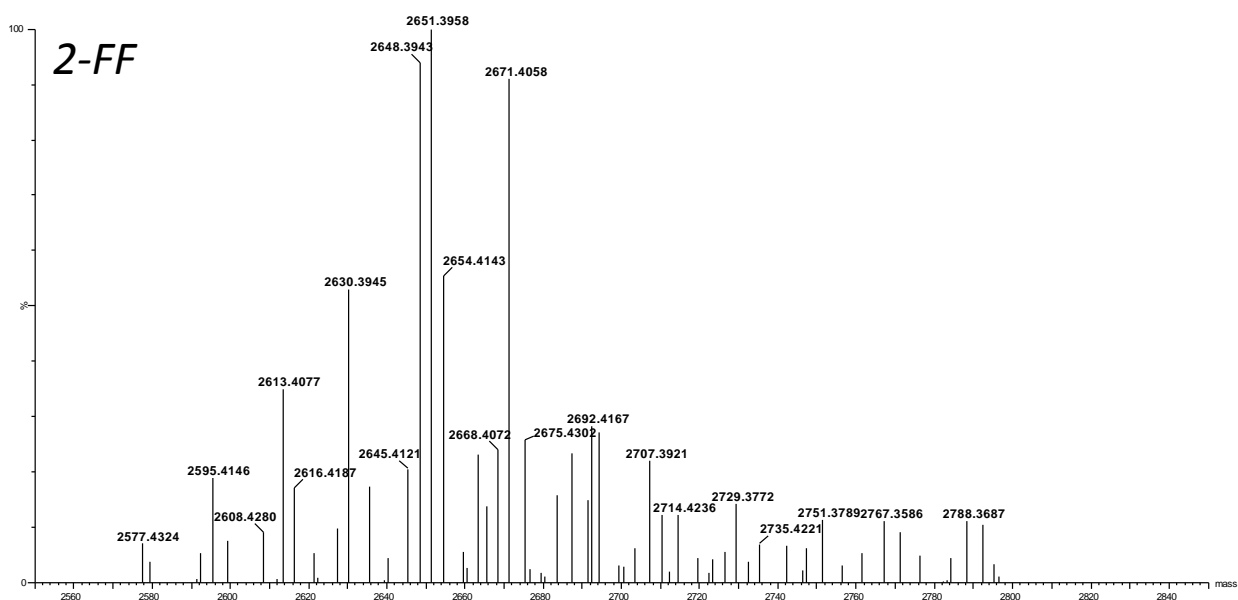


*Figure 3.16* ESMS mass-spectra generated using the MaxEnt 3 algorithm for 20 mM 2-FF supplemented deep-well culture extract of strain 5618 depicting mass-range for dimers and detected masses. Refer to Table 3.10 for % signal contribution of detected masses to this spectrum and Table 3.11 for possible dimer identities.

*Table 3.10* Detected MaxEnt 3 masses in dimer range for 2-FF supplemented culture contributing over 2% to total signal in this range.

Detected Mass (Da)	% Total Signal
2651.3958	10.47
2648.3943	9.82
2671.4058	9.53
2654.4143	5.79
2630.3945	5.55
2613.4077	3.66
2692.4167	2.96
2694.4170	2.84
2675.4302	2.69
2668.4072	2.50
2687.4155	2.45
2663.4016	2.41
2707.3921	2.30
2645.4121	2.14



Table 3.11 Theoretical dimer masses and constituent monomers determined from combinations of detected monomers in 2-FF extract. Highlighted masses are theoretical dimer masses which correspond with detected masses in Table 3.10.

TpcB/B' (2*2-FF)	TrcB/B' (2*2-FF)	TrcB/B' (1*2-FF)	TpcA (2*2-FF)	TrcA <sub>1</sub> (3*2-FF)	TrcA <sub>1</sub> (2*2-FF)	TrcA (3*2-FF)	TrcA (2*2-FF)	PhcA (4*2-FF)	PhcA (3*2-FF)	Monomer Abbreviation
2676.3019	2653.2859	2635.2954	2637.2910	2646.2813	2628.2907	2632.2656	2614.2750	2634.2613	2616.2707	PhcA (3*2-FF)
2694.2925	2671.2765	2653.2859	2655.2816	2664.2718	2646.2813	2650.2562	2632.2656	2652.2518		PhcA (4*2-FF)
2674.3063	2651.2903	2633.2997	2635.2954	2644.2856	2626.2950	2630.2700	2612.2794			TrcA (2*2-FF)
2692.2968	2669.2809	2651.2903	2653.2859	2662.2762	2644.2856	2648.2605				TrcA (3*2-FF)
2688.3219	2665.3059	2647.3153	2649.3110	2658.3012	2640.3107					TrcA <sub>1</sub> (2*2-FF)
2706.3125	2683.2965	2665.3059	2667.3016	2676.2918						TrcA <sub>1</sub> (3*2-FF)
2697.3222	2674.3063	2656.3157	2658.3113							TpcA (2*2-FF)
2695.3266	2672.3106	2654.3200								TrcB/B' (1*2-FF)
2713.3172	2690.3012									TrcB/B' (2*2-FF)
2736.3331										TpcB/B' (2*2-FF)

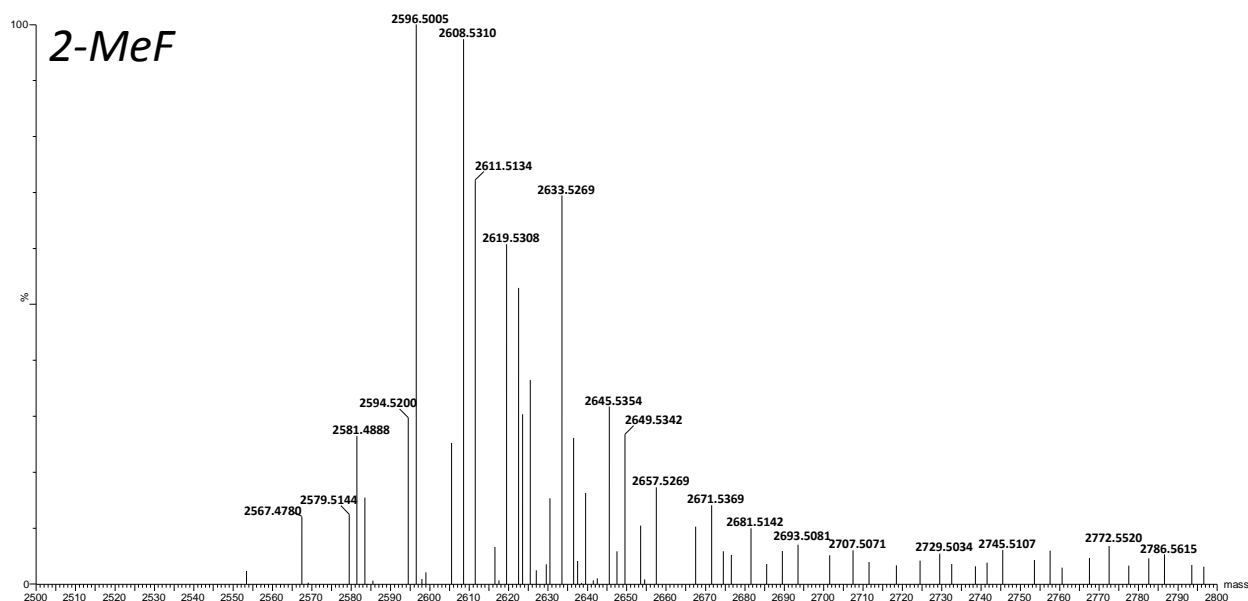


Figure 3.17 ESMS mass-spectra generated using the MaxEnt 3 algorithm for 20 mM 2-MeF supplemented deep-well culture extract of strain 5618 depicting mass-range for dimers and detected masses. Refer to Table 3.12 for % signal contribution of detected masses to this spectrum and Table 3.13 for possible dimer identities.

Table 3.12 Detected MaxEnt 3 masses in dimer range for 4-MeF supplemented culture contributing over 2% to total signal in this range.

Detected Mass (Da)	% Total Signal
2596.5005	10.34
2619.5308	6.28
2622.5415	5.47
2623.5383	3.14
2594.5200	3.07
2649.5342	2.77
2636.5396	2.70
2605.5212	2.61



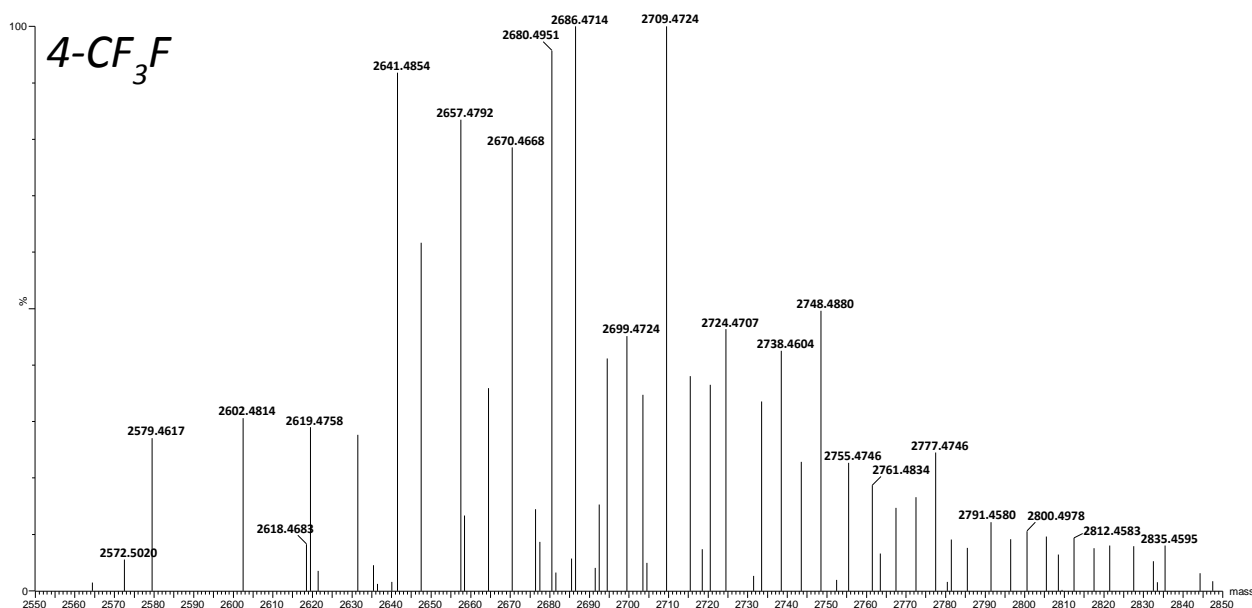


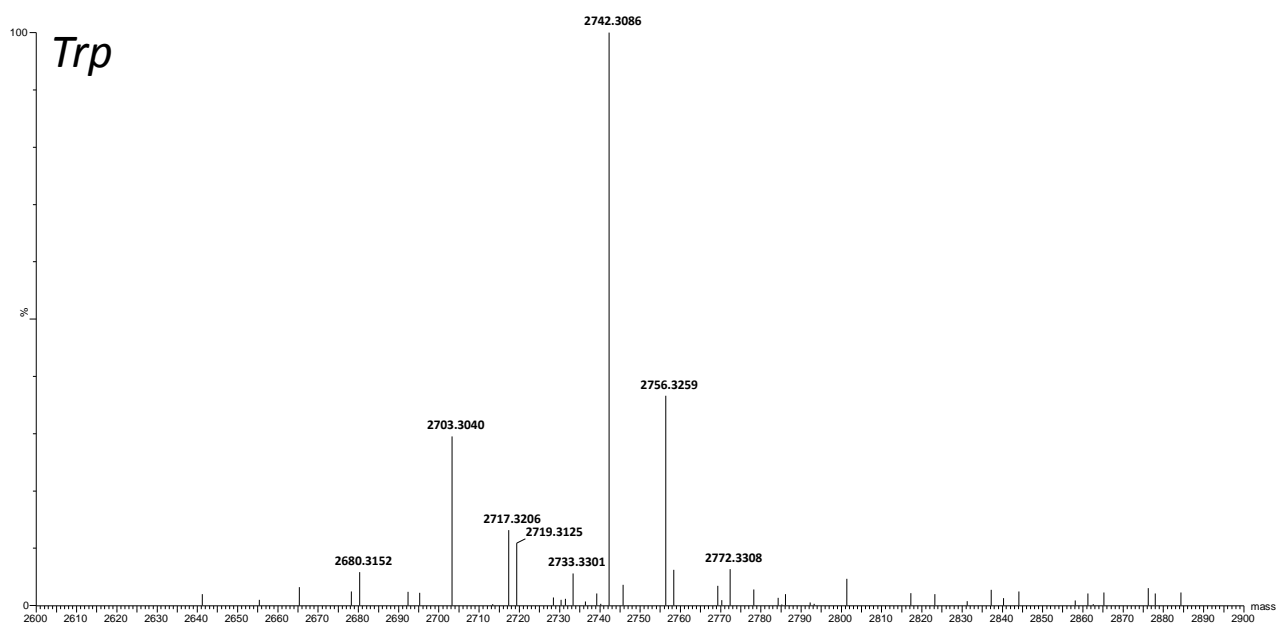
Figure 3.18 ESMS mass-spectra generated using the MaxEnt 3 algorithm for 20 mM 4-CF<sub>3</sub>F supplemented deep-well culture extract of strain 5618 depicting mass-range for dimers and detected masses. Refer to Table 3.14 for % signal contribution of detected masses to this spectrum and Table 3.15 for possible dimer identities.

Table 3.14 Detected MaxEnt 3 masses in dimer range for 4-CF<sub>3</sub>F supplemented culture contributing over 2% to total signal in this range.

Detected Mass (Da)	% Total Signal
2709.4724	6.75
2686.4714	6.75
2680.4951	6.46
2641.4854	6.20
2657.4792	5.64
2670.4668	5.30
2647.4534	4.16
2748.488	3.35
2724.4707	3.13
2699.4724	3.05
2738.4604	2.87
2694.4988	2.78
2715.4607	2.56
2720.4976	2.46
2664.5044	2.42
2703.5002	2.34
2733.4934	2.26
2602.4814	2.06

**Table 3.15** Theoretical dimer masses and constituent monomers determined from combinations of detected monomers in 4-CF<sub>3</sub>F extract. Highlighted masses are theoretical dimer masses which correspond with detected masses in Table 3.14.

TpcC	TrcC	TpcB/B'	TrcB <sub>1</sub> /B <sub>1</sub> '	TrcB/B'	TpcA (1*CF <sub>3</sub> F)	TpcA	TrcAv (1*CF <sub>3</sub> F)	TrcA (1*CF <sub>3</sub> F)	TrcA	Peptide Abbreviation
2641.3548	2618.3389	2602.3439	2593.3436	2647.3261	2631.3311	2563.3330	2594.2995	2608.3152	2540.3171	TrcA
2709.3529	2686.3370	2670.3420	2661.3417	2715.3241	2699.3292	2631.3311	2662.2976	2676.3132		TrcA (1*CF <sub>3</sub> F)
2695.3373	2672.3213	2656.3264	2647.3260	2701.3085	2685.3136	2617.3155	2648.2819			TrcAv (1*CF <sub>3</sub> F)
2664.3708	2641.3548	2625.3599	2616.3596	2670.3420	2654.3471	2586.3490				TpcA
2732.3689	2709.3529	2693.3580	2684.3577	2738.3401	2722.3452					TpcA (1*CF <sub>3</sub> F)
2680.3657	2657.3498	2641.3548	2632.3545	2686.3370						TrcB/B'
2748.3638	2725.3479	2709.3529	2700.3526	2754.3350						TrcB/B' (1*CF <sub>3</sub> F)
2694.3814	2671.3654	2655.3705	2646.3701							TrcB <sub>1</sub> /B <sub>1</sub> '
2703.3817	2680.3657	2664.3708								TpcB/B'
2719.3766	2696.3607									TrcC
2742.3926										TpcC



*Figure 3.19* ESMS mass-spectra generated using the MaxEnt 3 algorithm for 10 mM Trp supplemented deep-well culture extract of strain 5618 depicting mass-range for dimers and detected masses. Refer to Table 3.16 for % signal contribution of detected masses to this spectrum and Table 3.17 for possible dimer identities.

*Table 3.17* Detected MaxEnt 3 masses in dimer range for Trp supplemented culture contributing over 2% to total signal in this range.

Detected Mass (Da)	% Total Signal
2742.3086	36.12
2756.3259	13.22
2703.3040	10.64
2717.3206	4.75
2719.3125	3.92
2772.3308	2.28
2758.3206	2.25
2680.3152	2.11

*Table 3.16* Theoretical dimer masses and constituent monomers determined from combinations of detected monomers in Trp extract. Highlighted masses are theoretical dimer masses which correspond with detected masses in Table 3.17.

Peptide Abbreviation	TpcB	TrcC	TpcC	TpcC <sub>1</sub>
TpcB	2664.3708			
TrcC	2680.3657	2696.3607		
TpcC	2703.3817	2719.3767	2742.3926	
TpcC <sub>1</sub>	2717.3974	2733.3923	2756.4083	2770.4239

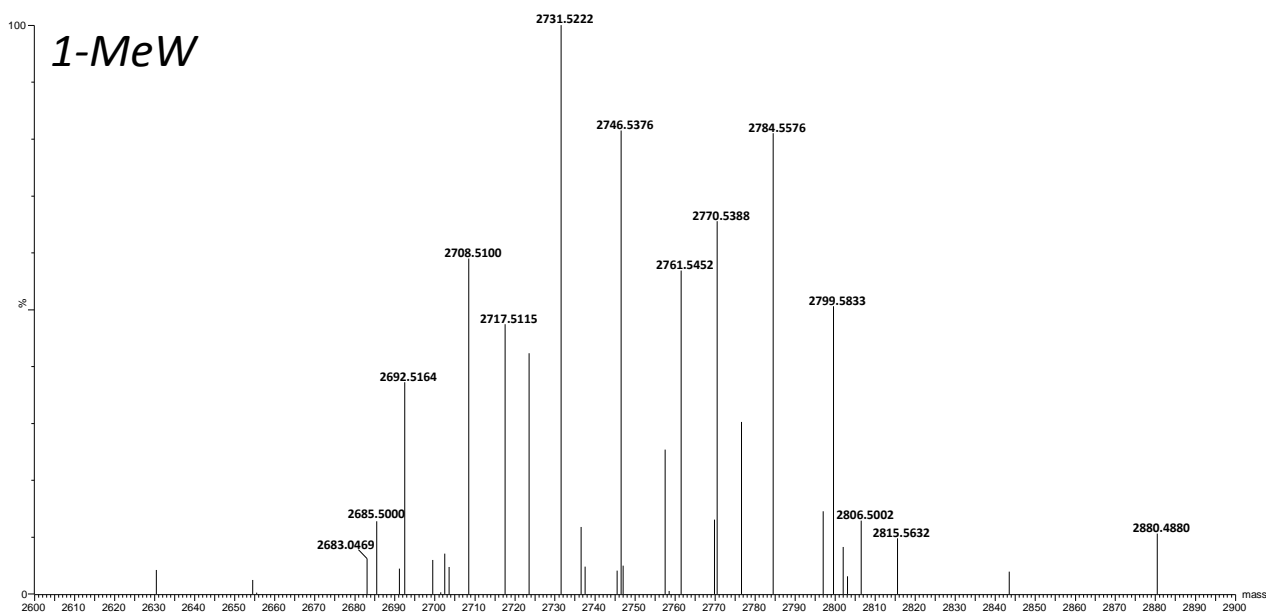


*Figure 3.20* ESMS mass-spectra generated using the MaxEnt 3 algorithm for 10 mM 1-MeW supplemented deep-well culture extract of strain 5618 depicting mass-range for dimers and detected masses. Refer to Table 3.18 for % signal contribution of detected masses to this spectrum Table 3.19 for possible dimer identities.

*Table 3.18* Detected MaxEnt 3 masses in dimer range for 1-MeW supplemented culture contributing over 2% to total signal in this range.

Detected Mass (Da)	% Total Signal
2731.5222	12.08
2746.5376	9.84
2784.5576	9.79
2770.5388	7.91
2708.5100	7.13
2761.5452	6.87
2799.5833	6.11
2717.5115	5.73
2723.5247	5.11
2692.5164	4.49
2776.5486	3.65
2757.5217	3.07

*Table 3.19* Theoretical dimer masses and constituent monomers determined from combinations of detected monomers in 1-MeW extract. Highlighted masses are theoretical dimer masses which correspond with detected masses in Table 3.18.

TpcC <sub>1</sub> (1*1MeW)	TpcC <sub>1</sub>	TpcC (2*1MeW)	TpcC (1*1MeW)	TpcC	TrcC <sub>1</sub> (1*1MeW)	TrcC <sub>1</sub>	TrcC (2*1MeW)	TrcC (1*1MeW)	TpcB/B' (1*1MeW)	TpcB/B'	Peptide Abbreviation
2731.413015	2717.397365	2731.413025	2717.397375	2703.381725	2708.397185	2694.381385	2708.397345	2694.381545	2678.386475	2664.370825	TpcB/B'
2745.428665	2731.413015	2745.428675	2731.413025	2717.397375	2722.412835	2708.397035	2722.412995	2708.397195	2692.402125		TpcB/B' (1*1MeW)
2761.423735	2747.408085	2761.423745	2747.408095	2733.392445	2738.407905	2724.392105	2738.408065	2724.392265			TrcC (1*1MeW)
2775.439535	2761.423885	2775.439545	2761.423895	2747.408245	2752.423705	2738.407905	2752.423865				TrcC (2*1MeW)
2761.423575	2747.407925	2761.423585	2747.407935	2733.392285	2738.407745	2724.391945					TrcC <sub>1</sub>
2775.439375	2761.423725	2775.439385	2761.423735	2747.408085	2752.423545						TrcC <sub>1</sub> (1*1MeW)
2770.423915	2756.408265	2770.423925	2756.408275	2742.392625							TpcC
2784.439565	2770.423915	2784.439575	2770.423925								Tpc C (1*1MeW)
2798.455215	2784.439565	2798.455225									TpcC (2*1MeW)
2784.439555	2770.423905										TpcC <sub>1</sub>
2798.455205											TpcC <sub>1</sub> (1*1MeW)



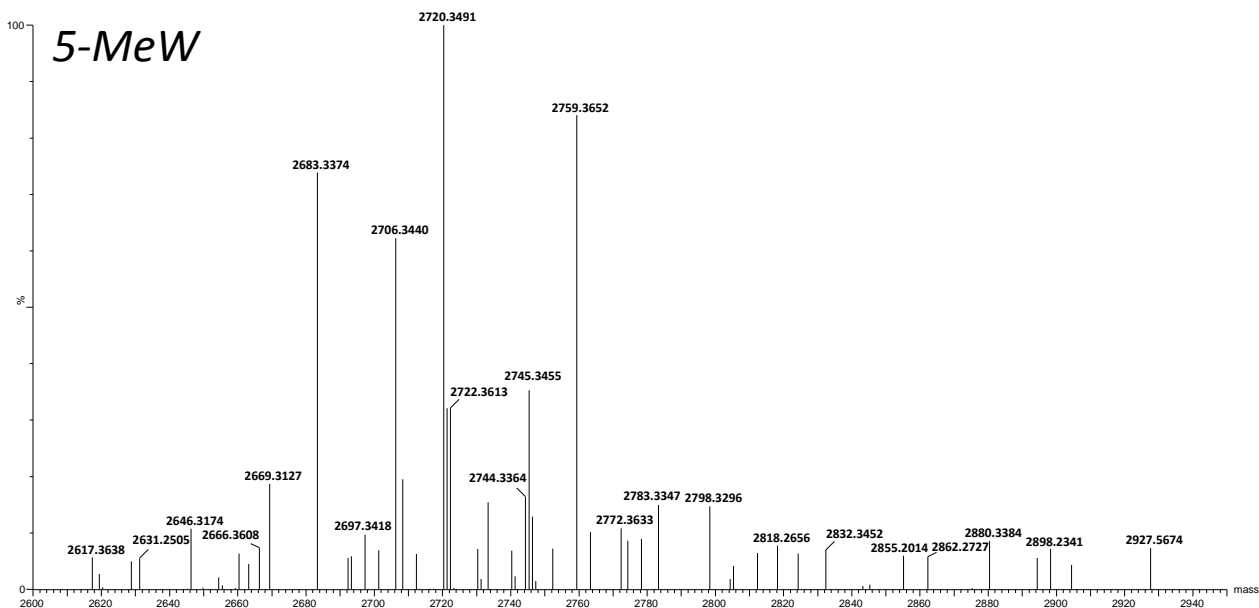


*Figure 3.21* ESMS mass-spectra generated using the MaxEnt 3 algorithm for 10 mM 5-MeW supplemented deep-well culture extract of strain 5618 depicting mass-range for dimers and detected masses. Refer to Table 3.20 for % signal contribution of detected masses to this spectrum and Table 3.21 for possible dimer identities.

*Table 3.20* Detected MaxEnt 3 masses in dimer range for 5-MeW supplemented culture contributing over 2% to total signal in this range.

Detected Mass (Da)	% Total Signal
2720.3491	13.13
2759.3652	11.03
2683.3374	9.70
2706.3440	8.17
2745.3455	4.63
2722.3613	4.22
2721.3516	4.21
2708.3269	2.56
2669.3127	2.45
2744.3364	2.14
2733.3340	2.02

*Table 3.21* Theoretical dimer masses and constituent monomers determined from combinations of detected monomers in 1-MeW extract. Highlighted masses are theoretical dimer masses which correspond with detected masses in Table 3.20.

TpcC <sub>1</sub> (1*5MeW)	TpcC <sub>1</sub>	TpcC (2*5MeW)	TpcC (1*5MeW)	TpcB <sub>1</sub> /B <sub>1</sub> ' (1*5MeW)	TpcB/B' (2*5MeW)	TpcB/B' (1*5MeW)	TrcB <sub>1</sub> /B <sub>1</sub> '	TrcB/B' (1*5MeW)	Peptide Abbreviation
2722.4127	2708.3970	2722.4127	2708.3970	2683.4018	2683.4018	2669.3861	2646.3702	2646.3702	TrcB/B' (1*5MeW)
2722.4127	2708.3970	2722.4127	2708.3970	2683.4018	2683.4018	2669.3861	2646.3701		TrcB <sub>1</sub> /B <sub>1</sub> '
2745.4287	2731.4130	2745.4287	2731.4130	2706.4178	2706.4178	2692.4021			TpcB/B' (1*5MeW)
2759.4443	2745.4287	2759.4443	2745.4287	2720.4334	2720.4334				TpcB/B' (2*5MeW)
2759.4443	2745.4287	2759.4443	2745.4287	2720.4334					Tpc B <sub>1</sub> /B <sub>1</sub> ' (1*5MeW)
2784.4396	2770.4239	2784.4396	2770.4239						TpcC (1*5MeW)
2798.4552	2784.4396	2798.4552							TpcC (2*5MeW)
2784.4396	2770.4239								TpcC <sub>1</sub>
2798.4552									TpcC <sub>1</sub> (1*5MeW)

## Chapter 4

### Medium scale production and characterisation of tyrocidine analogues containing non-natural aromatic amino acids

#### 4.1 Introduction

As discussed in the introduction of the previous chapter, the producer organism *Br. parabrevis* has the ability to produce a diverse array of non-ribosomally synthesized peptides. This occurs as a result of a lack of specificity of specific of modules 3,4,7 and 9 in the tyrocidine synthetase system for a single amino acid, resulting in the large array of cyclic decapeptides with the sequence cyclo- $f^1P^2X^3x^4N^5Q^6X^7V^8X^9L^{10}$  (variable residues depicted by X, lower case letters represent D-amino acids) observed by Tang *et al.* (1).

Vosloo *et al.* (2) adapted a media from Lewis *et al.* (3), termed TGS, consisting of tryptone, glucose and inorganic salts, as a base media for use in supplementation tyrocidine producer cultures with specific amino acids. Using the producer organism *Br. parabrevis* ATCC 10068 it was found that supplementation of the growth media with 5.5 mM Phe led to a marked increase in the more hydrophobic tyrocidine A-analogues with Phe at residue positions three and four, while supplementation of the growth media with 11 mM Trp led to a marked increase in more hydrophilic tyrocidine C-analogues (having Trp at positions 3 and 4) (2), as well as tryptocidines with Trp at position 7 (4). Modelling the incorporation of Trp and Phe into the tyrocidines and their analogues as a function of their concentration in the media gave an indication of the affinity of the adenylation domains at modules 3, 4 and 7 in the tyrocidine synthetase system (4). All these positions have a preference for Trp, but position four has the highest affinity for Phe relative to positions 3 and 7, being the first to incorporate Phe as its concentration in the growth media is increased, followed by position 3 then 7 (4).

The shift in production of crude extracts towards more A ( $F^3f^4$ ) analogues or more B ( $F^3w^4/W^3f^4$ ) and C ( $W^3w^3$ ) analogues also leads to alterations in antibacterial activity against *Micrococcus luteus* (2). Extracts from 5.5 mM Phe supplemented cultures, containing predominantly A and B analogues, gave an MIC (minimum inhibitory concentration) of 3.125  $\mu\text{g/mL}$  compared to extracts from 5.5 mM Trp supplemented culture containing predominantly B and C-analogues together with higher gramicidin A production, yielding an MIC of 6.25  $\mu\text{g/mL}$ . At very high Phe supplementation concentrations of 27.5 mM there was four-fold increase in the MIC. Supplementation with 5.5 mM Trp, as well as 2.5 mM Phe led to a high production of TrcB, which were previously shown to be

one of the most active analogues against Gram-positive bacteria (5, 6). For more detail refer to the introduction of Chapter 3 that highlights the differences in activity of six major tyrocidine analogues against three microorganisms. As mentioned in Chapter 3, synthetic modification of a TrcA led to alterations in its structure-activity relationship, with some modifications leading to enhanced activity against *M. luteus* together with reduced haemolytic activity, indicative of the ability to improve the selectivity of the tyrocidines and analogues for pathogens (7). There has been little work done on the ability of *Br. parabrevis* to incorporate non-natural amino acids into tyrocidine analogues, with the exception of work by Okuda *et al.* (8) who observed incorporation of  $\beta$ -2-thienylalanine using isotopic labelling and Ruttenberg *et al.* (9), where the preferential incorporation of allo-isoleucine over isoleucine was observed.

In earlier years the most commonly used methods to determine the incorporation of an amino acids into non-ribosomally synthesized peptides was through the use of radiolabelled tracers, but modern electrospray ionisation mass spectrometry (ESI-MS or ESMS) and improved nuclear magnetic resonance (NMR) spectrometry has greatly aided in the identification and characterisation of peptides (10). High-resolution mass-spectrometry can now provide accurate identification of peptides based on the detected  $m/z$  ratios, with ppm (parts per million) errors of 2-10 being achieved by the high resolution ESMS utilised in our group. Ultra-performance liquid chromatography (UPLC<sup>®</sup>) linked to ESMS (UPLC-MS) is also a valuable tool in calculating purity of tyrocidine extracts as well as estimating the concentration of the peptides present in the tyrothricin complex using a commercially available standard.

High performance liquid chromatography (HPLC) is an important tool in both the purification and analysis of peptides. In the case of the tyrocidines and analogues semi-preparative purification, as well as analysis of peptides is best achieved using reverse-phase separation, where the tyrocidines and analogues are separated based on interaction of their hydrophobic amino acid residues with the stationary phase (C<sub>18</sub> matrix) together with a polar solvent as the mobile phase, in this case acetonitrile. UPLC provides enhanced separation via smaller matrix particle sizes (having a larger analyte interaction surface) and higher operating pressures, providing improved separation and analysis of complex compounds such as the peptide complexes in this study. In the case of the tyrocidines and analogues, small differences in amino acid chemistry (such as the CH<sub>2</sub> difference between Lys and Orn variants) and sequence (Trc analogues with a F<sup>3</sup>W<sup>4</sup> or W<sup>3</sup>F<sup>4</sup> configuration) can make them difficult to separate via analytical HPLC, in which case UPLC-ESMS provides the best available too for analysis.

Semi-preparative HPLC is useful for isolating individual peptides for testing in isolation in terms of biological activity (6) and biophysical properties, such as levels of aggregation (4). In this way individual peptides can be compared to one another and to the mixture as a whole for optimising peptide compositions for use against different organisms. In addition, the isolation of pure peptide eases the process of determining its primary structure through tandem MS.

This chapter reports the utilisation of semi-preparative HPLC, UPLC-MS and biological activity to partially characterise novel tyrocidine analogues in medium scale extracts of *Br. parabrevis* cultures supplemented with Phe, Trp and their selected, non-natural, derivatives.

## 4.2 Materials

The producer organisms *Br. parabrevis* 5618 originate from the Deutsche Sammlung von Mikroorganismen und Zellkulturen (DSMZ) in Braunschweig, Germany. *M. luteus* NCTC 8340 was obtained from the UK National Collection of Type Cultures in Porton Down (Salisbury, England). Tryptic soy broth (TSB), LB (Luria Bertani) media, tryptone, agar, glucose, ethanol (EtOH), hydrochloric acid (HCl), sodium chloride (NaCl), were from Merck (Darmstadt, Germany). Commercial tyrothricin, gramicidin S (GS), trifluoroacetic acid (TFA, > 98% purity), and resazurin dye and were obtained from Sigma-Aldrich (St. Louis, USA). Acetonitrile (ACN, far UV cut-off, > 98% purity) was obtained from Romil Ltd (Cambridge, UK). Analytical grade, deionised water was obtained by filtering reverse osmosis water through a Milli-Q<sup>®</sup> water purification system from Merck Millipore (Burlington, Massachusetts, USA). The modified amino acid 2-fluorophenylalanine (2-FF) was from GL Biochem Ltd (Shanghai, China). L-Tryptophan (Trp), 5-methyl-DL-tryptophan (5-MeW) and L-phenylalanine (Phe) were from Sigma-Aldrich (Steinheim, Germany). TrcA, TrcB, PhcA, TpcB and TpcC (purity above 90% as determined by UPLC-ESMS) were donated by W Laubscher and JA Vosloo, and the tyrocidine mixture (>95% purity in terms of cyclodecapeptide content) was from the BIOPEP<sup>™</sup> peptide library.

Falcon<sup>®</sup> tubes were from Corning (Corning, NY). The Acquity UPLC<sup>®</sup> BEH Phenyl column (2.1 mm × 100 mm, 1.7 µm particle size) and semi-preparative NovaPak HR C<sub>18</sub> column (6 µm particle size, 7.8 mm X 300 mm) and 0.22 µm polycarbonate syringe filters were from Waters (Milford, MA, USA). Microplate readers utilised in the study were a Model 680 Microplate reader from Bio-Rad Laboratories (Hercules, California, United States) and the Spark 10M multimode plate reader from Tecan (Männedorf, Switzerland)

## 4.3 Methods

### 4.3.1 Medium-scale culturing and extraction using selected, non-natural amino acids

*Medium-scale culturing of producer organism:* The selected producer organism (*Br. parabrevis* 5618) was streaked out from frozen glycerol stocks onto TSA (3% (*m/v*) tryptic soy broth, 1.5% (*m/v*) agar) agar plates and incubated for 48 hours to allow for the formation of individual colonies. An individual colony was then used to inoculate 20 mL a starter culture containing TSB broth (3% (*m/v*) TSB in analytical grade water) in a 50 mL Falcon<sup>®</sup> tube to allow for incubation for 16 hours while shaking at 37 °C where an OD<sub>595</sub> of 0.6-0.9 was reached. This culture was then used to inoculate a medium-scale 200 ml cultures containing TGS (tryptone, glucose and inorganic salts, exact composition cannot be disclosed due to an existing non-disclosure agreement with the BIOPEP<sup>®</sup> group) media in a 200 mL Erlenmeyer flask. One percent of the volume of the medium-scale culture is used from the starter culture (i.e. 2 mL starter culture in 200 mL TGS). For Trp and 5-MeW supplemented TGS cultures, a final concentration 10 mM of the amino acid was used. For the Phe and 2-FF supplemented TGS cultures, a final concentration of 20 mM of the amino acid was used. Following inoculation, cultures were incubated at 37 °C in stationary cultures for a period of 10 days.

*Extraction of medium-scale culture:* Following the 10-day incubation period, the cultures were acidified using HCl to pH of 4 and allowed to stand overnight. The cultures were then extracted using an organic solvent, followed by a precipitation step and treatment with activated carbon (details cannot be disclosed due to a non-disclosure agreement).

### 4.3.2 Purification of medium-scale extracts

*Semi-preparative HPLC of extracts:* Medium-scale extracts were subjected to semi-preparative reverse phase HPLC following the methodology of Eyeghe-Bickong (11) and Rautenbach *et al.* (5), utilising the same a Waters<sup>®</sup> HPLC system to purify individual Trc analogues or subsets of analogues. Extracts were dissolved in 75% (*v/v*) ACN in analytical grade water to a concentration of either 10, 15 or 20 mg/mL. Dissolved culture extracts were then centrifuged at 2000 × *g* for 5 minutes to remove particulate and all preparations and collection of fractions were done in clean (pyrolysed) glassware. All extracts were initially injected at 10 mg/mL and concentrations were increased if it had no observable effect on the separation and peak shape that generally occurs due to aggregation of the peptides. A semi-preparative NovaPak C<sub>18</sub> column (6 µm particle size, 7.8 mm × 300 mm) was used at a temperature of 37 °C and chromatograms were generated by monitoring absorbance at 254 nm using a Waters Model 440 UV-detector at a wave length of 254 nm. A two-solvent system was used, with eluent A containing 0.1 % TFA in analytical quality water and eluent

B consisting of 90% HPLC grade ACN and 10% eluent A (v/v). Injections of 100  $\mu$ L were made and chromatographed using the gradient program depicted in Table 4.1 developed by Eyeghe-Bickong (11) and Rautenbach (5). All fractions collected via HPLC were freeze dried in preparation for later analysis via ESMS and UPLC-MS.

*Table 4.1* Gradient program used for reverse phase semi-preparative HPLC purification of modified peptides from the crude culture extracts. The flow rate was 3.00 mL/min for steps 1-5. Gradient type 5 and 6 refers to the Waters<sup>®</sup> gradient with type 6 being a linear gradient and type 5 being a non-linear concave-type gradient

Step	% Eluent B Start	% Eluent B End	Time interval (min)	Gradient Type	Comment
1	40	60	0.5	-	loading sample
2	40	100	0.5 - 27	5	Separation of peptides
3	100	100	27 - 29	6	Cleaning of column
4	40	60	29 - 30	6	Return to starting conditions
5	40	60	30 - 35	6	Condition column

#### 4.3.2 ESMS Analysis of Trcs and analogues

*Direct-injection ESMS analysis:* Both crude and purified samples were analysed via direct-injection ESMS analysis. Samples were made up to 1.00 mg/mL (for crude extracts) and 0.500 mg/mL for purified extracts in 75% ACN (%v/v) and centrifuged for 10 minutes  $8600 \times g$  to remove insoluble material and particulate. Three microliters of sample were then injected and analysed on a Waters<sup>®</sup> Synapt G2 mass spectrometer using the same conditions as in Chapter 2.

*UPLC-ESMS analysis:* Crude and purified samples were made up in 75% ACN (v/v) in analytical grade water and diluted down to a final concentration of 1.00 mg/mL for crude extracts and 0.50 mg/mL for purified samples and an ACN concentration of 2.5 % (v/v). Three microliters of sample were injected and chromatographed via ultra-performance liquid chromatography (UPLC) on an Acquity UPLC<sup>®</sup> instrument utilising a BEH Phenyl UPLC column at flow rate of 300  $\mu$ L/min. Column temperature of 60 °C was used together with a two-solvent system (eluent A: 1% (v/v) formic acid in analytical grade water, eluent B: 100% (v/v) ACN) profile at a flow rate of 0.3 mL/min and chromatography was conducted using the gradient program given in Table 4.2.

*Table 4.2* UPLC linear gradient program used for separation of peptides during the UPLC-MS analysis of crude extracts and purified fractions

Step	% eluent B Start	% eluent B End	Time interval (min)
1	0	0	0 - 0.5
2	0	30	0.5 - 1
3	30	60	1 - 10
4	60	80	10 - 15
5	80	100	15 - 15.1
6	100	100	15.1-18

ESI-MS monitoring of the chromatography was done inline (i.e. UPLC-MS) on a Waters Synapt G2 QTOF mass spectrometer in positive mode at a capillary voltage of 3.0 kV together with a sample cone voltage of 15 V. The source temperature was 120 °C and the flow rate of desolvation gas (N<sub>2</sub>) was 650 L/hour with a desolvation temperature of 275 °C. Data acquisition took place over a mass-to-charge (*m/z*) range of 300 to 2000 in continuum mode at a rate of 0.2 scans per second. All ESMS data was analysed using the Waters® MassLynx 4.01 software package.

#### **4.3.3 Growth inhibition against *M. luteus***

*Preparation of peptides for use in spot plate and growth inhibition assay:* Selected novel cyclic decapeptide analogues with unnatural aromatic residues, enriched from the crude extract following semi-preparative HPLC, were used for the spot plate and growth inhibition assays. In addition to the novel analogues, equivalent natural purified tyrocidine, phenycidine and tryptocidine analogues were also tested. Selected purified peptides and enriched peptide fractions were analytically weighed and made up to 2.500 mg/mL in 50% (*v/v*) DMSO.

For the spot plate assay on nutrient agar, the stock solutions were added to the first column in a 300 µL round-bottom microtiter plate, in which analytical quality water had already been added, to dilute the peptide down to 0.050 mg/mL and a DMSO concentration of 1% (*v/v*). A series of five-fold dilutions were then made, using 1% (*v/v*) DMSO, starting at a concentration of 0.050 mg/mL going down to 2.00 µg/mL (3 dilutions). In addition to the selected peptides, a commercially available mixture of tyrocidine analogues (TrcMix) as well as gramicidin S (GS) were used as control and diluted in the same manner. A solvent control was also made up using 1% (*v/v*) DMSO alone.



For the growth inhibition assay in culture broth, the 2.500 mg/mL peptide stock solution in 50% (v/v) DMSO was added to the first column in a 300  $\mu$ L round bottom plate (dilution plate) in which analytical-grade water had already been added, to achieve a final peptide concentration of 0.500 mg/mL and a DMSO concentration of 10% (v/v). A series of five-fold dilution was then done in the wells using 10% (v/v) DMSO for a concentration range from 0.500 mg/mL to 20.0  $\mu$ g/mL (3 dilutions). The TrcMix as well as gramicidin S (GS) were used as control and diluted in the same manner. A solvent control consisting of only 10% (v/v) DMSO was also made.

*Spot plate assay:* The spot plate method used was adapted from Du Toit and Rautenbach (12). A colony of previously grown *M. luteus*, grown on TSA agar plates (3% (m/v) TSB, 1.5% (m/v) agar) was used to inoculate 20 mL of LB (1% (m/v) tryptone, 0.5% (m/v) yeast extract, 1% (m/v) NaCl) media which was then incubated for 16 hours at 37 °C while shaking to allow for the formation of an OD<sub>595</sub> of between 0.6-0.9 to be reached. Following this initial incubation period, a sub-culture was done by inoculating 20 mL of TSB broth (3% (m/v) TSB) with 500  $\mu$ L of the LB culture, and allowed to grow to an OD<sub>595</sub> of 0.6 (between 3.5 to 4.5 hours, checking periodically). An OD<sub>595</sub> of 0.625 was reached and diluted using TSB down to an OD<sub>595</sub> of 0.6. Seven-hundred microliters of this culture was then added on top of TSB-agar plates, which had been pre-warmed to 37 °C, and spread evenly across the surface by tilting the plate, any excess culture was poured off and the plates were allowed to dry. Five microliters of each peptide at each dilution was spotted onto the plates using a pipette and allowed to dry. Commercial GS and TrcMix were used at a concentration of 10  $\mu$ g/mL as positive controls while 1% (v/v) DMSO was used as a negative solvent control. The plates were incubated at 37 °C for 24 hours after which pictures were taken to display zones of inhibition of growth.

*Turbidimetric growth inhibition assay:* The growth inhibition assay was adapted from Du Toit and Rautenbach (12). Cultures of *M. luteus* were prepared in the same manner as for the spot plate assay, only once the subculture of *M. luteus* reached an OD<sub>595</sub> of 0.6, it was diluted down to an OD<sub>595</sub> of 0.2 using TSB (3% (m/v)) broth. Ninety microliters of this diluted culture were then added to the wells of a 200  $\mu$ L flat-bottomed 96-well plate, with the exception of four wells which were left open for sterile TSB alone, to serve as a negative growth control. Ten microliters of the previously prepared peptide dilutions in 10% (v/v) DMSO was then added on top of the 90  $\mu$ L of target organism, meaning a ten-times dilution of peptide was made from the preparatory dilution plate, resulting in a final dilution series in the flat-bottomed plate starting at 50.0  $\mu$ g/mL and going down to 0.20  $\mu$ g/mL with a final DMSO concentration of 1% (v/v). Ten microliters of 10% (v/v) DMSO was added to negative and the positive controls, with the positive control used to determine

maximal growth without any influence of peptide. Following the addition of the peptide, the plates were incubated at 37 °C for 16 hours and the OD<sub>595</sub> was then measured using a Model 680 BioRad™ microplate reader, following shaking of the plate, to determine % growth inhibition. Four analytical repeats were done per peptide per dilution ( $n=4$ ). Percentage growth inhibition was done using the following equation:

$$\% \text{ Growth inhibition} = 100 - \frac{100 \times (\text{OD}_{595} \text{ of well} - \text{Mean OD}_{595} \text{ of Blank})}{\text{Mean OD}_{595} \text{ of growth control} - \text{Mean OD}_{595} \text{ of Blank}}$$

*Metabolic inhibition assay:* This assay was adapted from the Alamar Blue assay® developed by O'Brien *et al* (13). The dye resazurin, commonly used in the Alamar Blue® assay, can be used to assess the effects of a given compound, in this case peptides, on cell metabolism and viability (14). Following incubation of the plate used to measure growth inhibition (for 16 hours), and an additional nine hours at room temperature, 10 µL of resazurin (which is reduced to resorufin by actively metabolising cells) was added to the wells and incubated for 37 °C for an hour. Following incubation, the emitted fluorescence (F) of the wells was measured using an excitation wavelength of 530 nm and an emission wavelength of 590 nm (at which resorufin fluoresces). The percentage inhibition of metabolic activity is determined using the same equation as for the turbidimetric assay, but using the fluorescence values instead of optical density at 595 nm. The fluorescence was determined using a Tecan™ Spark 10M multimode microplate reader, together with the SparkControl™ software suite.

## 4.4 Results

### 4.4.1 Medium-scale culturing and extraction using selected, non-natural amino acids

#### *extracts*

The extract mass of each of the crude extracts were determined by weighing the freeze-dried mass following extraction with organic solvent. The extract mass per litre of the culture ranged from 1.523 g for the 10 mM 2-FF supplemented culture to 3.546 g for the 10 mM Trp supplemented culture. The grams extract mass per litre media was less for the non-natural Phe analogue 2-FF, while the tryptophan analogue 5-MeW produced a marginally lower crude extract yield per liter compared to tryptophan.

*Table 4.3* Summary of the Extract masses obtained for combined cultures following two rounds of extraction with organic solvent

Amino Acid (AA)	AA Concentration (mM)	Total Culture Volume (mL)*	Combined Crude Extract mass (mg)	Extract mass (g) per litre of culture
2-FF	10	400	609.4	1.523
Phe	10	400	1051.9	2.630
5-MeW	10	400	1401.5	3.504
Trp	10	600	2127.8	3.546

\*Individual cultures of 200 mL were combined, hence total culture volume/200 gives the number of cultures combined

#### 4.4.2 ESMS Analysis of crude extracts of Trcs and analogues

*ESMS analysis of medium-scale 5-MeW extract:* Figure 4.1 shows the UPLC chromatograms for the Trp and 5-MeW supplemented medium-scale extracts as well as the major detected  $m/z$  values for the major peptide in each peak. The letters in bold above the peaks in Figure 4.1, A, correspond with the extracted peaks of this extract in Figure 4.2. UPLC-ESMS analysis of the 10 mM 5-MeW supplemented crude extract revealed extensive incorporation of this analogue into the tyrocidines. Analogues were identified by tracking and extracting the relevant doubly charged  $m/z$  value in each UPLC-MS profile (see addendum at end of thesis for a list of theoretical monomer masses) (Figure 4.2). Methylated tyrocidine analogues of TrcC, TpcC, TrcB/B', TrcB<sub>1</sub>/B<sub>1</sub>' and TpcB<sub>1</sub>/B<sub>1</sub>' were observed. In some cases, it was difficult to determine the identity of a peptide as its  $m/z$  matched exactly with another non-natural analogue. This overlap of masses occurred due to the fact that the mass gained by the addition of an extra CH<sub>2</sub> in the case of an ornithine to lysine substitution is same as the mass gained by the substitution of a methyl group for a hydrogen group on 5-MeW. As a result, one could not readily tell the difference between a TpcC incorporating two 5-MeW analogues or a TpcC incorporating one 5-MeW analogue and having a lysine instead of an ornithine at position 9.

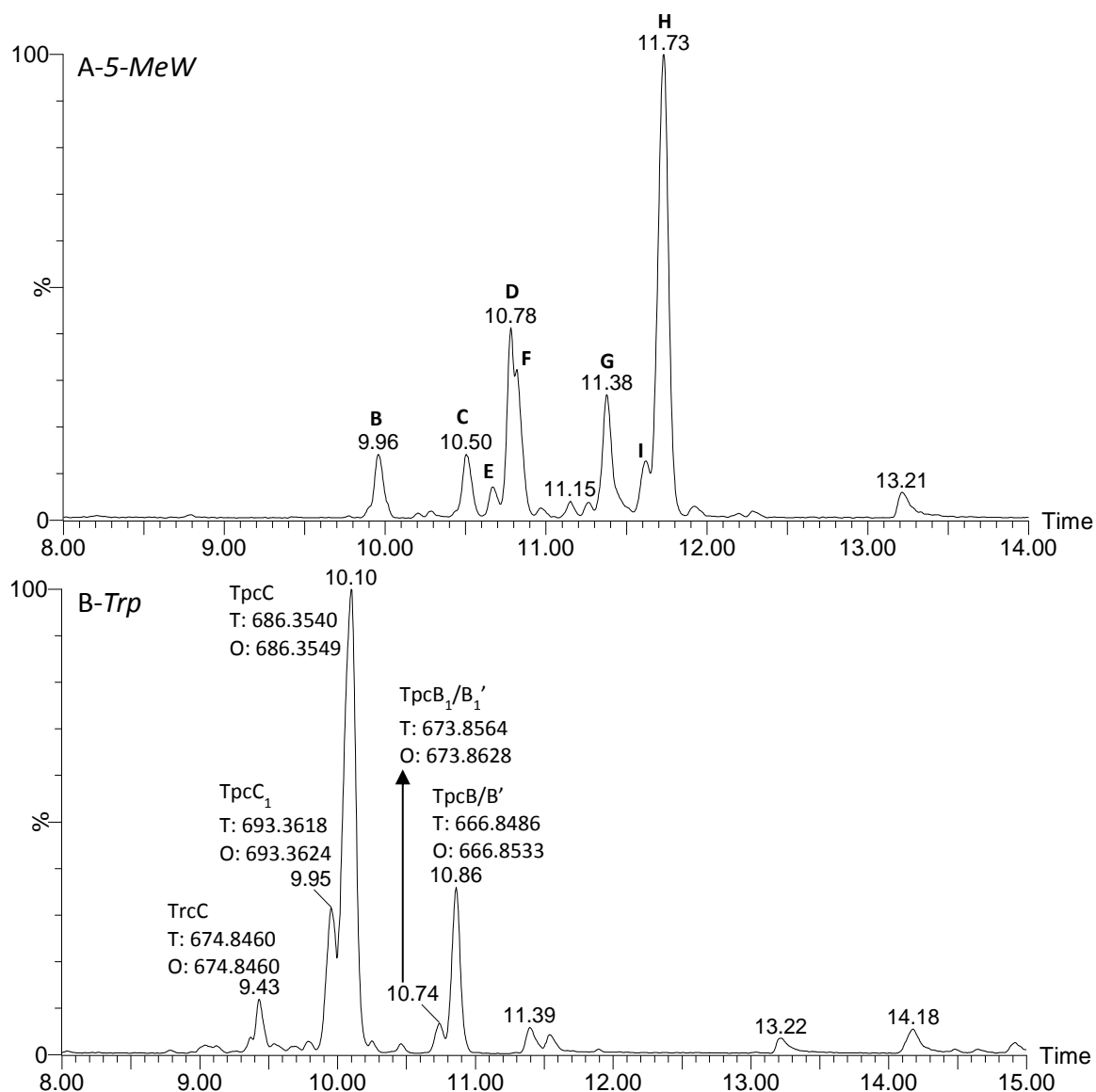


**Figure 4.1** UPLC-ESMS base-peak chromatograms of large scale extracts. **A**, 5-MeW supplemented extract (letters correspond with  $m/z$  values and peptide identified in Figure 4.2) **B**, Trp supplemented extract showing major peptides identified by doubly charged  $m/z$  values  $[M+2H]^{2+}$

In the case of a masses overlapping between an analogue which theoretically contains no 5-MeW analogues, and one which does (e.g. a TrcC<sub>1</sub> versus a TrcC(1\*5-MeW)), the peptide identity could be determined on the basis of differences in retention times between the natural and non-natural analogues. Here it can be seen that the peptide observed in Figure 4.2, B, is a TrcC incorporating a single 5-MeW residue and not a TrcC<sub>1</sub> due to the large difference in retention time, with the non-natural analogue being retained longer and having an apparent more hydrophobic nature as determined by its retention time (9.96 min versus 9.43 min for TrcC seen in Figure 4.1, B). This

principle could also be used to identify a TpcC(1\*MeW) versus a TpcC<sub>1</sub>, a TpcB/B'(1\*5MeW) versus as TpcB<sub>1</sub>/B<sub>1</sub>' and lastly a TrcB/B'(1\*5MeW) versus a TrcB<sub>1</sub>/B<sub>1</sub>' (not observed in Trp supplemented extract, determined by comparison with commercial TrcMix).

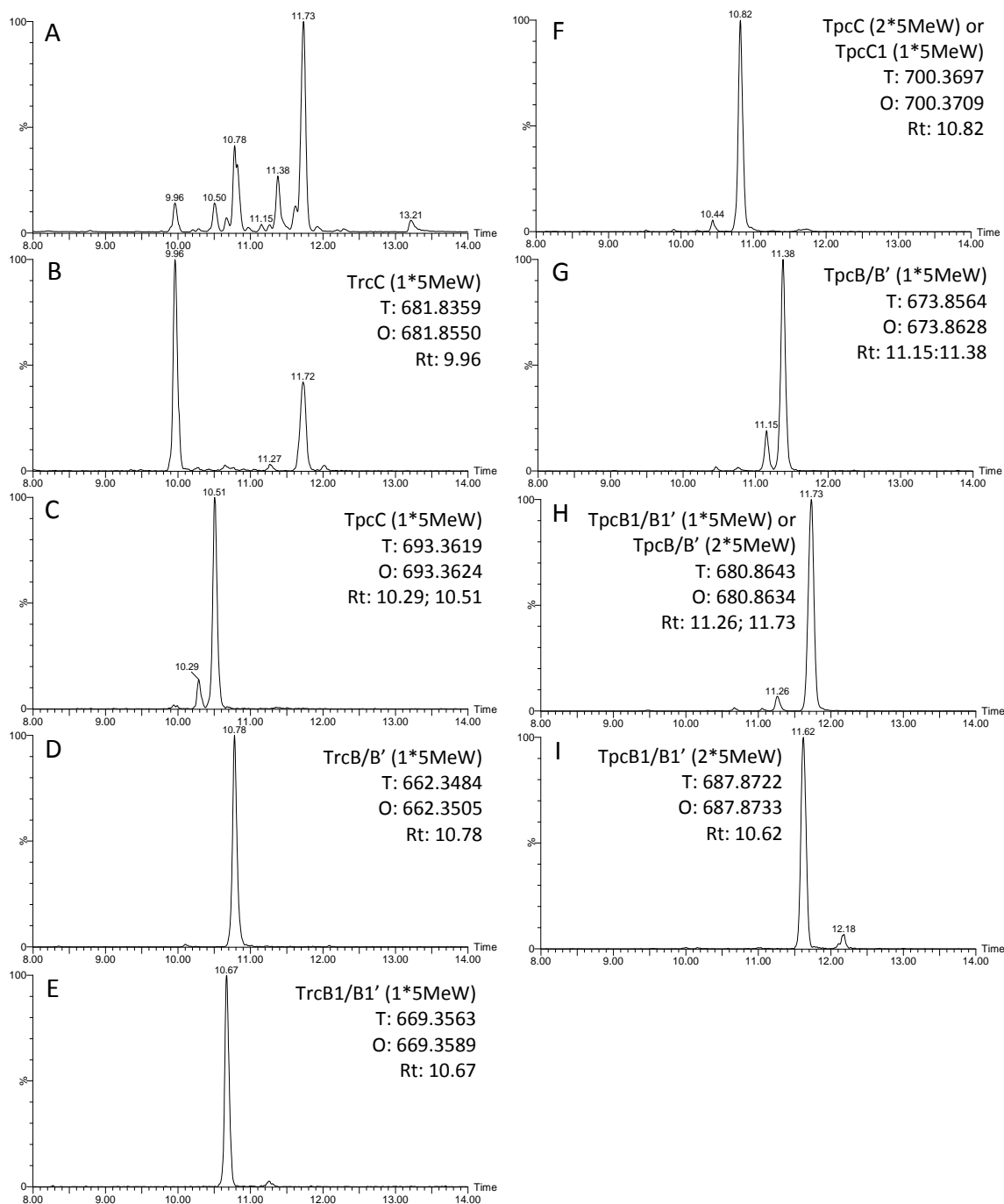


**Figure 4.2** UPLC-MS analysis of 5-MeW supplemented culture extract. **A** Base peak chromatogram (BPC) of the crude extract, **B-I** extracted  $m/z$  chromatogram component peaks ( $[M+2H]^{2+}$ ) in the culture extract indicating the proposed main analogue in the extracted peak, retention time (Rt) in minutes, theoretical  $m/z$  (T) and observed  $m/z$  (O). See thesis addendum for a list of theoretical masses

Looking at the crude extract in Figure 4.2, A, and assuming a similar response factor for all the tyrocidine analogues, it appears that the analogues produced in the highest abundance are a TrcB/B' incorporating a single 5-MeW residue and either a TpcB<sub>1</sub>/B<sub>1</sub>' incorporating a single 5-MeW residue or a TpcB/B' incorporating two 5-MeW residues, respectively (Figure 4.2, D & H). In some cases, there are two major peaks for an extracted  $m/z$  value, as observed for TrcC<sub>1</sub>(1\*5MeW) in Figure 4.2, B. Here, the peak at 11.72 minutes has a different overlapping isotope peak profile with a monoisotopic  $m/z$  of 680.8643 mapping it to a TpcB<sub>1</sub>/B<sub>1</sub>'(1\*5MeW) or a TpcB/B'(2\*5MeW) (as identified in Figure 4.2, H). In such cases the retention time (Rt) shown beneath the theoretical (T) and observed (O) masses indicates which peak is being referred to by the peptide identity and mass. In cases where there are two retention times shown (e.g. Figure 4.2, C), this indicates that there are two similar peptides with the same  $m/z$  and isotopic peak profiles, but with different retention times.

*ESMS analysis of medium-scale 2-FF extract:* Figure 4.3 compares the 2-FF and Phe supplemented cultures. The letters in bold above the peaks in Figure 4.3, A, correspond with the extracted peaks of this extract in Figure 4.4. This shows the similar retention time of the fluorinated analogues to the natural analogues. The peptide produced in the highest abundance in both extracts was a TrcA in the Phe supplemented culture extract and TrcA with three or two fluorinated residues in the 2-FF supplemented culture extract (Figure 4.4, F and G respectively). The TrcA(3\*2-FF) analogues had a retention time that was only 0.03 minutes longer than its natural counterpart, indicating a similar hydrophobicity, while the TrcA (2\*2-FF) produced two peaks. The two peaks are likely due to different incorporation sites, as there are three possible positions (1, 3 and 4) for incorporation of the 2-FF residue in TrcA.

In Figure 4.4 we can see the breakdown of the UPLC-MS analysis of the crude 2-FF supplemented extract. This fluorinated Phe analogue was readily incorporated into the tyrocidines and analogues with observable amounts of TrcB/B', TrcB<sub>1</sub>/B<sub>1</sub>', TpcB/B', TpcB<sub>1</sub>/B<sub>1</sub>', TrcA, TrcA<sub>1</sub>, PhcA and TpcA incorporating one or more 2-FF residue (see thesis addendum for a list of theoretical monomer masses). Fortunately, the substitution of a fluorine for a hydrogen in these analogues did not produce overlapping masses, making their identification based on  $m/z$  ratios an easier process relative to peptides incorporating the 5-MeW analogue. Looking at Figure 4.4, A & G, it appears that a TrcA incorporating three 2-FF residues was produced in the highest relative amount (again assuming similar response factors), with TrcB/B'(2\*2-FF) and TpcA(3\*2-FF) also being produced in significant amounts (Figure 4.4, B & K respectively).

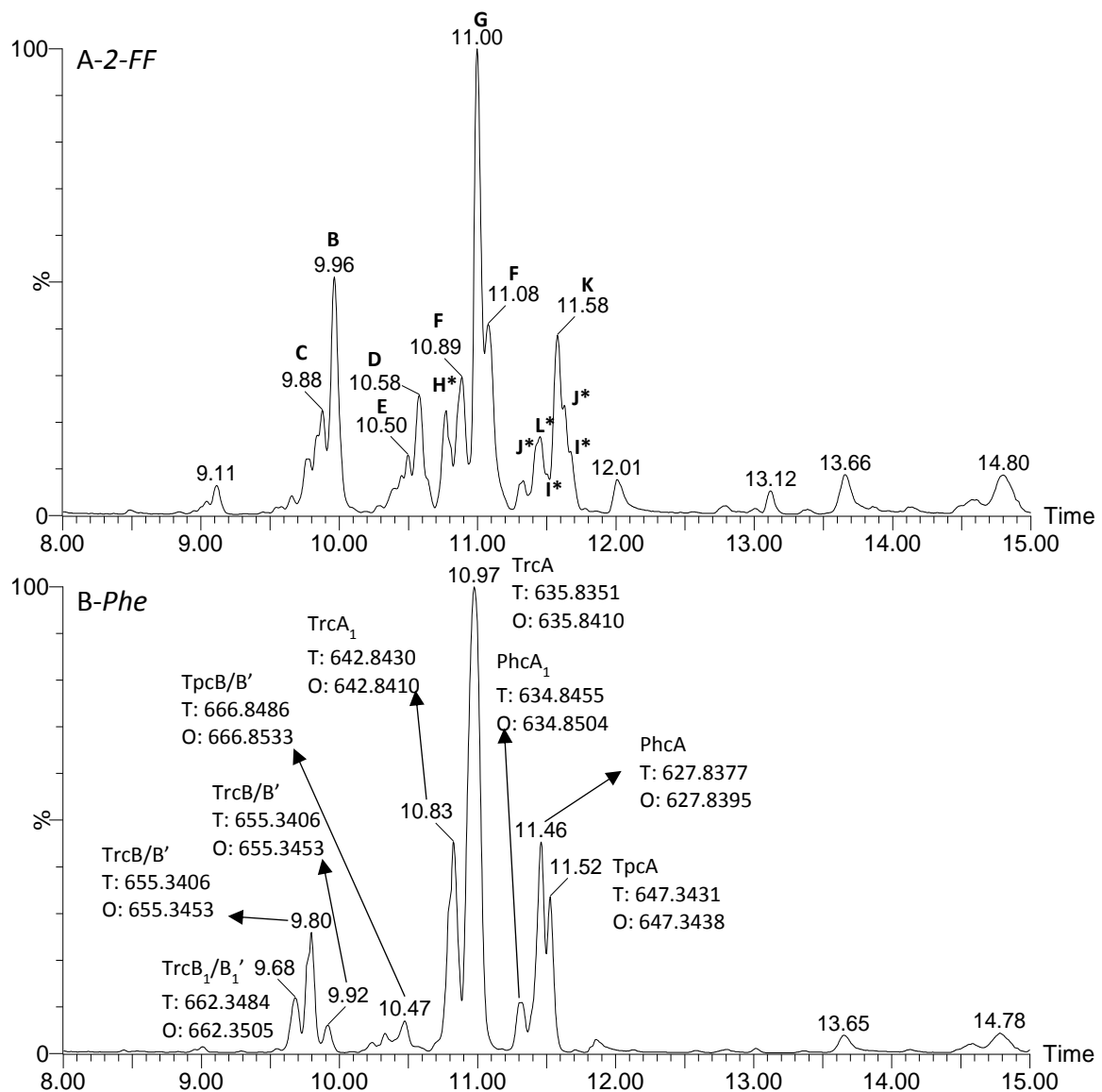


**Figure 4.3** UPLC-ESMS base-peak chromatograms of large scale extracts. **A**, 2-FF supplemented extract (letters correspond with  $m/z$  values and peptide identified in Figure 4.2 (\*Retention time not displayed, letter\* placed approximately where peptide elutes). **B**, Phe supplemented extract showing major peptides identified by their doubly charged  $m/z$  values  $[M+2H]^{2+}$

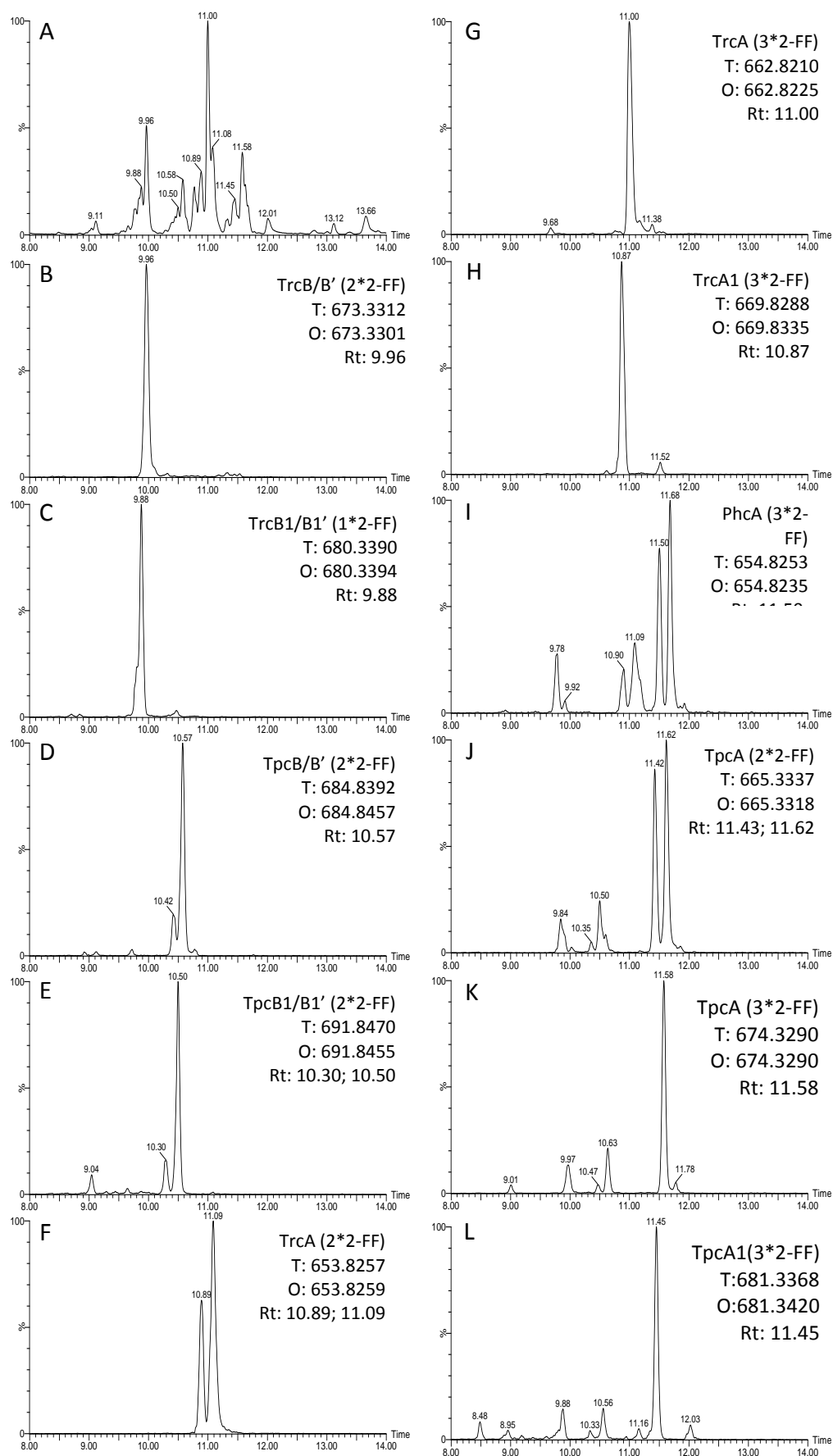


**Figure 4.4** UPLC-MS analysis of 2-FF supplemented culture extract. **A.** BPC of the crude extract, **B-L,** extracted  $m/z$  chromatograms of component peaks ( $[M+2H]^{2+}$ ) in the culture extract indicating the proposed main analogue in the extracted peak, Rt in minutes, theoretical  $m/z$  (T) and observed  $m/z$  (O)



#### 4.4.3 Reverse-phase semi-preparative HPLC purification and ESMS analysis of fractions

*Purification and ESMS analysis of medium-scale 5-MeW extract fractions:* Figure 4.5 represents the HPLC chromatogram produced by separation of the peptides in the extract based on hydrophobicity. Eight fractions were collected in total (2-9). These fractions were then analysed via UPLC-MS. Based on UPLC-MS analysis, fractions 3 and 8 were chosen for further analysis and use in biological activity testing.

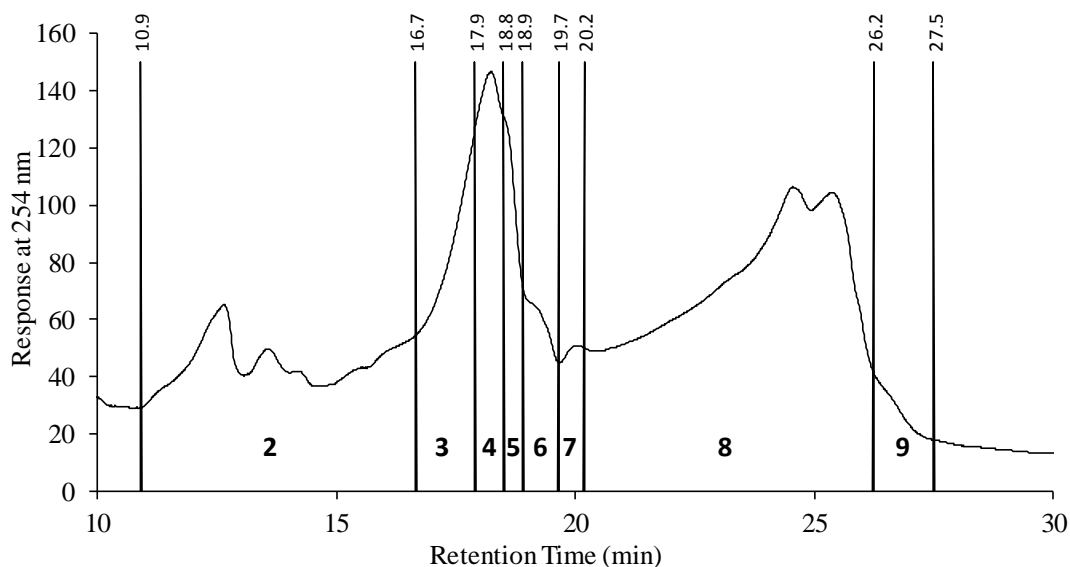


*Figure 4.5* A representative chromatogram showing the semi-preparative HPLC and fractions collected for 5-MeW supplemented culture extract. Numbers in bold above *x*-axis indicate the fraction number and numbers above the vertical lines are the retention time cut-offs of the fractions

Figure 4.6, A, represents the UPLC-MS analysis of fraction 3 showing the integration of the observed peaks to determine the area-under-curve (AUC) for these peaks. The peak at 10.73 minutes, together with the shoulder at 10.81 minutes were the only peaks observed containing tyrocidine analogues, with the peak at 11.69 contained unidentifiable compounds and the peak at 14.59 minutes also containing contaminants together with trace amounts of gramicidins, which were not analysed further. Figure 4.6, B & C, represent the isolated peaks selected using the predominant peptide *m/z* in the peak and shoulder respectively. These peaks were then combined and analysed further using the MaxEnt 3 algorithm. Table 4.4 shows the % total AUC for the peak and shoulder determined by the contribution of their AUCs to the total AUCs for all the peaks integrated. MaxEnt 3 analyses of the peak and shoulder indicated an impure peptide preparation enriched in certain peptide analogues. The % signal intensity was determined for the enriched peptide analogue preparations. This % signal intensity represents the contribution of these peptides to the total ESMS

signal for all the compounds in this peak, only considering the monomer signals and assuming comparable response factors. The peak at 10.73 minutes is enriched for a TrcB analogue containing a single 5-MeW residue (TrcB/B'(1\*5MeW)), with a sodium adduct also present giving a total % signal intensity of 33.4%. This analogue proved to have a very similar retention time to a TpcC analogue containing two 5-MeW residues (TpcC(2\*5MeW)), which partially co-eluted with this analogue. The shoulder at 10.8 minutes contained a higher percentage of this tryptocidine analogue, producing a % signal intensity of 38.1% (including the TpcC(2\*5MeW) sodium adduct). Again, due to the partially resolved peak separation, TrcB(1\*5MeW) is also observed. Taking both AUC and % signal intensity together, fraction 3 contains the highest relative amount of TrcB/B'(1\*5MeW). The possible structures for this peptide are shown in Figure 4.7.

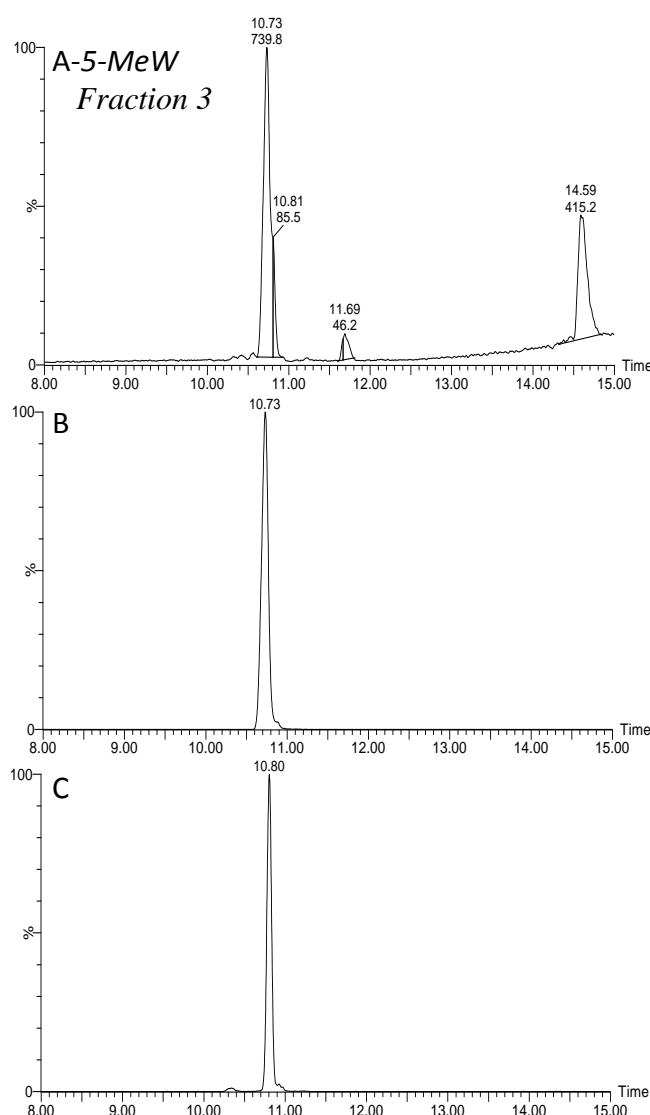


*Figure 4.6* UPLC-MS analysis of semi-preparative reverse phase HPLC fraction 3 of 5-MeW supplemented extract. **A**, BPC (Base Peak Chromatogram) of integrated peaks together with area-under-curve (AUC) below retention time. Extracted mass chromatograms **B** & **C** show peak at 10.73 minutes ( $m/z = 1323.6958$ ) and shoulder at 10.80 minutes ( $m/z = 1399.7439$ ) respectively

**Table 4.4** Mass analysis of peak and shoulder from HPLC fraction 3 containing 5-MeW tyrocidine analogues showing the % contribution to the total AUC of all integrated peaks. MaxEnt 3 analysis was used to determine the % signal contribution of the analogues in the peak and shoulder which contributed to over 10% of the total signal intensity as well as their mass and identity

Peak Rt (min)	% Total AUC	MaxEnt Spectra	Peptide (Theor. mass/Obs. Mass)	% Signal Intensity
10.73	52.98		TrcB/B' 1*5MeW) 17.66 1323.6890/1323.6847 TrcB/B'(1*5MeW)[Na] 15.74 1345.6709/1345.6666 TpcC(2*5MeW) 10.96 1399.7315/1399.7251	
10.80	10.98		TpcC(2*5MeW) 24.38 1399.7315/1399.7299 TpcC(2*5MeW)[Na] 13.72 1421.7166/1421.7135 TrcB/B'(1*5MeW) 13.35 1323.6890/1323.6878	

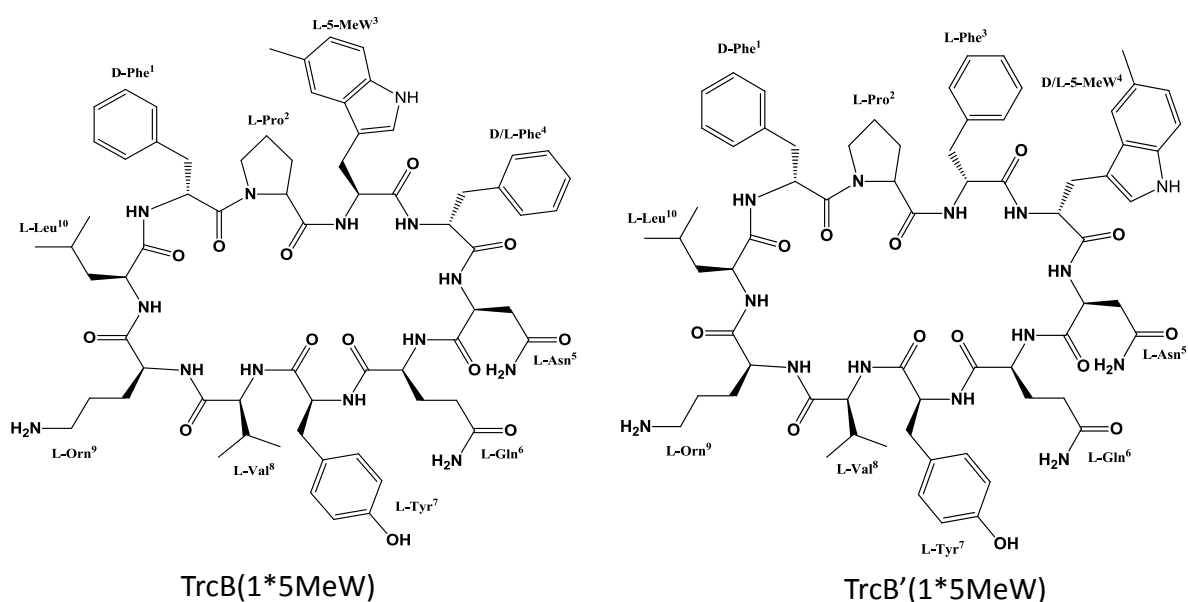


**Figure 4.7** Possible structures for novel TrcB/B' analogue containing a single 5-MeW residues enriched for in fraction 3

Figure 4.8, A, represents the UPLC chromatogram for fraction 8 showing the AUCs and retention times for the major peaks. Here the peaks were better resolved, with no major overlap. The peak at 11.40 minutes (Figure 4.8, B) contained majority TpcB/B'(1\*5MeW) while the peak at 11.73 minutes (Figure 4.8, C) was enriched for TpcB/B'(2\*5MeW), as shown by the % signal intensities in Table 4.5. With the peak at 11.73 minutes giving the highest % total AUC and containing predominantly TpcB/B'(2\*5MeW), this fraction is enriched primarily for this peptide. Figure 4.9 shows the possible structures for this peptide.

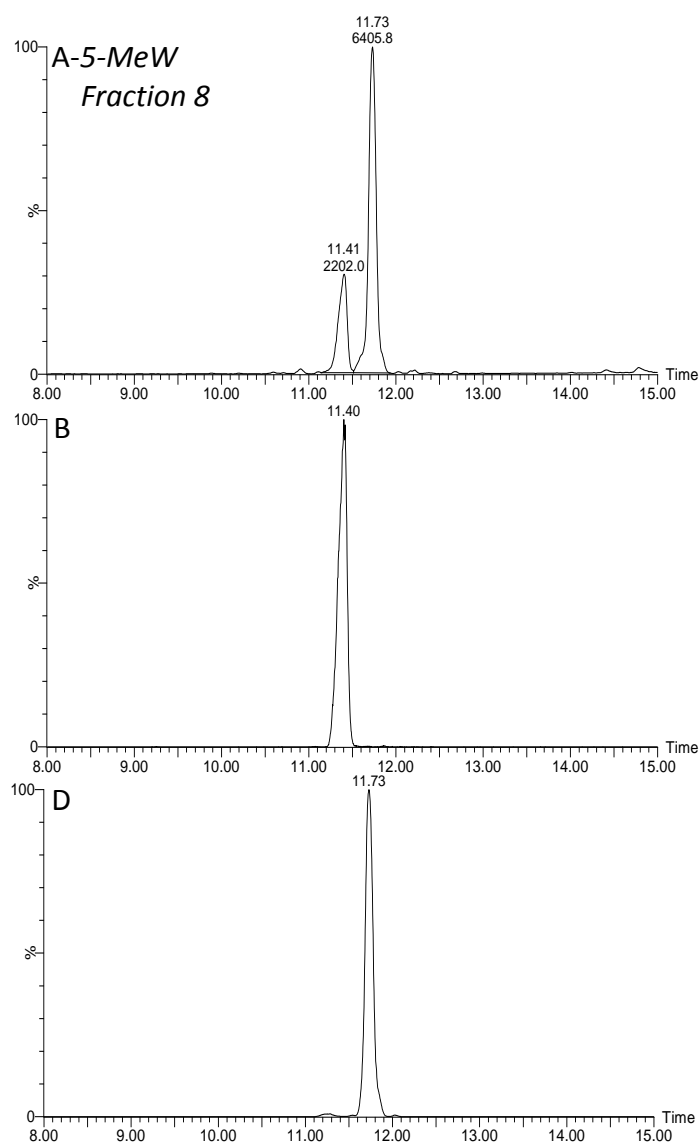
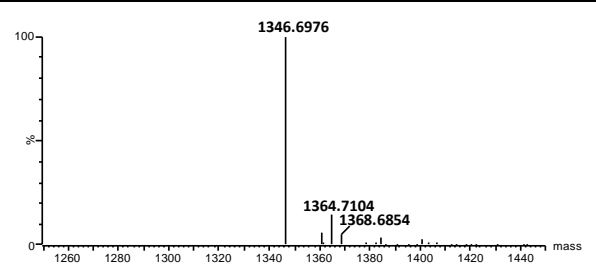
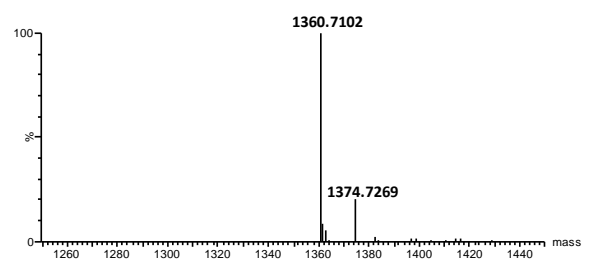
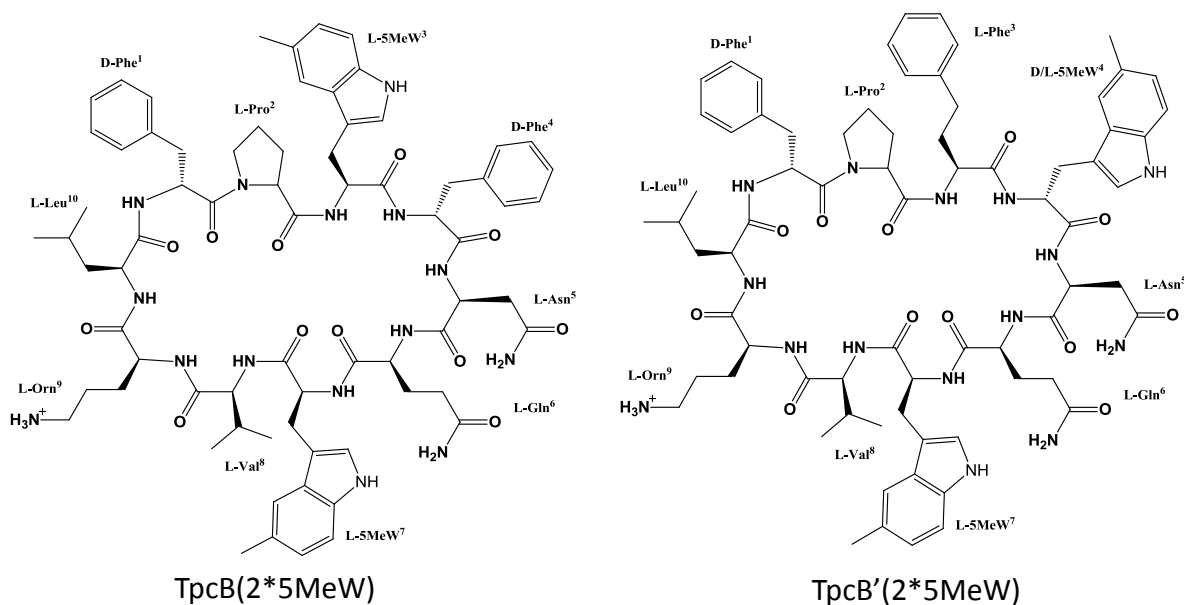


Figure 4.8 UPLC-MS analysis of semi-preparative reverse phase HPLC fraction 8 of 5-MeW supplemented extract. **A**, BPC of integrated peaks together with area-under-curve (AUC) below retention time. **B** & **C** show extracted mass chromatograms with peaks at 11.40 minutes ( $m/z = 1346.7039$ ) and 11.73 minutes ( $m/z = 1360.7295$ )

**Table 4.5** Mass analysis of UPLC peaks from Fraction 8 containing 5-MeW tryptocidine analogues showing the % contribution to the total AUC of all integrated peaks. MaxEnt 3 analysis was used to determine the % signal contribution of the analogues in the peak and shoulder which contributed to over 10% of the total signal intensity as well as their mass and identity

Peak Rt (min)	% Total AUC	MaxEnt Spectra	Peptide (Theo. mass/Obs. Mass)	% Signal Intensity
11.40	25.58		TpcB/B'(1*5MeW) 1346.7050/1346.6976	70.89
11.73	74.42		TpcB/B'(2*5MeW) 1360.7206/1360.7102 TpcB1/B1'(2*5MeW) 1374.7363/1374.7269	70.22 14.23



**Figure 4.9** Possible structures for novel TpcB/B' analogue containing two 5-MeW residues enriched for in fraction 8

*Purification and ESMS analysis of medium-scale 2-FF extract fractions:* Figure 4.10 shows the 10 fractions collected (2-11) for the 10 mM 2-FF supplemented crude extract. Following UPLC-MS analysis of these fractions, fractions 8 and 9 were selected for further analysis.

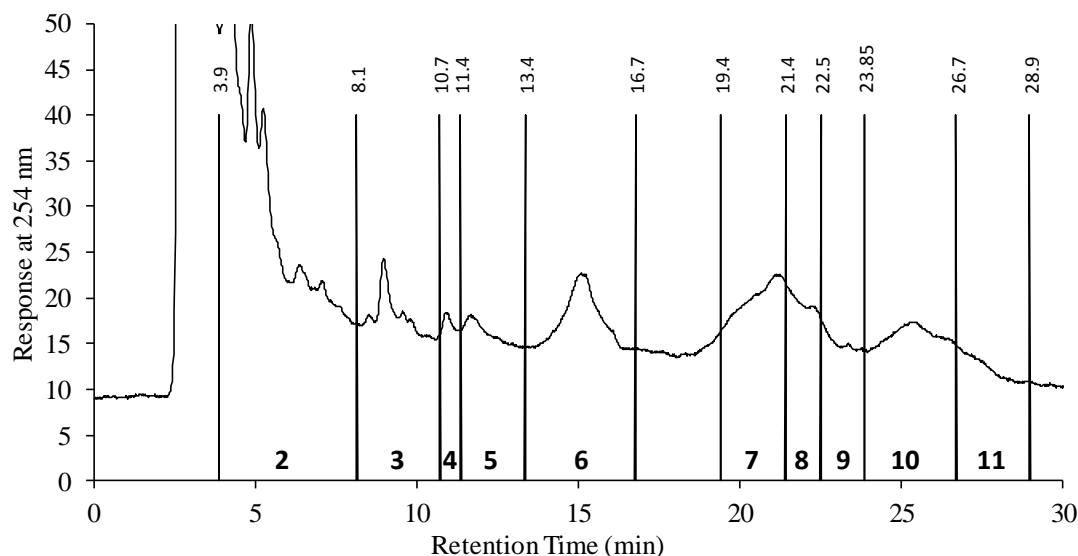


*Figure 4.10* A representative chromatogram showing the semi preparative HPLC and fractions collected for 2-FF supplemented culture extract. Numbers in bold above *x*-axis indicate the fraction number and numbers above the vertical line are the retention time cut-offs of the fractions

Figure 4.11, A, shows the UPLC-MS analysis and AUCs for integrated peaks of fraction 8. The peak present at 14.39 minutes contained a contaminant with an  $m/z$  of 317.115, possibly a potassium adduct of dibutyl-phthalate, a common plasticiser from laboratory plastic ware, such as micropipette tips, Falcon<sup>®</sup> tubes and Eppendorf<sup>®</sup> tubes. Three major peaks were detected with retention times of 10.87, 10.99 and 11.11 minutes respectively (Figure 4.11, B-D). The peak at 10.87 minutes contains predominantly TrcA<sub>1</sub> incorporating three 2-FF residues, with a % signal intensity of 20.75% (Table 4.6). The peak at 10.99 minutes has the largest % total AUC at 74.6%. The predominant peptide in this peak is a TrcA incorporating three 2-FF residues, with a % signal intensity of 65.5%. The predominant peptide in the peak at 11.11 minutes is also a TrcA incorporating three 2-FF residues. One would expect the TrcA(3\*2-FF) peptide to only elute as one peak, given that if all the sites for 2-FF incorporation are occupied, only one structural configuration is possible and therefore should interact with the UPLC-column in the same manner. However, looking in detail at the extracted peaks for this analogue from the crude 2-FF extract in Figure 4.4, G, we also see another small peak eluting immediately after the main peak. The high levels of oligomerisation of the 2-FF extracts (as observed in Chapter 3) means that it is possible that the TrcA(3\*2-FF) analogue is undergoing high levels of oligomerisation with of the TrcA(2\*2-

FF) analogue that elutes at 11.09 minutes (Figure 4.4, F). It is regularly observed in our research group with TrcA purification that more than one peak corresponds to TrcA, particularly in purer samples, where more oligomerisation is expected. The two peptide containing peaks with the largest % total AUC both contain TrcA(3\*2-FF) in the highest relative amounts. This fraction can therefore be considered to be enriched for this peptide, but also containing some TrcA<sub>1</sub> and TrcA with varying levels of incorporation of 2-FF residues, ranging from one to three. The fluorinated TrcA analogues observed in this fraction have very similar retention times to the natural analogue, as is can be seen in Figure 4.3. Proposed structure for the enriched peptide in this fraction, TrcA(3\*2-FF), is given in Figure 4.12.

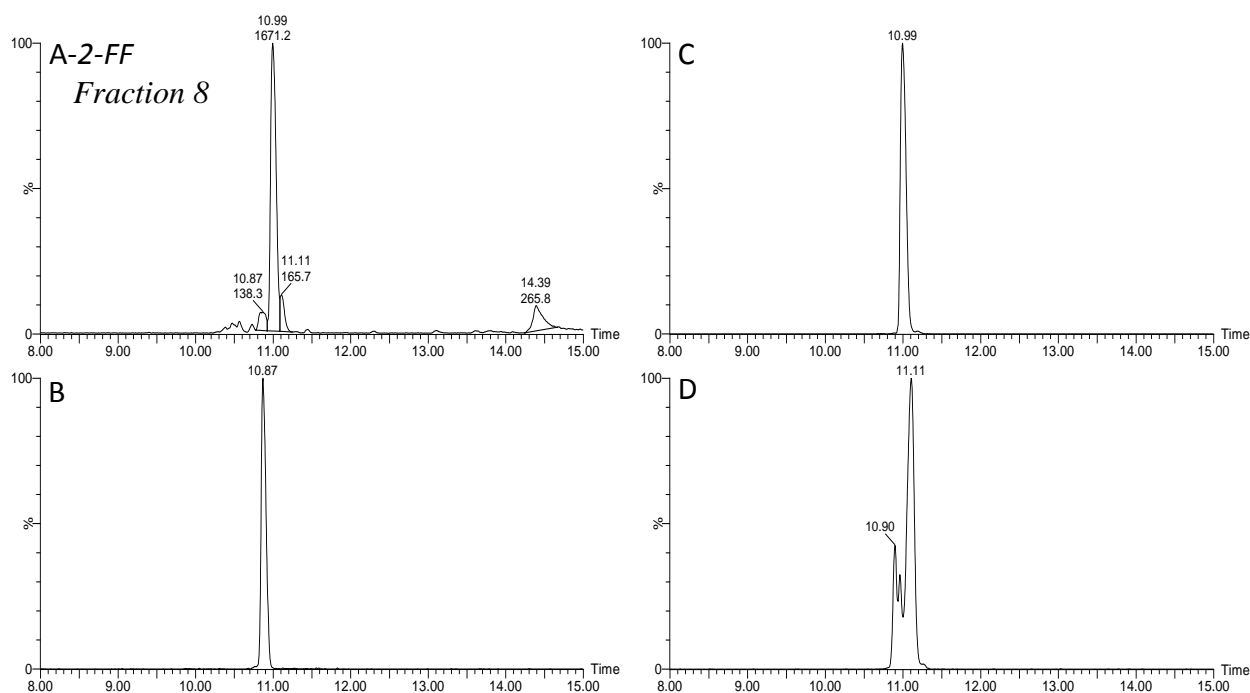


**Figure 4.11** UPLC-MS analysis of semi-preparative reverse phase HPLC fraction 8 of 2-FF supplemented extract. **A**, BPC of integrated peaks together with AUC below retention time. **B-D** show extracted mass chromatograms with peaks at retention times 10.87 ( $m/z = 669.8222$ ), 10.99 ( $m/z = 1324.6333$ ) and 11.11 minutes ( $m/z = 1306.6410$ ) respectively

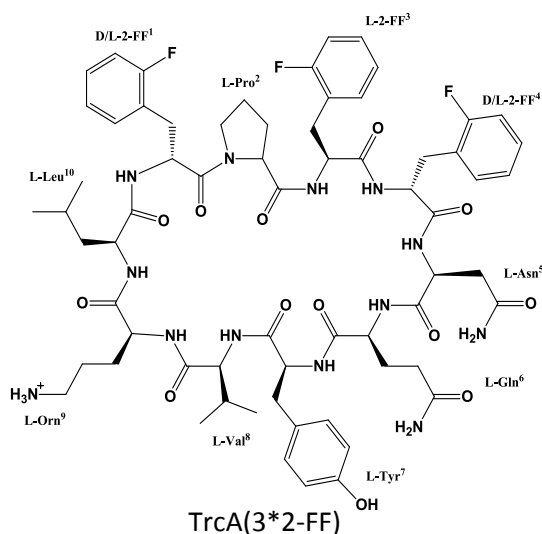


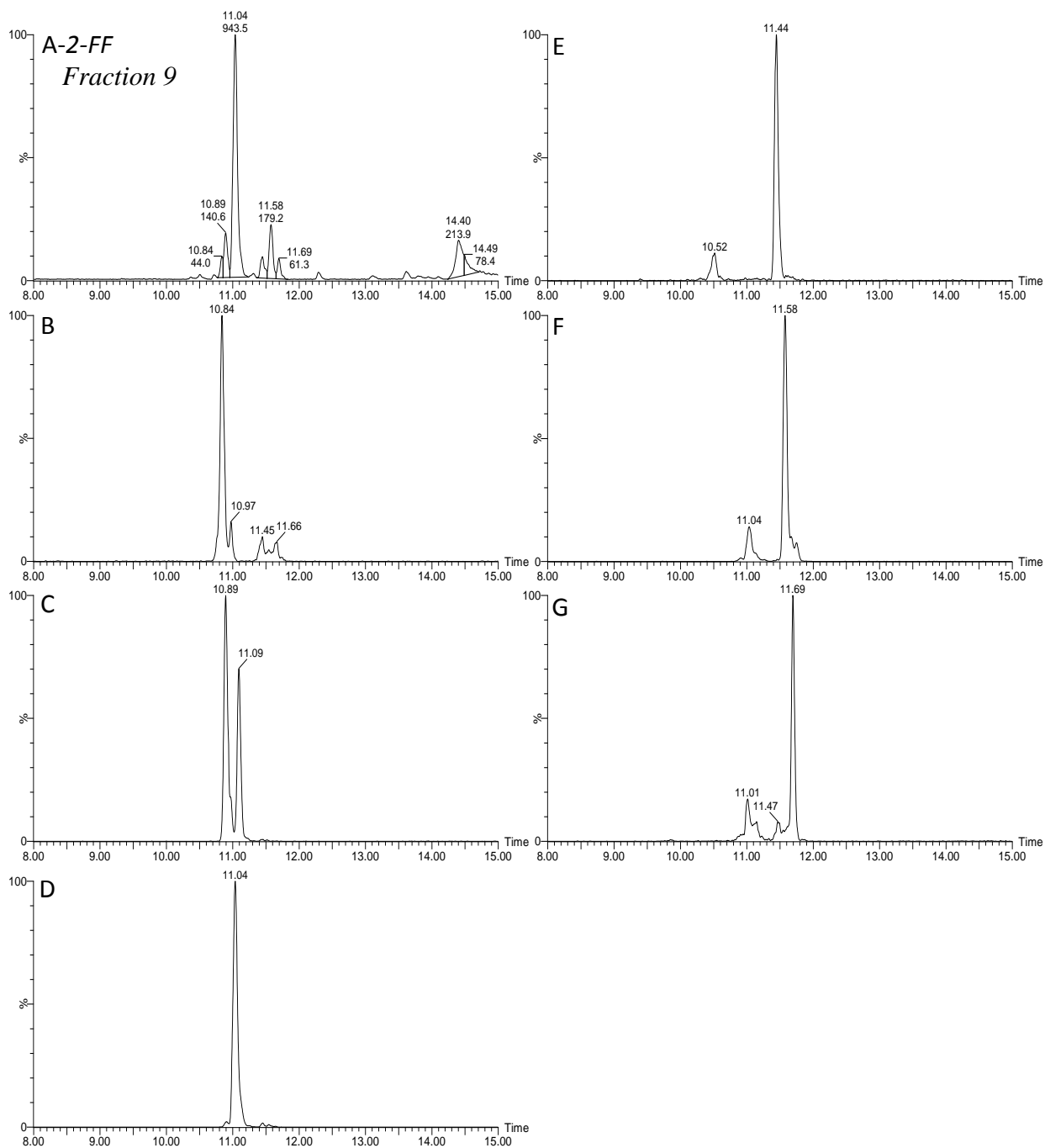
Figure 4.12 Structure for novel TrcA analogue containing three 2-FF residues enriched for in fraction 8

Figure 4.13, A, shows the UPLC-MS analysis and integrated peaks for fraction 9. The peak at 14.40 minutes is the same contaminant that is present in fraction 8, with an  $m/z$  of 317.115. This fraction had six peaks that could clearly be observed. The major peak at 11.04 minutes contributed most to the % total AUC, with a contribution of 54.26%. The predominant peptide in this peak is a TrcA containing two 2-FF residues (Table 4.7), which is also found to be the major peptide in the peaks at 10.84 and 10.97 minutes, meaning that this fraction is enriched for this peptide. TpcA(2\*2-FF) (with a sodium adduct) and PhcA(3\*2-FF) were detected in the remaining peaks (Table 4.7). From the peak and signal analysis it was deduced that fraction 9 of the 2-FF extract is enriched for the TrcA analogues with two 2-FF residues, denoted TrcA(2\*2-FF), whose possible structural configurations are shown in Figure 4.14.



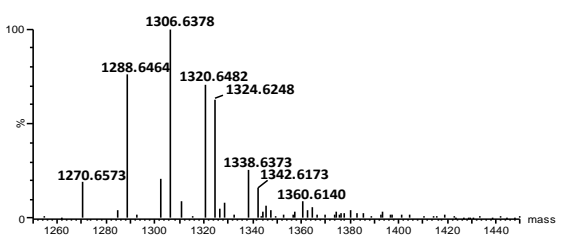
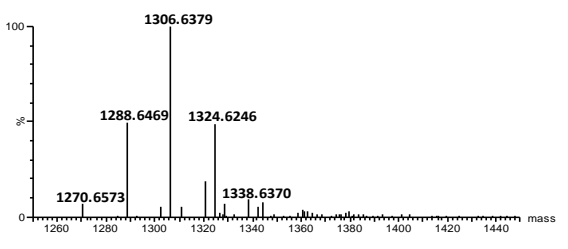
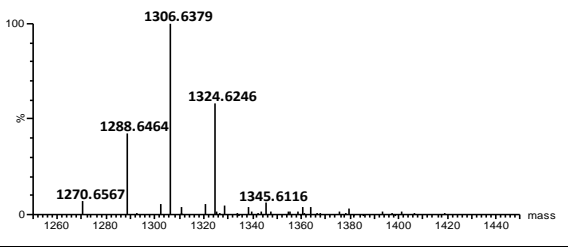
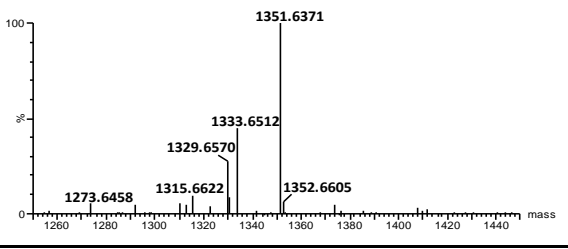
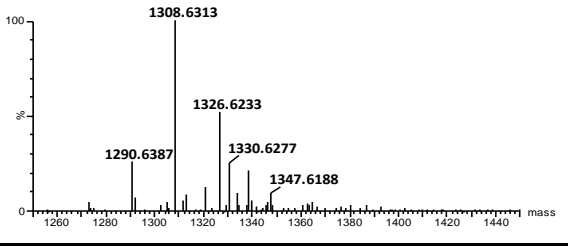
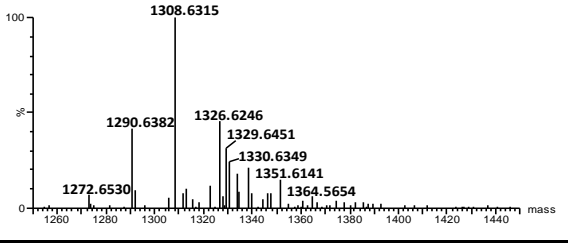
**Table 4.6** Mass analysis of peaks from HPLC Fraction 8 containing 2-FF tyrocidine analogues showing the % contribution to the total AUC of all integrated peaks. MaxEnt analysis was used to determine the % signal contribution of the analogues in the peak and shoulder which contributed to over 10 % of the total signal intensity as well as their mass and identity

Peak Rt (min)	% Total AUC	MaxEnt Spectra	Peptide (Theo. mass/Obs. Mass)	% Signal Intensity
10.87	6.2		TrcA <sub>1</sub> (3*2-FF) 1338.6498/1338.6426 TrcA <sub>1</sub> (2*2-FF) 1320.6592/1320.6508 TrcA(2*2-FF) 1306.6436/1306.6379 TrcA(1*2-FF) 1288.6530/1288.6473	20.75 15.44 15.04 13.03
10.99	74.6		TrcA(3*2-FF) 1324.6342/1324.6246 TrcA(2*2-FF) 1306.6436/1306.6376	65.50 13.96
11.11	7.4		TrcA(3*2-FF) 1324.6342/1324.6246 TrcA(2*2-FF) 1306.6436/1306.6375	45.07 20.25



**Figure 4.13** UPLC-MS analysis of semi-preparative reverse phase HPLC fraction 9 of 2-FFsupplemented extract. **A**, BPC of integrated peaks together AUC below retention time. **B-G** show extracted peaks at retention times 10.84 ( $m/z = 660.8342$ ), 10.89 ( $m/z = 1288.6462$ ), 11.04 ( $m/z = 1306.6410$ ), 11.44 ( $m/z = 676.3248$ ), 11.58 ( $m/z = 1308.6464$ ) and 11.69 ( $m/z = 1326.6366$ ) minutes at respectively

*Table 4.7* Mass analysis of peaks from HPLC fraction 9 containing 2-FF tyrocidine analogues showing the % contribution to the total AUC of all integrated peaks. MaxEnt analysis was used to determine the % signal contribution of the analogues in the peak and shoulder which contributed to over 10 % of the total signal intensity as well as their mass and identity

Peak Rt (min)	% Total AUC	MaxEnt Spectra	Peptide (Theo. mass/Obs. Mass)	% Signal Intensity
10.84	2.53		TrcA(2*2-FF) 1306.6436/1306.6378 TrcA(1*2-FF) 1288.6530/1288.6464 TrcA <sub>1</sub> (2*2-FF) 1320.6592/1320.6482 TrcA(3*2-FF) 1324.6342/1324.6248	19.4 14.7 13.7 12.2
10.89	8.09		TrcA(2*2-FF) 1306.6436/1306.6379 TrcA(1*2-FF) 1288.6530/1288.6469 TrcA(3*2-FF) 1324.6342/1324.6246	32.39 16.05 15.09
11.04	54.26		TrcA(2*2-FF) 1306.6436/1306.6379 TrcA(3*2-FF) 1324.6342/1324.6246 TrcA(1*2-FF) 1288.6530/1288.6462	36.17 21.03 14.92
11.44	4.49		TpcA(2*2-FF)[Na] 1351.6415/1351.6371 TpcA(1*2-FF)[Na] 1333.6509/13336512 TpcA(2*2-FF) 1329.6596/1329.6570	40.75 18.16 11.03
11.58	10.30		PhcA(3*2-FF) 1308.6393/1308.6313 PhcA(4*2-FF) 1326.6298/1326.6233	26.14 13.59
11.69	3.53		Phc(3*2-FF) 1308.6393/1308.6315 PhcA(4*2-FF) 1326.6298/1326.6246	22.00 9.95

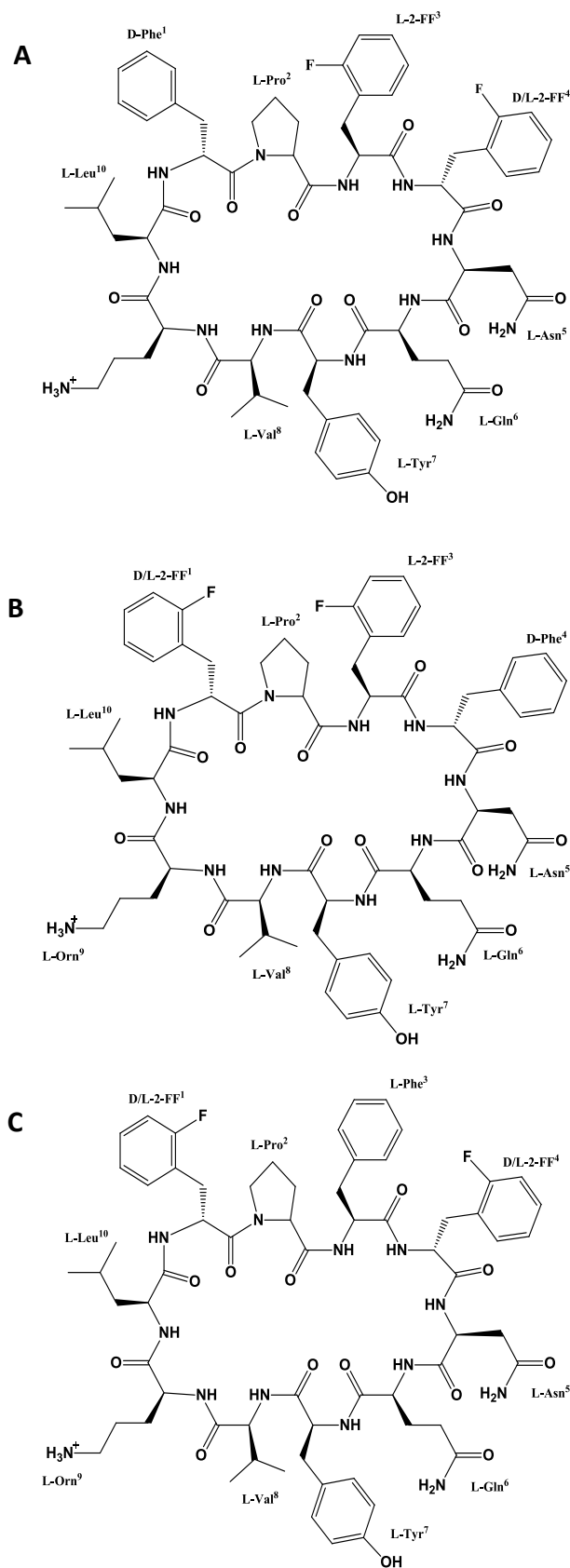


*Figure 4.14* Possible structural configurations for novel TrcA analogue containing two 2-FF residues enriched for in fraction 9. **A-C** represent the three different possible structural configurations based on theoretical sites of incorporation for phenylalanine

#### 4.3.4 Growth inhibition against *M. luteus*

For the HPLC fractions used in the biological activity assay, the fraction number will no longer be used, but rather the identity of the peptide present in the largest relative amount as determined by ESMS analysis. The 5-MeW fractions 3 and 8 were denoted TrcB(1\*5MeW) and TpcB(2\*5MeW) respectively. The 2-FF fractions 8 and 9 were denoted TrcA(3\*2-FF) and TrcA(2\*2-FF) respectively.

*Spot plates against M. luteus*: Figure 4.15 shows the effects of the selected HPLC fractions and selected natural analogues spotted on top of a lawn of *M. luteus*

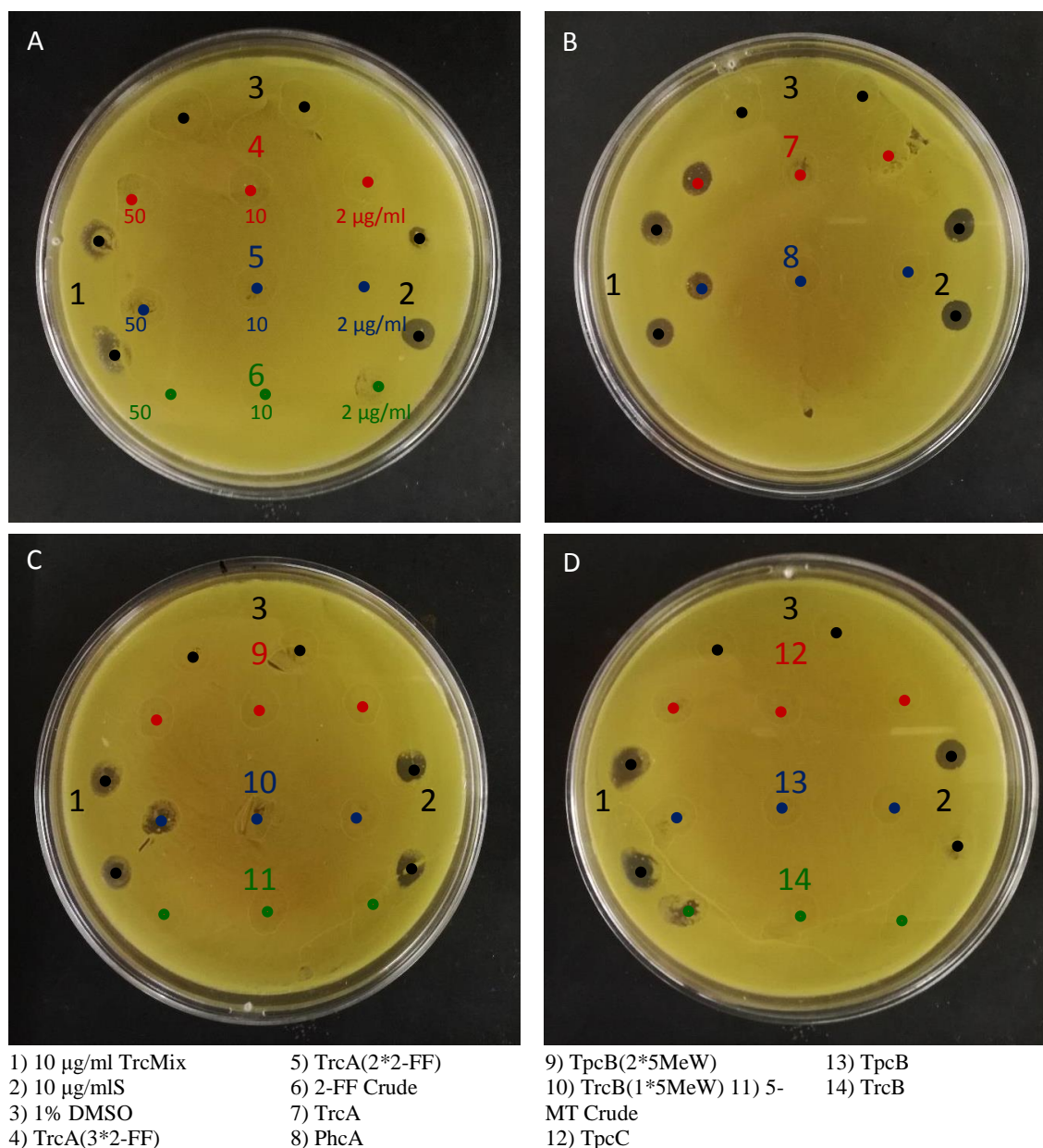


**Figure 4.15** Spot plates of selected HPLC fractions for 5-MeW and 2-FF. A volume of 5µL was spotted for all samples. Fractions and controls (TrcMix, GS and solvent) were all tested against *M. luteus*

In Figure 4.15, A, there were no clear zones of inhibition against the target organism by either of the 2-FF fractions or the crude extract. The positive controls (spotted in duplicate at positions 1 and 2) did not all have very clear zones of inhibition relative to the other plates (Figure 4.15, B-D) indicating that the organism concentration was slightly too high on parts of the plate. This is possibly due to uneven spreading and growth over the plate. The natural analogues (Figure 4.15, B) represented by spots at 7 and 8 (TrcA and PhcA), only showed zones of inhibition at the highest concentration of 50 µg/mL (spot to the furthest left).

For the 5-MeW analogues, only the spot at 10 (Figure 4.15, C-10, TrcB(1\*5MeW)) showed a zone of inhibition at 50 µg/mL. Only the natural analogue of this peptide (Figure 4.15, D-14, TrcB) showed some inhibition of growth, also at 50 µg/mL. It was previously found by Troskie (15) that solid media such as agar can influence the activity of tyrocidines against certain fungi. To overcome the problem of uneven spreading of the indicator organism on the assay plate and the possible effect that agar can have on the activity of the peptides, the activity assay was repeated in a liquid culture broth.

*Turbidimetric growth inhibition assay:* Figure 4.16 A and B represent the % growth inhibition of *M. luteus* by determining the optical density (OD) or turbidity produced by the dividing bacterial cells in solution after 16 hours of incubation. Figure 4.16, A, represents the peptides % growth inhibition of the selected natural and non-natural analogues against the target organism at the highest concentration used of 50 µg/mL. All peptides showed very good inhibition of growth at this concentration, with the exception of PhcA showing only about 30% growth inhibition. Figure 4.16, B, compares the activity of the same peptides at a five-fold lower concentration of 10 µg/mL. Here again most peptides show good inhibition of growth after 16 hours, again with the exception of PhcA, but also TpcC, having a marked decrease in growth inhibition, inhibiting only about 35% of bacterial growth.

*Resazurin growth inhibition assay:* Figure 4.12, C and D, represent the loss of actively metabolising cells, which can reduce the dye resazurin to resorufin, due to cell death by the peptide preparations. The % inhibition of metabolism (or % cell death) by the peptide preparations at 50 µg/mL (Figure 4.12, C) is similar to the % growth inhibition produced by the peptides tested at the same concentration. However, at a lower concentration of 10 µg/mL, the % inhibition of metabolic activity decreased markedly for most peptides, as surviving cells will metabolise the dye. If a peptide inhibits cell growth effectively, but there are still actively metabolising cells (surviving cells as determined by Alamar Blue<sup>®</sup> assay), it is a more bacteriostatic peptide, whereas if there is loss in cell growth and metabolism, it is a more bactericidal peptide (acting either through disruption of

the cell wall and/or other mechanisms) (16). These results indicated that 10 µg/mL was below the MIC and below the minimum bacteriocidal concentration (MBC) of these peptides. MIC is defined as the lowest concentration at which visible inhibition of growth is observed using OD measurements, whereas MBC is defined by the minimum concentration at which over a 99% percent loss in cell viability occurs (usually as a result of lysis of the bacterial membrane) (17). The commercial TrcMix, commercial GS, TrcB and its non-natural analogue TrcB(1\*5MeW), and the fluorinated TrcA analogue TrcA(3\*2-FF) did not show such a decrease in activity, indicating that 10 µg/mL is close to their MICs and/or MBCs.

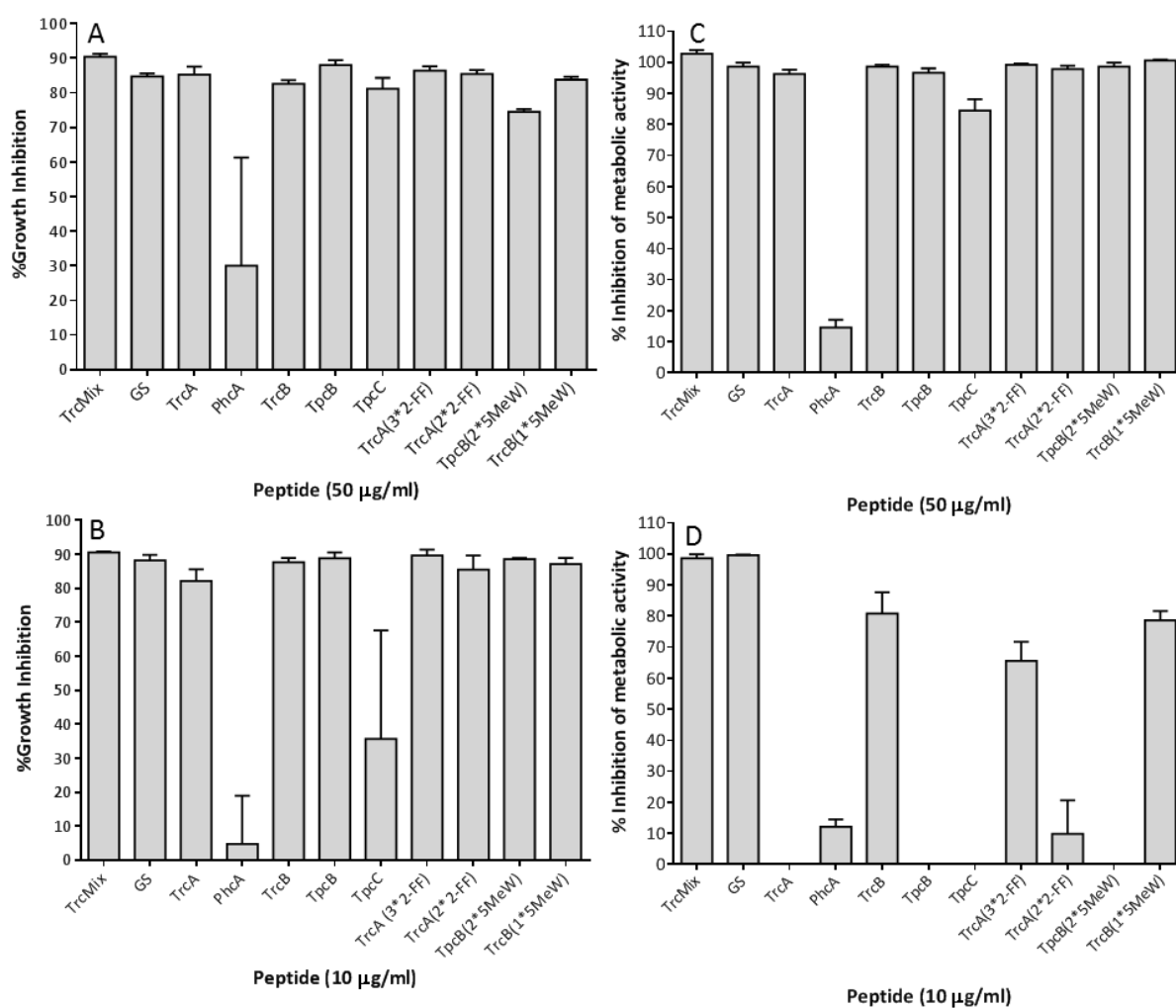


**Figure 4.16** Activity of selected peptides against *M. luteus* showing. **A** and **B** show the percentage inhibition of bacterial growth as a function of decrease in OD<sub>595</sub> following 16 hours of incubation. **C** and **D** show inhibition of metabolic activity as a function of increase in fluorescence at 590 nm after 25 hours by incubating the plates for an hour after adding resazurin dye then taking the reading.

## 4.5 Discussion

The non-natural amino acid analogues 2-flouro-phenylalanine and 5-methyl-tryptophan have been shown to be readily incorporated into tyrocidine-analogues by the producer organism *Br. parabrevis* DSMZ 5618 in TGS media. Preliminary analysis of extracts of cultures supplemented with the 1-methyl-L-tryptophan and 4-methyl-L-phenylalanine also showed incorporation of these analogues into peptides produced by this organism (Chapter 3), indicating the ability of the tyrocidine peptide synthetase complex to incorporate unnatural aromatic amino acid derivatives of Phe and Trp.

The increased incorporation of certain amino acid residues by supplementation in the growth media is supported by Vosloo *et al.* (2) who showed that the production profile of *Br. parabrevis* ATCC 10068 could be shifted towards analogues containing enriched in either Trp or Phe residues. These results indicate a promising avenue for the biosynthesis of novel tyrocidines, tryptocidines and phenycidines.

Like the natural analogues incorporated into the variable positions, the non-natural analogues also have variable incorporation into different sites, as is evident by certain non-natural tyrocidine analogues having two different retention times as observed by UPLC analysis. In Figure 4.1, B, there are two peaks which contain significant proportions of a peptide corresponding to TpcC with one 5MeW residue (TpcC(1\*5MeW)), indicating that there are likely only two favourable positions of incorporation (of the three theoretically available). Given the fact that position 4 in any tyrocidine analogue contains a D-amino acid residue that is converted from L to D configuration by the epimerase activity in the E-domain, it seems more likely that the 5-MeW residue is incorporated into either position 3 or position 7, resulting in a different retention time for the two analogues. The double peak phenomenon is also observed for the 2-FF-containing tyrocidine analogues. For example, Figure 4.6, F, shows two clear peaks with different retention times both containing TrcA with two 2-FF residues (TrcA (2\*2-FF)), indicating that there are two possible sites of incorporation. Given that this analogue only contains three likely sites for incorporation of a Phe analogue, it would seem likely that the 2-FF residue can be incorporated at positions 1 and/or 3 and/or 4, with both positions 1 and 4 having a D-configuration. This implies that a 2-FF residue could be epimerised by the E-domain, or at the very least can still be incorporated at this module in the NRPS.

The purification of single peptides from a mixture of non-natural analogues proved to be difficult due to the extra level of structural diversity provided by the incorporation of non-natural amino acid residues at different positions, as well as the possible increased levels of aggregation resulting from



changes in structure and hydrophobicity. An emphasis should be placed on optimising semi-preparative HPLC purification of these peptides, either using lower concentrations, exploring different solvent systems, alternative chromatographic matrix/HPLC program or driving the production profile towards one or two major analogues using specific amino acid supplementation concentrations during incubation. This could also involve the creation of a mathematical model determining the levels of productions of certain analogues as a function of supplemented amino acid concentration in a manner similar to that done by Vosloo *et al* (2). It would also be essential to confirm the amino acid sequence of novel peptide(s) in the purified/enriched fractions utilising tandem mass spectrometry (MS/MS). In MS/MS the collisional induced dissociation (CID) of a novel cyclic decapeptide and comparing the fragment spectra with that of the natural analogue would allow validation of our current identification of the different peptides.

Of particular interest would be the purification of single analogues with fluorinated aromatic amino acid residues for use in fluorine-NMR studies, possibly to explore the interaction of these residues with model membranes. The incorporation of a fluorinated tryptophan would potentially allow for the production of various tyrocidine analogues with all the aromatic amino acid residues being fluorinated. Using TrcA as an example, the similar retention times of fluorinated analogues of TrcA (Figure 4.8) with the natural analogue, together with their similar levels of inhibition of bacterial growth (Figure 4.11, A & B) indicate that the incorporation of 2-FF residues into TrcA does not significantly alter its structure-activity relationship. The modified TrcA with 2-FF residue(s) can therefore be an NMR traceable analogue of TrcA in biological systems. In terms of inhibition of metabolic activity, the fluorinated TrcA analogues (TrcA(3\*2-FF) and TrcA(2\*2-FF), appear to be more active at lower concentrations, where the anti-metabolic activity of the natural TrcA disappeared completely. It is possible that these analogues depress cell growth by causing cell death (i.e. have lower MBCs), rather than just causing reversible inhibition of cell growth (bacteriostatic action).

The incorporation of 5-MeW into the tyrocidines resulted in an increase in the hydrophobicity of these peptides as determined by the increase in their retention times compared to the natural analogues (Figure 4.1). The incorporation of this analogue did not appear to have any marked effect on inhibition of microbial growth (Figure 4.16, A and B). Both TrcB and TrcB(1\*5MeW) appeared to be strong inhibitors of bacterial growth, as is evident by the zones of inhibition on the spot plates in Figure 4.11 C and D. Both these analogues were also relatively good inhibitors of bacterial metabolism retaining over 70% inhibition of bacterial metabolic activity at the lower concentrations of 10 µg/ml (Figure 4.12, D), indicating a more bacteriostatic nature (as discussed earlier for TrcA and its analogues). Of all the peptides tested these therefore appear to be the most active against *M.*

*luteus*, a result supported by Spathelf and Rautenbach (6) and Leussa and Rautenbach (18). Both TpcB and TpcB(2\*5MeW) showed similar levels of inhibition of bacterial growth and bacterial metabolic activity. For these analogues, the lack of inhibition of metabolism at a concentration of 10 µg/mL (Figure 4.16, D) indicates that these are less active peptides.

This work shows a promising avenue for the biosynthesis of a wide array of novel Trc analogues, with the possibility of developing novel anti-microbial peptides with unique structure-activity relationships, which is becoming ever more important as the efficacy of existing antibiotics is rapidly dwindling. In addition, the cost of production is lower compared to synthetic synthesis, implying a higher feasibility for large-scale production of these novel peptides if they prove to have practical applications in clinical and industrial settings.

Future work would include improving the purification process of these peptide to characterise individual analogues, sequencing novel peptides using MS fragmentation, testing a more diverse array of amino acid analogues for incorporation, testing biological activity against a wider variety of organisms (particular to observe if activity against Gram negative bacteria occurs) and looking at production of novel peptides in producer organisms which also synthesize subsets of structurally similar peptides using non-ribosomal peptide synthesis.

## 4.6 References

1. Tang, X-J., Thibault, P., and Boyd, R. K. (1992) Characterisation of the tyrocidine and gramicidin fractions of the tyrothricin complex from *Bacillus brevis* using liquid chromatography and mass spectrometry. *Int. J. Mass Spectrom. Ion Process.* **122**, 153–179
2. Vosloo, J. A., Stander, M. A., Leussa, A. N. N., Spathelf, B. M., and Rautenbach, M. (2013) Manipulation of the tyrothricin production profile of *Bacillus aneurinolyticus*. *Microbiol. (United Kingdom)*. **159**, 2200–2211
3. Lewis, J. C., Dimick, K. P., and Feustel, I. C. (1945) Production of tyrothricin in cultures of *Bacillus brevis*. *Ind. Eng. Chem.* **37**, 996–1004
4. Vosloo, J. A. (2016) Optimised bacterial production and characterisation of natural antimicrobial peptides with potential application in agriculture. **Ph.D. thesis**, University of Stellenbosch, <http://scholar.sun.ac.za/handle/10019.1/98411>
5. Leussa, N.-N. A. (2014) Characterisation of small cyclic peptides with antilisterial and antimalarial activity. **Ph.D. thesis**, University of Stellenbosch, <http://hdl.handle.net/10019.1/86161>
6. Spathelf, B. M., and Rautenbach, M. (2009) Anti-listerial activity and structure-activity relationships of the six major tyrocidines, cyclic decapeptides from *Bacillus aneurinolyticus*. *Bioorganic Med. Chem.* **17**, 5541–5548
7. Marques, M. A., Citron, D. M., and Wang, C. C. (2007) Development of tyrocidine A analogues with improved antibacterial activity. *Bioorg. Med. Chem.* **15**, 6667–6677

8. Okuda, K., Edwards, G. C., and Winnick, T. (1963) Biosynthesis of gramicidin and tyrocidine in the Dubos strain of *Bacillus brevis*. I. Experiments with growing cultures. *J. Bacteriol.* **85**, 329–338
9. Ruttenberg, M., and Mach, B. (1966) Studies on amino acid substitution in the biosynthesis of the antibiotic polypeptide tyrocidine. *Biochemistry.* **5**, 2864–2869
10. Süßmuth, R. D., and Mainz, A. (2017) Nonribosomal peptide pynthesis—principles and prospects. *Angew. Chemie - Int. Ed.* **56**, 3770–3821
11. Eyeghe-Bickong, H. (2011) Role of surfactin from *Bacillus subtilis* in protection against antimicrobial peptides produced by *Bacillus* species. **Ph.D. thesis**, Stellenbosch University, <http://hdl.handle.net/10019.1/6773>
12. Du Toit, E. A., and Rautenbach, M. (2000) A sensitive standardised micro-gel well diffusion assay for the determination of antimicrobial activity. *J. Microbiol. Methods.* **42**, 159–165
13. O’Brien, J., Wilson, I., Orton, T., and Pognan, F. (2000) Investigation of the Alamar Blue (resazurin) fluorescent dye for the assessment of mammalian cell cytotoxicity. *Eur. J. Biochem.* **267**, 5421–5426
14. Riss, T. L., Moravec, R. A., Niles, A. L., Duellman, S., Benink, H. A., Worzella, T. J., and Minor, L. (2004) Cell Viability Assays, Eli Lilly & Company and the National Center for Advancing Translational Sciences, [online] <http://www.ncbi.nlm.nih.gov/pubmed/23805433> (Accessed January 2, 2018)
15. Troskie, A. M. (2013) Tyrocidines , cyclic decapeptides produced by soil bacilli , as potent inhibitors of fungal pathogens. **Ph.D. thesis**, Stellenbosch University, <http://hdl.handle.net/10019.1/86162>
16. Brogden, K. A. (2005) Antimicrobial peptides: Pore formers or metabolic inhibitors in bacteria? *Nat. Rev. Microbiol.* **3**, 238–250
17. Hancock, R. E. W., and Rozek, A. (2002) Role of membranes in the activities of antimicrobial cationic peptides. *FEMS Microbiol. Lett.* **206**, 143–149
18. Leussa, A. N. yango N., and Rautenbach, M. (2014) Detailed SAR and PCA of the tyrocidines and analogues towards leucocin A-sensitive and leucocin A-resistant *Listeria monocytogenes*. *Chem. Biol. Drug Des.* **84**, 543–557

## Chapter 5

### Summary, conclusions and future work

#### 5.1 Introduction

The Tcn extract produced by the producer organism, *Brevibacillus parabrevis*, contains a diverse array of cationic cyclodecapeptides, such as the tyrocidines, tryptocidines and phenycidines, as well as the neutral linear pentadecapetides, the gramicidins. The different structural analogues arise as a result of the non-ribosomal synthesis process of these peptides, where the tyrocidine peptide synthetases enzymatically incorporate amino acids, with certain domains having the ability to incorporate more than one amino acid (1). These peptides are produced in varying amounts within the Tcn extract depending on a variety of factors, including the producer strain (2) used and media compositions (3). In addition, it has been found that supplementing the growth media with Phe and/or Trp can drive the production towards different subsets of Trcs incorporating more of these amino acids at their variable positions (4). The activity of the individual Trcs isolated from these mixtures against Gram-positive bacteria (5) and *Plasmodium falciparum* (6) varies depending on their structure and biophysical characteristics, which effect their hydrophobicity and their levels of oligomerisation (3, 7).

The goal of this study was to make use of the ability of the producer organism to incorporate different amino acids into the Trcs, specifically to determine whether non-natural derivatives of Phe and Trp could be incorporated, to produce novel Trcs. In order to achieve this, different strains of the producer organism were first analysed in terms of their Trc production profiles without amino acid supplementation under varying conditions (Chapter 2). Following this, the strains were assessed on their ability to grow in the presence of the selected non-natural amino acid derivatives and to determine their production profiles (using a selected strain) following supplementation with these amino acids under various growth conditions (Chapter 3). In chapter 4 large scale productions using the selected strain was done using supplementation with the selected amino acid derivatives in an attempt to purify and partially characterise novel Trcs.

## 5.2 Summary of findings and future work

### 5.2.1 Strain production profile characterisation and optimisation of carbon, nitrogen and sulphate sources

Initially, extracts of large scale cultures of the four available *Br. parabrevis* strains (DSMZ 5618, DSMZ 362, ATCC 8185 and ATCC 10068) were characterised using UPLC-ESMS analysis to determine differences in their production profiles. These cultures were grown in TGS media (combinations tryptone, glucose and inorganic salts) as used in cultures by Vosloo (4) based on a media composition developed by Lewis *et al* (8). UPLC-MS analysis revealed differences in the production profiles of the major Trc analogues, which is likely given differences in the production of the structurally similar GS observed between different producer strains (9, 10). The major Trcs detected in the extracts (based previous extracts done in our lab) were identified and their contributions to the production profiles were calculated. Here it was observed that the 5618-strain gave the best production of C-analogues, with TpcC and TrcC<sub>1</sub> being the predominant analogues. There was no strain with a clear preference for production of B-analogues, but the 362-strain did produce the highest relative amounts of TpcB<sub>1</sub> and TrcB<sub>1</sub>, indicating a higher level production of Lys<sup>9</sup> containing analogues. The 362-strain showed the best overall production of A-analogues.

The effects of altering nitrogen, sulphate and carbon sources (using TGS as a base media) on the growth rates of the 5618, 8185 and 362 strains were also determined using various combinations and concentrations of urea (CO(NH<sub>2</sub>)<sub>2</sub>), sodium sulphate (Na<sub>2</sub>SO<sub>4</sub>), ammonium sulphate ((NH<sub>4</sub>)<sub>2</sub>SO<sub>4</sub>), glucose and glycerol. The nitrogen and sulphate containing compounds were well tolerated by all the strains as determined by their growth rates relative to TGS. Urea appeared to produce a slightly higher growth rate (either on its own or in combination with sodium sulphate) for the 5618 and 362 strains compared to TGS. Some of the tested nutrient conditions also had an effect on the nature of the growth of the strain, producing multi-auxic (more than one apparent exponential growth phase) growth curves and varying lag times.

In terms of the carbon sources tested (using TGS as a base media), glycerol appeared to be an overall poor supporter of growth for all strains, with a clear preference for glucose shown by all the strains tested. When testing combinations of these carbon sources the results were more ambiguous, with the combination of glucose and glycerol sometimes producing higher or lower growth rates (and not for all concentrations) compared to either glucose or glycerol alone. Glucose alone at a concentration of 30 g/L produced the highest growth rates for all carbon source concentrations and combinations tested. Like the nitrogen and sulphate sources, different glucose and glycerol

concentrations and compositions also had an observable effect on lag times and number of apparent exponential growth phases.

Selected concentrations of urea (since it had the largest apparent improvement in on growth rate compared to all other nutrient conditions tested) were selected for used in deep-well extracts to determine its effects on Trc production on the 5618, 362 and 8185 strains. In terms of the ratio of cell mass to extract mass, the 5618 and 8185 strains showed the best production of peptide with added urea. For the 5618-strain the addition of 8 g/L urea to TGS produced the best cell mass to extract mass ratio compared to all other strains and conditions, but with an improvement in this ratio of 0.11 over TGS, it is dubious whether this difference would be statistically significant and ultimately lead to a significant in production of peptide.

In terms of production profiles following urea supplementation, the 5618-strain showed the best production in the sense that it produced all the major Trc analogues tested for in readily detectable amounts (with the exception of TpcC, which was suppressed by the addition of urea to TGS). The relationship between growth rate and peptide production is unclear, with variable relationships between growth rate, extract masses and peptide signals.

The 5618-strain was chosen going forward for subsequent chapters based on the fact that it was the best producer of TrcC-analogues (but also had an all-round good production of other analogues). This was initially of interest as the first non-natural analogue initially tested for incorporation into the Trcs was the Trp derivative 5-MeW. The strain was then chosen for testing with other amino acid derivatives for the sake of simplicity and comparison of production of Trcs by this strain under different conditions.

Future studies of this nature would benefit from a more comprehensive growth curve experiment in which more data in captured in an individual experiment. This means that following the determination of growth rate in the microtiter plates, incubation of these plates should be done for a longer period to allow for Trc synthesis. Following this incubation small-scale extraction can be done in the wells and the supernatant can be tested for Trc production in a higher throughput manner using any number of assays or combinations of assays, including antimicrobial growth inhibition assays, assays to determine peptide aggregation, as well as haemolysis assays. In this way the one can directly determine the effect of growth rate and growth conditions on peptide productions before selecting conditions for deep-well assays.

### ***5.2.2 Determination of the incorporation of non-natural amino acids into the tyrocidines and analogues***

As described previously, the mechanism of Trc synthesis allows for the production of a variety of cyclo-decapeptide analogues thanks to variable amino acid incorporation (4). This provides the primary basis for exploring the possibility of incorporation of the selected non-natural amino acid derivatives. Some work has been done on the effect of non-natural amino acids on growth rates of different producer organisms as well as Trc production (but not looking at incorporation of the tested amino acid into the produced Trcs) (11), with some non-natural amino acids inhibiting protein synthesis by the producer organism. Little work, however, has been done on testing for the incorporation of non-natural amino acids into the Trcs, with the exception of some work by Ruttenberg *et al.* (12). The possibility of the producer organism to incorporate non-natural amino acids provides a promising avenue for the creation of novel antimicrobial peptides, which may help in the fight against antimicrobial resistance.

This chapter aimed to determine the effects of selected non-natural amino acids on the growth rate of the 5618, 362 and 8185 strains and to characterise the production of Trcs by the 5618-strain following supplementation with Phe and Trp as well as their non-natural derivatives 2-FF (2-flouro-phenylalanine), 4-MeF (4-methyl-phenylalanine), CF<sub>3</sub>F (4-triflouro-phenylalanine), 1-MeW (1-methyl-trpytophan) and 5-MeW (5-mehtyl-trpytophan).

Supplementation of TGS with the selected amino acids at varying concentrations produced both improved and reduced growth rates relative to TGS alone. There was generally an inhibitory effect on growth as amino acid concentration was increased, with some strains showing no change, particularly at the maximum concentration tested of 22 mM. Increasing Trp concentration led to an improvement in growth rate for the 5618-strain. The 5-MeW derivative was best tolerated by the 5618-strain while the 1-MeW derivative was best tolerated by the 362-strain. For the phenylalanine derivatives, the 8185-strain appeared to be the most tolerant to increasing concentrations of all the Phe derivatives, with the exception of the CF<sub>3</sub>F derivative, which showed increasing toxicity with an increase in growth rate for all the strains.

Medium-throughput small scale cultures were done using the 5618-strain, which was selected as it had already been used for initial deep-well cultures with Trp and 5-MeW (for which it gave the best growth rates and production profiles). Analysis of these deep-well culture extracts, using ESMS, showed extensive incorporation of all the amino-acid analogues tested (with the exception of the CF<sub>3</sub>F derivative). Identification of novel peptides was done based on comparing the detected versus the theoretical masses (see addendum at end of thesis) if amino acids had been incorporated. In



addition, levels of oligomerisation were analysed, and found to vary from natural to non-natural analogues. All the non-natural Phe derivative extracts showed increased formation of higher order oligomers (trimers and tetramers) relative to the Phe extract, while there was a marginal increase in tetramer formation for the non-natural Trp derivatives relative to Trp.

The relative quantification of natural and non-natural peptides produced under varying incubation conditions was done following extraction of deep-well cultures to assess differences in production profiles as well as any possible correlation between growth rates under varying conditions and Trc production under varying conditions. For Phe and its derivatives, there was no clear correlation between a growth rates at amino acid supplementation concentrations of 11 and 22 mM, and peptide production at 10 and 20 mM, with the exception of the CF<sub>3</sub>F derivative, which showed both decreasing growth rates and peptide production as its concentration increased. There was no clear effect of sodium sulphate and urea supplementation and concentration on peptide production, with some peptides showing increased production relative to TGS alone and some having decreased production relative to TGS alone. The same is true for quantification of peptides in Trp and Trp-derivative supplemented samples. It may be possible than some amino acid derivatives are selective inhibitors or protein synthesis but not Trc synthesis.

Production of novel Trcs by incubation of the producer organism with non-natural amino acids proved to be successful. Future work would include testing a wider variety of non-natural amino acids for incorporation. The process of peptide identification and quantification would benefit from automated identification and quantitation of peptides using ESMS mass spectra. In addition, the use of ion-mobility analysis linked to ESMS would aid in the identification of novel Trcs (when there are too many samples to be processed by UPLC-MS), which have overlapping masses with natural Trcs, on the basis of differing drift-times (as determined by ion-mobility analysis). Ion mobility would also aid in the analysing levels of oligomerisation and deconvoluting oligomers and monomers with overlapping  $m/z$  values to aid in the determination of masses using MaxEnt 3 analysis.

### ***5.2.3 Medium scale production and characterisation of tyrocidine analogues containing non-natural aromatic amino acids***

Medium-scale in-culture production of Trcs allows for subsequent extraction, purification and analysis of both the crude extract and individual Trc analogues. This is achieved using a large-scale extraction process to maximise the purity of the Trcs before further purification and analysis. UPLC-MS is a valuable tool which is then used to analyse the extracts for quantification and identification or peptides within the mixture using its high degree of sensitivity. Semi-preparative



reverse-phase HPLC can be used to purify or enrich certain analogues within the crude extract, which can then be further characterised in a number of ways, including their activity against selected microorganisms and their unique biophysical characteristics.

In this chapter we aimed to produce, purify and partially characterise novel Trcs isolated following incubation of the producer organism with the Phe derivative 2-FF and the tryptophan derivative 5-MeW.

Both 2-FF and 5-MeW were readily incorporated into the Trcs to produce a host of novel cyclo-decapeptides. Identification was achieved by comparing the detected masses of these analogues to their theoretical masses (given in thesis addendum) and comparison of production profiles and UPLC retention times for extracts supplemented with Phe and Trp. In the case of the 2-FF supplemented extract, a TrcA incorporating three fluorinated phenylalanine residues produced the largest signal, and with a similar retention time to TrcA (differing by 0.03 minutes), indicating a very similar hydrophobicity. In the 5-MeW supplemented extract a TpcB/B' incorporating a single 5-MeW residue produced the highest signal and a retention time of 11.73 minutes, but was significantly more hydrophobic than its natural counterpart which eluted at 10.86 minutes. The UPLC analysis of the 5-MeW analogues indicated an increase in retention time for all methylated analogues, indicating the more hydrophobic nature of these analogues.

Semi-preparative reverse-phase HPLC purification of individual peptides proved to be difficult. This was primarily due to the large increase in structural diversity of Trc analogues produced when incorporating an additional amino acid. This increases the odds of creating peptides with overlapping retention times. As a result, it was only possible to enrich HPLC fractions for a certain peptide (as determined by UPLC-MS analysis). For the 2-FF extract two fractions were used for subsequent analysis, one enriched for a TrcA incorporating three fluorinated phenyl residues (TrcA(3\*2-FF)), and one incorporating two (TrcA(2\*2-FF)). In the case of the HPLC fractions of the 5-MeW supplemented culture extract, two fractions were also used for subsequent analysis, one enriched for a TrcB/B' incorporating single 5-MeW residue (TrcB/B'(1\*5MeW)) and one a TpcB/B' incorporating two 5-MeW residues (TpcB/B'(2\*5MeW)).

The peptide enriched for in these fractions were then characterised by testing them against the Gram-positive target organisms *Micrococcus luteus*, together with their natural equivalents as well as PhcA and TpcC. An initial spot plate assay indicated that the most active peptides were the natural analogues TrcA, PhcA and the non-natural analogue TrcB(1\*5MeW), however further tests were required. Growth inhibition and metabolic activity inhibition assays were done against *M. luteus* to give a more in-depth idea of their activity. All peptides tested appeared to be good

inhibitors of bacterial growth ( $\pm 80\%$  -  $90\%$  growth inhibition) at concentrations of  $50 \mu\text{g/mL}$  (with the exception of PhcA) and  $10 \mu\text{g/mL}$  (with the exception of PhcA and TpcC). The % inhibition of metabolic activity by the selected peptides at  $50 \mu\text{g/mL}$  were also good ( $\pm 80\%$  -  $90\%$ ), again with the exception of PhcA. At a concentration of  $10 \mu\text{g/mL}$  the inhibition of metabolic activity decreased for TrcA, TpcB, TpcC and TpcB(2\*5MeW) and decreased less, but still considerably, for TrcA(2\*2-FF). This indicates that the MBC (minimum bactericidal concentration) for these peptides is above  $10 \mu\text{g/mL}$ , while TrcB, TrcA(3\*2-FF) and TrcB(1\*5MeW) retained good inhibition of bacterial metabolism, making them more potent bactericidal peptides. The large increase in % metabolic inhibition by the TrcA(3\*2-FF) peptide, and to a lesser degree the TrcA(2\*2-FF) peptide, indicates that these non-natural derivative are more active than TrcA. TpcB and TrcB and their non-natural analogues had similar growth and metabolic activity inhibition, with TrcB and its non-natural analogues being more active than TpcB and its analogues.

### **5.3 Last word**

Growth curve analysis can be rapidly used to determine the viability of certain culture conditions and non-natural amino acid supplementations on cell growth. Medium throughput deep-well assays can then be used to test for the levels of peptide production, as well as the identification of novel peptides, under selected conditions. This can be scaled up even further to allow for the production, isolation and characterisation of novel Trcs.

This study has shown that it is possible to create novel Trcs using simple in-culture methodology and this may prove to be an exciting avenue in the development of novel antimicrobial peptides for use in clinical and industrial settings.

## 5.4 References

1. Marahiel, M. A., Stachelhaus, T., and Mootz, H. D. (1997) Modular peptide synthetases involved in nonribosomal peptide synthesis. *Chem. Rev.* **97**, 2651–2674
2. Dubos, R. J., and Hotchkiss, R. D. (1941) The production of bactericidal substances by aerobic sporulating bacilli. *J. Exp. Med.* **73**, 629–640
3. Vosloo, J. A. (2016) Optimised bacterial production and characterisation of natural antimicrobial peptides with potential application in agriculture. **Ph.D. thesis**, University of Stellenbosch, <http://scholar.sun.ac.za/handle/10019.1/98411>
4. Vosloo, J. A., Stander, M. A., Leussa, A. N. N., Spathelf, B. M., and Rautenbach, M. (2013) Manipulation of the tyrothricin production profile of *Bacillus aneurinolyticus*. *Microbiol. (United Kingdom)*. **159**, 2200–2211
5. Dubos, R. J. (1939) Studies on a bactericidal agent extracted from a soil bacillus I. Preparation of the agent. Its activity *in vitro*. *J. Exp. Med.* **70**, 1–10
6. Leussa, N.-N. A. (2014) Characterisation of small cyclic peptides with antilisterial and antimalarial activity. **Ph.D. thesis**, Stellenbosch University, <http://scholar.sun.ac.za/handle/10019.1/86161>
7. Munyuki, G., Jackson, G. E., Venter, G. a., Kövér, K. E., Szilágyi, L., Rautenbach, M., Spathelf, B. M., Bhattacharya, B., and Van Der Spoel, D. (2013)  $\beta$ -sheet structures and dimer models of the two major tyrocidines, antimicrobial peptides from *Bacillus aneurinolyticus*. *Biochemistry*. **52**, 7798–7806
8. Lewis, J. C., Dimick, K. P., and Feustel, I. C. (1945) Production of tyrothricin in cultures of *Bacillus brevis*. *Ind. Eng. Chem.* **37**, 996–1004
9. Lykov, V. P., Bodnar, I. V., Khovrychev, M. P., and Polin, A. N. (1986) Biosynthesis of the antibiotic gramicidin S by a *Bacillus brevis* culture associated with a change in growth kinetics. *Mikrobiologiya*. **55**, 792–795
10. Winnick, R. E., and Winnick, T. (1961) Biosynthesis of gramicidin S II. Incorporation experiments with labelled amino acids analogs, and the amino acid activation process. *Biochem. Biophys Acta*. **53**, 461–468
11. Okuda, K., Edwards, G. C., and Winnick, T. (1962) Biosynthesis of gramicidin and tyrocidine in the dubos strain of *bacillus brevis* I. Experiments with growing cultures. *J. Bacteriol.* **85**, 329–338
12. Ruttenberg, M. A, and Mach, B. (1966) Studies on amino acid substitution in the biosynthesis of the antibiotic polypeptide tyrocidine. *Biochemistry*. **5**, 2864–2869

## Peptide Reference Tables

**Table 1** List of theoretical monomer masses and primary structures for natural Trcs and Grcs (1). For this and subsequent tables,  $M_r$  = theoretical mass,  $[M+H]^{1+} = (M_r + \text{hydrogen})/1$  (singly charged  $m/z$ ),  $[M+2H]^{2+} = (M_r + 2 \text{ hydrogens})/2$  (doubly charged  $m/z$ ),  $[M+Na]^{1+} = \text{mass} + \text{sodium adduct}$ ,  $[M+Na+H]^{2+} = (M_r + \text{hydrogen} + \text{sodium})/2$  (doubly charged  $m/z$ )

Abbreviations	Primary structure	$M_r$	$[M+H]^{1+}$	$[M+2H]^{2+}$	$[M+Na]^{1+}$	$[M+Na+H]^{2+}$
A analogues						
PhcA	Cyclo-(fPFfNQFVOL)	1253.6597	1254.6675	627.8377	1276.6495	638.8286
PhcA <sub>1</sub>	Cyclo-(fPFfNQFVKL)	1267.6753	1268.6832	634.8455	1290.6651	645.8365
TrcA	Cyclo-(fPFfNQYVOL)	1269.6546	1270.6624	635.8351	1292.6444	646.8261
TrcAv <sup>1</sup>	Cyclo-(fPFfNQYVOV)	1255.6390	1256.6468	628.8273	1278.6287	639.8183
TrcA <sub>1</sub>	Cyclo-(fPFfNQYVKL)	1283.6703	1284.6781	642.8430	1306.6600	653.8339
TpcA	Cyclo-(fPFfNQWVOL)	1292.6706	1293.6784	647.3431	1315.6604	658.3341
TpcA <sub>1</sub>	Cyclo-(fPFfNQWVKL)	1306.6862	1307.6941	654.3509	1329.6760	665.3419
B analogues						
PhcB <sup>2</sup>	Cyclo-(fPWfNQFVOL)	1292.6706	1293.6784	647.3431	1315.6604	658.3341
TrcB	Cyclo-(fPWfNQYVOL)	1308.6655	1309.6733	655.3406	1331.6553	666.3316
TrcB <sup>1</sup>	Cyclo-(fPFwNQYVOL)	1308.6655	1309.6733	655.3406	1331.6553	666.3316
TrcB <sub>1</sub>	Cyclo-(fPWfNQYVKL)	1322.6812	1323.6890	662.3484	1345.6709	673.3394
TrcB <sub>1</sub> <sup>1</sup>	Cyclo-(fPFwNQYVKL)	1322.6812	1323.6890	662.3484	1345.6709	673.3394
TpcB	Cyclo-(fPWfNQWVOL)	1331.6815	1332.6893	666.8486	1354.6713	677.8395
TpcB <sup>1</sup>	Cyclo-(fPWfNQWVOL)	1331.6815	1332.6893	666.8486	1354.6713	677.8395
TpcB <sub>1</sub>	Cyclo-(fPWfNQWVKL)	1345.6971	1346.7050	673.8564	1368.6869	684.8474
TpcB <sub>1</sub> <sup>1</sup>	Cyclo-(fPFwNQWVKL)	1345.6971	1346.7050	673.8564	1368.6869	684.8474
C analogues						
PhcC <sup>2</sup>	Cyclo-(fPWwNQFVOL)	1331.6815	1332.6893	666.8486	1354.6713	677.8395
TrcC	Cyclo-(fPWwNQYVOL)	1347.6764	1348.6842	674.8460	1370.6662	685.8370
TrcC <sub>1</sub>	Cyclo-(fPWwNQYVKL)	1361.6921	1362.6999	681.8539	1384.6818	692.8448
TpcC	Cyclo-(fPWwNQWVOL)	1370.6924	1371.7002	686.3540	1393.6822	697.3450
TpcC <sub>1</sub>	Cyclo-(fPWwNQWVKL)	1384.7080	1385.7159	693.3618	1407.6978	704.3528
Gramicidins (GrCs)						
VGA	VGAIAvVvW-IWIWIW	1881.0783	1882.0862	941.5470	1904.0681	952.5380
VGB	VGAIAvVvW-IFIWIW	1842.0674	1843.0753	922.0415	1865.0572	933.0325
VGC	VGAIAvVvW-IYIWIW	1858.0624	1859.0702	930.0390	1881.0521	941.0300
IGA	IGAIAvVvW-IWIWIW	1895.0940	1896.1018	948.5548	1918.0838	959.5458
IGB	IGAIAvVvW-IFIWIW	1856.0831	1857.0909	929.0494	1879.0729	940.0403
IGC	IGAIAvVvW-IYIWIW	1872.0780	1873.0858	937.0468	1895.0678	948.0378

<sup>1</sup> Very rarely detected in Trc extracts using ESMS

<sup>2</sup> Never detected in ESMS extracts using ESMS

**Table 2** List of theoretical monomer masses for Trcs incorporating Phe derivative 2-FF. The F residues with the a, b, c and d superscripts show the modification sites of F to 2-FF. In the cases of a single 2-FF substitution, 'a', 'b', 'c' and 'd' show the possible sites of modification from most to least likely (assuming a preference for the natural analogue over 2-FF). If there is more than one possible sequence due to more than one 2-FF substitution in a Trc analogue, the possible sequences are shown by corresponding superscripts in the structure e.g. PhcA(2\*2-FF) = Cyclo-(<sup>f</sup>Pf<sup>a</sup><sup>f</sup>NQF<sup>b</sup>VOL), where F<sup>a</sup> is the most likely modification to a 2-FF residue, and subsequent modifications are at any of the positions with the 'b' subscript. The order of incorporation of modified Phe residues (from most to least likely), is based on the work of Vosloo (2) using Phe

Abbreviations <sup>1</sup>	Primary structure/s	No. of theoretical sequences <sup>2</sup>	<i>M<sub>r</sub></i>	[M+H] <sup>+</sup>	[M+2H] <sup>2+</sup>	[M+Na] <sup>+</sup>	[M+Na+H] <sup>2+</sup>
<b>A analogues</b>							
PhcA(1*2-FF)	Cyclo-( <sup>f</sup> Pf <sup>a</sup> <sup>f</sup> NQF <sup>c</sup> VOL)	4	1271.6503	1272.6581	636.8330	1294.6400	647.8239
PhcA(2*2-FF)	Cyclo-( <sup>f</sup> Pf <sup>a</sup> <sup>f</sup> NQF <sup>b</sup> VOL)	6	1289.6409	1290.6487	645.8283	1312.6306	656.8192
PhcA(3*2-FF)	Cyclo-( <sup>f</sup> Pf <sup>a</sup> <sup>f</sup> NQF <sup>b</sup> VOL)	4	1307.6314	1308.6393	654.8235	1330.6212	665.8145
PhcA(4*2-FF)	Cyclo-( <sup>f</sup> Pf <sup>a</sup> <sup>f</sup> NQF <sup>b</sup> VOL)	1	1325.6220	1326.6298	663.8188	1348.6118	674.8098
PhcA <sub>1</sub> (1*2-FF)	Cyclo-( <sup>f</sup> Pf <sup>a</sup> <sup>f</sup> NQF <sup>c</sup> VKL)	4	1285.6659	1286.6737	643.8408	1308.6557	654.8318
PhcA <sub>1</sub> (2*2-FF)	Cyclo-( <sup>f</sup> Pf <sup>a</sup> <sup>f</sup> NQF <sup>b</sup> VKL)	6	1303.6565	1304.6643	652.8361	1326.6463	663.8270
PhcA <sub>1</sub> (3*2-FF)	Cyclo-( <sup>f</sup> Pf <sup>a</sup> <sup>f</sup> NQF <sup>b</sup> VKL)	4	1321.6471	1322.6549	661.8314	1344.6368	672.8223
PhcA <sub>1</sub> (4*2-FF)	Cyclo-( <sup>f</sup> Pf <sup>a</sup> <sup>f</sup> NQF <sup>b</sup> VKL)	1	1339.6377	1340.6455	670.8267	1362.6274	681.8176
TrcA(1*2-FF)	Cyclo-( <sup>f</sup> Pf <sup>a</sup> <sup>f</sup> NQYVOL)	3	1287.6452	1288.6530	644.8304	1310.6350	655.8214
TrcA(2*2-FF)	Cyclo-( <sup>f</sup> Pf <sup>a</sup> <sup>f</sup> NQYVOL)	3	1305.6358	1306.6436	653.8257	1328.6255	664.8167
TrcA(3*2-FF)	Cyclo-( <sup>f</sup> Pf <sup>a</sup> <sup>f</sup> NQYVOL)	1	1323.6264	1324.6342	662.8210	1346.6161	673.8120
TrcAv(1*2-FF) <sup>3</sup>	Cyclo-( <sup>f</sup> Pf <sup>a</sup> <sup>f</sup> NQYVOV)	3	1273.6295	1274.6374	637.8226	1296.6193	648.8136
TrcAv(1*2-FF) <sup>3</sup>	Cyclo-( <sup>f</sup> Pf <sup>a</sup> <sup>f</sup> NQYVOV)	3	1291.6201	1292.6280	646.8179	1314.6099	657.8089
TrcAv(1*2-FF) <sup>3</sup>	Cyclo-( <sup>f</sup> Pf <sup>a</sup> <sup>f</sup> NQYVOV)	1	1309.6107	1310.6185	655.8132	1332.6005	666.8041
TrcA <sub>1</sub> (1*2-FF)	Cyclo-( <sup>f</sup> Pf <sup>a</sup> <sup>f</sup> NQYVKL)	3	1301.6608	1302.6687	651.8382	1324.6506	662.8292
TrcA <sub>1</sub> (2*2-FF)	Cyclo-( <sup>f</sup> Pf <sup>a</sup> <sup>f</sup> NQYVKL)	3	1319.6514	1320.6592	660.8335	1342.6412	671.8245
TrcA <sub>1</sub> (3*2-FF)	Cyclo-( <sup>f</sup> Pf <sup>a</sup> <sup>f</sup> NQYVKL)	1	1337.6420	1338.6498	669.8288	1360.6318	680.8198
TpcA(1*2-FF)	Cyclo-( <sup>f</sup> Pf <sup>a</sup> <sup>f</sup> NQWVOL)	3	1310.6612	1311.6690	656.3384	1333.6509	667.3294
TpcA(2*2-FF)	Cyclo-( <sup>f</sup> Pf <sup>a</sup> <sup>f</sup> NQWVOL)	3	1328.6518	1329.6596	665.3337	1351.6415	676.3247
TpcA(3*2-FF)	Cyclo-( <sup>f</sup> Pf <sup>a</sup> <sup>f</sup> NQWVOL)	1	1346.6423	1347.6502	674.3290	1369.6321	685.3200
TpcA <sub>1</sub> (1*2-FF)	Cyclo-( <sup>f</sup> Pf <sup>a</sup> <sup>f</sup> NQWVKL)	3	1324.6768	1325.6846	663.3462	1347.6666	674.3372
TpcA <sub>1</sub> (2*2-FF)	Cyclo-( <sup>f</sup> Pf <sup>a</sup> <sup>f</sup> NQWVKL)	3	1342.6674	1343.6752	672.3415	1365.6572	683.3325
TpcA <sub>1</sub> (3*2-FF)	Cyclo-( <sup>f</sup> Pf <sup>a</sup> <sup>f</sup> NQWVKL)	1	1360.6580	1361.6658	681.3368	1383.6477	692.3278
<b>B analogues</b>							
PhcB(1*2-FF) <sup>4</sup>	Cyclo-( <sup>f</sup> PW <sup>a</sup> <sup>f</sup> NQF <sup>b</sup> VOL)	3	1310.6612	1311.6690	656.3384	1333.6509	667.3294
PhcB(2*2-FF) <sup>4</sup>	Cyclo-( <sup>f</sup> PW <sup>a</sup> <sup>f</sup> NQF <sup>b</sup> VOL)	3	1328.6518	1329.6596	665.3337	1351.6415	676.3247
PhcB(3*2-FF) <sup>4</sup>	Cyclo-( <sup>f</sup> PW <sup>a</sup> <sup>f</sup> NQF <sup>b</sup> VOL)	1	1346.6423	1347.6502	674.3290	1369.6321	685.3200
TrcB(1*2-FF)	Cyclo-( <sup>f</sup> PW <sup>a</sup> <sup>f</sup> NQYVOL)	2	1326.6561	1327.6639	664.3359	1349.6459	675.3268
TrcB(2*2-FF)	Cyclo-( <sup>f</sup> PW <sup>a</sup> <sup>f</sup> NQYVOL)	1	1344.6467	1345.6545	673.3312	1367.6364	684.3221
TrcB'(1*2-FF)	Cyclo-( <sup>f</sup> PW <sup>a</sup> <sup>w</sup> NQYVOL)	2	1326.6561	1327.6639	664.3359	1349.6459	675.3268
TrcB'(2*2-FF)	Cyclo-( <sup>f</sup> PW <sup>a</sup> <sup>w</sup> NQYVOL)	1	1344.6467	1345.6545	673.3312	1367.6364	684.3221
TrcB <sub>1</sub> (1*2-FF)	Cyclo-( <sup>f</sup> PW <sup>a</sup> <sup>f</sup> NQYVKL)	2	1340.6717	1341.6796	671.3437	1363.6615	682.3347
TrcB <sub>1</sub> (2*2-FF)	Cyclo-( <sup>f</sup> PW <sup>a</sup> <sup>w</sup> NQYVKL)	1	1358.6623	1359.6701	680.3390	1381.6521	691.3300
TrcB <sub>1</sub> '(1*2-FF)	Cyclo-( <sup>f</sup> PW <sup>a</sup> <sup>w</sup> NQYVKL)	2	1340.6717	1341.6796	671.3437	1363.6615	682.3347
TrcB <sub>1</sub> '(2*2-FF)	Cyclo-( <sup>f</sup> PW <sup>a</sup> <sup>w</sup> NQYVKL)	1	1358.6623	1359.6701	680.3390	1381.6521	691.3300
TpcB(1*2-FF)	Cyclo-( <sup>f</sup> PW <sup>a</sup> <sup>f</sup> NQWVOL)	2	1349.6721	1350.6799	675.8439	1372.6618	686.8348
TpcB(2*2-FF)	Cyclo-( <sup>f</sup> PW <sup>a</sup> <sup>f</sup> NQWVOL)	1	1367.6627	1368.6705	684.8392	1390.6524	695.8301
TpcB'(1*2-FF)	Cyclo-( <sup>f</sup> PW <sup>a</sup> <sup>w</sup> NQWVOL)	2	1349.6721	1350.6799	675.8439	1372.6618	686.8348
TpcB'(2*2-FF)	Cyclo-( <sup>f</sup> PW <sup>a</sup> <sup>w</sup> NQWVOL)	1	1367.6627	1368.6705	684.8392	1390.6524	695.8301
TpcB <sub>1</sub> (1*2-FF)	Cyclo-( <sup>f</sup> PW <sup>a</sup> <sup>f</sup> NQWVKL)	2	1363.6877	1364.6955	682.8517	1386.6775	693.8427
TpcB <sub>1</sub> (2*2-FF)	Cyclo-( <sup>f</sup> PW <sup>a</sup> <sup>f</sup> NQWVKL)	1	1381.6783	1382.6861	691.8470	1404.6681	702.8379
TpcB <sub>1</sub> '(1*2-FF)	Cyclo-( <sup>f</sup> PW <sup>a</sup> <sup>w</sup> NQWVKL)	2	1363.6877	1364.6955	682.8517	1386.6775	693.8427
TpcB <sub>1</sub> '(2*2-FF)	Cyclo-( <sup>f</sup> PW <sup>a</sup> <sup>w</sup> NQWVKL)	1	1381.6783	1382.6861	691.8470	1404.6681	702.8379
<b>C-analogues</b>							
PhcC(1*2-FF) <sup>4</sup>	Cyclo-( <sup>f</sup> PWwNQF <sup>b</sup> VOL)	2	1349.6721	1350.6799	675.8439	1372.6618	686.8348
PhcC(2*2-FF) <sup>4</sup>	Cyclo-( <sup>f</sup> PWwNQF <sup>b</sup> VOL)	1	1367.6627	1368.6705	684.8392	1390.6524	695.8301
TrcC(1*2-FF)	Cyclo-( <sup>f</sup> PWwNQYVOL)	1	1365.6670	1366.6748	683.8413	1388.6568	694.8323
TrcC <sub>1</sub> (1*2-FF)	Cyclo-( <sup>f</sup> PWwNQYVKL)	1	1379.6826	1380.6905	690.8491	1402.6724	701.8401
TpcC(1*2-FF)	Cyclo-( <sup>f</sup> PWwNQWVKL)	1	1388.6830	1389.6908	695.3493	1411.6727	706.3403
TpcC <sub>1</sub> (1*2-FF)	Cyclo-( <sup>f</sup> PWwNQWVKL)	1	1402.6986	1403.7064	702.3571	1425.6884	713.3481

<sup>1</sup> The number followed by the \* indicated the number of residues of the non-natural amino acid (shown after \*) in that structure

<sup>2</sup> Shows the structural configurations possible given the same sites of incorporation for Phe in the natural equivalent of the analogue

<sup>3</sup> Natural analogue (TrcAv) very rarely detected in Trc extracts using ESMS

<sup>4</sup> Natural analogues (PhcB and PhcC) not detected in Trc extracts using ESMS

**Table 2** List of theoretical monomer masses for Trcs incorporating Phe derivative 4-MeF. The F residues with the a, b, c and d superscripts show the modification sites of F to 4-MeF substitution. In the cases of a single 4-MeF substitution, 'a', 'b', 'c' and 'd' show the possible sites of modification from most to least likely (assuming a preference for the natural analogue over 4-MeF). If there is more than one possible sequence due to more than one 4-MeF substitution in a Trc analogue, the possible sequences are shown by corresponding superscripts in the structure e.g. PhcA(2\*4-MeF) = Cyclo-(<sup>f</sup>bPF<sup>a</sup><sup>b</sup>NQF<sup>b</sup>VOL), where F<sup>a</sup> is the most likely modification to a 4-MeF residue, and subsequent modifications are at any of the positions with the 'b' subscript. The order of incorporation of modified Phe residues (from most to least likely), is based on the work of Vosloo (2) using Phe

Abbreviations <sup>1</sup>	Primary structure/s	No. of theoretical sequences <sup>2</sup>	$M_r$	[M+H] <sup>1+</sup>	[M+2H] <sup>2+</sup>	[M+Na] <sup>1+</sup>	[M+Na+H] <sup>2+</sup>
<b>A analogues</b>							
PhcA(1*4-MeF)	Cyclo-( <sup>f</sup> dPF <sup>a</sup> <sup>b</sup> NQF <sup>c</sup> VOL)	4	1267.6863	1268.6941	641.8643	1290.6760	652.8552
PhcA(2*4-MeF)	Cyclo-( <sup>f</sup> bPF <sup>a</sup> <sup>b</sup> NQF <sup>b</sup> VOL)	6	1281.7129	1282.7207	655.8908	1304.7026	666.8818
PhcA(3*4-MeF)	Cyclo-( <sup>f</sup> bPF <sup>a</sup> <sup>b</sup> NQF <sup>b</sup> VOL)	4	1295.7394	1296.7473	669.9174	1318.7292	680.9084
PhcA(4*4-MeF)	Cyclo-( <sup>f</sup> aPF <sup>a</sup> <sup>b</sup> NQF <sup>a</sup> VOL)	1	1309.7660	1310.7738	683.9440	1332.7558	694.9350
PhcA <sub>1</sub> (1*4-MeF)	Cyclo-( <sup>f</sup> dPF <sup>a</sup> <sup>b</sup> NQF <sup>c</sup> VKL)	4	1281.7019	1282.7097	648.8721	1304.6917	659.8630
PhcA <sub>1</sub> (2*4-MeF)	Cyclo-( <sup>f</sup> bPF <sup>a</sup> <sup>b</sup> NQF <sup>b</sup> VKL)	6	1295.7285	1296.7363	662.8987	1318.7183	673.8896
PhcA <sub>1</sub> (3*4-MeF)	Cyclo-( <sup>f</sup> bPF <sup>a</sup> <sup>b</sup> NQF <sup>b</sup> VKL)	4	1309.7551	1310.7629	676.9252	1332.7448	687.9162
PhcA <sub>1</sub> (4*4-MeF)	Cyclo-( <sup>f</sup> aPF <sup>a</sup> <sup>b</sup> NQF <sup>a</sup> VKL)	1	1323.7817	1324.7895	690.9518	1346.7714	701.9428
TrcA(1*4-MeF)	Cyclo-( <sup>f</sup> cPF <sup>a</sup> <sup>b</sup> NQYVOL)	3	1283.6812	1284.6890	649.8617	1306.6710	660.8527
TrcA(2*4-MeF)	Cyclo-( <sup>f</sup> bPF <sup>a</sup> <sup>b</sup> NQYVOL)	3	1297.7078	1298.7156	663.8883	1320.6975	674.8793
TrcA(3*4-MeF)	Cyclo-( <sup>f</sup> aPF <sup>a</sup> <sup>b</sup> NQYVOL)	1	1311.7344	1312.7422	677.9149	1334.7241	688.9058
TrcAv(1*4-MeF) <sup>3</sup>	Cyclo-( <sup>f</sup> cPF <sup>a</sup> <sup>b</sup> NQYVOV)	3	1269.6656	1270.6734	642.8539	1292.6553	653.8449
TrcAv(1*4-MeF) <sup>3</sup>	Cyclo-( <sup>f</sup> bPF <sup>a</sup> <sup>b</sup> NQYVOV)	3	1283.6921	1284.7000	656.8805	1306.6819	667.8714
TrcAv(1*4-MeF) <sup>3</sup>	Cyclo-( <sup>f</sup> aPF <sup>a</sup> <sup>b</sup> NQYVOV)	1	1297.7187	1298.7265	670.9071	1320.7085	681.8980
TrcA <sub>1</sub> (1*4-MeF)	Cyclo-( <sup>f</sup> cPF <sup>a</sup> <sup>b</sup> NQYVKL)	3	1297.6968	1298.7047	656.8695	1320.6866	667.8605
TrcA <sub>1</sub> (2*4-MeF)	Cyclo-( <sup>f</sup> bPF <sup>a</sup> <sup>b</sup> NQYVKL)	3	1311.7234	1312.7312	670.8961	1334.7132	681.8871
TrcA <sub>1</sub> (3*4-MeF)	Cyclo-( <sup>f</sup> aPF <sup>a</sup> <sup>b</sup> NQYVKL)	1	1325.7500	1326.7578	684.9227	1348.7398	695.9137
TpcA(1*4-MeF)	Cyclo-( <sup>f</sup> cPF <sup>a</sup> <sup>b</sup> NQWVOL)	3	1306.6972	1307.7050	661.3697	1329.6869	672.3607
TpcA(2*4-MeF)	Cyclo-( <sup>f</sup> bPF <sup>a</sup> <sup>b</sup> NQWVOL)	3	1320.7238	1321.7316	675.3963	1343.7135	686.3873
TpcA(3*4-MeF)	Cyclo-( <sup>f</sup> aPF <sup>a</sup> <sup>b</sup> NQWVOL)	1	1334.7503	1335.7582	689.4229	1357.7401	700.4138
TpcA <sub>1</sub> (1*4-MeF)	Cyclo-( <sup>f</sup> cPF <sup>a</sup> <sup>b</sup> NQWVKL)	3	1320.7128	1321.7206	668.3775	1343.7026	679.3685
TpcA <sub>1</sub> (2*4-MeF)	Cyclo-( <sup>f</sup> bPF <sup>a</sup> <sup>b</sup> NQWVKL)	3	1334.7394	1335.7472	682.4041	1357.7292	693.3951
TpcA <sub>1</sub> (3*4-MeF)	Cyclo-( <sup>f</sup> aPF <sup>a</sup> <sup>b</sup> NQWVKL)	1	1348.7660	1349.7738	696.4307	1371.7557	707.4217
<b>B analogues</b>							
PhcB(1*4-MeF) <sup>4</sup>	Cyclo-( <sup>f</sup> cPW <sup>a</sup> <sup>b</sup> NQF <sup>b</sup> VOL)	3	1306.6972	1307.7050	661.3697	1329.6869	672.3607
PhcB(2*4-MeF) <sup>4</sup>	Cyclo-( <sup>f</sup> bPW <sup>a</sup> <sup>b</sup> NQF <sup>b</sup> VOL)	3	1320.7238	1321.7316	675.3963	1343.7135	686.3873
PhcB(3*4-MeF) <sup>4</sup>	Cyclo-( <sup>f</sup> aPW <sup>a</sup> <sup>b</sup> NQF <sup>a</sup> VOL)	1	1334.7503	1335.7582	689.4229	1357.7401	700.4138
TrcB(1*4-MeF)	Cyclo-( <sup>f</sup> cPW <sup>a</sup> <sup>b</sup> NQYVOL)	2	1322.6921	1323.6999	669.3672	1345.6819	680.3581
TrcB(2*4-MeF)	Cyclo-( <sup>f</sup> bPW <sup>a</sup> <sup>b</sup> NQYVOL)	1	1336.7187	1337.7265	683.3937	1359.7084	694.3847
TrcB'(1*4-MeF)	Cyclo-( <sup>f</sup> bPF <sup>a</sup> <sup>w</sup> NQYVOL)	2	1322.6921	1323.6999	669.3672	1345.6819	680.3581
TrcB'(2*4-MeF)	Cyclo-( <sup>f</sup> aPF <sup>a</sup> <sup>w</sup> NQYVOL)	1	1336.7187	1337.7265	683.3937	1359.7084	694.3847
TrcB <sub>1</sub> (1*4-MeF)	Cyclo-( <sup>f</sup> bPW <sup>a</sup> <sup>b</sup> NQYVKL)	2	1336.7077	1337.7156	676.3750	1359.6975	687.3660
TrcB <sub>1</sub> (2*4-MeF)	Cyclo-( <sup>f</sup> aPW <sup>a</sup> <sup>b</sup> NQYVKL)	1	1350.7343	1351.7421	690.4016	1373.7241	701.3925
TrcB <sub>1</sub> '(1*4-MeF)	Cyclo-( <sup>f</sup> bPF <sup>a</sup> <sup>w</sup> NQYVKL)	2	1336.7077	1337.7156	676.3750	1359.6975	687.3660
TrcB <sub>1</sub> '(2*4-MeF)	Cyclo-( <sup>f</sup> aPF <sup>a</sup> <sup>w</sup> NQYVKL)	1	1350.7343	1351.7421	690.4016	1373.7241	701.3925
TpcB(1*4-MeF)	Cyclo-( <sup>f</sup> bPW <sup>a</sup> <sup>b</sup> NQWVOL)	2	1345.7081	1346.7159	680.8752	1368.6978	691.8661
TpcB(2*4-MeF)	Cyclo-( <sup>f</sup> aPW <sup>a</sup> <sup>b</sup> NQWVOL)	1	1359.7347	1360.7425	694.9017	1382.7244	705.8927
TpcB'(1*4-MeF)	Cyclo-( <sup>f</sup> bPF <sup>a</sup> <sup>w</sup> NQWVOL)	2	1345.7081	1346.7159	680.8752	1368.6978	691.8661
TpcB'(2*4-MeF)	Cyclo-( <sup>f</sup> aPF <sup>a</sup> <sup>w</sup> NQWVOL)	1	1359.7347	1360.7425	694.9017	1382.7244	705.8927
TpcB <sub>1</sub> (1*4-MeF)	Cyclo-( <sup>f</sup> bPW <sup>a</sup> <sup>b</sup> NQWVKL)	2	1359.7237	1360.7315	687.8830	1382.7135	698.8739
TpcB <sub>1</sub> (2*4-MeF)	Cyclo-( <sup>f</sup> aPW <sup>a</sup> <sup>b</sup> NQWVKL)	1	1373.7503	1374.7581	701.9096	1396.7401	712.9005
TpcB <sub>1</sub> '(1*4-MeF)	Cyclo-( <sup>f</sup> bPF <sup>a</sup> <sup>w</sup> NQWVKL)	2	1359.7237	1360.7315	687.8830	1382.7135	698.8739
TpcB <sub>1</sub> '(2*4-MeF)	Cyclo-( <sup>f</sup> aPF <sup>a</sup> <sup>w</sup> NQWVKL)	1	1373.7503	1374.7581	701.9096	1396.7401	712.9005
<b>C-analogues</b>							
PhcC(1*4-MeF) <sup>4</sup>	Cyclo-( <sup>f</sup> bPW <sup>w</sup> NQF <sup>b</sup> VOL)	2	1345.7081	1346.7159	680.8752	1368.6978	691.8661
PhcC(2*4-MeF) <sup>4</sup>	Cyclo-( <sup>f</sup> aPW <sup>w</sup> NQF <sup>a</sup> VOL)	1	1359.7347	1360.7425	694.9017	1382.7244	705.8927
TrcC(1*4-MeF)	Cyclo-( <sup>f</sup> bPW <sup>w</sup> NQYVOL)	1	1361.7030	1362.7108	688.8726	1384.6928	699.8636
TrcC <sub>1</sub> (1*4-MeF)	Cyclo-( <sup>f</sup> aPW <sup>w</sup> NQYVKL)	1	1375.7186	1376.7265	695.8804	1398.7084	706.8714
TpcC(1*4-MeF)	Cyclo-( <sup>f</sup> aPW <sup>w</sup> NQWVKL)	1	1384.7190	1385.7268	700.3806	1407.7087	711.3716
TpcC <sub>1</sub> (1*4-MeF)	Cyclo-( <sup>f</sup> bPW <sup>w</sup> NQWVOL)	1	1398.7346	1399.7424	707.3884	1421.7244	718.3794

<sup>1</sup> The number followed by the \* indicated the number of residues of the non-natural amino acid (shown after \*) in that structure

<sup>2</sup> Shows the structural configurations possible given the same sites of incorporation for Phe in the natural equivalent of the analogue

<sup>3</sup> Natural analogue (TrcAv) very rarely detected in Trc extracts using ESMS

<sup>4</sup> Natural analogues (PhcB and PhcC) not detected in Trc extracts using ESMS



**Table 3** List of theoretical monomer masses for Trcs incorporating Trp derivatives 5- or 1-mehtyl-tryptophan (5/1-MeW). The W residues with the ‘a’ and ‘b’ superscripts show the modification sites of W to 5/1-MeW. In the cases of a single 5/1-MeW substitution, ‘a’ and ‘b’ show the possible sites of modification from most to least likely (assuming a preference for the natural analogue over 5/1-MeW). If there is more than one possible sequence due to more than one 5/1-MeW substitution in a Trc analogue, the possible sequences are shown by corresponding superscripts in the structure e.g.  $\text{TpcC}(2^*5/1\text{-MeW}) = \text{Cyclo}(\text{fPW}^{\text{b}}\text{w}^{\text{a}}\text{NQW}^{\text{b}}\text{VOL})$ , where  $\text{W}^{\text{a}}$  is the most likely modification to a 5/1-MeW residue, and subsequent modifications are at any of the positions with the ‘b’ subscript. The order of incorporation of modified Trp residues (from most to least likely), is based on the work of Vosloo (2) using Trp

Abbreviations <sup>1</sup>	Primary structure/s	No. of theoretical sequences <sup>2</sup>	$M_r$	$[\text{M}+\text{H}]^{1+}$	$[\text{M}+2\text{H}]^{2+}$	$[\text{M}+\text{Na}]^{1+}$	$[\text{M}+\text{Na}+\text{H}]^{2+}$
A analogues							
TpcA(1*5/1-MeW)	Cyclo-(fPFfNQW <sup>a</sup> VOL)	1	1306.6864	1307.6942	654.3511	1329.6762	665.3420
TpcA <sub>1</sub> (1*5/1-MeW)	Cyclo-(fPFfNQW <sup>a</sup> VKL)	1	1320.7020	1321.7099	661.3589	1343.6918	672.3498
A analogues							
PhcA(1*5/1-MeW) <sup>3</sup>	Cyclo-(fPW <sup>a</sup> fNQFVOL)	1	1306.6863	1307.6941	654.3510	1329.6760	665.3419
TrcA(1*5/1-MeW)	Cyclo-(fPW <sup>a</sup> fNQYVOL)	1	1322.6812	1323.6890	662.3484	1345.6709	673.3394
TrcA'(1*5/1-MeW)	Cyclo-(fPFw <sup>a</sup> NQYVOL)	1	1322.6812	1323.6890	662.3484	1345.6709	673.3394
TrcA <sub>1</sub> (1*5/1-MeW)	Cyclo-(fPFw <sup>a</sup> NQYVKL)	1	1336.6968	1337.7046	669.3563	1359.6866	680.3472
TrcA <sub>1</sub> '(1*5/1-MeW)	Cyclo-(fPFw <sup>a</sup> NQYVKL)	1	1336.6968	1337.7046	669.3563	1359.6866	680.3472
TpcA(1*5/1-MeW)	Cyclo-(fPW <sup>a</sup> fNQW <sup>b</sup> VOL)	2	1345.6972	1346.7050	673.8564	1368.6869	684.8474
TpcA(2*5/1-MeW)	Cyclo-(fPW <sup>a</sup> fNQW <sup>a</sup> VOL)	1	1359.7128	1360.7206	680.8643	1382.7026	691.8552
TpcA'(2*5/1-MeW)	Cyclo-(fPFw <sup>a</sup> NQW <sup>a</sup> VOL)	1	1359.7128	1360.7206	680.8643	1382.7026	691.8552
TpcA'(1*5/1-MeW)	Cyclo-(fPFw <sup>a</sup> NQW <sup>b</sup> VOL)	2	1345.6973	1346.7051	673.8565	1368.6871	684.8474
TpcA <sub>1</sub> (1*5/1-MeW)	Cyclo-(fPW <sup>a</sup> fNQW <sup>b</sup> VKL)	2	1359.7128	1360.7206	680.8643	1382.7026	691.8552
TpcA <sub>1</sub> '(1*5/1-MeW)	Cyclo-(fPW <sup>a</sup> fNQW <sup>a</sup> VKL)	1	1373.7284	1374.7363	687.8721	1396.7182	698.8630
TpcA <sub>1</sub> '(1*5/1-MeW)	Cyclo-(fPFw <sup>a</sup> NQW <sup>b</sup> VKL)	2	1359.7129	1360.7208	680.8643	1382.7027	691.8553
TpcA <sub>1</sub> '(2*5/1-MeW)	Cyclo-(fPFw <sup>a</sup> NQW <sup>a</sup> VKL)	1	1373.7287	1374.7366	687.8722	1396.7185	698.8632
C analogues							
PhcC(1*5/1-MeW) <sup>3</sup>	Cyclo-(fPW <sup>b</sup> w <sup>a</sup> NQFVOL)	2	1345.6973	1346.7051	673.8565	1368.6871	684.8474
PhcC(2*5/1-MeW) <sup>3</sup>	Cyclo-(fPW <sup>b</sup> w <sup>a</sup> NQFVOL)	1	1359.7131	1360.7209	680.8644	1382.7029	691.8553
TrcC(1*5/1-MeW)	Cyclo-(fPW <sup>b</sup> w <sup>a</sup> NQYVOL)	2	1361.6922	1362.7000	681.8540	1384.6820	692.8449
TrcC(2*5/1-MeW)	Cyclo-(fPW <sup>b</sup> w <sup>a</sup> NQYVOL)	1	1375.7080	1376.7158	688.8619	1398.6978	699.8528
TrcC <sub>1</sub> (1*5/1-MeW)	Cyclo-(fPW <sup>b</sup> w <sup>a</sup> NQYVKL)	2	1375.7079	1376.7157	688.8618	1398.6976	699.8527
TrcC <sub>1</sub> (2*5/1-MeW)	Cyclo-(fPW <sup>b</sup> w <sup>a</sup> NQYVKL)	1	1389.7237	1390.7315	695.8697	1412.7134	706.8606
TpcC(1*5/1-MeW)	Cyclo-(fPW <sup>b</sup> w <sup>a</sup> NQW <sup>b</sup> VOL)	3	1384.7081	1385.7159	693.3619	1407.6978	704.3528
TpcC(2*5/1-MeW)	Cyclo-(fPW <sup>b</sup> w <sup>a</sup> NQW <sup>b</sup> VOL)	3	1398.7237	1399.7315	700.3697	1421.7135	711.3606
TpcC(3*5/1-MeW)	Cyclo-(fPW <sup>b</sup> w <sup>a</sup> NQW <sup>a</sup> VOL)	1	1412.7394	1413.7472	707.3775	1435.7291	718.3685
TpcC <sub>1</sub> (1*5/1-MeW)	Cyclo-(fPW <sup>b</sup> w <sup>a</sup> NQW <sup>b</sup> VKL)	3	1398.7237	1399.7315	700.3697	1421.7135	711.3606
TpcC <sub>1</sub> (2*5/1-MeW)	Cyclo-(fPW <sup>b</sup> w <sup>a</sup> NQW <sup>b</sup> VKL)	3	1412.7393	1413.7472	707.3775	1435.7291	718.3685
TpcC <sub>1</sub> (3*5/1-MeW)	Cyclo-(fPW <sup>b</sup> w <sup>a</sup> NQW <sup>a</sup> VKL)	1	1426.7550	1427.7628	714.3854	1449.7448	725.3763

<sup>1</sup> The number followed by the \* indicated the number of residues of the non-natural amino acid (shown after \*) in that structure

<sup>2</sup> Shows the structural configurations possible given the same sites of incorporation for Trp in the natural equivalent of the analogue

<sup>3</sup> Natural analogues (PhcA and PhcC) not detected in Trc extracts using ESMs

## References

1. Tang, X.-J., Thibault, P., and Boyd, R. K. (1992) Characterisation of the tyrocidine and gramicidin fractions of the tyrothricin complex from *Bacillus brevis* using liquid chromatography and mass spectrometry. *Int. J. Mass Spectrom. Ion Process.* **122**, 153–179
2. Vosloo, J. A. (2016) Optimised bacterial production and characterisation of natural antimicrobial peptides with potential application in agriculture. **Ph.D. thesis**, University of Stellenbosch, <http://scholar.sun.ac.za/handle/10019.1/98411>
3. Vosloo, J. A., Stander, M. A., Leussa, A. N. N., Spathelf, B. M., and Rautenbach, M. (2013) Manipulation of the tyrothricin production profile of *Bacillus aneurinolyticus*. *Microbiol. (United Kingdom)*. **159**, 2200–2211